The University of Nottingham

UNITED KINGDOM · CHINA · MALAYSIA

# Investigation of Dormancy in Acute Myeloid Leukaemia Cells and the Induction of Dormancy in their Response to Genotoxic Stress


**Mazin Ghalib Hussein Al-Asadi**

**MBChB, MSc. Haematology**


**Thesis submitted to the University of Nottingham for the degree of Doctor of Philosophy**

**May 2017**

# ABSTRACT

Cancer cells can exist in a reversible state of dormancy (G0 phase of the cell cycle). Relapse of acute myeloid leukaemia (AML) is likely due to dormant cells escape frontline treatment. Dormant AML cells have been identified in the bone marrow (BM) endosteal region which is characterised by an excess of TGFβ1 and a shortage of nutrients.

As the first step in this project, we developed an *in vitro* model of AML cell dormancy by exploiting these features. Following a preliminary investigation of four AML cell lines, the $CD34^{+}CD38^{-}$ line TF1-a was selected for in-depth investigation. TF1-a showed significant inhibition of proliferation, with features of dormancy and stemness, in response to 72 hours of TGFB1+mTOR inhibitor treatment (mTOR pathway inhibition mimics major effects of nutrient scarcity) without affecting cell viability or inducing differentiation of these cells.

Secondly, whole human genome gene expression profiling using Affymetrix microarray strips (HuGene2.1ST) was conducted to molecularly characterise the dormancy-induced TF1-a cells. As a result, we identified 240 genes which were significantly up-regulated by at least twofold, including genes involved in adhesion, stemness, chemoresistance, tumor suppression and genes involved in canonical cell cycle regulation. The most upregulated gene was osteopontin (17.1fold). Immunocytochemistry of BM biopsies from AML patients confirmed high levels of osteopontin in the cytoplasm of blasts near the paratrabecular BM. Osteopontin and other genes identified in this model, including well-characterised genes (e.g. CD44, CD47, CD123, ABCC3 and CDKN2B) as well as little-known ones (e.g. ITGB3, BTG2 and PTPRU), are potential therapeutic targets in AML.

AML cells which are identified in the bone marrow (BM) endosteal region are likely to survive chemotherapy for several reasons including the low concentration of the drug delivered to this poorly perfused area of the BM. We hypothesised that these cells might induce dormancy features that help them escaping chemotherapy. Moreover, little is known regarding the molecular changes in those AML cells surviving genotoxic stress.

The third aim of this study was to investigate the AML cells surviving genotoxic stress. Therefore, we developed and characterised an *in vitro* model of prolonged sub-lethal genotoxicity in AML cells by utilising the TF1-a cells treated with etoposide for 6 days. TF1-a cells survived this conditioning with significant inhibition of proliferation and limited damage and apoptosis. The molecular signature of these cells was characterized using GEP of the whole human genome and was compared to that of the dormancy-induced TF1-a cells in an aim to identify genes commonly up-regulated in both scenarios that might act as possible drivers of dormancy in AML cells residing in a sub-lethal genotoxic environment. In this context, 31 genes were significantly commonly upregulated in both scenarios including ITGB3, SLFN5, C15orf26 and GRAP2 which are candidates for in-depth investigation in AML.

To sum up, in this study we developed and molecularly characterised in vitro models of dormancy and sub-lethal genotoxicity in AML cells with stemness characteristics through novel approaches that took bone marrow microenvironmental features into consideration. These features likely contribute to the resistance of the residual sub-population of AML cells that causing disease relapse. The current models helped to overcome the obstacles facing the in-depth studying of these rare AML cells due to the difficulty in obtaining them from clinical samples. Finally, the molecular findings of this study paved the way to potentially important future directions of research that could help to achieve the ultimate goal of eradicating AML cells and preventing relapse.

# ACKNOWLEDGEMENTS

First and foremost, it is a great honor and an enormous pleasure to express my deep thank and gratitude to my supervisors; **Professor Nigel Russell, Dr. Monica Pallis and Associate Professor Claire Seedhouse**, for their continuing support throughout this study. A special thank goes to Dr. Monica Pallis who has taught me, both consciously and unconsciously, how to deal with the challenges in my study and for her patience, clarity, and the scientific criticism in her advice to bring this work to the best. I am also thankful to Associate Professor Claire Seedhouse for offering her precious time generously to review my writings and in providing materials for performing the molecular experiments.

In the department, I thank Dr. Martin Grundy (a postdoc) and my colleagues Sahar Aldosari, Hiba Al-masmum, Hayaa Alhuthali and Ning Yu. The joy and enthusiasm you all have in your work were contagious and motivational for me. I learned many things from you in lab works and in discussions; thank you all indeed.

This work could not be completed without the contributions of many other people who I am indebted to them in my life. Here, I would like to thank our collaborators in the NASC research group; particularly the research technicians Iqbal Khan and Naofel Aljafer for processing the RNA preps for the GEP experiments. Also, Dr. Marcos Castellanos who taught me how to use Partek Genomic Suite software for analysing the GEP data. In my work on the IHC investigations of the BM biopsies, I thank the members of the the Nottingham Health Science Biobank (NHSB) team who kindly provided me with the BM sections. Also, a big thank goes to the members of the academic rheumatology Dr. Laura Wyatt and Dr. Seyed Shahtaheri for their help in performing the IHC experiments. I would like to thank Mohammed Al-Ameedee (PhD candidate/school of pharmacy) for offering his experience in managing long Word document which helped me in formatting the thesis. I, also, would like to express my thank to Nikita Dutta (MSc student) who

I enjoyed working with her in investigating osteopontin (OPN) in AML. I wish her all the success in her future career.

I gratefully thank the funding source that made my PhD study possible. I was funded by a scholarship from the Iraqi government represented by the Iraqi Ministry of Higher Education and Scientific Research (MOHESR).

Lastly, I would like to express my love and thank to my wife **Lina** for the endless time and support she provided to push me forward to complete this work. Her existence besides me was indispensable to accomplish this work. My thank, also, goes to other members of my family including my kids; **Zain, Yousif and Haya**, my brothers, my sisters and my mother for their love, encouregements and continuous prayers that immensely helped me to overcome the work pressure.

# LIST OF ABBREVIATIONS

| | |
|---|---|
| 7AAD | 7-amino-actinomycin D |
| ABC | ATP-binding cassette |
| ADLH | Aldehyde Dehydrogenase |
| AML | acute myeloid leukaemia |
| Ang1 | Angiopoietin |
| ANOVA | analysis of variance |
| APC | Allophycocyanin |
| B2M | β2-microglobulin |
| BAAA | Bodipy-aminoacetaldehyde |
| BAAA-DA | Bodipy-aminoacetaldehyde diethyl acetal |
| BM | bone marrow |
| BMP | bone morphogenic protein |
| BrdU | bromodeoxyuridine |
| BSA | bovine serum albumin |
| BT | bone trabeculae |
| CAR | CXCL12-abundant reticular cells |
| CD | cluster of differentiation |
| CDK | cyclin dependent kinase |
| CDKI | cyclin dependent kinase inhibitor |
| cDNA | complementary deoxyribonucleic acid |
| CHIP | clonal haematopoiesis of indeterminate potential |
| CM | complete medium |
| CML | chronic myeloid leukaemia |
| CO2 | carbon dioxide |
| CT | Chemotherapy |
| DAB | 3,3'-diaminobenzidine |
| DAPI | 4'-6-Diamidino-2-phenylindole |
| DEAB | diethylaminobenzaldehyde |
| DMSO | dimethyl sufloxide |

| | |
|---|---|
| DNA | deoxyribonucleic acid |
| DREAM | DP, RB-like, E2F, and MuvB-like proteins |
| DSB | DNA double strands breaks |
| DYRK1B | dual specificity tyrosinephosphorylation- regulated kinase 1B |
| ECM | cell-extracellular matrix |
| ES | enrichment scores |
| FAB | French-American-British |
| FACS | Fluorescence Activated Cell Sorting/Scanning |
| FCS | foetal calf serum |
| FDR | false discovery rate |
| FFPE | formalin-fixed paraffin-embedded |
| FITC | Fluorescein Isothiocyanate |
| FLT3-ITD | FMS-like tyrosine kinase 3-internal tandem duplication |
| FSCs | fixed and stained cells |
| G0 | gap 0 |
| G1 | gap 1 |
| G-CSF | granulocyte colony stimulating factor |
| GEP | gene expression profiling |
| GO | gene ontology |
| GSK-3 | glycose synthase kinase 3 |
| H&E | haematoxylin and eosin |
| HCL | hydrochloric acid |
| HRP | horseradish peroxidase |
| HSC | haematopoietic stem cell |
| HSPC | haematopoietic stem and progenitor cell |
| IC20 | dose that inhibits 20% of cells |
| IHC | immunohistochemistry |
| IR | ionizing radiaton |
| KEGG | Kyoto Encyclopaedia of Genes and Genomes |
| LIC | leukaemia initiating cell |
| LRC | lipid raft clustering |

| | |
|---|---|
| LSC | leukaemia stem cell |
| LSK | Lin- Sca-1+ c-Kit+ |
| LT-HSCs | long-term HSCs |
| mAb | monoclonal antibody |
| MFU | mean fluorescence unit |
| miniGEP | mini gene expression profile |
| MRD | minimal residual disease |
| mTOR | mammalian target of Rapamycin |
| N:C | nucleus to cytoplasm |
| NASC | Nottingham arabidopsis stock centre |
| NGS | normal goat serum |
| NHSB | Nottingham Health Science Biobank |
| NOD/SCID | non-obese diabetic/ severe combined immune deffecient |
| OPN | Osteopontin |
| PB | peripheral blood |
| PBS | phosphate buffered saline |
| PCA | Principal Components Analysis |
| PE | PhycoErythrin |
| PGS | partek genomic suite |
| PI | propidium iodide |
| prS6 | phosphorylated ribosomal S6 |
| qPCR | quantitative polymerase chain reaction |
| Rb | Retinoblastoma |
| RFU | relative fluorescence unit |
| RIN | RNA Integrity Number |
| RNA | ribo nucleic acid |
| ROS | reactive oxygen species |
| RPMI | Roswell Park Memorial Institute medium |
| SCM | serum-containing media |
| SFM | serum-free culture medium |
| SPSS | Statistical Package for Social Sciences, version 23 |

| | |
|---|---|
| STR | short tandem repeat |
| TCGA | the Cancer Genomic Atlas |
| TGFβ1 | transforming growth factor-β1 |
| THBS | Thrombospondin |
| TPO | Thrombopoietin |
| UV | Ultraviolet |
| VLA-4 | very late antigen-4 |
| VLA-5 | very late antigen-5 |
| WHO | world health organization |

# TABLE OF CONTENTS

**ABSTRACT** ..... **II**
**ACKNOWLEDGEMENTS** ..... **IV**
**LIST OF ABBREVIATIONS** ..... **VI**
**TABLE OF CONTENTS** ..... **X**
**LIST OF FIGURES** ..... **XV**
**LIST OF TABLES** ..... **XVIII**
**CHAPTER ONE INTRODUCTION AND REVIEW OF LITERATURE** ..... **1**
1.1. Background ..... 2
1.2. Acute Myeloid Leukaemia; Definition, epidemiology and classification ..... 3
1.2.1. Classification of AML ..... 3
1.2.2. Mutations in AML; prognostic impacts and functional categorization ..... 5
1.2.3. The stem cell theory in AML ..... 5
1.2.4. From CHIP to AML ..... 6
1.2.5. Relapse in AML ..... 8
1.3. Theories explaining LIC survival of chemotherapy ..... 8
1.4. Dormancy in LICs ..... 10
1.5. Dormancy as a defence mechanism against genotoxic insults ..... 11
1.6. Targeting dormant LICs to eradicate AML ..... 12
1.7. Components of the bone marrow ..... 13
1.7.1. Cellular components of the normal bone marrow ..... 14
1.7.2. Additional components of the bone marrow ..... 15
1.8. Dormant HSC and LIC niche ..... 16
1.9. Regulatory mechanisms of dormancy in HSC and LIC ..... 19
1.9.1. Extrinsic regulators of HSCs and LICs dormancy ..... 19
1.9.2. Intrinsic regulators of HSC and LIC dormancy ..... 28
1.10. Stemness markers identifying LICs ..... 30
1.11. Markers for *in vitro* identification of dormant LICs ..... 31
1.12. Molecular signature of dormant HSCs and LICs ..... 33
1.13. Concluding remarks ..... 34
1.14. Aims of the study ..... 35
**CHAPTER TWO MATERIALS AND METHODS** ..... **36**
2.1. AML Cell Lines and Cell Cultures ..... 37
2.2. AML Cell Lines Treatment ..... 38
2.2.1. TGFβ1 treatment ..... 38

2.2.2. Rapamycin treatment .....39
2.2.3. Etoposide treatment (Etoposide-chemosensitivity assay).....39
2.3. Viable Cells Counting .....40
2.3.1. Trypan Blue Exclusion-Haemocytometer Method .....40
2.3.2. FSCs/7AAD-Flowcytometry Method .....40
2.4. Cell lines morphology assessment .....42
2.5. Indirect Immunofluorescence analysis of FOXO3a expression .....42
2.6. Immunohistochemistry analysis of human bone marrow biopsies .....43
2.7. Flowcytometry-based assays .....44
2.7.1. AML cells surface membrane immunophenotyping .....44
2.7.2. Aldehyde Dehydrogenase (ADLH) expression assay .....45
2.7.3. AML cells viability assessment by AnnexinV/PI method .....46
2.7.4. Ki-67 expression assay .....47
2.7.5. Investigating the apoptotic markers (γH2AX, aCASPAS3, and cPARP) .....47
2.7.6. Ribosomal protein S6 (rpS6) expression measurement .....48
2.7.7. PKH26 Labelling assay .....48
2.8. Molecular biology assays .....49
2.8.1. Total RNA extraction .....49
2.8.2. Complementary DNA (cDNA) synthesis .....50
2.8.3. Primers and primers designing .....50
2.8.4. Real-time quantitative polymerase chain reaction (qPCR) assay .....50
2.9. Affymetrix Whole Human Genome Gene Expression Profile (GEP) Assay .51
2.9.1. TF1-a cells treatment protocol for the GEP.....51
2.9.2. Total RNA extraction and assessment of RNA integrity for the GEP ..52
2.9.3. Generating, fragmentation and hybridization of the Sense cDNA on the Array strips .....54
2.9.4. Microarray data (the CEL files) handling and statistical analysis of the differentially expressed genes .....54
2.10. Statistical Analysis.....56
**CHAPTER THREE SELECTING AND INVESTIGATING THE CANDIDATES LEUKAEMIA CELL LINES FOR THE TGFB1-DEPENDENT IN VITRO DORMANCY MODEL ..... 57**
3.1. Background .....58
3.2. Results .....59
3.2.1. AML cell lines Characteristics .....59
3.2.3. TGFβ1 inhibits the AML cells proliferation in a dose-dependent manner .....64

3.2.4. AML cell lines response to culture in serum-free medium .....66
3.2.5. TGFβ1 inhibitory effect was persistent to up to 6 days of continuous treatment .....69
3.2.6. No effect on AML cells viability was observed due to TGFβ1 treatment .....71
3.2.7. The response of the cyclin-dependent kinase inhibitors (CDKI) p21, p27, and p57 to TGFβ1 treatment .....72
3.2.8. TGFβ1-treated AML cells showed features of dormancy .....74
3.2.9. TGFβ1-treatment up-regulates ALDH expression .....78
3.2.10. TGFβ1-treated TF1-a cells showed additional feature of dormancy .81
3.2.11. TGFβ1 treatment up-regulates stemness-related markers in TF1-a cells .....82
3.3. Discussion .....86
**CHAPTER FOUR MTOR PATHWAY INHIBITION AUGMENTS THE TGFB1-DEPENDENT DORMANCY FEATURES IN TF1-A LEUKAEMIA CELLS ..... 92**
4.1. Background .....93
4.2. Results .....95
4.2.1. The mTOR inhibition by Rapamycin augments TF1-a growth inhibition by TGFβ1 without detrimentally affecting cellular viability .....95
4.2.2. Combining mTOR inhibition with TGFβ1 enhances features of dormancy in TF1a cells .....98
4.2.3. TF1-a cells induced to dormancy did not show signs of differentiation .....102
4.3. Discussion .....104
**CHAPTER FIVE MOLECULAR SIGNATURE OF DORMANCY IN THE $CD34^{+}CD38^{-}$ ACUTE MYELOID LEUKAEMIA CELLS TF1-A..... 106**
5.1. Background .....107
5.2. Results .....108
5.2.1. MiniGEP by qPCR for optimizing the time point for the GEP of Affymetrix Microarrays Experiments .....108
5.2.2. Investigating the molecular signature of dormant TF1-a cells using whole human gene expression profiling .....112
5.2.3. Validation of the GEP microarray results using qPCR .....127
5.3. Discussion .....129
5.3.1. MiniGEP of the dormant TF1-a cells .....129
5.3.2. The functional importance of the genes of TF1-a dormancy signature in AML biology .....130
**CHAPTER SIX INVESTIGATION OF OSTEOPONTIN AND ITS RECEPTORS IN AML CELLS ..... 134**
6.1. Background .....135

6.2. Results ..... 137

6.2.1. Investigating the role of osteopontin in the *in vitro* dormancy induction of TF1-a cells ..... 137

6.2.2. Immunocytochemistry study of BM biopsies of AML patients ..... 142

Table 6.2: The clinical characteristics of the 14 BM biopsies of the 7 AML patients. ..... 144

6.3. Discussion ..... 155

6.3.1. comparison between OPN receptors expression on primary AML cells with that on TF1-a cells. ..... 155

6.3.2. Lack of an inhibitory effect for exogenous osteopontin as a cytokine on TF1-a cells proliferation ..... 156

6.3.3. Myeloid Leukaemia cells in the bone marrow biopsies of AML patients were positive for expression of osteopontin and CD44 ..... 157

**CHAPTER SEVEN INVESTIGATION OF $CD34^{+}CD38^{-}$ ACUTE MYELOID LEUKAEMIA TF1-A CELLS SUBJECTED TO PROLONGED SUB-LETHAL GENOTOXIC STRESS ..... 161**

7.1. Background ..... 162

7.2. Results ..... 164

7.2.1. Selection of etoposide treatment dose and duration in TF1-a cells . 164

7.2.2. Validating the genotoxicity in the Etoposide-treated TF1-a cells .... 166

7.2.3. Tracking TF1-a cellular division using PKH26 viability dye ..... 169

7.2.4. Molecular signature of the Etoposide-treated TF1-a cells ..... 171

7.2.5. Molecular features of dormancy in the CD34+CD38- Acute Myeloid Leukaemia TF1-a Cells subjected to prolonged sub-lethal genotoxic stress ..... 178

7.3. Discussion ..... 184

7.3.1. Selecting the etoposide IC20 for modelling sub-lethal genotoxicity in TF1-a cells ..... 184

7.3.2. Molecular signature of TF1-a cells under a prolonged sub-lethal genotoxic stress ..... 184

7.3.3. Induction of dormancy in the CD34+CD38- Acute Myeloid Leukaemia Cells TF1-a subjected to prolonged sub-lethal genotoxic stress ..... 187

**CHAPTER EIGHT GENERAL DISCUSSIONS, CONCLUSIONS AND FUTURE WORK ..... 190**

8.1. Study aims and objectives ..... 191

8.2. Establishing dormancy model in AML by mimicking the LICs niche using TGFβ1+rapamycin *in vitro* treatment of TF1-a AML cell line ..... 192

8.2.1. A comparison of the current study with previous studies investigating dormancy signature ..... 193

8.3. Molecular signature of dormancy in the CD34+ CD38- AML cells TF1-a showed a marked presentation of the adhesion-related genes ..... 196

8.5. Induction of dormancy in the response of AML cells to sub-lethal genotoxic insult ..... 200
8.6. Conclusions ..... 203
8.7. Limitations of the study ..... 204
8.8. Future directions ..... 205
**REFERENCES ..... 206**
**APPENDICES ..... 229**

# LIST OF FIGURES


| Number | Title | Page |
|---|---|---|
| **Figure 1.1** | The hierarchical arrangement of haematopoiesis in normal status and in AML | 7 |
| **Figure 1.2** | Stem cells defence mechanisms in response to various insults and the possible outcomes | 9 |
| **Figure 1.3** | The HSCs niche | 18 |
| **Figure 1.4** | Regulatory mechanisms of dormancy in HSC and LIC | 24 |
| **Figure 1.5** | The mTOR pathway | 27 |
| **Figure 2.1** | The FSCs/7AAD gating strategy used to count the viable cells by flowcytometry | 41 |
| **Figure 2.2** | TF1-a cells treatment protocol for the GEP experiments | 53 |
| **Figure 2.3** | Assay Schematic for generating Sense cDNA | 55 |
| **Figure 3.1** | The Four AML Cell lines Morphology | 60 |
| **Figure 3.2** | Immunophenotyping of the AML cell lines | 63 |
| **Figure 3.3** | The inhibitory effect of TGFβ1 on the cell lines growth | 65 |
| **Figure 3.4** | AML Cell lines survival in Serum-Free Medium Culture | 67 |
| **Figure 3.5** | AML Cell lines viability in Serum-Free Medium Culture | 68 |
| **Figure 3.6** | The inhibitory effect of prolonged TGFβ1 treatment on the cell lines growth | 70 |
| **Figure 3.7** | The viability of Kasumi-3, TF1-a and M0-91 cells after 3 days culture with 4ng/mL of TGFβ1. | 71 |
| **Figure 3.8** | The expression of the cyclin dependant kinase inhibitors p21, p27 and p57 genes in M0-91, TF1-a and Kasumi-3 cells in response to TGFβ1 treatment. | 73 |
| **Figure 3.9** | Ki-67 expression in M0-91, Kasumi-3, and TF1-a cells before and after culture with 4ng/ml of TGFβ1 | 76 |
| **Figure 3.10** | CD71 expression on M0-91, TF1-a and Kasumi-3 cells | 77 |
| **Figure 3.11** | ALDH expression modulation by TGFβ1 treatment in TF1-a, M0-91, and Kasumi-3 cells | 79 |

| | | |
|---|---|---|
| **Figure 3.12** | Total RNA content in TF1-a before (Cycling TF1-a) and after (Dormant TF1-a) 3 days culture with 4ng/ml of TGFβ1 | 81 |
| **Figure 3.13** | CD34 expression modulation on TF1a cells by TGFβ1 treatment | 83 |
| **Figure 3.14** | Immunofluorescence microscopy for the subcellular localization of FOXO3a protein in TF1-a cells | 85 |
| **Figure 4.1** | The inhibitory effect of TGFβ1+Rapamycin combination on the TF1-a cell line growth. | 95 |
| **Figure 4.2** | The expression of the phosphorylated ribosomal protein S6 (rpS6) in TF1-a cells | 96 |
| **Figure 4.3** | TF1-a cells viability after 3 days culture with 4ng/ml of TGFβ1 or 100nM of Rapamycin or both | 97 |
| **Figure 4.4** | The effect of TGFβ1 and Rapamycin treatment on the CD71 expression on TF1-a cells surface membrane | 98 |
| **Figure 4.5** | Ki-67 expression in TF1-a cells induced to dormancy | 100 |
| **Figure 4.6** | Total RNA content in TF1-a cells induced to dormancy. | 101 |
| **Figure 4.7** | TF1-a Cell line Morphology before (Cycling TF1-a) and after (Dormant TF1-a) 3 days culture with 4ng/ml of TGFβ1 or 100nM of rapamycin or Both | 103 |
| **Figure 5.1** | The Expression of the 6 selected genes in TF1-a cells for the miniGEP | 111 |
| **Figure 5.2** | Genes of interest selected in the dormant TF1-a cells | 114 |
| **Figure 5.3** | Analysis of the 240 upregulated genes GEP of TF1-a cells cultured with TGFβ1 and/or Rapamycin. | 119 |
| **Figure 5.4** | The heat maps of the molecular signature of the TF1-a cells induced to dormancy | 120 |
| **Figure 5.5** | The three biologically related groups of genes markedly represented in the dormancy signature of dormant TF1-a cells | 125 |
| **Figure 5.6** | The possible interactions of some of the detected adhesion-related genes products in the TF1-a dormancy signature | 126 |
| **Figure 5.7** | The qPCR validation of the top 7 adhesion-related genes in TF1-a cells | 128 |
| **Figure 6.1** | The expression of OPN receptors on TF1-a cells | 140 |

| | | |
|---|---|---|
| **Figure 6.2** | TF1-a cells proliferation in response to OPN treatment | 140 |
| **Figure 6.3** | TF1-a cell proliferation in response to OPN treatment in fibronectin or hyaluronic acid coated plates | 141 |
| **Figure 6.4** | BM biopsies of AML patient number one stained with H&E | 145 |
| **Figure 6.5** | Immunohistochemistry of OPN Expression in BM biopsies of AML patients | 147 |
| **Figure 6.6** | Immunohistochemistry of OPN Expression in BM biopsies of AML patients | 148 |
| **Figure 6.7** | Immunohistochemistry study of CD44 expression in BM biopsies of AML patients | 150 |
| **Figure 6.8** | KI67 expression scoring of the BM biopsies of the AML patients | 152 |
| **Figure 6.9** | Immunohistochemistry of Ki-67 Expression in BM biopsy of AML patient | 154 |
| **Figure 7.1** | Etoposide treatment optimization for TF1-a cells | 165 |
| **Figure 7.2** | Validation of genotoxicity in etoposide-treated TF1-a cells | 168 |
| **Figure 7.3** | Tracking of TF1-a cell division by PKH26 labelling | 170 |
| **Figure 7.4** | Principal Component Analysis (PCA) of the 15 samples of TF1-a cells | 172 |
| **Figure 7.5** | Molecular signature of TF1-a cells surviving etoposide treatment | 173 |
| **Figure 7.6** | Genes commonly upregulated between the dormancy and genotoxicity signature of TF1-a cells. | 179 |
| **Figure 7.7** | The 31 genes significantly upregulated by at least 1.5 fold change with FDR unadjusted p value in TF1-a under prolonged sub-lethal genotoxic stress with comparison to the degree of upregulation of the same genes in the dormancy signature of TF1-a cells. | 181 |
| **Figure 7.8** | The qPCR validation of the expression of the 4 significantly commonly upregulated genes in the genotoxicity and dormancy signatures of TF1-a cells | 183 |
| **Figure 8.1** | Suggested regulatory mechanisms of dormancy in LIC according to the TF1-a dormancy and genotoxcity models | 199 |

# LIST OF TABLES


| Number | Title | Page |
|---|---|---|
| **Table 1.1** | Classes of AML with recurrent genetic abnormalities according to the WHO classification (2016) | 4 |
| **Table 1.2** | Prognostic impacts and functional categorization of mutations in AML | 5 |
| **Table 2.1** | Information about the panel of human AML cell lines used in this study | 38 |
| **Table 3.1** | Summary of the immunophenotyping of the four human AML cell lines used in this study. | 62 |
| **Table 5.1** | The 240 genes significantly upregulated in dormant TF1-a cells | 115 |
| **Table 5.2** | Significantly enriched biological processes/signalling pathways in the dormancy signature of TF1-a cells cultured with TGFβ1 and rapamycin | 122 |
| **Table 6.1** | Osteopontin-related receptor genes expression in leukaemia patients according to The Cancer Genomic Atlas database. | 138 |
| **Table 6.2** | The clinical characteristics of the 14 BM biopsies of the 7 AML patients. | 144 |
| **Table 6.3** | Comparison between the osteopontin receptors genes expression in leukaemia cells from two sources; the TCGA data base and dormant TF1-a cells. | 156 |
| **Table 7.1** | The 88 significantly up regulated and 25 significantly downregulated genes by at least 1.5 fold in TF1-a cells which survived prolonged sub-lethal etoposide-mediated genotoxic stress | 174 |

# CHAPTER ONE
# INTRODUCTION AND REVIEW OF LITERATURE

## 1.1. Background

Acute myeloid leukaemia (AML) is a heterogeneous malignant neoplasm of the primitive myeloid progenitors. It shows a high rate of relapse despite the initial induction of remission. This is mainly attributed to the incomplete eradication of those leukemic cells capable of re-initiating the disease. Since most chemotherapeutic agents tend to target proliferating cells, dormant leukaemia stem cells (LSCs, also known as leukaemia initiating cells (LICs)) are likely to be spared. Consequently, significant efforts need to be spent to improve strategies and techniques to study dormant LICs in the attempt to achieve deeper understanding and effective targeting of these rare sub-populations of leukaemia cells. This literature review will focus on the current knowledge of the possible mechanisms that regulate dormancy in haematopoietic stem cells (HSCs) and similarly in the LICs. It will also shed light on the recent advances in the understanding of the components of the bone marrow microenvironment that form the HSC and LIC niche. Other issues linked to dormant LICs will also be briefly discussed such as markers of stemness and dormancy and the up-to-date findings in the molecular characterization of dormant AML cells and AML cells surviving genotoxic stress.

## 1.2. Acute Myeloid Leukaemia; Definition, epidemiology and classification

Leukaemia is a term used to describe a large and heterogeneous group of malignancies of the precursors of white blood cells. Based on the cell of origin and the course of the disease, the leukaemias are broadly classified into myeloid, lymphoid or biphenotypic and chronic or acute leukaemias respectively. Acute myeloid leukaemia is one of the most virulent and difficult-to-treat types of human malignancies that results in death within weeks or months if untreated. It is characterized by uncontrolled proliferation of immature malignant myeloid precursors known as 'blast' cells. With time, the blasts accumulate in the bone marrow (BM) and the peripheral blood (PB) at the expense of the normal haematopoietic cells, leading to failure of production of normal white blood cells, red blood cells and platelets. This results in diverse clinical manifestations and serious complications including severe anaemia, infections and bleeding diathesis.

Epidemiologically, AML is considered as a disease of the older population although it might occur in any age group. It has an incidence rate of 2-3/100 000 per year in paediatric age groups which increase to 15/100 000 per year in adults with a peak incidence in the seventh decade (Burnett 2006).

### 1.2.1. Classification of AML

AML is a heterogeneous group of diseases that have been subjected to several classification systems. The two most widely accepted and clinically applied classification systems are the FAB (French-American-British; first established in 1976) and the WHO classification (first published in 2001 and updated in 2016) (Bain 2003, Provan D 2015, Arber, Orazi *et al.* 2016, Dohner, Estey *et al.* 2017). Despite the usefulness of both systems, there are several major differences between them. Firstly, the FAB system requires blast counts of at least 30% of the PB and/or the BM to diagnose AML (Bain 2003) whereas a blast proportion of

20% is enough for AML diagnosis in the WHO system and less than 20% in cases of AML with recurrent genetic abnormalities including t(15;17), t(8;21), inv(16), or t(16;16) (Arber, Orazi *et al.* 2016, Dohner, Estey *et al.* 2017). Secondly, the FAB classification is based solely on the morphological examination of the cytology and cytochemistry of PB and BM smears of AML patients. On the other hand, the WHO classification takes into consideration the underlying cytogenetic and molecular genetic abnormalities in AML cells (table 1.1) which carry a major importance in leukemogenesis of AML (Viny and Levine 2016), affect the choice of treatment and allow prognostic stratification of AML patients (Kansal 2016, Papaemmanuil, Dohner *et al.* 2016). Also, the WHO classification pays consideration to the etiological background and the presence of coexisting myelodysplasia which are both ignored by the FAB system. Therefore, in the WHO classification, groups such as AML with Downs syndrome, AML with dysplasia and therapy-related AML are classified as separate entities.

Despite the importance of the WHO classification, the FAB classification system still being used in many centres worldwide as a preliminary categorization of AML patients pending the results of cytogenetic and molecular genetic testing (Bain 2003) or due to the lack of these technologies in under-resourced laboratories.

**Table 1.1: Classes of AML with recurrent genetic abnormalities according to the WHO classification (2016) (Dohner, Estey et al. 2017).**

| |
|---|
| AML with t(8;21)(q22;q22.1); RUNX1-RUNX1T |
| AML with inv(16)(p13.1q22) or t(16;16)(p13.1;q22); CBFB-MYH11 |
| Acute promyelocytic leukemia with PML-RARA |
| AML with t(9;11)(p21.3;q23.3); MLLT3-KMT2A |
| AML with t(6;9)(p23;q34.1); DEK-NUP214 |
| AML with inv(3)(q21.3q26.2) or t(3;3)(q21.3;q26.2); GATA2,MECOM(EVI1) |
| AML (megakaryoblastic) with t(1;22)(p13.3;q13.3); RBM15-MKL1 |
| Provisional entity: AML with BCR-ABL1 |
| AML with mutated NPM1 |
| AML with biallelic mutations of CEBPA |
| Provisional entity: AML with mutated RUNX1 |

### 1.2.2. Mutations in AML; prognostic impacts and functional categorization

The heterogeneity of AML cells considered an important obstacle facing the treatment of AML. Indeed, despite the advances in the detection of many important mutations in AML, approximately half of AML cases carry no identifiable mutations. Nevertheless, some of these mutations guided the clinicians to stratify AML patients into three prognostic categories. For instance, the two commonest genetic mutations in AML, NPM1 and FLT3-ITD, are known to be associated with favourable and adverse prognosis respectively (Patel, Gonen et al. 2012). Those three categories are significantly different in overall survival. Importantly, these identified mutations in AML are found to alter different biological processes in AML cells including cellular proliferation, differentiation and the self-renewal potential of leukemic stem cells (table 1.2) (Khwaja, Bjorkholm et al. 2016).

**Table 1.2: Prognostic impacts and functional categorization of mutations in AML.**

| Gene | Functional class | Frequency (%)* | Prognostic impact |
|---|---|---|---|
| NPM1 | Not clear | 30 | Favourable |
| FLT3-ITD | Proliferation | 25 | Adverse |
| DNMT3A | Epigenetic modification | 22 | Adverse |
| TET2 | Epigenetic modification and differentiation | 14 | None or adverse |
| NRAS | Proliferation | 12 | None |
| ASXL1 | Epigenetic modification | 10 | Adverse |
| IDH2 | Epigenetic modification | 10 | Higly variable |
| RUNX1 | Transcriptional regulation | 10 | Adverse |
| CEBPA | Differentiation and stem cell self-renewal | 8 | Favourable (biallelic) |
| FLT3-TKD | Proliferation | 7 | unclear |
| IDH1 | Epigenetic modification | 7 | None |
| WT1 | Epigenetic modification and differentiation | 7 | Adverse |
| TP53 | Tumour suppression | 6 | Adverse |
| KIT | Proliferation | 5 | Adverse |
| KRAS | Proliferation | 5 | None |
| GATA2 | Differentiation and stem cell self-renewal | NI** | None or adverse |
| | | | |

* Frequency in adult AML patients. ** No Information available.

### 1.2.3. The stem cell theory in AML

The current knowledge supports the fact that AML blasts are organized in a hierarchical manner similar to their normal haematopoietic cells counterparts. In this arrangement, AML cells divided into daughter blasts cells that constitute the

majority of AML cells in bone marrow and peripheral blood and rare mother cells called the leukemic stem cells (LSCs) or leukaemia initiating cells (LICs) which have the self-renewal potential similar to their normal HSCs counterparts (figure 1.1) (Khwaja, Bjorkholm et al. 2016). Indeed, the available evidence confirm the distinct biological characteristics of the LICs if compared to the bulk of blast cells that makes these rare mother cells insensitive to the current chemotherapeutic agents (discussed in section 1.3). In addition, many studies were targeted to identify and investigate peculiar features of LICs that could help in differentiating them from their normal HSCs counterparts (discussed in section 1.10).

### 1.2.4. From CHIP to AML

In such discussed stem cell model of AML, it is believed that before the development of overt leukaemia, AML can originate from a pre-leukaemic clone which is gradually acquired additional mutations (Sperling, Gibson et al. 2017). Indeed, investigations of human normal haematopoiesis demonstrated that ageing population can carry this clone of HSCs harbouring mutations and producing a clonal haematopoiesis. This pre-leukemic clone has subsequently been termed clonal haematopoiesis of indeterminate potential (CHIP) (Steensma, Bejar et al. 2015). Genomic studies demonstrate that AML mutations including DNMT3A, TET2 and ASXL1 occur within this asymptomatic clonal haematopoiesis and represents an early stage in the evolution of AML. The incidence of this phenomenon is rare in people younger than 40 years old and sharply increase in older age groups reaching approximately 10% and 19% of those older than 70 and 90 years respectively (Jaiswal, Fontanillas et al. 2014).

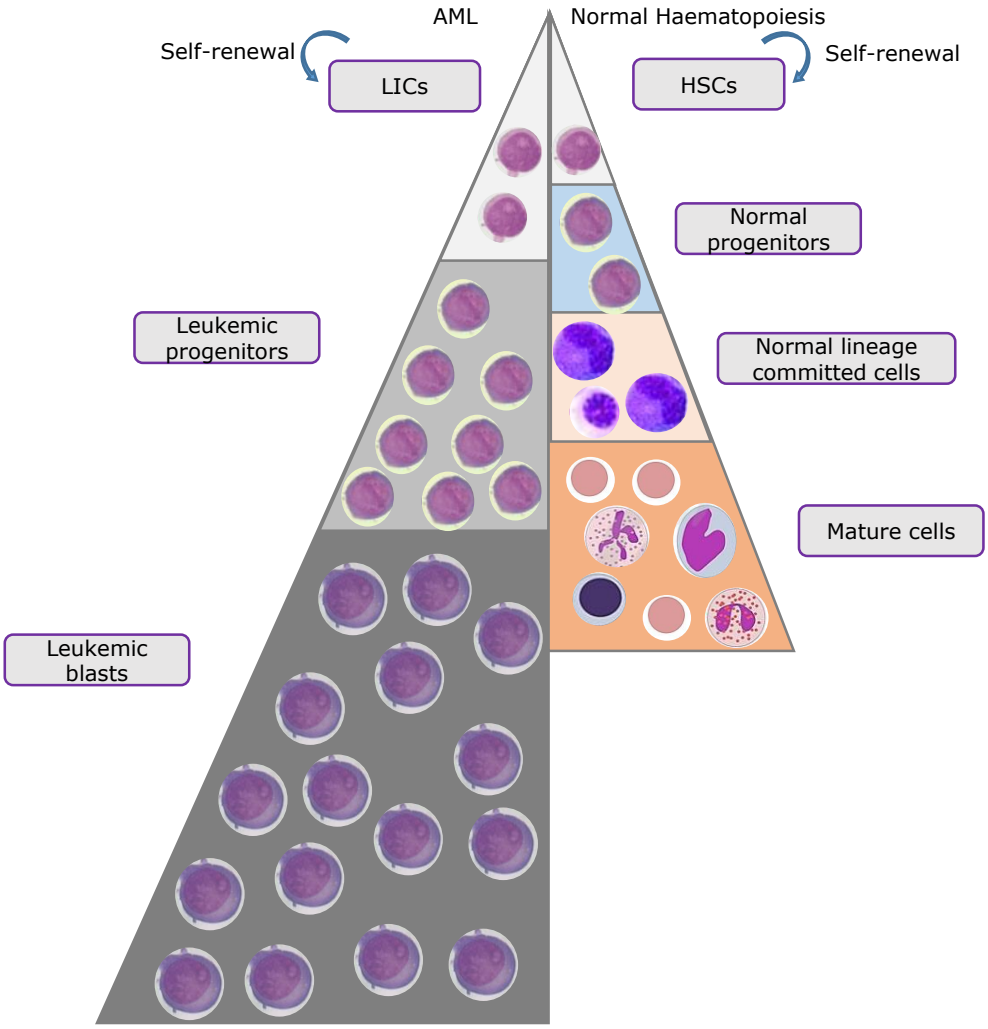



**Figure (1.1): The hierarchical arrangement of haematopoiesis in normal status and in AML.** A simplified schematic diagram illustrates how both normal and AML haematopoiesis originate from a mother cells named HSCs and LICs respectively. These cells are distinguished from the other cells down in the hierarchy by their self-renewal potential that give them the repopulating potential. The figure adapted from (Khwaja, Bjorkholm et al. 2016).

### 1.2.5. Relapse in AML

Despite the advance in the molecular characterization and targeted therapy of AML, this neoplasm remains associated with a high rate of relapse. It has been reported that the rate of the initial induction of remission can reach up to 80% in young adults and 40% of elderly patients with AML (Dombret and Gardin 2016). Nevertheless, the majority of these patients relapsed within 3 years of diagnosis (Dohner, Weisdorf *et al.* 2015). This is mainly attributed to the incomplete eradication of the leukemic cells that are capable of re-initiating the disease. These cells are collectively known as leukemic stem cells (LSCs) or leukaemia initiating cells (LICs).

## 1.3. Theories explaining LIC survival of chemotherapy

There are several mechanisms could explain why this sub-population of leukemic cells survive chemotherapeutic (CT) treatment (figure 1.2). Firstly, accumulating data have demonstrated that leukaemia cells which are responsible for relapse in AML, like HSCs, reside in a low perfusion microenvironment in the endosteal region of the bone marrow relatively far from the regional fenestrated sinusoids, which impedes the delivery of CT drugs (Ishikawa, Yoshida *et al.* 2007, Essers and Trumpp 2010, Winkler, Barbier *et al.* 2010, Cui, Skretting *et al.* 2013, Kunisaki, Bruns *et al.* 2013, Morrison and Scadden 2014, Itkin, Gur-Cohen *et al.* 2016). As a result, the concentrations of the CT reaching the AML cells might not be adequate to eradicate these cells. Secondly, LICs are found to possess intrinsic features such as efficient DNA repair pathways and various transmembrane pumps belong to the ATP-binding cassette (ABC) family; the later protects them by extruding the CT drugs (Lainey, Sebert *et al.* 2012). Thirdly, it has been recently found that HSCs,

and similarly LICs, have an autophagy major stress response pathway that has been identified as a mechanism protecting HSCs from metabolic stress. Autophagy is a self-catabolic process through which cellular components are sequestered into double-membrane vacuoles, known as autophagosomes, and degraded by the

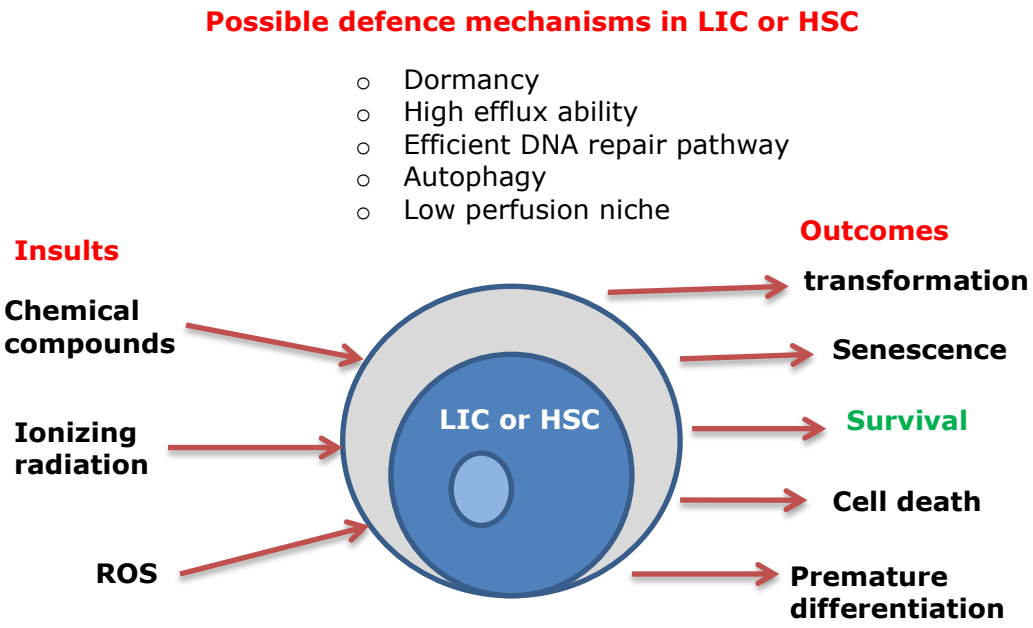



**Figure 1.2:** Stem cells defence mechanisms in response to various insults.

lysosomes. It plays an essential "adaptive" survival role by maintaining nutrient and energy levels during periods of metabolic starvation or stress (Warr, Binnewies *et al.* 2013).

Finally and importantly, the LICs are suggested to enter the cell cycle very infrequently and reside in a prolonged state of very slow cycling or dormancy. This might simulate the reversible state of quiescence that characterizes, and contributes to the maintenance of, the HSCs (Pietras, Warr *et al.* 2011). This dormancy is likely to protect them from the current CT agents which target cycling cells and also may render them insensitive to inhibitors of signalling pathways due to their minimal metabolic activities (Essers and Trumpp 2010).

## 1.4. Dormancy in LICs

In non-transformed cells, quiescence is a distinct biological phenomenon that can be defined as a state of arrest of proliferation during which the cells are found in the G0 phase of the cell cycle (Coller, Sang *et al.* 2006). Unlike the terminally differentiated cells which are found in an irreversible G0 phase, stem cells are suggested to survive in a reversible state of quiescence (dormancy).

In malignant stem cells such as the LICs, dormancy is ill defined and difficult to understand due to several reasons. Firstly, leukaemia cells, including LICs, are found to carry different types of genetic and epigenetic (Conway O'Brien, Prideaux *et al.* 2014) aberrations that could variably alter their proliferation potential and response to inhibitory signals in their niche. Secondly, the phenotype of the leukemic stem cells is heterogeneous and may evolve further following chemotherapy (Ho, LaMere *et al.* 2016) if compared to the well-defined phenotype of their normal counterparts (discussed in section 1.8). Consequently, tracking these cells is a complex process. Finally, kinetics of cell division and rates of self-renewal of LIC are difficult to monitor *in vivo* (Wright 2012, Lutz, Hoang *et al.* 2013, Stiehl, Baran *et al.* 2015) due to the lack of viable cell markers for quiescence. Indeed, the lack of viable markers for identifying the G0 phase of the cell cycle was a major obstacle facing the *in vivo* studying of quiescence in normal and cancer stem cells. Nevertheless, a recent study has been reported which is targeted to track and identify cells in the G0 phase of cellular division. In this study, a viable marker has been developed as a fusion protein consisting of mVenus and a defective mutant of cyclin dependent kinase inhibitor (CDKI), p27 used for *in vivo* detection of murine muscle stem cells in G0 phase (Oki, Nishimura *et al.* 2014). No similar attempts have been reported for *in vivo* identification and tracking of human AML or other hematopoietic cancer stem cells in their G0 phase of cell cycle.

Similarly, occasional *in vitro* approaches to identify viable and dormant cells have been reported that confirm dormancy in the leukemic stem cells. For instance, from the peripheral blood of chronic myeloid leukaemia (CML) patients the ($Lin^{-}CD34^{+}$) stem cells were labelled with carboxy-fluorescein diacetate succinimidyl diester dye. The labelled cells were sorted, thereafter, and were confirmed to be viable in a quiescent state (Graham, Jorgensen *et al.* 2002).

## 1.5. Dormancy as a defence mechanism against genotoxic insults

In pre-treatment conditions, there is growing evidence suggests that dormancy is a feature of stem cells that maintains their function as a mother cell in physiological or cancerous cellular systems. During or post-treatment however, induction of reversible dormancy in these cells is incompletely understood as a possible protective response of these stem cells surviving genotoxic stress against other possible outcomes: senescence, cell death, transformation and premature differentiation (Suda, Takubo *et al.* 2011).

In this context, several studies directed to uncover the response of the normal or tumour genetic machinery to various external genotoxic stresses (Welch and Link 2011). An example of these studies, the one that was carried out by Zhou and colleagues (2006). By using telomerase-expressing human diploid fibroblast cell lines subjected to ionizing radiation (IR) insults, they identified that these cells showed synchronization behind the G1 checkpoint in a G0-like state of dormancy with prominent induction of genes of G0 dormancy like *GAS1* (Zhou, Chou *et al.* 2006).

IR-induced DNA damage was also reported to result in impaired G1 arrest of $p21^{-/-}$ mouse embryo fibroblasts in comparison to $p21^{+/+}$ cells. This evidence highlights the role of the up-regulation of the CDK inhibitor p21 as a checkpoint response to

safeguard genomic integrity by dormancy induction (Brugarolas, Bronson *et al.* 1998). Similarly, Cuadrado *et al.* (2009) reported the role of p27, another CDK inhibitor, in the induction of dormancy in response to DNA damage. In this study, the human lung cancer cell line; A549 was treated with doxorubicin to induce DNA double strand breaks. They concluded that p27 stabilization is required for cell cycle arrest in response to DNA damage (Cuadrado, Gutierrez-Martinez *et al.* 2009). Of note, this evidence supports the hypothesis of the presence of an association between the induction of possible drivers of dormancy and the cellular response to genotoxic insults.

This notion has not been studied in AML cells, but there is evidence to support it in solid malignancies ((Sosa, Bragado *et al.* 2014) and references therein). For example, in ovarian cancer cells, the kinase DYRK1B (dual specificity tyrosinephosphorylation- regulated kinase 1B) was found to have a role in inducing dormancy in cells surviving in sub-optimal conditions by interfering with cyclin D1, CDK4 and p27 functions (Hu, Nakhla *et al.* 2011). Similarly, breast cancer cells were reported to enter a dormancy-like state *in vitro* in response to treatment with farnesyl transferase inhibitors (Chatterjee and van Golen 2011).

The lack of information in AML in regards to the possible dormancy induction post-chemotherapy highlights the need for a thorough investigation to achieve an effective targeting of the residual leukaemia cells and hence preventing relapse.

## 1.6. Targeting dormant LICs to eradicate AML

If the presence of residual dormant LICs is one of the main reasons for AML resistance to chemotherapy, one could postulate a two-step therapy strategy by which the dormant LSCs can be eradicated using an initial dormancy switching-off strategy followed by targeted therapy. This strategy is based on the fact that leukemic haematopoiesis responds to growth factors that are known to regulate proliferation of normal haematopoiesis (Russell 1992, Caceres-Cortes 2013).

Indeed, attempts to implement this strategy have been carried out in *in vivo* experimental systems and in clinical practice. For instance, the growth factor G-CSF has been used in combination with cytarabine-based chemotherapy in an attempt to help in eliminating the residual LSCs in a mouse AML model (Essers and Trumpp 2010) and to increase the sensitivity of leukemic cells to chemotherapy (Lowenberg, van Putten *et al.* 2003) in AML patients. However, more recent evidence based on randomized clinical studies reported that the G-CSF priming of AML patients showed no improvement in the overall survival, event-free survival and relapse rates if compared to patients who did not receive G-CSF (Pabst, Vellenga *et al.* 2012). This might be due to the heterogeneity of AML that can defy single approach treatment strategies. In addition, these results illustrate the need for deeper investigations to characterize the dormant LICs and to understand the complexity of the mechanisms that regulate dormancy in these cells.

These mechanisms are found to be mediated by signals originating from the complex microenvironment surrounding the LICs (Moore and Lemischka 2006). Before discussing these factors, however, it is important to shed light on the bone marrow histology and its different cellular and additional components forming the haematopoietic and leukemic stem cells niches.

## 1.7. Components of the bone marrow

The bone marrow (BM) is the largest organ in the body which occupies, in adults, the cavities inside the proximal ends of the long bones and the axial skeletal bones including the skull, sternum, ribs, vertebrae and the hip bone. Histologically, the bone marrow is not a random mixture of cells, but it is a highly specialized tissue containing haematopoietic and non-haematopoietic cellular components. In addition to cells, the BM includes additional structures such as nerve endings, blood vessels and extracellular matrix that occupy the inter-cellular spaces as well

as the bone tissue which surrounds the bone marrow. Together, these components provide a complex microenvironment supporting haematopoiesis (Calvi and Link 2014) and also leukemogenesis.

### 1.7.1. Cellular components of the normal bone marrow

The process of haematopoiesis (i.e. blood cell production) is the function of the haematopoietic precursor cells of the bone marrow. This functionally related group of cells consists of three main subgroups each possessing a distinct functional and histological distribution within the bone marrow (David Brown 2006). Firstly, the granulopoietic cells are responsible for the production of the granular white blood cells (i.e. neutrophils, eosinophils and basophils). The most immature cells of this group are reported to occupy the paratrabecular area of the bone marrow and the more mature cells extend towards the central regions. Secondly, the erythropoietic series of cells which are responsible for the red blood cells production are found to form islands in the central areas among the bone trabeculae. Finally, the megakaryopoietic cells which are responsible for the production of platelets are demonstrated to be evenly distributed throughout the bone marrow regions.

In addition, there are many non-haematopoietic cells (known as stromal cells) in the bone marrow. Although these numerically constitute a minority, many of them are reported to be part of the HSC and LSC niche and play a key role in dormancy regulation (Anthony and Link 2014). These include, but are not limited to, perivascular and endothelial cells (Ding, Saunders *et al.* 2012), CXCL-12-abundant cells (CAR) (Sugiyama, Kohara *et al.* 2006), mesenchymal stem cells (Mendez-Ferrer, Michurina *et al.* 2010), osteoblasts (Calvi, Adams *et al.* 2003, Zhang, Niu *et al.* 2003, Arai, Hirao *et al.* 2004), nonmyelinated Schwann cells (Yamazaki, Ema *et al.* 2011) and fat cells. Some of these cells show unique localization in the BM. For example, the osteoblasts form a continuous sheet of mono-cellular layer lining

the endosteal region. Whereas, most other non-haematopoietic cells show non-specific distribution throughout different BM regions.

### 1.7.2. Additional components of the bone marrow

The spaces separating the bone marrow cells are filled by the extracellular matrix, blood vessels and nerve endings. Proteins forming the extracellular matrix include collagen, fibronectin, hyaluronan and other proteins secreted by the BM cells such as osteopontin and others. Some of these proteins are found to be concentrated more in certain areas of the BM. For example, osteopontin is found to be more abundantly expressed in the extracellular compartment adjacent to the bone trabeculae compared to other parts of the BM. This is mainly attributed to the presence of cells of the osteoid tissue such as osteoblasts which are reported to produce osteopontin.

As regards the blood vessels of the BM, it has been frequently reported that there are two networks of blood vessels, the sinusoids and the arterioles, which have a distinct distribution within the BM and a distinct influence on the haematopoietic and leukemic cell biology. The arterioles mainly occupy the paratrabecular areas of the BM (i.e. areas near the endosteal region) and the sinusoids are mainly distributed in the central parts among the bone trabeculae.

Histologically, the arterioles' wall is thick and non-permeable. This makes the passage of oxygen and nutrients through the wall to the adjacent cells extremely limited. In contrast, the sinusoids' wall is thin and fenestrated and the blood flows slowly in their lumen. Both these features of the sinusoids facilitate the rapid delivery of oxygen and nutrients to the perisinusoidal cells. Consequently, HSCs and LICs resides near those two different blood vessels networks will adapt to different external signals and might also be subjected, theoretically, to different concentrations of chemotherapeutic agents.

## 1.8. Dormant HSC and LIC niche

The relationship between HSCs and their niche has been widely investigated and has made the basis of understanding the LIC niche. Despite the fact that the LICs harbour genetic mutations that result in increased proliferation and resistance to apoptosis, they retain similar interactions with cells of the BM niche as the HSCs (Riether, Schurch *et al.* 2015). Importantly, these interactions between HSCs and their niche have been found to play a key role in preserving the HSC's self-renewal ability (Anthony and Link 2014) and dormancy (Matsumoto and Nakayama 2013).

Through different approaches involving *in vivo* and *in vitro* systems, many components of the BM were reported to be part of the niche that regulates dormancy in HSC. These include megakaryocytes (Bruns, Lucas *et al.* 2014), vascular endothelial cells (Winkler, Barbier *et al.* 2012), macrophages (Barbier, Winkler *et al.* 2012), osteoblasts (Ishikawa, Yoshida *et al.* 2007) and mesenchymal stem cells (Krause, Scadden *et al.* 2013, Kunisaki, Bruns *et al.* 2013). Among those cells, osteoblasts seem to play a central role in regulating dormancy in HSCs through direct contact (Calvi, Adams *et al.* 2003, Zhang, Niu *et al.* 2003) or through cytokines (Arai, Hirao *et al.* 2004) and extracellular protein secretion (Nilsson, Johnston *et al.* 2005, Stier, Ko *et al.* 2005). Covering all these components is beyond the scope of this section, but one important component of the dormant HSC niche needs to be highlighted, namely particular types of BM blood vessels.

Based on the relation to different types of BM blood vessels, it has been suggested that two anatomically distinct niches exist in the BM; one harbours the potentially cycling HSCs and the other forms the home for the dormant ones (figure 1.3). To illustrate, dormant HSCs are found to be near the arteriolar blood vessels whereas the cycling HSCs reside the peri-sinusoidal compartment. Indeed, such a discovery has changed the previous understanding of two principal biologically distinct BM

sub-compartments from being identified as endosteal and perivascular to become periarteriolar and perisinusoidal (Silberstein and Lin 2013). This reflects the influence of the type and distribution of the BM blood vessels, through forming the basis of the impact of shortage of nutrients, on the behaviour and biology of the different BM cells.

The first evidence that confirmed the relationship between dormant HSCs and arterioles was published by Kunisaki Y. and colleagues (2013). These researchers used an *in vivo* study a in mouse model and a novel approach that combined whole-mount confocal immunofluorescence imaging and computational modelling to analyse the three-dimensional associations among cells and vascular structures in the bone marrow. They were able to identify the specific association of dormant HSCs with small arterioles near the endosteal BM. Importantly, the report demonstrated two distinct peri-vascular mesenchymal stem cell subsets that were found to ensheath the arteriole and the sinusoids. Interestingly, the periarteriolar mesenchymal stem cells were found in a dormant state similar to those HSCs adjacent to the arterioles (Kunisaki, Bruns *et al.* 2013). These findings were supported recently by Itkin T. and colleagues (2016) who reported that arterioles with low permeability maintain HSCs in a low reactive oxygen species (ROS) state. In contrast, the highly permeable sinusoids promote haematopoietic stem and progenitor cell (HSPC) activation (Itkin, Gur-Cohen *et al.* 2016).

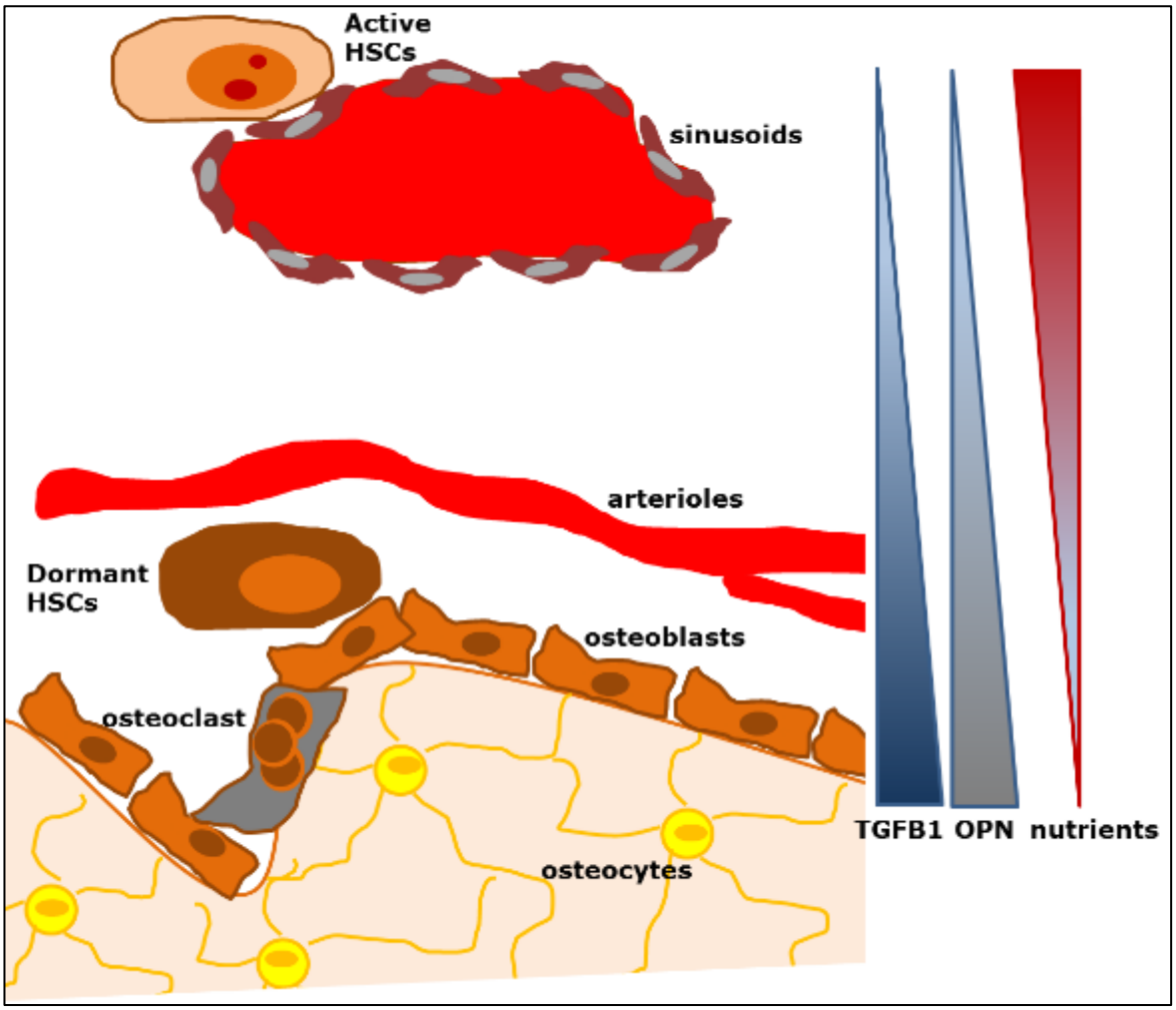



**Figure (1.3): The HSCs niche.** A simplified schematic diagram illustrates the two anatomically distinct niches of the HSCs; the periarteriolar (endosteal) and the perisinusoidal niches. Gradient of the amount of TGFβ1 and osteopontin (OPN) decreases when moving away from the endosteal area whereas the opposite happens regarding the amount of nutrients.

## 1.9. Regulatory mechanisms of dormancy in HSC and LIC

It has been reported that many intrinsic and extrinsic factors cooperate in regulating dormancy in HSCs (Matsumoto and Nakayama 2013). Indeed, a number of external signals originating locally from various components of the HSC niche have been identified, and their role in modulating HSC dormancy is currently well known (Frenette, Pinho *et al.* 2013, Schepers, Campbell *et al.* 2015). For example, Lane *et al.* (2009) listed more than fifteen pathways implicated in the HSC-niche interaction several of which probably play a role in dormancy regulation (Lane, Scadden *et al.* 2009). Among these the roles of transforming growth factor-β1(TGFβ1), osteopontin (OPN), and mTOR pathway inhibition were supported by the findings of many researchers later on (Ichihara, Kaneda *et al.* 2011, Boyerinas, Zafrir *et al.* 2013, Pallis, Burrows *et al.* 2013, Tabe, Shi *et al.* 2013). Interestingly, those intrinsic and extrinsic mechanisms of dormancy regulation are tightly linked (Wilson and Trumpp 2006) as most extrinsic (niche) factors induce dormancy through intracellular molecular pathways. Also, unique responses characterize the HSCs, and similarly LICs, when compared to their differentiated counterparts despite the fact that they are exposed to the same extrinsic dormancy inducers, and this might be explained by unique intrinsic features of these cells.

The following section is a discussion on the most important extrinsic and intrinsic players in HSC dormancy regulation which were subjected to investigation in this study.

### 1.9.1. Extrinsic regulators of HSCs and LICs dormancy

There seem to be many cellular and extracellular components of the BM microenvironment that can play a role in regulating HSC and LSC self-renewal, differentiation and dormancy (Ema and Suda 2012). However, the key extracellular factors and the precise molecular mechanisms underlying HSC hibernation remain largely elusive. It has been suggested that residual tumour

cells (such as those responsible for MRD in AML) might live in a state of dormancy with little metabolic activity and if those residual cancer cells share some of the properties of normal stem cells such as low cycling, sensitivity to inhibitory signals from micro-environment and niche location, they could hibernate and persist for years (Quesnel 2013).

The so-called stromal cells that form the HSC BM niche; including osteoblasts, MSCs, adipocytes, endothelial cells, nonmyelinating Schwann cells (Yamazaki, Ema *et al.* 2011) and others, produce several secretory and membrane-bound proteins (Pietras, Warr *et al.* 2011, Ema and Suda 2012) that cooperate to keep HSCs and LICs in a state of dormancy. These can encompass, but are not limited to, TGFβ1 (Tabe, Shi *et al.* 2013), osteopontin (OPN) (Boyerinas, Zafrir *et al.* 2013), angiopoietin, thrombopoietin, CXCL12 and β-catenin in addition to other extrinsic factors such as hypoxia and shortage of nutrients (figure 1.4). This section will discuss the role of TGFβ1 (Tabe, Shi *et al.* 2013) and OPN (Boyerinas, Zafrir *et al.* 2013) as well as the evidence that support the less perfused niche as key players in maintaining dormancy of the HSCs.

1.9.1.1. Transforming Growth Factor β-1

The Transforming Growth Factor β signalling pathway exerts a pleiotropic effect on different cells and controls a diverse set of cellular processes including inhibition of proliferation (Shi and Massague 2003). TGFβ1 is the prototype member of a structurally related superfamily which also includes TGFβ2, activins and bone morphogenic protein (BMP) (Larsson and Karlsson 2005). It was firstly discovered by De Larco and Todaro in 1978 (Fortunel, Hatzfeld *et al.* 2000). TGFβ1 mediates its action by binding to TGF-type II receptor which then forms a complex with TGF-type I receptor. Subsequently, the activation of this receptor complex phosphorylates receptor-activated Smads (R-Smad2 and R-Smad3) which eventually form a complex with the common mediator Smad4. This complex is

then translocated to the nucleus where it recruits transcriptional cofactors to control the expression of genes, including those involved in cell cycle regulation (Massague 2000, Larsson and Karlsson 2005, Matsumoto and Nakayama 2013).

A large body of evidence supports the role of TGFβ1 in the regulation of haematopoietic stem cell dormancy and inhibition of proliferation (Fortunel, Hatzfeld *et al.* 2000, Morita, Yamamoto *et al.* 2003, Larsson and Karlsson 2005, Ruscetti, Akel *et al.* 2005, Matsumoto and Nakayama 2013).

TGFβ1 is secreted in the bone marrow microenvironment by many stromal cells including megakaryocytes, osteoclasts, nonmyelinated Schwann cells (Blank and Karlsson 2015) and MSCs as paracrine TGFβ1, or by the HSCs and progenitors themselves as a para- and autocrine TGFβ1 (Fortunel, Batard *et al.* 1998). However, its role is thought to vary considerably in relation to the degree of cellular maturation. It has been suggested that TGFβ1 is one of those inhibitors that controls the dormant and undifferentiated HSCs (Fortunel, Batard *et al.* 1998, Scandura, Boccuni *et al.* 2004) while those more committed progenitors are less responsive to its inhibitory effects (Scandura, Boccuni *et al.* 2004).

Although the mechanism by which TGFβ1 mediates its cytostatic effect is not well understood, two possible explanations have been suggested. Firstly, in normal CD34+ HSCs, the cyclin-dependent kinase inhibitor (CDKI) p57 is found to be an early target gene activated by TGFβ1 proved by gene expression profiling (Scandura, Boccuni *et al.* 2004, Yamazaki, Iwama *et al.* 2009). The CDK inhibitor p57, thereafter, acts on inhibiting the cell cycle progression. Other CDKIs such as p21 and p27 are also possible targets for TGFβ1 (reviewed in (Blank and Karlsson 2015)). Secondly, a body of evidence suggests the role of lipid raft clustering (LRC) on the plasma membrane of HSCs in regulating their state of dormancy (Yamazaki, Iwama *et al.* 2006, Yamazaki, Iwama *et al.* 2007). The induced LRC by growth cytokines is essential for HSCs to boost their proliferation signals to the

required level to re-enter the cell cycle. TGFβ1 has been found to suppress the HSCs lipid raft clustering, resulting in survival of HSCs without proliferation (Yamazaki, Iwama *et al.* 2009).

In contrast to the clearer role of TGFβ1 in dormancy regulation of HSCs, its role in LICs is less well investigated. In general, it is frequently claimed that the loss of the inhibitory effect of TGFβ1 on malignant haematopoietic cells is derived from the frequent mutations that interfere with the canonical TGFβ1 signalling pathway (reviewed in(Dong and Blobe 2006)). For example, it has been found that AML cells harbouring mutated onco-protein EVI1 are less responsive to the inhibitory effect of TGFβ1 (Kurokawa, Mitani *et al.* 1998, Jakubowiak, Pouponnot *et al.* 2000). However, this finding could not be replicated in leukaemia cells with stemness features (i.e. the LICs) possibly reflecting a difference in the response of the relatively more differentiated leukaemia cells to the inhibitory effect of TGFβ1 in comparison to the mother LICs similar to that documented in normal cells. A recent finding which supports this possibility describes a key role played by TGFβ1 in maintaining leukaemia stem cells of CML through FOXO3a activation by inducing its nuclear localization (Naka, Hoshii *et al.* 2010) whereas TGFβ1 did not efficiently induce nuclear localization of FOXO3a in non-LICs cells. In this study the LICs also showed a significant decrease in the proliferation marker Ki-67 expression which is a feature of dormancy. Nevertheless, the role of TGFβ1 in regulating AML LICs is not fully understood yet.

1.9.1.2. Osteopontin

Osteopontin (OPN) is an extracellular matrix protein secreted mainly by osteoblastic cells among other BM niche cells. Its role in HSCs and leukemic cell dormancy is incompletely understood and less investigated in comparison to TGFβ1. OPN was first identified by Franzen and Heinegard (1985) as a secretory protein. Its phosphorylated or non-phosphorylated protein forms were reported

to determine its binding to cellular receptors such as CD44 or β1-integrin, or to extracellular matrix proteins, fibronectin or collagen (Haylock and Nilsson 2006). The first evidence supporting the role of OPN in HSC dormancy regulation was published by Nilsson and colleagues in 2005 through analysing *in vivo* and *in-vitro* experiments. These researchers found that besides the role of OPN in attraction, retention and regulation of HSCs within the endosteal niche it also has a direct role in the maintenance of HSC dormancy (Haylock and Nilsson 2006). This role was demonstrated by examining the cell cycle status using bromodeoxyuridine (BrdU) incorporation of HSCs which were isolated from $OPN^{-/-}$ mice. This showed that the cells, in contrast to the wild-type HSC, were in a proliferative state (Nilsson, Johnston *et al.* 2005).

In malignant haematopoietic cells, OPN's role in dormancy regulation was reported in ALL leukemic cells, whereas no evidence has been reported in AML. In ALL, the expression of OPN was found to be higher in areas adjacent to endosteal region of the bone marrow of a mouse model. Additionally, it has been suggested that the leukemic cells themselves were a source of the extracellular OPN. Furthermore, the dormant leukemic cells, but not the proliferating ones, were found to express OPN *in vivo* suggesting the likely role of OPN in dormancy induction of leukemic cells (Boyerinas, Zafrir *et al.* 2013).

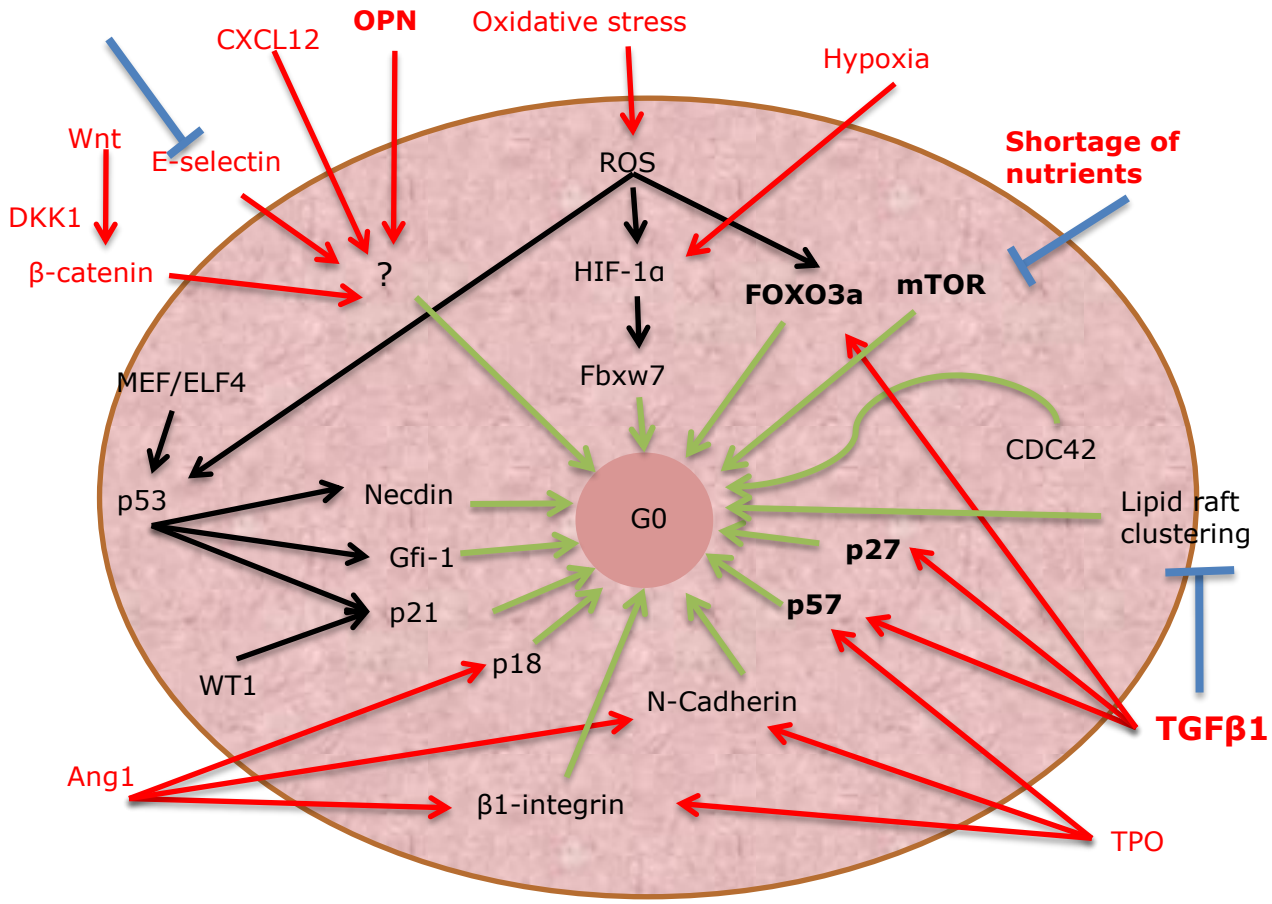



**Figure 1.4: Regulatory mechanisms of dormancy in HSC and LIC**. Data collected from different published papers (see text) to include the frequently reported intrinsic (black) and extrinsic (red) regulatory mediators of dormancy in HSC and LIC. For details of the abbreviations see abbreviation list please. The ones written in bold were covered in the current study to investigate AML cells dormancy.

1.9.1.3. Nutrient-low niche and mTOR pathway inhibition

Accumulating data have demonstrated that leukaemia cells which are responsible for relapsed AML, similar to the HSCs, reside in a low perfusion microenvironment in the peri-arteriolar (endosteal) region of the bone marrow (Ishikawa, Yoshida *et al.* 2007, Winkler, Barbier *et al.* 2010, Kunisaki, Bruns *et al.* 2013, Morrison and Scadden 2014, Itkin, Gur-Cohen *et al.* 2016). This low perfusion is largely associated with the thick-wall arteriole which prevent the free movements of nutrients from its lumen to the adjacent cells. In addition, these less permeable blood vessels have been reported to provide a microenvironment enhancing $ROS^{low}$ HSC which promote their dormancy (Itkin, Gur-Cohen *et al.* 2016). In support of this finding, bone marrow arterioles were found to retain long term and dormant HSC through downregulation of nitric oxide production, promoting adhesion and inhibiting migration (Gur-Cohen, Itkin *et al.* 2015). Finally, the scarcity of nutrients of this limited perfusion niche could contribute to leukaemia cell dormancy and resistance to chemotherapy as they survive in a low metabolic state that protects them from chemotherapeutic agents targeting metabolically active cells (Ishikawa, Yoshida *et al.* 2007).

The mTOR (mammalian target of Rapamycin) pathway is believed to be constitutionally active in cycling cancer cells and is largely regulated by the level of the extracellular nutrients (Zoncu, Efeyan *et al.* 2011). Moreover, it has been reported that mTOR pathway regulates several cellular functions including nutrient uptake (Chen, Liu *et al.* 2008); hence it is regarded as a nutrient sensor pathway in cancer and other cells (Fingar and Blenis 2004, Jewell and Guan 2013, Blagosklonny 2014).

More importantly, mTOR inhibition by rapamycin was used as a strategy for the *in vitro* maintenance of haematopoietic stem cells (Huang, Nguyen-McCarty *et al.* 2012) and, recently, for the *in vitro* induction of stemness characteristics in T-cells (Scholz, Jandus *et al.* 2016). Furthermore, it has been reported that mTOR-inhibited leukaemia cell lines (Pallis, Burrows *et al.* 2013) and prostatic cancer

cells (Kim, Jung *et al.* 2013) by rapamycin showed features of dormancy and resistance to chemotherapy. Finally, a combination of mTOR inhibition with TGFβ1 was reported to potentiate the inhibitory effect of TGFβ1 in transformed cells (Law, Chytil *et al.* 2002). It is worth mentioning here rapamycin act through inhibiting the mTORC1 complex activity of the mTOR pathway and sparing the mTORC2 complex activity (Shimobayashi and Hall 2014). The former is mainly regulating protein synthesis and inhibiting autophagy (Kim, Jung et al. 2015) whereas the lator involved in biological processes essential for cell survival (figure 1.5).

Interestingly, manipulation in the intrinsic pathways regulating dormancy has been exploited as an *ex vivo* approach to maintain HSCs in G0 phase of the cell cycle. This was through induction of dormancy by F-box and WD-40 domain protein 7 (Fbxw7) which has been reported by Iriuchishima and colleagues (2011). Indeed, mTOR was reported as one of the substrates of Fbxw7, besides cyclin E, c-Myc and Notch1, important for G0 state maintenance in HSCs (Mao, Kim *et al.* 2008, Onoyama and Nakayama 2008). Iriuchishima and colleagues used retrovirus transduction to induce Fbxw7α expression in $Lin^-$ $Sca\text{-}1^+$ $c\text{-}Kit^+$ (LSK) murine cells which were cultured on fibronectin-coated plates in serum-free medium. They found that forced Fbxw7α expression represses HSC cell-cycle progression by reducing c-Myc, Notch1, and mTOR proteins (Iriuchishima, Takubo *et al.* 2011) and by up-regulation of p53 which was reported to control the cell cycle entry of murine HSCs (Liu, Elf *et al.* 2009).

Finally, another interesting recent *in vitro* study published by Huang J *et al.* (2012) highlights the possibility of maintenance of human and mouse long-term HSCs (LT-HSCs) by dual inhibition of both glycose synthase kinase 3 (GSK-3) by lithium and mTOR by rapamycin in serum-free culture medium in the absence of feeder cells or cytokines (Huang, Nguyen-McCarty *et al.* 2012). Importantly, they found a significant increase in dormant cells after treatment suggesting dormancy as a cause for HSC maintenance *in vitro* (Masuda, Li *et al.* 2013).

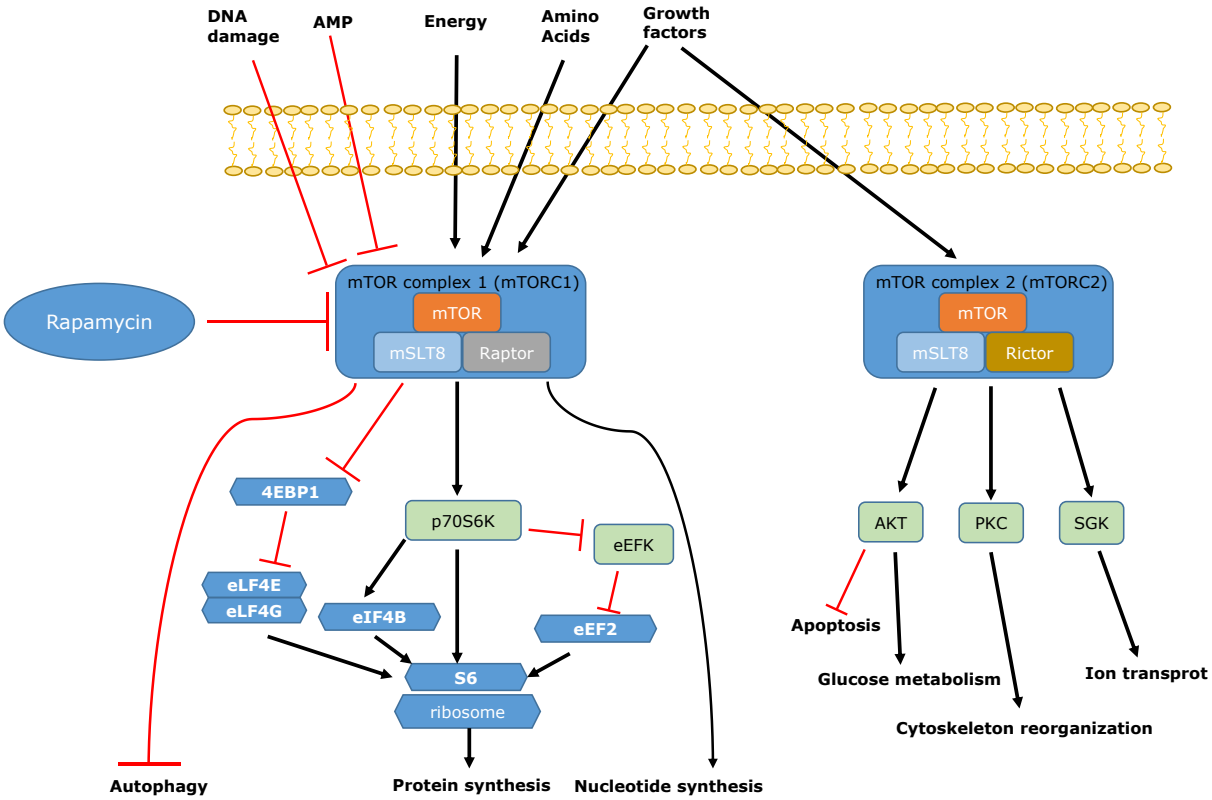



**Figure (1.5): The mechanistic target of rapamycin (mTOR) pathway.** A simplified schematic diagram illustrates the two major effector complexes of the mTOR pathway, the mTOR complex 1 and mTOR complex 2. The figure also shows the extracellular signals that can stimulate these two complexes and the major biological processes that are regulated by them. Rapamycin inhibits the mTORC1 only and leaving the mTORC2 active. (data in this figure were collected from different sources).

### 1.9.2. Intrinsic regulators of HSC and LIC dormancy

Researchers have investigated the role of intracellular molecules or pathways controlling dormancy in HSCs. The proteins regulating the cell cycle, such as p57, were a focus of study in many of these investigations.

1.9.2.1. The cyclin-dependent enzyme inhibitor p57

Among the four main phases of the cell cycle (i.e. gap1 phase, DNA synthesis phase, gap 2 phase and mitosis phase; G1, S, G2, and M respectively), the decision to start cycling is restricted to G1 phase and is dependent on growth factor stimulation. Progression to S phase and proliferation only occurs in the presence of these external stimuli, while in their absence, cells enter a dormant gap 0 (G0) phase. If cells pass the G1/S checkpoint ''restriction point'', they are committed to continuing through an entire cycle and no longer require growth factors to complete division (Coller 2007, Tesio and Trumpp 2011). Furthermore, regulation of cell cycle progression is controlled by many protein kinases and their inhibitors. P57 is one the cyclin-dependent kinase inhibitors that have been identified to possess a key role in regulating HSC dormancy (Matsumoto and Nakayama 2013). In their papers, Matsumoto *et al.* (2011) and Zou *et al.* (2011) highlighted the role of p57 in HSCs dormancy of adult mice (Matsumoto, Takeishi *et al.* 2011, Zou, Yoshihara *et al.* 2011). Further, by gene expression profiling a study of cord blood $CD34^+$ cells and the M091 AML cell line, found p57 to be an early target gene up-regulated by transforming growth factor-β (TGFβ1) that results in the induction of dormancy (Scandura, Boccuni *et al.* 2004). A severe self-renewal capacity defect was observed in HSCs which are deficient in p57 in addition to a significant decrease in the proportion of non-cycling cells (Matsumoto, Takeishi *et al.* 2011, Tesio and Trumpp 2011, Zou, Yoshihara *et al.* 2011). Melania Tesio and Andreas Trumpp (2011) have thoroughly and critically discussed the role of p57 and other related cyclin-dependent kinase inhibitors, p27, and p18, in the initiation and maintenance of dormancy in HSCs (Tesio and

Trumpp 2011). They concluded that, through the effect of TGFβ and thrombopoietin (TPO) that are secreted by the stromal cells of HSC niche, HSC dormancy is induced and maintained by the induction and maintenance of cytoplasmic p57 expression. P57, in turn, forms a complex with Hsc70-cyclinD1 and prevents cyclinD1 from entering the nucleus and activating retinoblastoma (Rb) -mediated G1 phase progression. Interestingly, it has been reported that 30-55% of patients with AML and other haematological malignancies were found to carry a silenced p57 gene in the leukemic clone which may suggest the role of p57 as a tumour suppressor gene in these diseases ((Scandura, Boccuni *et al.* 2004) and references therein) and also may explain the poor response of leukemic cells to the inhibitory signals of TGFβ.

1.9.2.2. FOXO3

Another intracellular protein with a tumour suppression role has been found to be involved in the maintenance of LICs which is the forkhead transcription factor FOXO3. The FoxO subfamily of transcription factors is involved in diverse physiologic processes including cell cycle arrest at G1/S checkpoint (Brunet, Sweeney *et al.* 2004). Upon activation by growth factors, Akt kinase directly phosphorylates FoxO3 resulting in its translocation out of the nucleus and consequent degradation. In the absence of growth factors or in the presence of stressful stimuli, FoxO3 is shifted to the nucleus to upregulate the expression of several target genes that subsequently promote cell-cycle arrest and stress resistance. Importantly, it has been reported that TGFβ–FOXO pathways interaction is implicated in the maintenance of LICs in CML (Naka, Hoshii *et al.* 2010). As shown in mammalian cells, the mechanism might be involved in the role of FOXO3 in organismal longevity and stress resistance through the deacetylase SIRT1 as the latter was found to potentiate FOXO3's effect on cell cycle arrest and DNA repair target genes and also attenuate FOXO3-dependent apoptosis in the presence of stress stimuli (Brunet, Sweeney *et al.* 2004).

## 1.10. Stemness markers identifying LICs

Relapse in AML is believed to be initiated by sub-populations of AML cells that carry the repopulating (i.e. stemness) potential when compared to the other relatively differentiated counterparts. Therefore, it is important to review the current knowledge in regards to the phenotyping of these AML repopulating cells.

Several surface receptors proteins were reported as marker for identifying LICs. While some of these markers are common between normal and leukemic stem cells such as CD34 and ALDH (aldehyde dehydrogenase), other are believed to be exclusively expressed in LICs.To illustrate, by transplantation studies using mouse model (the xenogeneic NOD/SCID system), a specific primary phenotype of CD34+/CD38- was assigned to LICs (Lapidot, Sirard *et al.* 1994, Jordan 2002). Later on, the phenotype of the LICs was reported to include: $CD34^+$, $CD38^-$, $CD71^-$, HLA-$DR^-$, $CD90^-$, $CD117^-$ and $CD123^+$. In contrast to the CD34+/CD38- pattern, the expression of the markers CD90, CD117 and CD123 is believed to be specific for LICs in comparison to the normal HSCs (Lapidot, Sirard *et al.* 1994, Jordan 2002, Ishikawa, Yoshida *et al.* 2007). Similarly, the T cell immunoglobulinmucin-3 **(**TIM-3) has been more recently discovered to mark LICs whereas it is absent on normal HSCs (Kikushige, Shima *et al.* 2010, Kikushige and Akashi 2012). Moreover, $CD96^+$, but not $CD96^-$, AML cells have been found to efficiently reconstitute AML in the immune-deficient mice (Kikushige and Akashi 2012). Finally, it has been reported that CD25 and CD32 were highly expressed in dormant and chemotherapy resistant LICs by an *in vivo* study (Saito, Kitamura *et al.* 2010).

Of note, in contrast to the constant finding of HSCs phenotypes within the $CD34^+$ and $CD38^-$ population, LICs show a substantial variability among different AML patients and LICs have been isolated from $CD34^-$ AML cells (Taussig, Vargaftig *et al.* 2010). In addition, it has been suggested that the HSCs have also been isolated from the $CD34^-$ BM cells of an adult human (Bhatia, Bonnet *et al.* 1998, Zanjani,

Almeida-Porada *et al.* 1998, Gallacher, Murdoch *et al.* 2000). Taking these data into consideration, it might be worth including AML cell lines and primary BM AML cells lacking the CD34 expression in potential *in vitro* models of dormancy, as this will allow broader comparison among diverse cellular responses to external dormancy inducers.

Finaly, investigations, also, focused on biochemical markers of stemness such as ALDH in AML. ALDH is a cytoplasmic enzyme involved in various biological functions including the metabolism of retinoic acid and the detoxification of alkylating drugs (Tomita, Tanaka et al. 2016). Both haematopoietic and AML stem cells were enriched among ALDH high subpopulation of cells. Indeed, $ALDH^{high}$ AML cases were reported to be show an adverse prognosis. Interestingly, AML cases with numerous $ALDH^{+}$ leukemic cells were more ARA-C resistant and dormant than $ALDH^{-}$ cells. This ha been concluded from investigating BM aspiration samples of AML patients before and after induction chemotherapy which confirmed that $CD34^{+}$ $CD38^{-}$ $ALDH^{-}$ cells were more effectively eliminated by chemotherapy than the $CD34^{+}$ $CD38^{-}$ $ALDH^{+}$ cells suggesting the correlation between chemoresistance and high ALDH activity *in vivo* (Hoang, Buss et al. 2015).

## 1.11. Markers for *in vitro* identification of dormant LICs

Despite the absence of a marker specific for dormant cells, researchers have sought to identify G0 cells among cells in a different proliferative state through several approaches. All these strategies are based mainly on the fact that dormant cells lack expression of markers of proliferation. As a result, biomarkers and stains, alone or in combinations, were adopted for this purpose for example transferrin receptor (CD71), nuclear protein Ki-67, the nucleic acid stain Hoechst 33342 and the measurement of the RNA contents using RNA-specific stain Pyronin Y or the nanodrop. However, each single marker has its own pros and cons that necessitate a careful selection to suit the system used.

The expression of Ki-67 is strictly associated with cell proliferation (Gerdes, Lemke *et al.* 1984). It is present during all active phases of the cell cycle (G1, S, G2, and M), but is absent from dormant cells (G0), making it an excellent marker for G0 cell identification (Scholzen and Gerdes 2000). However, detection of Ki-67 is not possible in viable cells as it requires fixation and permeabilization of cells that then render further functional assays impossible. On the other hand, all other mentioned markers can be used at certain concentrations without affecting cell viability.

The absence of CD71 expression has been suggested to characterize the dormant HSCs while the active proliferating counterparts are $CD71^+$ (Blair, Hogge *et al.* 1998). Further, in AML patients it has been found that CD71 expression is related to proliferative capacity and is expressed by the leukemic progenitor cell fraction (Kozlowski, Reilly *et al.* 1988). Whilst detection of the surface marker CD71 is easy in the laboratory, a problem is that CD71 is found to be highly expressed in erythroid progenitors and erythroleukemic cells regardless their maturation status (Dong, Wilkes *et al.* 2011) and this might render the interpretation of CD71 expression on these cells more complicated.

Finally, a combination of DNA and RNA dyes has been used as an approach to identify and isolate G0 cells (Gothot, Pyatt *et al.* 1997, Ladd, Pyatt *et al.* 1997, Holyoake, Jiang *et al.* 1999). Indeed, based on DNA content alone G0 cells cannot be discriminated from cells in the proliferative G1 phase, as DNA content remains constant until S-phase entry. In contrast, by combining measuring RNA content in addition to DNA content, cells can be assigned to G0 (Darzynkiewicz, Traganos *et al.* 1980, Schmid 2007). Several DNA dyes have been used such as the supravital dye Hoechst 33342. However, the limitation for the use of this dye is that it requires a flow cytometry instrument with ultraviolet dye for analysis which is a feature not present on all types of flowcytometers. Thus, researchers have used a

different DNA dye known as 7-aminoactinomycin D (7AAD) in combination with Pyronin Y (Schmid 2007) or in combination with the nuclear marker Ki-67 (Holyoake, Jiang *et al.* 1999) to identify dormant cells.

## 1.12. Molecular signature of dormant HSCs and LICs

Much of the current knowledge, including breakthrough discoveries in the field of haematological malignancies, came from studying the molecular signatures of cancer cells with the help of whole-exome or whole-genome gene expression profiling (GEP) (Godley, Cunningham *et al.* 2011) which has become indispensable for basic biological research. Many studies used GEP were directed to uncover the response of the genetic machinery controlling cellular proliferation and dormancy to various external signals (Coller, Sang *et al.* 2006).

In the field of haematopoietic cells these efforts were mostly applied to investigation of the dormancy signature of HSCs, whereas negligible data is available on the dormancy signature of AML LICs. Venezia *et al.* (2004) examined the gene expression profile in the HSCs of adult mice after inducing proliferation and return to dormancy in an *in vivo* study (Venezia, Merchant *et al.* 2004). They reported that in order to reset dormancy, the HSCs expressed a high level of the anti-proliferative genes such as BTG1 and p21, and genes related to JAK/STAT signal transduction pathway. Moreover, Forsberg EC *et al.* (2010) studied and compared the molecular signature of dormant bone marrow HSCs, non-self-renewing multipotent progenitor cells, G-CSF-treated HSC to stimulate their exit from the bone marrow, and leukemic stem cells in a chronic myeloid leukaemia mouse model (Forsberg, Passegue *et al.* 2010). They demonstrated a subset of molecules that are downregulated in all three circumstances which seem to be particularly important for the maintenance and function of dormant HSCs. In support of this and by also using a mouse model, it has been reported that long-term HSC function in reconstituting of haematopoiesis is critically based on their

state of dormancy which is tightly regulated by several cell cycle regulator genes such as p18, p27, and p57 (Passegue, Wagers *et al.* 2005).

The scarcity of knowledge about the molecular feature of dormancy in LICs might be due to the difficulty in isolating these cells from clinical samples due to their rarity and lack of specific dormancy markers. Therefore, all attempts to characterize these sub-populations of leukaemia cells which are responsible for relapse will help to pave the way towards the ultimate goal of eradicating leukaemia.

## 1.13. Concluding remarks

Dormancy is an important phenomenon characterizing those leukemic cells capable of re-initiating the disease after remission induction. This phenomenon both maintains stemness characteristics of these cells and protects them from chemotherapeutic agents. In addition, dormancy, *per se*, could be a protective response of leukaemia cells surviving sub-lethal genotoxicity. Consequently, intensive research is required to be directed to study the functional and genetic signature of dormant LICs, under niche-induced or genotoxicity-induced external signals, that will help to develop a targeted therapy to eradicate AML cells.

## 1.14. Aims of the study

1. To establish an *in vitro* culture system that mimics features of the LIC niche to model dormancy in AML by primarily using TGFβ1 with or without the mTOR pathway inhibitor, rapamycin to treat a $CD34^+$ AML cell line.
2. To characterize the dormant AML cells using whole-human genome gene expression profiling to study the molecular signature of AML cells induced to dormancy.
3. To model and molecularly characterize AML cells surviving prolonged sub-lethal genotoxic stress and compare their molecular signature with that of the dormant counterparts.

# CHAPTER TWO
# MATERIALS AND METHODS

## 2.1. AML Cell Lines and Cell Cultures

Four growth factor-independent human acute myeloid leukaemia-derived cell lines were used in this study; Kasumi-3, TF1-a, KG-1a, and M0-91 cell lines (table 2.1). Kasumi-3 and KG-1a were maintained in serum-containing medium (SCM) consisting of RPMI-1640 (R0883-500ML; Sigma) with 20% foetal calf serum (FCS: 02-00-850; First Link, Birmingham, UK), 2mM L-glutamine (G7513, Sigma), 100 U/mL penicillin, and 10 µg/mL streptomycin. TF1-a and M0-91 cells were maintained as above but with 10% FCS. All cultures were maintained at ordinary culture atmosphere (37°C, 5% CO2) in an ordinary incubator (Thermo Electron Corporation, model 3141). All experiments were carried out with cells in log phase between 5-30 passage numbers. For the serum-free culture medium (SFM) experiments the studied AML cell lines were cultured in StemSpan SFEM II (09655) complete SFM which was purchased from stem cell technology.

Kasumi-3 has been established from the bone marrow of a 57-year-old Japanese man with minimally differentiated AML (AML-M0). TF1-a is a subclone of the AML cell line TF1 which has been established from a patient with erythroleukemia. Similarly, KG-1a is a subclone of the AML cell line KG-1 which was established from the bone marrow of a 59-year-old man with erythroleukemia. Established from a Japanese patient with undifferentiated AML (AML-M0) (Okabe, Kunieda *et al.* 1995).

Kasumi-3 was purchased from The American Collection of Animal Cell Culture (USA). Both TF1-a and KG-1a cell lines were purched from The European Collection of Animal Cell Culture (Salisbury, UK) whereas M0-91 was A kind gift from Dr. Joseph M. Scandura (Sloan-Kettering Institute, USA).

**Table 2.1: Information about the panel of human AML cell lines used in this study.**

| Name | Doubling time | Immunophenotyping | Specific Mutation | P53 status | FLT3 | MDR[#] |
|---|---|---|---|---|---|---|
| **Kasumi-3** | 5-6 days | $CD34^+$ $CD38^+$ $CD33^+$ $CD13^+$ | EVI1 | mutant | NI[*] | +ve |
| **TF1-a** | 24 hours | $CD34^+$ $CD38^-$ $CD33^+$ $CD13^+$ | NI | wild+mutant | No | +ve |
| **KG-1a** | 24 hours | $CD34^+$ $CD38^-$ $CD33^+$ $CD13^+$ | NI | mutant | NI | +ve |
| **M0-91** | 18 hours | $CD34^-$ $CD38^+$ $CD33^+$ | NI | wild | NI | -ve |

*NI: no information available. #MDR: multi drug resistance protein expreesion.

All cell lines were continuously authenticated toward the final passage of each newly thawed patch by genetic fingerprinting using short tandem repeat (STR)(Powerplex 16,Promega) and by a panel of monoclonal antibodies to validate the cell lines. In addition, mycoplasma contamination was excluded by regular testing for mycoplasma using the mycoalert detection kit (Lonza, Rockland, USA).

## 2.2. AML Cell Lines Treatment

### 2.2.1. TGFβ1 treatment

Recombinant human TGFβ1 cytokine was purchased from Peprotech (CAT No. 100-21). For the dose response assays, an escalating dose of TGFβ1 in final concentrations of 0.25, 0.5, 1, 2 and 4 ng/mL was added to cells seeded at a concentration of $2x10^5$cells/ml in 96 or 48 flat-bottomed well plates. Untreated cells from the same cell line were cultured in the same plate as controls by adding the same volume of complete medium (CM; the vehicle of TGFβ1) to the cell culture. Each condition was in triplicate. The TGFβ1-treated and untreated cells were then incubated for the indicated time for each experiment. At the end of the incubation period, the viable cells were counted by the trypan blue exclusion method and/or FSCs/7AAD flowcytometry method as described below. A final concentration of 4 ng/mL of TGFβ1 was selected to treat the cells for the rest of experiments. For the 6 days of incubation assays, two doses of 4 ng/mL of TGFβ1 were added at day0 and day3 of incubation. For the gene expression profiling

(GEP) experiments, CM and TGFβ1 were added to cells seeded at a concentration of $2x10^5$cells/ml in 10ml flasks on a daily basis, throughout the 3 days of incubation, to avoid cellular confluence.

### 2.2.2. Rapamycin treatment

The final dose of the mTOR pathway inhibitor, rapamycin (LC labs), was selected to be 100nM based on previous optimization steps carried out and published from our lab (Pallis, Burrows *et al.* 2013). The rapamycin effect was validated by measuring the phosphorylated ribosomal S6 (prS6) expression (an mTOR downstream effector) by flowcytometry (chapter four). Untreated and DMSO (the vector of rapamycin)-treated cells were used as controls for rapamycin treatment during the validation experiments (chapter four). Based on how many cells were required, 96 or 48 flat-bottomed wells plates or 10 ml flasks were used for cells cultured with rapamycin.

### 2.2.3. Etoposide treatment (Etoposide-chemosensitivity assay)

Etoposide (Tocris biosciences Cat No. 1226) was selected to the in-vitro modelling of sub-lethal genotoxicity in AML cells. For this purpose, IC20 was selected as the target Etoposide concentration to treat TF1-a cells in suspension culture medium. Therefore, for dose response assays, an escalating dose of Etoposide in final concentrations of 31.25, 62.5, 125, 250, 500, 2000, and 8000 nM was added to cells seeded at a concentration of $2x10^5$cells/ml in 96 flat-bottomed wells plates. Untreated and DMSO-treated cells from the same cell line were cultured in the same plate as controls by adding the same volume of the CM or DMSO (the vector of Etoposide) to the cells. Each condition was in triplicate. The TGFβ1-treated and untreated cells were then incubated for 72 hours before counting the viable cells by the trypan blue exclusion and/or FSCs/7AAD flowcytometry methods as described below. Final concentrations of 205 nM and 430 nM of Etoposide were selected as IC20 and IC50 respectively for the GEP experiments (chapter seven).

For the 6 days of Etoposide treatment assays, at Day3, the Etoposide-treated cells sub-cultured into the starting concentration of $2x10^5$cells/ml by centrifuging them at 200g in room temperature in a sterile universal tube and then resuspending the cells in Etoposide-containing CM to ensure continuous Etoposide treatment. For the gene expression profiling (GEP) experiments, Etoposide-containing CM was added to cells seeded at a concentration of $2x10^5$cells/ml in 10ml flasks on a daily basis, throughout the 6 days of incubation, to avoid cellular confluence.

## 2.3. Viable Cells Counting

### 2.3.1. Trypan Blue Exclusion-Haemocytometer Method

This method was used as the standard method for counting viable cells in the suspension medium. After thorough mixing, 100µl of cells in suspension medium were mixed with the same volume of Trypan blue dye (Sigma) in 0.6ml Eppendorf tube. Then, 100µl of the cells-dye mixture was gently dispensed to fill the potential space beneath the cover slide on the haemocytometer. After waiting for 30-60 seconds, the haemocytometer was examined by inverted light microscope to count the viable cells (the transparent ones which exclude the dye) from the dead cells (the blue ones which uptake the dye). Cells in two large opposite squares were counted and the result was multiplied by $10^4$ to determine the viable cell count in cells/ml of culture medium.

### 2.3.2. FSCs/7AAD-Flowcytometry Method

The fixed CD45-stained cells/ 7-amino actinomycin-D (FSCs/7AAD) method was adapted from Pallis and colleagues (1999) (Pallis, Syan *et al.* 1999). It was used as the method of choice for counting viable cells in experiments with a considerably large number of conditions where the manual standard Trypan blue method was not reproducible.

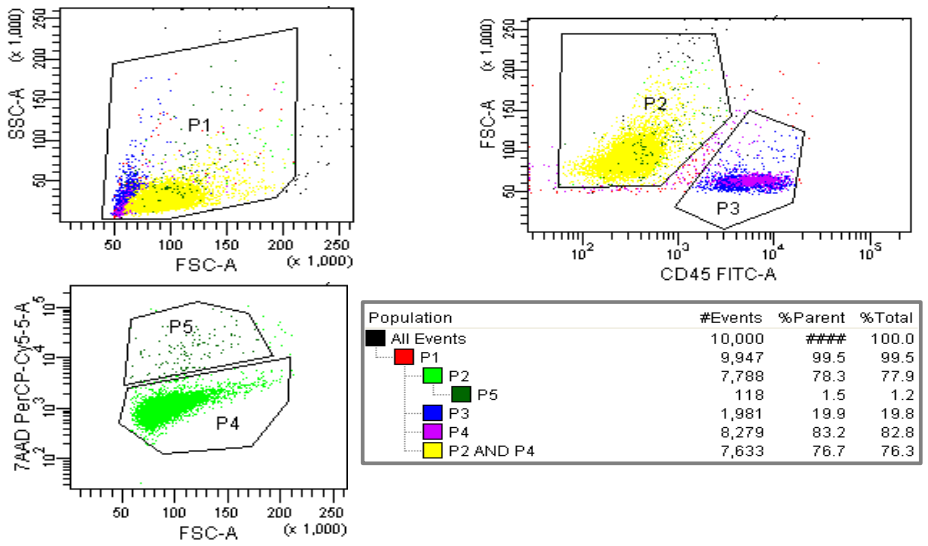



**Figure 2.1: The FSCs/7AAD gating strategy used to count the viable cells by flowcytometry.** P1 was gated to select all events and excluding cellular debris. P2 was gated to select all cells of interest ($CD45^-$). P3 was gated to select FSCs only ($CD45^+$). P4 was gated to select viable cells only (7AAD low). P5 was gated to select dead cells (7AAD high).

The mononuclear cells surplus from the stem cell harvest of the healthy donors was used to prepare the FSCs. Simply, these cells, which consist mainly of lymphocytes with variable proportions of monocytes, were suspended in 200 µl of phosphate buffer saline (PBS) (BR0014G; Dulbecco A) containing 1% BSA and 0.1% sodium azide (PBSAA buffer) and stained with mouse anti-human CD45-FITC monoclonal antibody (BD Biosciences) for 20 min in a dark place at room temperature. Following incubation, the cells washed twice in PBSAA and fixed by resuspending them in 2 ml of freshly prepared 2% paraformaldehyde solution (P/0840/53; Fisher Scientific). FSCs concentration then counted using haemocytometer and stored at $4^0$C until needed for up to 1 year with no significant deterioration.

Viable cell counting was carried out by harvesting a specific volume of cells (50-80µl for instance) in suspension medium from each well of the wells plate, after thorough mixing, into a pre-labelled flowcytometry tube. Then, 7AAD in a final concentration of 12 µg/ml was added to the cells and incubated for 20 min in a

dark place at room temperature. A volume of FSCs, same as the test cells volume, was added into each flowcytometry tube. The tubes were, then, kept on ice until flowcytometric analysis. Five gates were created to differentiate the viable cells from the dead cells, FSCS, and the cellular debris (figure 2.1). The concentration of viable cells (N) was calculated from the following equations:

$$N = Cf\ x\ \left(\frac{\%\ of\ P2\ AND\ P4}{\%\ of\ P3}\right); Cf = FSCs\ count\ x\ \left(\frac{FSCs\ volume}{Test\ Cells\ volume}\right)$$

## 2.4. Cell lines morphology assessment

The morphology of Kasumi-3, TF1-a & M0-91 cell lines was examined, at different points in this study, using Wright-Giemsa (WG16-500ML Sigma) stained smears. The cell lines smears were prepared by centrifugation of cells in suspension medium followed by removing most of the supernatant leaving the cells suspended in a high concentration (about $1X10^6$cells/ml). A small drop of the concentrated cells in suspension was put on one end of the slide and spread using the edge of a spreader slide. After fixation by complete rapid air drying, the smears were stained by the ordinary staining method according to the manufacturer recommendations and they were examined and pictured using the light microscope (Carl Zeiss).

## 2.5. Indirect Immunofluorescence analysis of FOXO3a expression

The Sub-cellular localization of FOXO3a was investigated by indirect immunofluorescence technique as recommended by the antibody manufacturer and as published previously (Naka, Hoshii *et al.* 2010, Thepot, Lainey *et al.* 2011). In brief, un-manipulated and TGFβ1-treated TF1-a cells were harvested and allowed to adhere on Poly-D-Lysine (PDL, p6407 Sigma)-coated 16mm glass round coverslips (PDL was diluted into a concentration of 10μg/ml in sterile DW and allowed to coat the coverslips for 2-4hours at room temperature before twice

washing with DW and then allowed to completely dry in a sterilized environment). The adherent cells then subjected to fixation with 4% paraformaldehyde for 15 min at 37 °C followed by permeabilization and blocking for 1 hour in blocking buffer (5% normal goat serum (NGS) + 2% BSA + 0.2% Triton X-100 in PBS). For immune-staining, the permeabilized cells were incubated with the rabbit anti-FOXO3a (75D8; Cell Signalling) antibody (1:400) at 4 °C overnight. The primary antibody was visualized by incubating the cells with FITC-conjugated goat anti-rabbit IgG (F0382 Sigma) antibody (1:400). Nuclei were stained and slides were mounted with the DAPI-containing mounting medium (Vectashield-H-1200; Vector Laboratories). Images were acquired using Olympus fluorescent microscope and analysed by ImageJ software.

## 2.6. Immunohistochemistry analysis of human bone marrow biopsies

The expressions of Osteopontin (OPN), CD44, and Ki-67 in human bone marrow (BM) were investigated by immunohistochemistry (IHC) analysis of formalin-fixed paraffin-embedded (FFPE) BM biopsies sections using mouse anti-human monoclonal anti-OPN AB (ab166709; abcam), rabbit anti-human polyclonal anti-CD44 AB (ab97478; abcam), and mouse anti-human monoclonal anti-Ki-67 AB (ab16667; abcam) at concentrations of 1:250, 1:400, and 1:50 respectively. The BM biopsies were obtained following approval from Nottingham Research Committee 1 (reference 06/Q2403/16) and from the Nottingham Health Science Biobank (NHSB) review board. The BM biopsies were sectioned (5μm thickness) and prepared by the NHSB team according to their standard protocol. The steps of IHC procedure were detailed in appendix A1. In brief, the BM sections slides were heated on a hot plate before tissue dewaxing and rehydration steps. Antigen retrieval was done using a hot water bath (95$^{o}$C for 20 min) with the slides embedded in acidic Citrate buffer solution (pH 6.0). Endogenous peroxidase was

blocked for 5 min at room temperature using 0.3% hydrogen peroxidase blocking reagent (ab94666; abcam). The primary antibodies (diluted in blocking antibody dilution buffer) were incubated overnight at 4$^{o}$C. The detection system X-Cell Plus Universal Polymer HRP (MP-XCP-U25; Menarini Diagnostics) and the chromogen DAB (ab94665; abcam) were used to visualize the staining. The stained sections were counter-stained with Mayer's haematoxylin (LAMB/170-D; Fisher Scientific), dehydrated, and mounted with DPX, thereafter; to be examined and pictured using Zeiss light microscopy system.

The Ki-67 scoring index were performed according to previously published methodology with some modification (Klapper, Hoster et al. 2009, Polley, Leung et al. 2015). In brief, all biopsies were scored using digital images taken from at lease three pictures representing each area of interest using oil immersion lense with 1000X magnification. Image J software was used for the process of digital scoring. All leukaemia cells with positive brown nuclear staining (DAB stain) were considered positive for Ki-67 expression regardless the intensity of staining. The measurement of Ki-67 index is based on manually counting and classifying at least 500 malignant cells into Ki-67 positive or negative cells to present the index as a percentage of Ki-67 positive cells. The process of leukaemia cells morphology assessement and Ki-67 positive cells identification were totally dependent on the experience of the researcher in haematopathology.

## 2.7. Flowcytometry-based assays

All flowcytometric analyses were carried out using the FACS Canto II (BD Biosciences) instrument with Diva software. Automated compensation calculations were made from single antibody-labelled tubes whenever required.

### 2.7.1. AML cells surface membrane immunophenotyping

Surface markers immunophenotyping was carried out using fluorescein-conjugated anti-human monoclonal antibody (mAB) to CD34, CD38, and CD117

(BD Biosciences). Background fluorescence was assessed using isotype-matched fluorescein-conjugated mAB. The proportion of cells that were positive for a particular marker was used as a measure of expression. The proliferation marker transferrin receptor (CD71) assessment was carried out by using allophycocyanin (APC)-conjugated mAB against CD71. The relative fluorescence unit (RFU) was used to compare the CD71 expression between untreated and TGFβ1-treated cells. The RFU was calculated from the following equation:

$$RFU = \frac{CD71\ mean\ flourscence}{Isotype\ control\ mean\ flourescence}$$

### 2.7.2. Aldehyde Dehydrogenase (ADLH) expression assay

The ALDEFLUOR™ reagent kit (Stem Cell Technology CAT No. 01700) was used to measure the intracellular activity of the enzyme ALDH in the viable AML cells according to the manufacturer instructions. The reagent is supplied in the form of Bodipy-aminoacetaldehyde diethyl acetal (BAAA-DA) which is converted to Bodipy-aminoacetaldehyde (BAAA) by exposure to hydrochloric acid (HCL). BAAA, a fluorescent substrate for ALDH, is uncharged and can diffuse across the cell membrane of intact viable cells readily and is converted into fluorescent negatively charged BAA which can be detected by flowcytometry. As a negative control, an identical concentration of the same tested cells was analysed under identical conditions but in the presence of the specific ALDH inhibitor diethylaminobenzaldehyde (DEAB). Briefly, 0.5 ml of cells at a concentration of $2.5X10^5$cells/ml (suspended in ALDEFLUOR Assay Buffer) were added into two 1.5ml Eppendorf tubes; test tube and control tube (contains 5µl DEAB reagent). 5µl of activated ALDEFLUOR reagent was added at the same time to both tubes and mixed by repeated pipetting. Both tubes were incubated for 45 min at room temperature in the dark. The tubes were pelleted, the supernatant was removed, and cells were resuspended in 250µl ALDEFLUOR Assay Buffer. The tubes were kept on ice until flowcytometry. The proportion of cells that were ALDH positive

(in comparison to DEAB-control expression) was used as a measure of the baseline ALDH activity, whereas, the relative fluorescence unit (RFU) was used to compare the ALDH activity between untreated and TGFβ1-treated cells. The RFU was calculated from the following equation:

$$RFU = \frac{ALDH\ mean\ flourscence}{DEAB\ control\ mean\ flourescence}$$

### 2.7.3. AML cells viability assessment by AnnexinV/PI method

The viability of the tested AML cell lines in response to different types of treatments was assessed by flowcytometry using Annexin V and propidium iodide (PI) labelling (Trevigen Annexin V kit, Cat No. 4830-250-K) as described in the manufacturer's instructions. The principle of this assay is that Annexin V-FITC conjugate helps in the accurate and precise quantification of early and late apoptotic cells through its binding to the cell membrane phosphatidylserine which flipped into the outer surface during apoptosis. The presence of PI in the kit adds an additional benefit in detecting late apoptotic and dead cells that lost membrane integrity. The assay procedure, in brief, consisted of pelleting a similar number of cells (ex. $10^5$-$10^6$) from each condition need in a labelled flowcytometry tube and washed once with iced PBS then resuspended in 100µl of Annexin V-FITC/PI incubation reagent. Then, the tubes were incubated at room temperature in the dark for 15 min before adding 200µl of 1X binding buffer for all tubes which then kept in ice until flowcytometry within 1 hour. Flowcytometry compensation was done for this experiment using unstained, FITC-stained (Annexin V), and PE-stained (PI) cells. Early apoptotic cells were identified when they showed positive expression for Annexin V but were negative for PI whereas the late apoptotic cells should express both markers. Necrotic cells, on the other hand, were identified by positive expression for PI and negative expression for Annexin V.

### 2.7.4. Ki-67 expression assay

The mouse anti-human anti-Ki-67-FITC (#556026; BD Pharmingen, Oxford, UK) was used for detecting the expression of the nuclear protein Ki-67 in fixed and permeabilized AML cells. The protocol was performed according to the manufacturer's instructions and, also, based on a previously published method with some modifications (Jordan, Yamasaki *et al.* 1996). Briefly, the untreated (proliferating) AML cells and those induced to dormancy (treated) were harvested, counted ($5X10^5$ cells per condition) and pelleted according to the standard procedure and then resuspended in a freshly prepared 4% paraformaldehyde solution and incubated at room temperature for 15 min. Subsequently, the fixed cells washed twice with PBS and resuspended in freshly prepared 0.1% of Triton X-100 in PBS followed by overnight incubation at $4^oC$ temperature for gentle permeabilization. In the second day, the cells were washed twice with PBSAA buffer and incubated for 30 min in the dark with the anti-Ki-67-FITC or its isotype control provided in the kit (mouse anti-human IgG-FITC). The tubes then were washed twice again with PBSAA buffer and the cells were resuspended in 300µl PBSAA and were kept on ice in dark place until flowcytometry.

### 2.7.5. Investigating the apoptotic markers (γH2AX, aCASPAS3, and cPARP)

The Anti-activated Caspase3-PE AB (No. 561011; BD), the Anti-γH2AX-FITC (Ser139) AB (No. 16-202A; Millipore), and the Anti-Cleaved-PARP-Alexa F647 AB (No. 558710; BD) were used to measure the expression of these 3 intracellular markers of apoptosis. Fixation and permeabilization of the tested cells were required prior to incubation with the ABs. For this purpose, 4% paraformaldehyde was used to fix the cells (see section 2.7.4.). Subsequently, fixed cells were permeabilized by adding 3.5ml of iced 100% methanol slowly into 0.5ml of cells suspended in PBS while gentle vortexing. Then, the cells were incubated at $-20^oC$

for at least 2 hours before flowcytometry analysis. Matched fluorescent-labelled isotype ABs were used as controls.

### 2.7.6. Ribosomal protein S6 (rpS6) expression measurement

The expression of the phosphorylated rpS6, a downstream sensitive marker of the mTORC1 pathway ((Pallis, Harvey *et al.* 2016)and references therein), was measured by flowcytometry using Alexa Fluor 647-conjugated anti-rpS6 p-ser235/236 AB (No. 4851; CST). As rpS6 is an intracellular protein, it was investigated in fixed and permeabilized AML cells using the same previously discussed paraformaldehyde/ methanol method (section 2.7.6.). The AB in a dilution of 1:50 was then added to permeabilized cells resuspended in PBSAA and incubated for 1hour on ice in the dark before flowcytometry analysis. As the rpS6 was expected to be constitutionally phosphorylated in proliferating cells, cells treated with rapamycin and the ERK-pathway inhibitor (U0126) for 1 hour at 37$^{o}$C were used as controls with minimal baseline phosphorylated rpS6 activity (Pallis, Harvey *et al.* 2016).

### 2.7.7. PKH26 Labelling assay

PKH26 (MIDI26; Sigma) is a lipophilic dye with fluorescence property (at the yellow-orange region of the spectrum) and it has been used in several *in vivo* and *in vitro* biological processes including tracking cellular division. The principle of this assay based on the fact that the stained cells will lose 50% of their dye fluorescence following each division which resulted in a decrease in fluorescence that can be measured by flowcytometry to track cellular proliferation. The assay was optimized according to manufacturer's recommendations and published works (Horan and Slezak 1989, Konopleva, Konoplev *et al.* 2002). In brief, 1X10$^{6}$ cells were washed once with RPMI, resuspended in 500µl of Diluent C (provided in the kit), and stained by mixing them with diluted PKH26 dye (6µl PKH26 dye in 500µl Diluent C) at room temperature for 3 min with repeated agitations. The reaction

then was stopped by adding 1 ml of 100% FCS followed by 4 times wash with CM (10% FCS and 1% glutamine in RPMI). Subsequently, the mean fluorescence intensity of the PKH26-stained cells was analysed by flowcytometry immediately after staining and at the end of the incubation time of treatment, thereafter, to track the cellular divisions. Unstained cells were used as negative controls.

## 2.8. Molecular biology assays

All steps of the qPCR assays were conducted as previously optimized and published from the department (Seedhouse, Mills *et al.* 2014) and according to the manufacturer's instructions. They included the following four steps.

### 2.8.1. Total RNA extraction

RNA was extracted and purified by using QIAamp RNA kits (52304; Qiagen) with DNase treatment according to the manufacturers' instructions (Qiagen). In brief, up to $10^6$ cells were counted by trypan blue-haemocytometer method, harvested, and pelleted into sterile 1.5ml Eppendorf tube and resuspended in 350µl RLT buffer with 3.5µl β-mercaptoethanol (βME). The resulted RNA lysate, thereafter, either stored immediately in -80$^o$C or subjected to further RNA purification steps. These steps included (in order): RNA homogenization using QIAshredder spin column, RNA collection into QIAamp spin column, on-column DNase digestion, RPE-buffer washing , and RNA elution into labelled 1.5ml Eppendorf tube using RNAase-free molecular grade water (All provided in the kit). The concentration and purity of the resulted purified RNA were analysed using Nanodrop-2000 (Thermo Scientific; UK) according to the manufacturer instructions before storage at -80$^o$C or proceed directly for complementary DNA synthesis. All RNA preps should show 280/260 and 260/230 ratios equal to or about 2 in order to pass the quality standards for further processing.

### 2.8.2. Complementary DNA (cDNA) synthesis

Two micrograms of RNA was used in the reverse transcription reaction using master mix consists of RNAase inhibitor (Promega), MMLV (Invitrogen) and reverse transcription mix containing first strand buffer (Invitrogen), dNTPs (Invitrogen), DTT (Invitrogen) and random primers (Invitrogen) in DEPC treated water. The reaction tubes were then placed in a pre-programmed cycler (PTC-100, Bio-Rad) to run for 60 min at 37°C, 10 min at 95°C and then cool down to 4°C. The resulted cDNA, then, was stored at -20°C until used for the qPCR reaction.

### 2.8.3. Primers and primers designing

All target genes were studied using primers purchased from Qiagen or designed using the 'primer-Blast' online primer designing software from the website 'http://www.ncbi.nlm.nih.gov/tools/primer-blast/'. The designed primers were selected to target the transcripts used the GEP chip and to span exon-exon junction, whenever possible, to avoid amplifying genomic DNA. The housekeeping gene β2-microglobulin (B2M) sequence was obtained from previously published papers (Pallisgaard, Clausen *et al.* 1999, Seedhouse, Grundy *et al.* 2007). Appendix A2 give information about the full list of the primers used in this study.

### 2.8.4. Real-time quantitative polymerase chain reaction (qPCR) assay

Quantitative PCR was performed on ABI prism-7700 (Applied Biosystems) using Mastermix with SYBR-green detection (Biogene, Cambridge, UK). Thermal cycler conditions included incubation at 95$^{o}$C 10 min followed by 40 cycles of 95$^{o}$C 15 s and 60$^{o}$C 1 min. Following the 40 cycles, the products were heated from 60$^{o}$C to 95$^{o}$C over 20 min to allow melting curve analysis to be done (appendix A3). This allowed the specificity of the products to be determined (single melting peak) and confirmed the absence of primer-dimers. To enable the levels of transcripts to be quantified, standard curves were generated using serial dilutions of cDNA for the suitable AML cell line (For examples TF1 cDNA for p21 and p57 genes while M0-

91 cDNA for the p27 gene). The housekeeping gene β2-microglobulin (B2M) was used to standardise the samples and the relative expression level of the target genes which, therefore, was calculated as the ratio between the level of test gene and the level of B2M housekeeping gene. Negative controls (no template) were included in each experiment and all reactions were run in triplicate.

## 2.9. Affymetrix Whole Human Genome Gene Expression Profile (GEP) Assay

Whole human genome gene expression profile of TF1-a cells was studied using the Affymetrix technology. These experiments were performed using four Human Gene 2.1 Array Strips (Code No. 902114; Affymetrix) to analyse the 15 TF1-a samples, as will be detailed below. Each strip contains 4 arrays and the necessary hybridization, wash and scan trays. The TF1-a cells were treated and their RNA was extracted in the department laboratory and then transferred in dry ice to Sutton Bonington Campus of the University of Nottingham to be processed in collaboration with the Nottingham Arabidopsis Stock Centre (NASC) laboratories team. The modern microarray system ,GeneAtlas$^{R}$ from Affymetrix, was used for sample processing and the software Partec Genomic Suite was used for the data analysis and generating the figures.

### 2.9.1. TF1-a cells treatment protocol for the GEP

TF1-a cells were selected for *in vitro* modelling of the AML dormancy (by treating them for 72 hours with of 4ng/ml of TGFβ1 and 100nM of the mTOR inhibitor Rapamycin) and the sublethal genotoxic stress (by treating them for 6 days with Etoposide at the IC20 concentration). Therefore, for the GEP experiments, TF1-a cells were cultured in 5 conditions: untreated, TGFβ1-treated, Rapamycin-treated, TGFβ1+Rapamycin-treated, and Etoposide-treated cells (figure 2.2). Three biological replicates were performed for this experiment resulted in 15 samples of

TF1-a cells. These were harvested, counted manually by Trypan Blue, lysed in RLT buffer, and stored in -80 for further processing.

### 2.9.2. Total RNA extraction and assessment of RNA integrity for the GEP

The total RNA was extracted using the same protocol described in section 2.8.1. The resulted 15 RNA preps were subjected to nanodrop testing for checking concentrations and purity before sending them to NASC laboratories in Sutton Bonington on dry ice for further analysis. All RNA preps showed 280/260 and 260/230 ratios equal to or about 2; thus passing the quality standards for further processing. To ensure suitability of the RNA samples for the GEP experiments, the RNA integrity was checked using Agilent 2100 Bioanalyzer to measure the RIN (RNA Integrity Number) for each sample. This number range from 0-10 with RIN=7 is recommended to be the minimum accepted limit for the RNA integrity. All the 15 TF1a RNA samples showed RIN ≥9.8 (appendix A4).

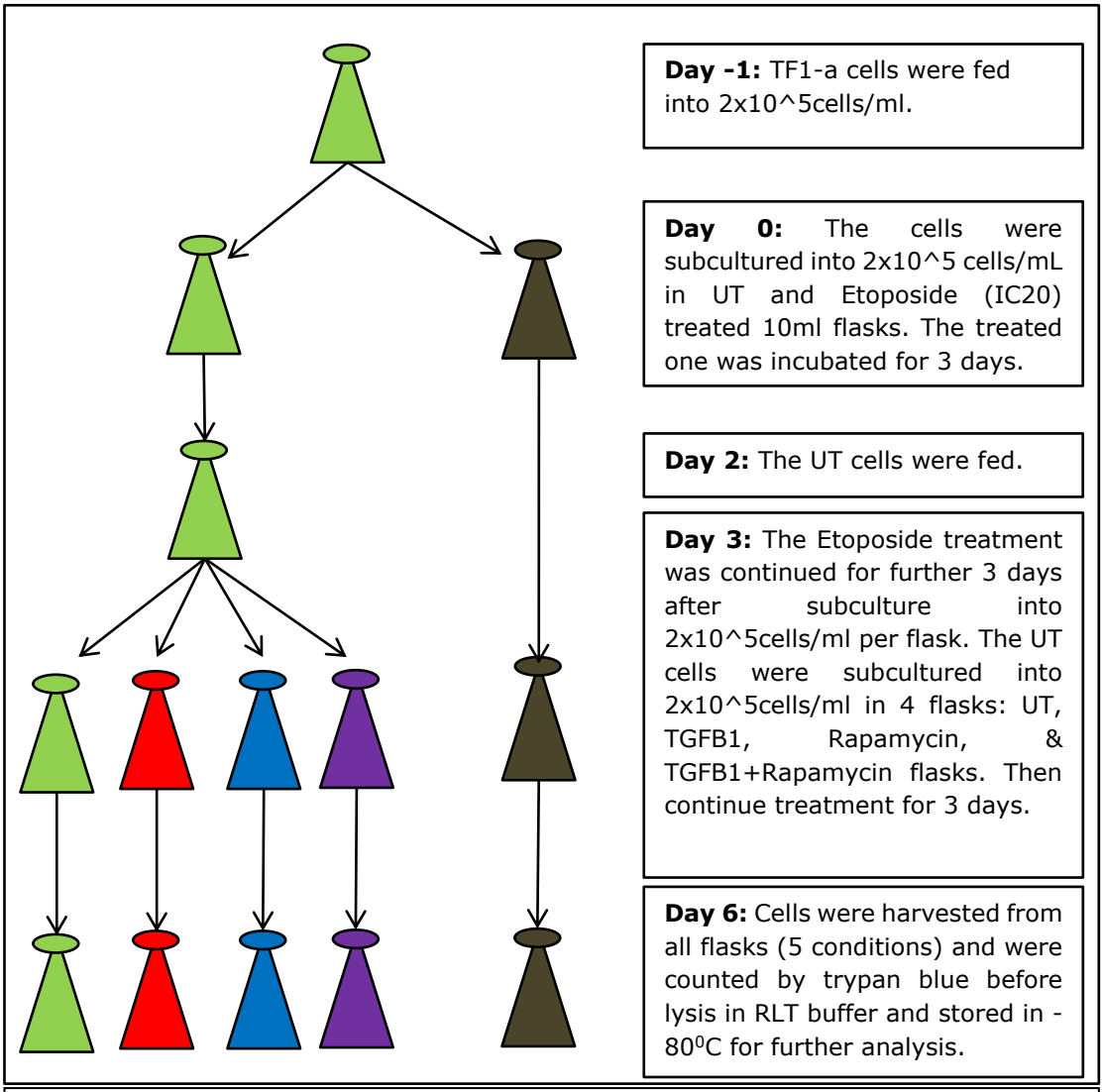



**Figure 2.2: TF1-a cells treatment protocol for the GEP experiments.** The green flasks refer to the untreated cells, the red for the TGFβ1-treated, the blue for the Rapamycin-treated, and the dark grey for the Etoposide-treated cells.

### 2.9.3. Generating, fragmentation and hybridization of the Sense cDNA on the Array strips

All steps of sense cDNA synthesis, fragmentation and hybridization were performed according to the manufacturer protocol (GeneAtlas$^{R}$ WT Expression Kit User Manual). Figure 2.3 summarizes these steps. To ensure optimum fragmentation the resulted fragmented sense cDNA was assessed using Agilent 2100 Bioanalyzer. The resulted fragmented whole transcript sense target was hybridized to Human Gene 2.1 Array Strips that have been designed with a median of 21 unique probes for each transcript. Each probe is 25 bases in length, which means that the array measures a median of 525 bases per transcript for more than 33500 NM and XM coding transcripts. All steps of hybridization, washing, and scanning were carried out automatically by the GeneAtlas$^{R}$ microarray system in the microarray facility of the NASC laboratories in Sutton Bonington.

### 2.9.4. Microarray data (the CEL files) handling and statistical analysis of the differentially expressed genes

The GEP data were generated by the Microarray scanner as CEL files and subjected to further analysis by the Partec Genomics Suite Software following the instruction manual. Briefly, the 'Gene Expression' workflow was selected which consists of several steps starting from importing the CEL files into the Software followed by checking the quality metrics. This followed by adding attributes to describe the sample groups before generating the Principal Components Analysis (PCA) to visualize the clustering and separations of the 15 samples of TF1a. The differentially expressed genes were identified using the ANOVA test to generate the main list of all genes for each condition. This followed by selecting the list of genes of interest which has included genes upregulated by at least 2 fold change with FDR (false discovery rate)-adjusted p value $<0.05$ and generating the necessary figures.

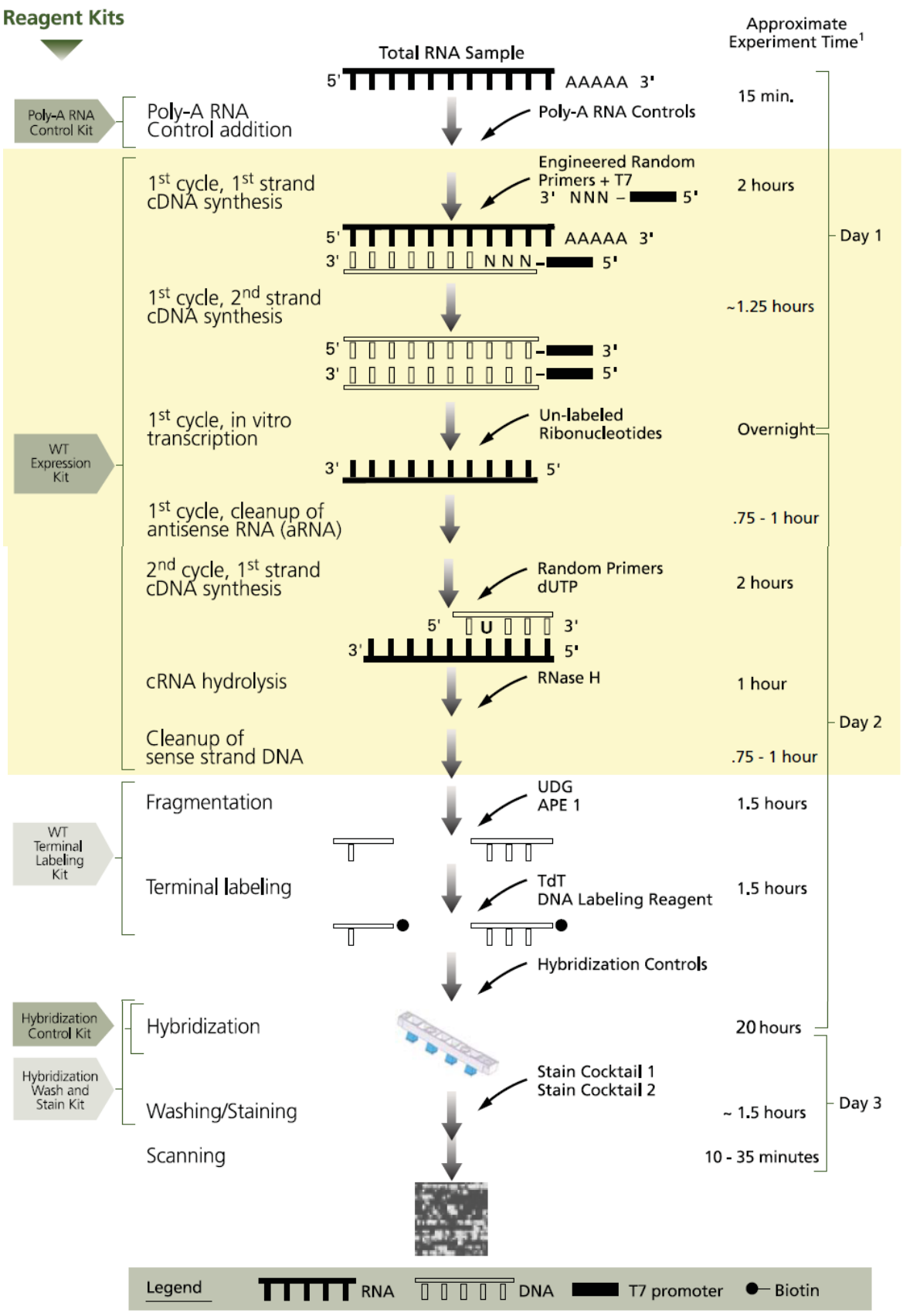



**Figure 2.3:** Assay Schematic for generating Sense cDNA (Source: GeneAtlas[R] WT Expression Kit User Manual)

## 2.10. Statistical Analysis

Statistical analysis was performed using the Statistical Package for Social Sciences, version 23 (SPSS, Chicago, IL, USA). P values of ≤0.05 were considered to be significance. Student Paired T-test was used to test the significance between treated and untreated AML cells while ANOVA test of significance was used for the GEP data analysis to select the differentially expressed genes.

The coefficient of drug interaction (CDI)(Xu, Sun et al. 2007) equasion was used to test weather the effect of TGFβ1+rapamycin combination was synergistic or aaditive if compared to each inhibitor alone.

$$CDI = AB/(A\,xB)$$

AB is the ratio of the combination of inhibitors to the untreated control, and A or B is the ratio of the single inhibitor to the untreated control. CDI <1 indicates synergism, CDI =1 indicates additivity, and CDI >1 indicates antagonism (Xu, Sun et al. 2007).

# CHAPTER THREE
# SELECTING AND INVESTIGATING THE CANDIDATES LEUKAEMIA CELL LINES FOR THE TGFB1-DEPENDENT IN VITRO DORMANCY MODEL

## 3.1. Background

The leukemic cells that are responsible for relapse in AML patients are generally believed to be phenotypically $CD34^+$ which was proven by repeated *in vivo* repopulating assays in xenograft models (Sutherland, Blair *et al.* 1996, Bonnet and Dick 1997, Blair, Hogge *et al.* 1998, Blair and Sutherland 2000, Ishikawa, Yoshida *et al.* 2007, Martelli, Pettirossi *et al.* 2010). Therefore, three $CD34^+$ AML cell lines were selected as candidates for the dormancy model, namely: KG-1a, TF1-a, and Kasumi-3. Recently, nevertheless, reports suggest that cells causing relapsed AML could, also, be isolated from $CD34^-$ fraction of the AML cells but with lower engraftment potential if compared to the $CD34^+$ phenotype (Martelli, Pettirossi *et al.* 2010, Taussig, Vargaftig *et al.* 2010). The $CD34^-$ AML cell line M0-91 , therefore, was included for the purpose of completion and also as a positive control for the TGFβ1 model due to a published work confirmed the response of these cells to the inhibitory signals of the exogenous TGFβ1 (Scandura, Boccuni *et al.* 2004).

As detailed in the introduction (section 1.5.2.1), TGFβ1 is a likely candidate for induction of dormancy in leukaemia cells. Therefore, the effect of the exogenous TGFβ1 on the four selected AML cell lines was studied in cells cultured in a suspension medium; and the focus was firstly on investigating its inhibitory effect on cellular proliferation before further studying its effect on cell cycle and stemness features.

## 3.2. Results

### 3.2.1. AML cell lines Characteristics

3.2.1.1. AML cell lines Morphology

The morphological examination of AML cells in stained smear continues to play a vital role in the diagnosis and classification of AML patients (Dohner, Estey *et al.* 2010). It has also an essential role, within the *in vitro* research context, in assessing the differentiation status of AML cells in response to various conditioning systems (Verhagen, Smit *et al.* 2016). Therefore, we sought to examine the four AML cell lines morphology as a baseline picture for further comparative assessment following dormancy induction.

In their suspension medium and under inverted light microscopy examination, the TF1-a cells were the largest cells among the studied AML cell lines. The M0-91 cells were the only cells showed some degree of adherence to the culture surface (figure 3.1, panel A). This adherence was weak that required no additional proteolytic step to harvest the cells.

All the four cell lines showed the characteristic morphological features of the myeloblasts in their Wright-Geimsa-stained smears. They showed large nucleus with variable nuclear shape and convolutions and high N:C (nucleus to cytoplasm) ratio. The chromatin was lacy opened with minimal condensation and the nucleolus was conspicuous single or, in many cells, multiple. Kasumi-3 cells, specifically, showed remarkable cytoplasmic vacuolation (figure 3.1, panel A) which could be related to its tendency of differentiation towards the monocytic lineage as it has been mentioned by the supplier.

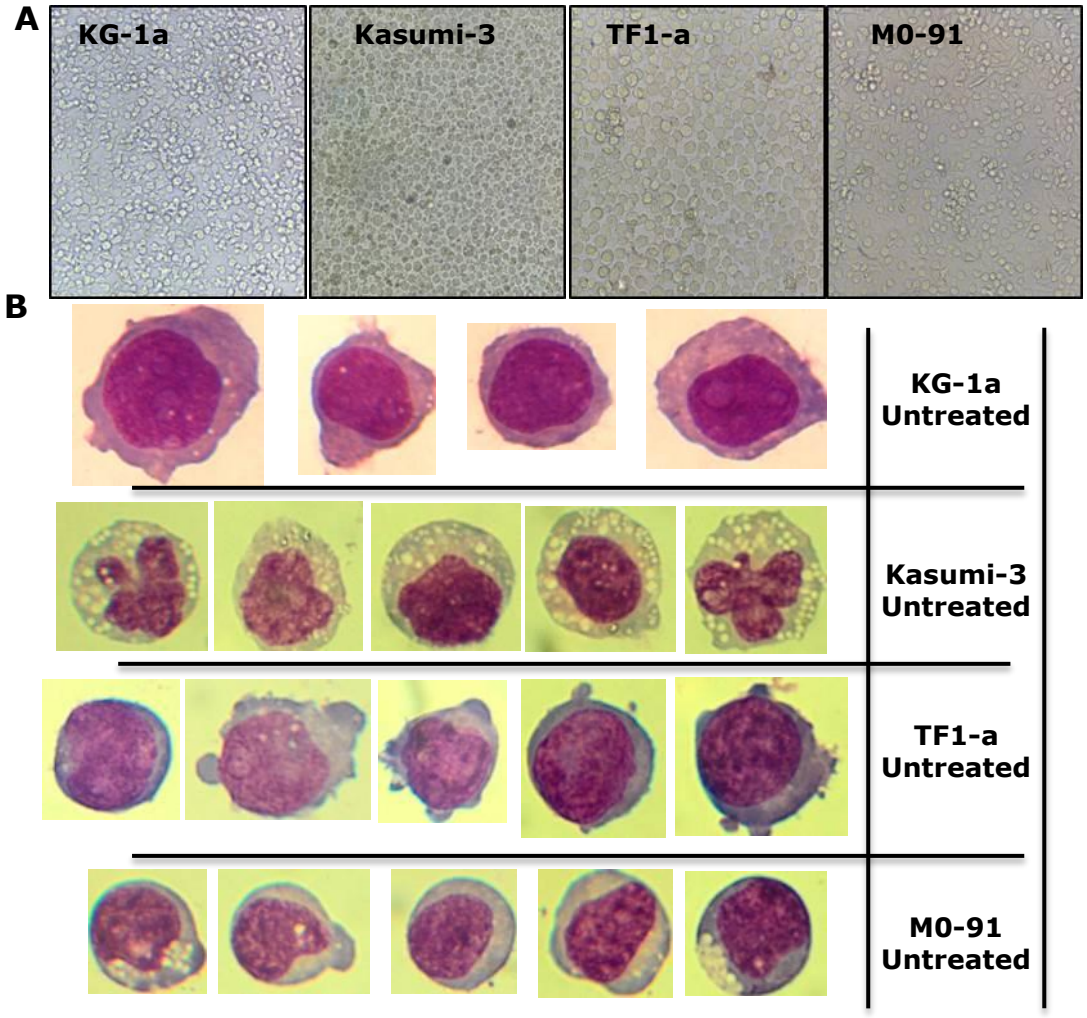



**Figure 3.1: The Four AML Cell lines Morphology. Panel A:** shows morphology of KG-1a, Kasumi-3, TF1-a, and M0-91 cells as they were examined under the inverted light microscope in their suspension medium. **Panel B:** illustrates the untreated cells as they appear in their smears which were prepared and dried by air before staining with Wright-Geimsa stain. Images of panel B were processed with Image J software.

3.2.1.2. AML cell lines Immunophenotyping

The cellular expression of three of the markers of stemness was studied in the four AML cell lines, namely; CD34, CD117, and ALDH (table 3.1). The expression of the surface protein CD34 was studied in combination with the expression of the differentiation marker CD38, as it is a well-adapted strategy for isolating normal and malignant haematopoietic cells with stemness features (Jan, Chao *et al.* 2011).

The $CD34^+$ AML cell lines (KG-1a, TF1-a, and Kasumi-3) showed a variable degree of CD34 expression. As regards KG-1a cell line, almost all the cells (99%) were $CD34^+$ and about 22% only were $CD38^+$. By contrast, in kasumi-3 85% of the cells were $CD34^+$ but with significant CD38 expression (64% of the cells). TF1-a had a relatively lower proportion of CD34 positivity and negligible CD38 expression resulted in approximately half of the cells was $CD34^+CD38^-$ and the other half was $CD34^-CD38^-$ (figure 3.2, panel A). These proportions of CD34 and CD38 expression were compatible with those provided by the suppliers except in the case of the CD34 expression of TF1-a which showed relatively lower expression than when it was first created (Hu, Moscinski *et al.* 1998). M0-91 cells, on the other hand, showed no CD34 expression with strong CD38 positivity on almost all the cells (figure 3.2, panel A).

The stem cell factor ligand CD117 is one of the surface markers that used to identify myeloid blasts by flow cytometry both clinically and for research purposes. Besides CD34, CD38 and others, CD117 is considered to be the marker for AML cells at the precursor stage of differentiation with stemness features (Dohner, Estey *et al.* 2010). Furthermore, due to the suggested correlation between CD117 expression and cell cycle regulation by TGFβ (Morita, Yamamoto *et al.* 2003) the expression of this receptor protein in the AML cell lines was studied. KG-1a, M0-

91, and TF1-a cells were CD117 low while Kasumi-3 was CD117 high (figure 3.2, panel B).

The expression of the cytoplasmic enzymatic protein ALDH was used by many researchers as a strategy, in association with CD34 expression, to identify cells with stemness characteristics in both normal haematopoietic cells ( in human bone marrow (Pierre-Louis, Clay *et al.* 2009) and cord blood (Christ, Lucke *et al.* 2007)) and also in AML patients (Nakamura, Tan *et al.* 2013). In the current study, a variable ALDH expression was noticed among the studied cell lines. Kasumi-3 and TF1-a showed 93% and 60% of ALDH activity respectively, whilst only, approximately, 5% of KG-1a and 10% of M0-91 cells were positive for ALDH (figure 3.2, panel C).

**Table 3.1: Summary of the immunophenotyping of the four human AML cell lines used in this study.**

| Cell line | CD34 | CD38 | CD117 | ALDH |
|---|---|---|---|---|
| **KG-1a** | +ve | Weak +ve | Weak +ve | -ve |
| **Kasumi-3** | +ve | +ve | Strong +ve | Strong +ve |
| **TF1-a** | +ve | -ve | Weak +ve | +ve |
| **M0-91** | -ve | Strong +ve | -ve | -ve |

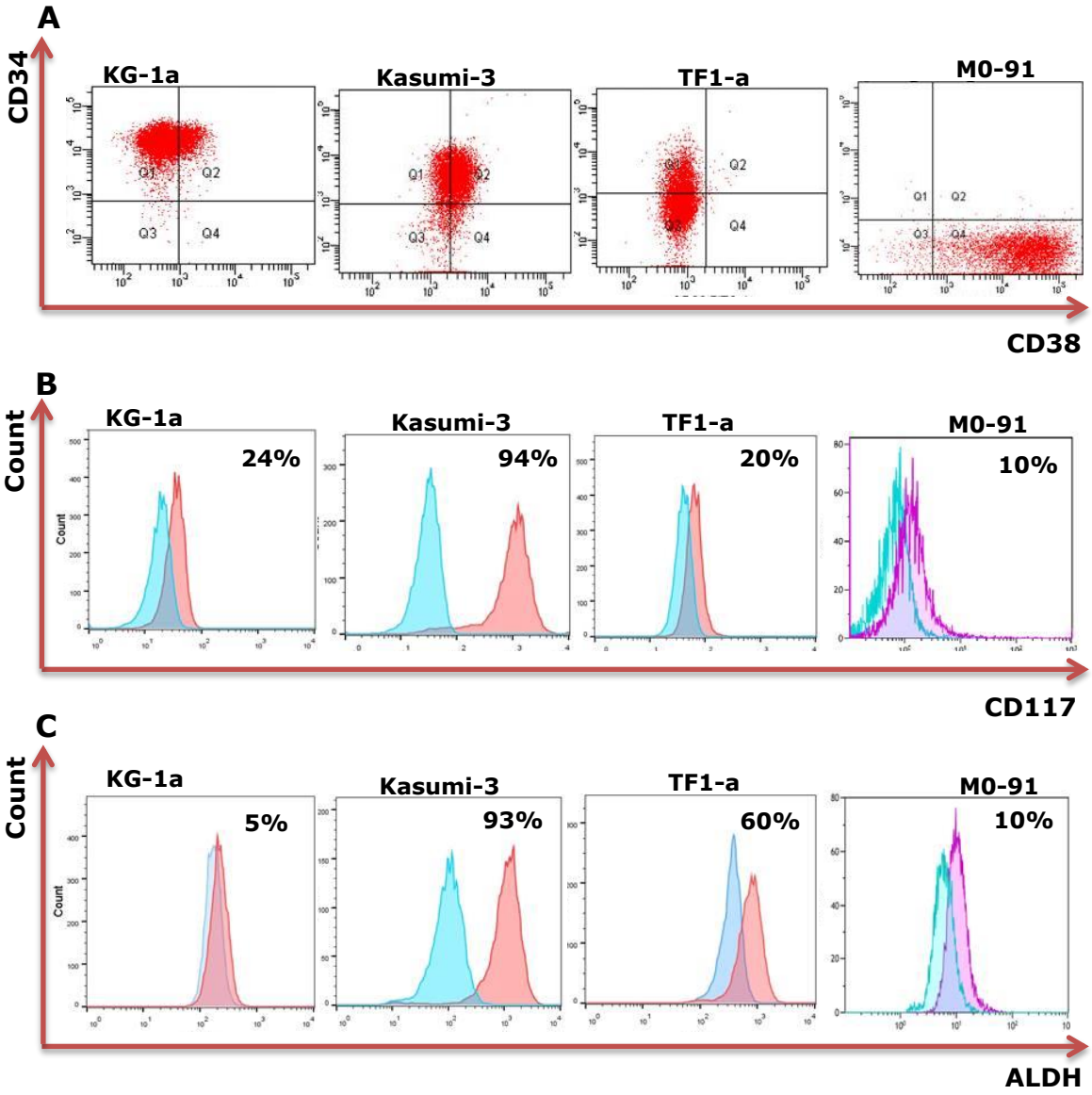



**Figure 3.2: Immunophenotyping of the AML cell lines. Panel A**: The expression of CD34 and CD38 in untreated KG-1a, Kasumi-3, TF1-a, and M0-91 cell lines. The four quadrants gates of each dot plot were adjusted according the isotype control for each cell line. **Panel B**: CD117 Expression on the four cell lines **Panel C**: Expression of ALDH in KG-1a, Kasumi-3, TF1-a, and M0-91 cell lines. The blue histograms represent the negative isotype control for CD117 and the negative DEAB control for ALDH . The percentages represent the proportion of positive cells for each condition.

### 3.2.3. TGFβ1 inhibits the AML cells proliferation in a dose-dependent manner

Variable concentrations of TGFβ1 have been previously used to treat leukaemia cell lines in different *in vitro* culture systems depending on the purpose of the study (Hu, Moscinski *et al.* 1998, Scandura, Boccuni *et al.* 2004, Xu, Tabe *et al.* 2008, Tabe, Shi *et al.* 2013). In this study, escalating doses of TGFβ1 ranging from 0.25-4 ng/ml were chosen to select the optimum TGFβ1 concertation for future experiments. All the four cell lines displayed a dose-dependent manner of growth inhibition where the minimal inhibition of growth was found at a concentration of 0.25 ng/ml of TGFβ1 and maximal inhibition was at 4ng/ml (figure 4.1; panel A).

Statistically, Kasumi-3 cell line showed a relatively slight, but significant inhibition of growth when compared to the untreated counterparts ($p < 0.05$). By contrast, TF1-a cells and M0-91 cells showed more significant proliferation inhibition in response to 3 days of incubation with 4ng/ml of TGFβ1 ($p< 0.001$ and $p< 0.01$ respectively). On the other hand, KG-1a proliferation was inhibited in a statistically non-significant degree following culture with the same range of TGFβ1 concentrations ($p= 0.128$) (figure 3.3). Consequently, KG-1a cell line was excluded from further investigations.

In preliminary experiments, which were not repeated for cost reasons, there was no significant increase in the inhibitory effect of TGFβ1 at 8ng/ml in comparison to 4ng/ml and also no increase of proliferation inhibition was noticed by using multiple daily doses of TGFβ1 at 4ng/ml. Therefore, 4ng/ml was selected for all future assays involving the use of TGFβ1.

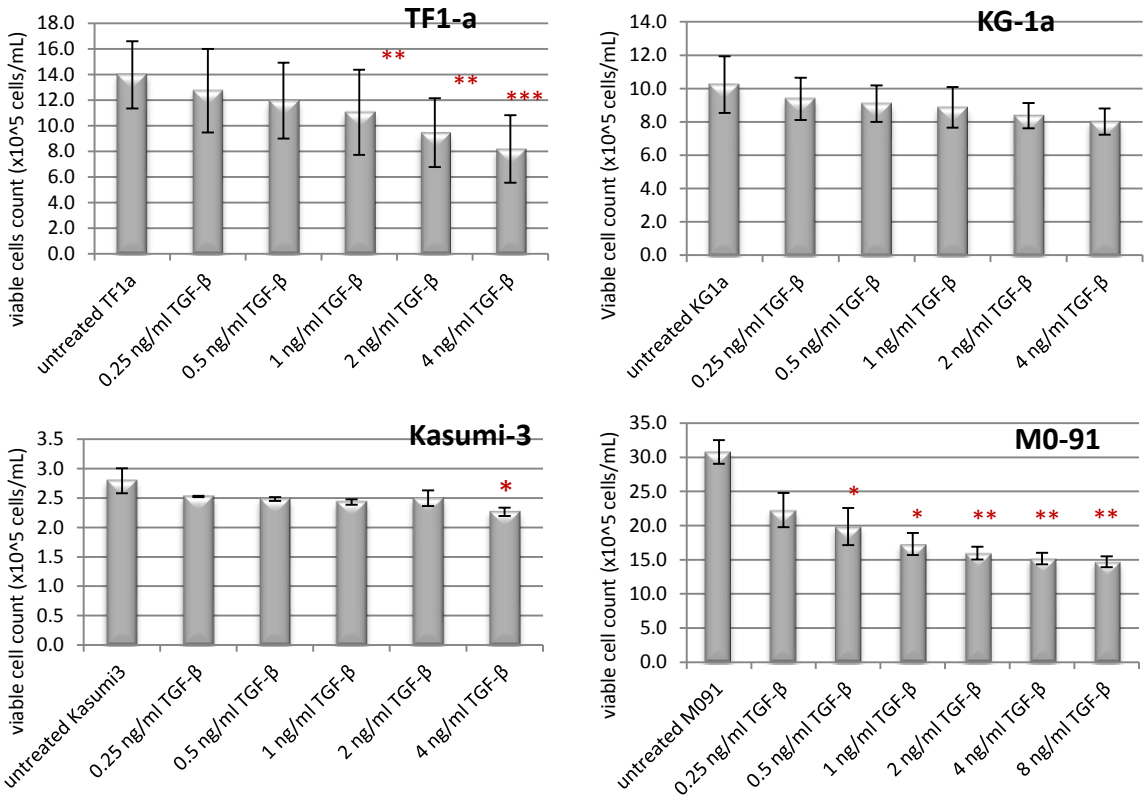



**Figure 3.3: The inhibitory effect of TGFβ1 on the cell lines growth.** It shows the effect of escalating doses of TGFβ1 on the proliferation of the four cell lines. All cells were seeded at a concentration of 2x10^5 cells/ml and incubated for 72 hrs. The columns represent mean values of three independent experiments. The error bars represent +/- 1SD. (*: $p < .05$; **: $p < .01$; ***: $p < .001$).

### 3.2.4. AML cell lines response to culture in serum-free medium

The present study based on an in vitro culture system consisted of AML cell lines cultured in suspension medium at ordinary conditioning circumstances (5%CO2 and 37$^{o}$C in humidified incubator). Nevertheless and before performing deep validation steps for the *in vitro* TGFβ1-dependent dormancy model, the suitability of serum withdrawal in replacing the serum-containing media (SCM) was studied in an attempt to exclude the animal serum that might contain variable amounts of TGFβ1 which could impose a degree of inconsistency among experimental replicates.

M0-91, TF1-a, and Kasumi-3 cells were maintained in the SFM (StemSpan SFEM II (09655); stem cell technology) in comparison to the ordinary SCM. All the 3 cell lines were cultured for 7 consecutive days during which they were sub-cultured 3 times to avoid confluence. M0-91 showed the least survival when most of the cells died within the period of the question (figure 3.4; panel A). TF1-a cells proliferated in considerably lower rates in SFM in comparison to their SCM-cultured counterparts (figure 3.4; panel B). Kasumi-3 cells were the only studied AML cell line that showed relatively similar rates of proliferation in SFM during the period in question (figure 3.4; panel C).

Despite the relatively better survival of TF1-a and Kasumi-3 cells in SFM, they showed a remarkable decrease in the proportion of viable cells in SFM from 92% to 34% and from 98% to 87% respectively (figure 3.5). This indicates the stressful influence of serum withdrawal on the viability of the three cell lines.

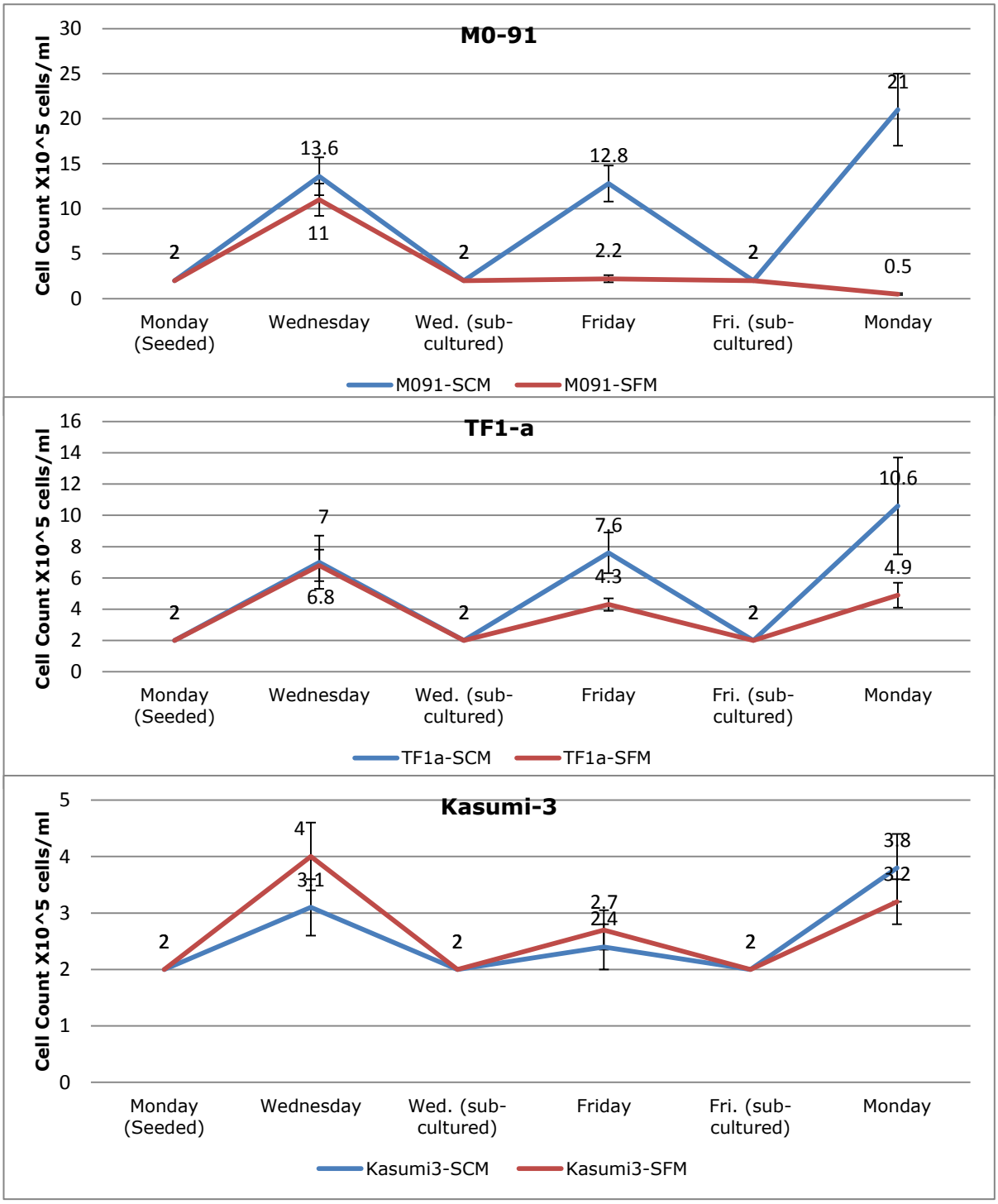



**Figure 3.4: AML Cell lines survival in Serum-Free Medium Culture.** The proliferation of M0-91 (Panel A), TF1-a (Panel B), and Kasumi-3 (Panel C) cells were followed for 7 consecutive days. During this period the cells were counted and then sub-cultured into the starting concentration of 2 X10^5 cells/ml on Monday, Wednesday, and Friday followed by 2 days, 2 days, and 3 days of culture in SCM (Blue lines) or SFM (Red lines) respectively. Cell count was measured by Trypan-Blue method and shown as mean +/- SD of 3 biological replicates.

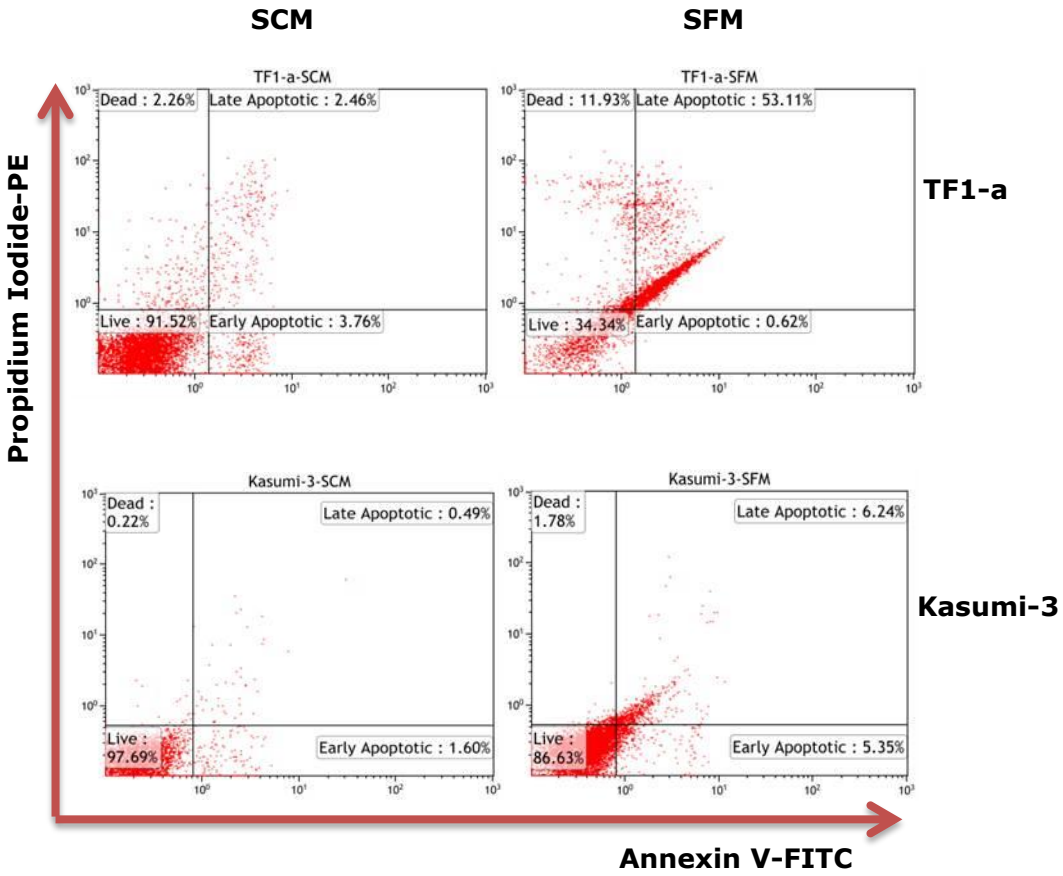



**Figure 3.5: AML Cell lines viability in Serum-Free Medium Culture.** The viability of TF1-a and Kasumi-3 cells were assessed by AnnexinV-Propidium Iodide-Flow cytometry assay after 7 days of continuous culture with SFM or SCM. The plots represent example of 2 biological replicates showed similar

### 3.2.5. TGFβ1 inhibitory effect was persistent to up to 6 days of continuous treatment

To confirm the consistency of TGFβ1 inhibitory effect on leukaemia cells proliferation, a series of experiments were carried out using a longer duration of incubation (6 days) and two doses of TGFβ1 (at day_0 and day_3 of incubation) to treat Kasumi-3, TF1-a cells, and M0-91. It was clear that the TGFβ1-treated leukaemia cells continued to express inhibition of proliferation which indicates that TGFβ1 effect was not transient. Nevertheless, the growth inhibition at days_6 of incubation was non-significant if compared to day_3 for Kasumi-3, TF1-a, and M0-91 ($p=0.1$, $p=0.05$, and $p=0.3$ respectively) (figure 3.6).

Collectively, these data indicate that a significant inhibition of proliferation in Kasumi-3, TF1-a, and M0-91 cells cultured in ordinary SCM can be achieved by a single dose of 4ng/ml TGFβ1 for 3 days.

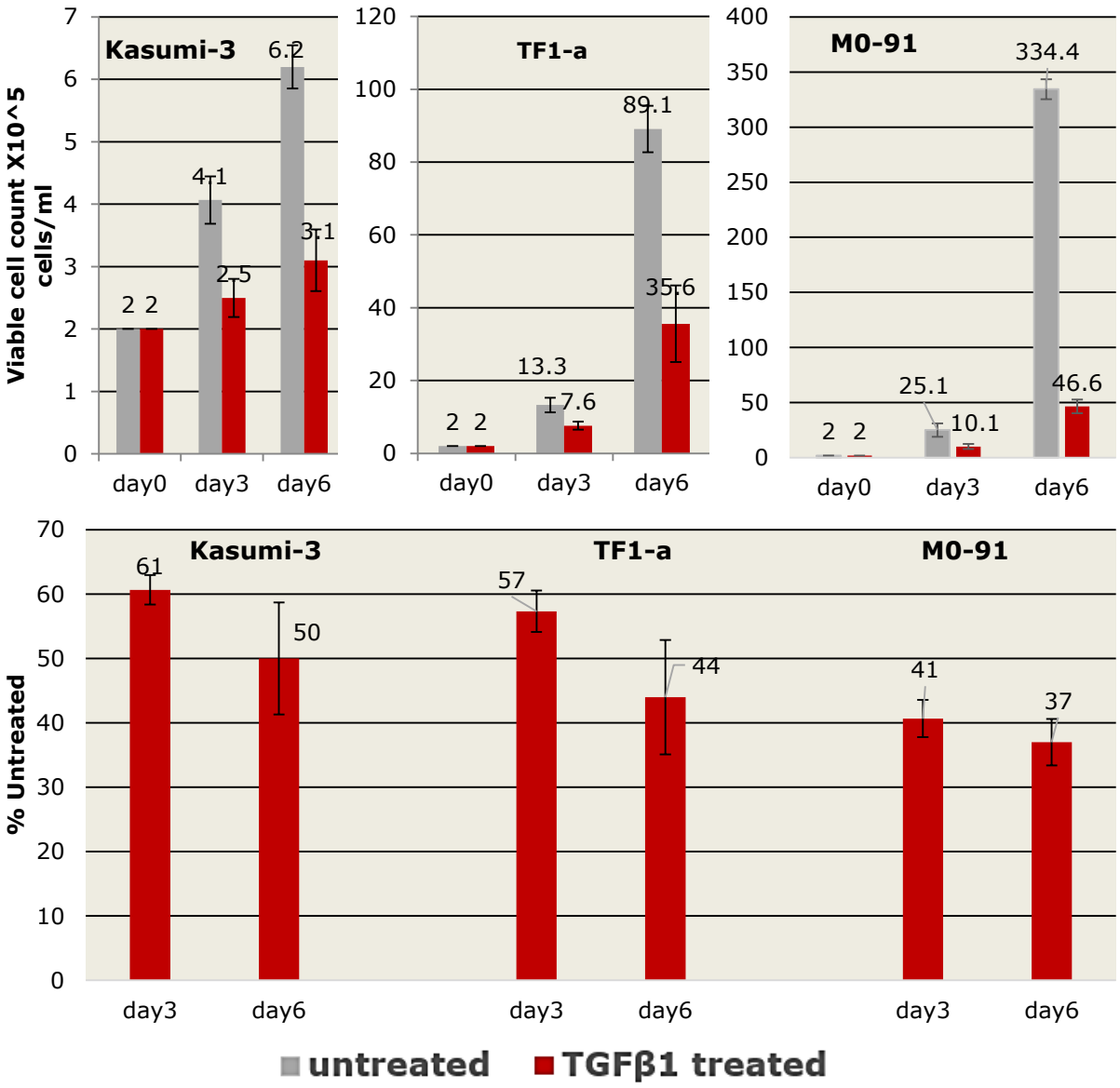



**Figure 3.6: The inhibitory effect of prolonged TGFβ1 treatment on the cell lines growth.** All cells were seeded at a concentration of 2x10^5 cells/ml and incubated for 6 days with or without continuous TGFβ1 treatment in a dose of 4ng/ml. The columns represent mean values of three independent experiments. The error bars represent +/- 1SD.

### 3.2.6. No effect on AML cells viability was observed due to TGFβ1 treatment

It is important to differentiate between a decrease in proliferation due to cellular dormancy from that due to apoptosis and loss of cell viability. Serum withdrawal, for instance, was associated with significant decrease in proliferation which was due to cell apoptosis (section 3.2.4.). In contrast, AML cells cultured with TGFβ1 was associated with no effect on cell viability. This was confirmed by labelling Kasumi-3, TF1-a, and M0-91 cells with propidium iodide (PI) and annexin V

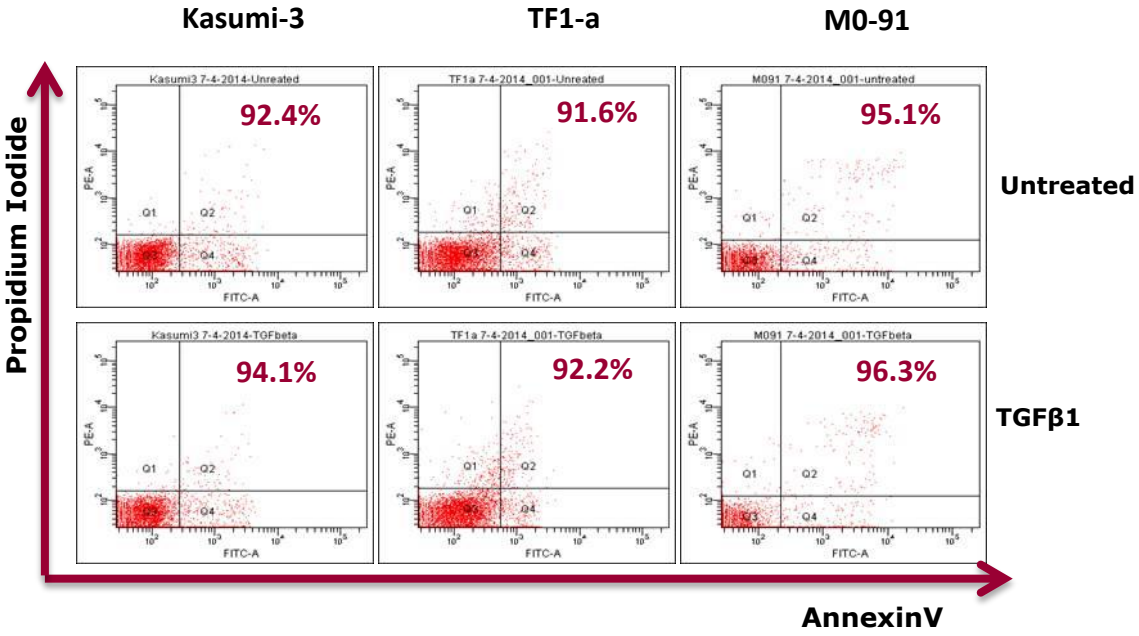



**Figure 3.7: The viability of Kasumi-3, TF1-a and M0-91 cells after 3 days culture with 4ng/mL of TGFβ1.** These cell lines were probed for AnnexinV and Propidium Iodide expression and subjected to flow cytometric analysis. The percentages represent the proportions of viable cells in quadrant 3 (Q3) for the untreated and the TGFβ1-treated cells. These plots are representative examples of two independent experiments for each cell line that showed similar results.

following 3 days culture with 4ng/ml TGFβ1. 94.1%, 92.2%, and 96.3% of the three cell lines, respectively, were negative for both markers (viable) after TGFβ1 treatment in comparison to 92.4%, 91.6%, and 95.1% of their untreated counterparts respectively (figure 3.7).

### 3.2.7. The response of the cyclin-dependent kinase inhibitors (CDKI) p21, p27, and p57 to TGFβ1 treatment

Although the definite mechanism through which TGFβ1 exerts its cytostatic effect is not well known yet, induction of the CDKI p57 is suggested to play a major role in cell cycle control in HSCs (Scandura, Boccuni *et al.* 2004, Matsumoto, Takeishi *et al.* 2011). Furthermore, the suggested role of p57 was reported to cooperate with the other CDKI p27 (Zou, Yoshihara *et al.* 2011) which is also reported playing a role in leukaemia stem cell dormancy (Zhang, Seet *et al.* 2013). Therefore, we sought to investigate the expression of the major 3 CDKI.s that controlling the cell cycle, namely; p21, p27, and p57.

The qPCR results demonstrated that p57 was up-regulated in M0-91, TF1a, and Kasumi-3 AML cells in response to culture with 4ng/ml of TGFβ1 (figure 3.8). The maximum induction of p57 expression was between 2-4 hours of treatment; thereafter, the expression showed a decline at 24 hours of treatment but did not reach the baseline within this time frame. This upregulation was only statistically significant in M0-91 cells in comparison to the other two leukaemia cell lines.

In contrary to p57, the other CDKIs (p21 and p27) showed a general trend of down-regulation after treatment during the period in question (figure 3.8).

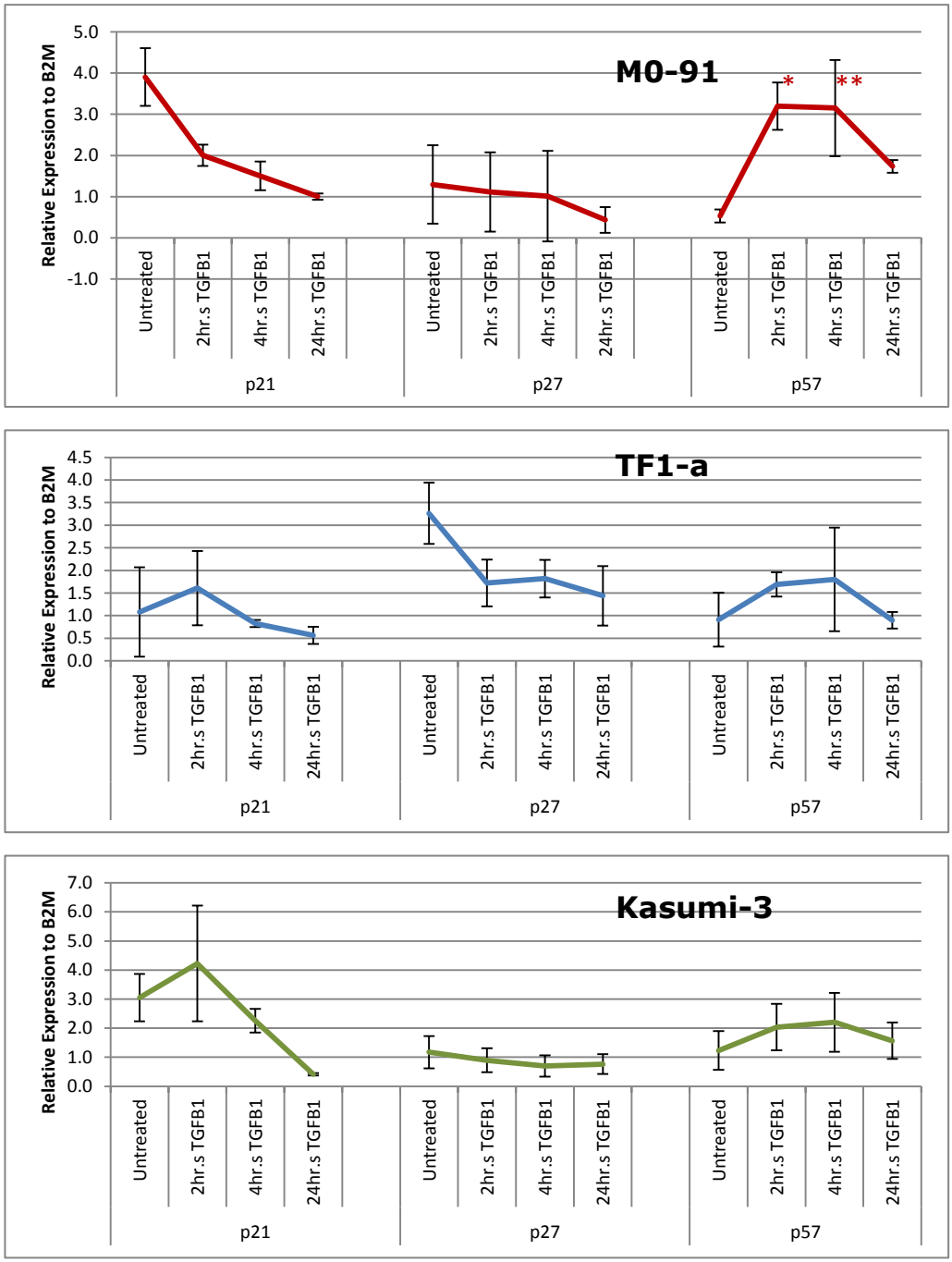



**Figure 3.8: The expression of the cyclin dependant kinase inhibitors p21, p27 and p57 genes in M0-91, TF1-a and Kasumi-3 cells in response to TGFβ1 treatment.** The cells were cultured with 4ng/mL of TGFβ1 for the indicated time. Untreated cells were used as a control. The expression of the target gene was calculated as a ratio to the house keeping gene β2M. The curves represent the means values of three independent experiments and the error bars represent +/- 1SD. The p value was calculated for the upregulated genes only (*: $p < .05$; **: $p < .01$).

### 3.2.8. TGFβ1-treated AML cells showed features of dormancy

The cell cycle status of untreated and TGFβ1 treated cells was assessed using the markers of proliferation Ki-67 and CD71. The nuclear protein Ki-67 is found to be expressed preferentially in G1 phase and proliferating cell, whereas cells in G0 phase are believed to be negative for Ki-67 expression (Scholzen and Gerdes 2000, Ishikawa, Yoshida *et al.* 2007). Similarly, AML cells with negative expression of the transmembrane transferrin receptor CD71 were reported to be dormant with high reconstituting ability in xenograft models (Blair, Hogge *et al.* 1998). Moreover, CD71 expression was found to be associated with cellular proliferation (Liu, Wang *et al.* 2014). In this study, we have examined the staining characteristics of Ki-67 and CD71 of cells cultured for 3 days with TGFβ1 in comparison to their untreated counterparts.

#### 3.2.8.1. Ki-67 assessment

As expected from continuously cycling cell lines, untreated TF1-a, M0-91 and Kasumi-3 cells showed high baseline Ki-67 staining (99%, 99%, and 81% Ki-67 positive cells, respectively). This indicates that the majority of these cells were in actively cycling at the harvesting time point. In response to TGFβ1 treatment, TF1-a cells showed remarkable increase in Ki-67 negative (dormant) cells from 1% to 42% ($p<0.01$). Similarly, Ki-67 negative M0-91 cells increased from 1% to 18% ($p<0.05$); whereas, Kasumi-3 cells showed a slight increase in G0 phase cells from 19% to 24% which was statistically non-significant despite the fact that Kasumi-3 cells showed the highest proportion of baseline Ki-67 negative cells, (figure 3.9).

Collectively, TF1-a cells showed the strongest response to the TGFβ1 inhibitory stimuli when they demonstrated the largest increase in the Ki-67 negative (dormant) cells. It is worth mentioning, however, all percentages of Ki-67 negative and positive cells were identified using gating of these two sub-population based

on the backgroung flourecence signal obtained from the isotype control. Although this is the standard method in flow cytometry assays, in case of the current Ki-67 experiemnt we might notice two visiaully distinct peaks in the histograms which might indicate two distinct population of cells. This could, potentially, alter the above mentioned proportions of Ki-67 positive and negative cells but does not alter the the fact that TF1-a cells remain the most cells with significant increase of Ki-67 negative (dormant) cells.

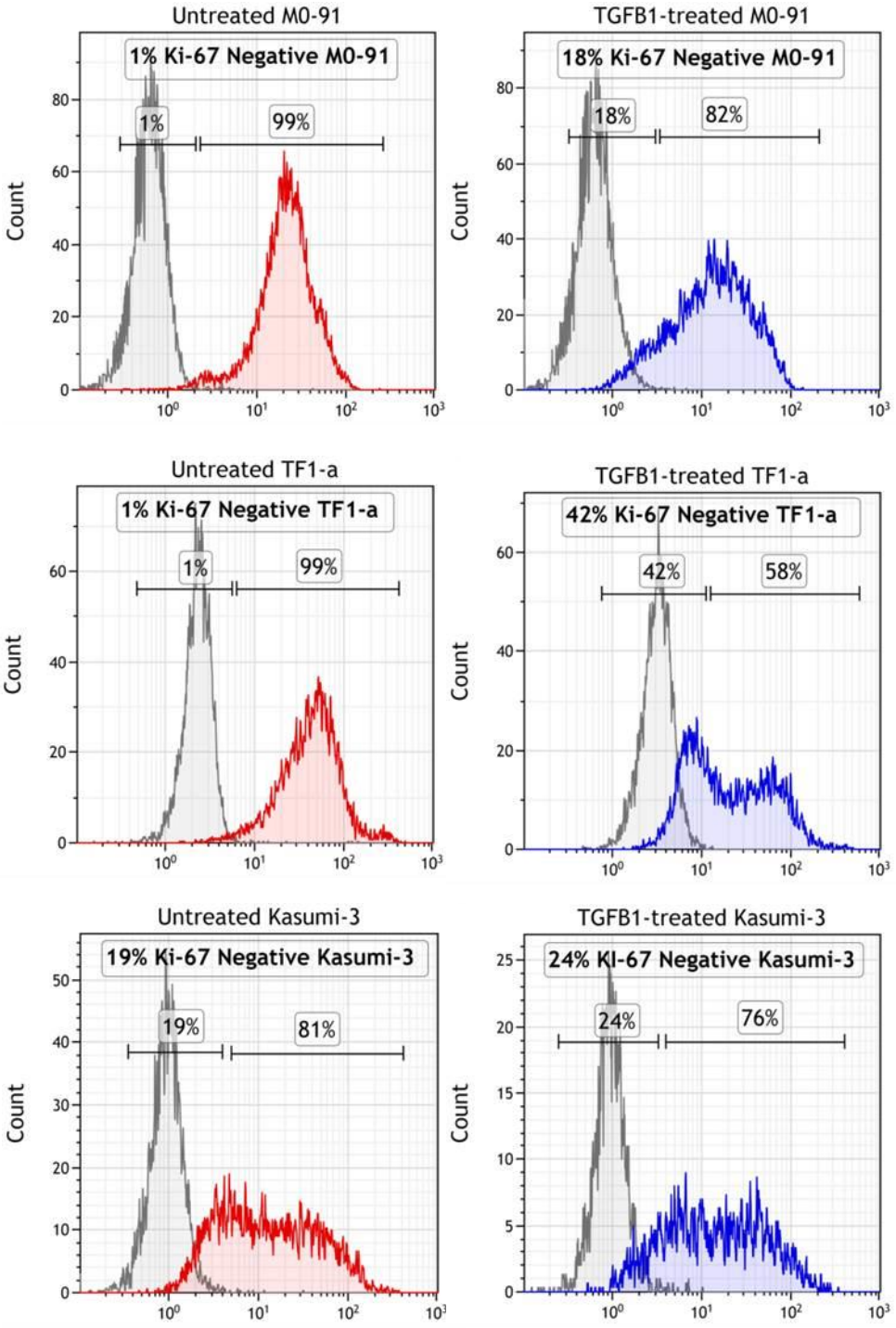



**Figure 3.9: Ki-67 expression in M0-91, Kasumi-3, and TF1-a cells before and after culture with 4ng/ml of TGFβ1.** FITC Mouse IgG1 isotype control (grey histograms) was used as a reference to determine the Ki-67 negative cells. The figure illustrates an example of at least 3 biological replicates showed similar results.

3.2.8.2. CD71 assessment

Following 3 days of TGFβ1 treatment, TF1-a showed a considerable reduction in CD71 staining from 163 RFU to 73 RFU ($p<0.05$). A reduction in CD71 expression was also observed on Kasumi-3 and M0-91 cells (from 45 RFU to 40 RFU and from 85 to 79 respectively) but was statistically non-significant (figure 3.10). Notably, the baseline CD71 expression on untreated TF1-a was remarkably higher than that on untreated Kasumi-3 or M0-91; 54133, 16792, and 19865 MFU respectively. This might be due to that TF1-a cells were considerably larger in size than Kasumi-3 and M0-91 cells (section 3.2.1.1). To avoid the bias due to the cell size variations, therefore, the RFU (section 2.7.1) was used instead of the MFU in assessing the CD71 expressions.

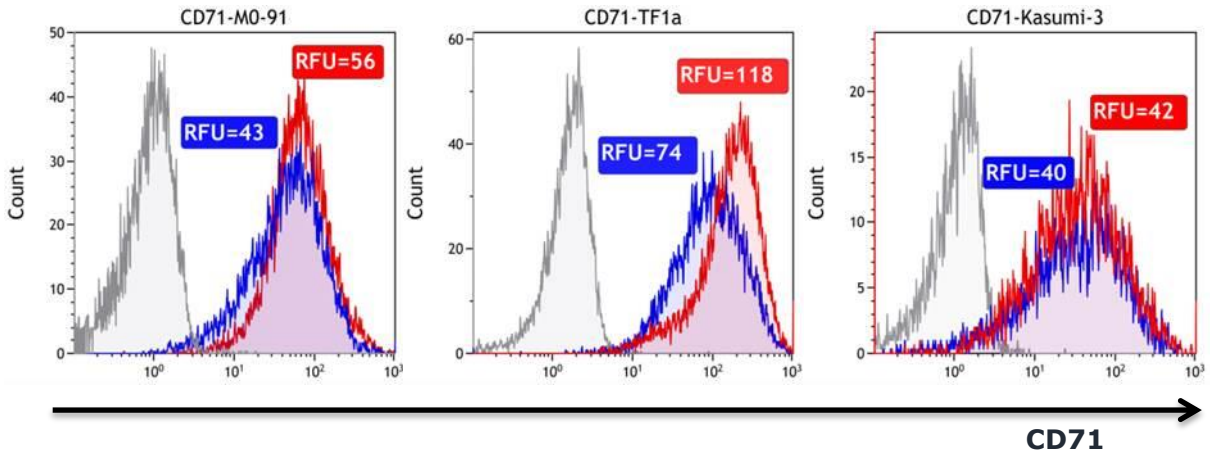



**Figure 3.10: CD71 expression on M0-91, TF1-a and Kasumi-3 cells.** The red and blue histograms represent CD71 expression before and after 3 days treatment with 4ng/ml TGFβ1 respectively. APC-conjugated isotype control antibody (grey histograms) was used to calculate the RFU values of CD71 expression for each condition. The histograms are representative examples of three assays for each cell line that showed similar results.

### 3.2.9. TGFβ1-treatment up-regulates ALDH expression

It has been reported that TGFβ1 increases the stem-like properties of cancer cells (Bhola, Balko *et al.* 2013). Therefore we sought to investigate the effect of the exogenous TGFβ1 on the marker of stemness ALDH in the leukaemia cells TF1-a, Kasumi-3, and M0-91. ALDH expression increased in TF1-a cells only (from 4.3 RFU to 7.6 RFU ($p<0.05$)) following 3 days culture with 4ng/ml of TGFβ1. In contrast, Kasumi-3 and M0-91 showed no increase in ALDH activity after TGFβ1 treatment; from 10.2 RFU to 9.8 RFU and from 1.7 RFU to 1.6 RFU before and after TGFβ1 treatment respectively (figure 3.11).

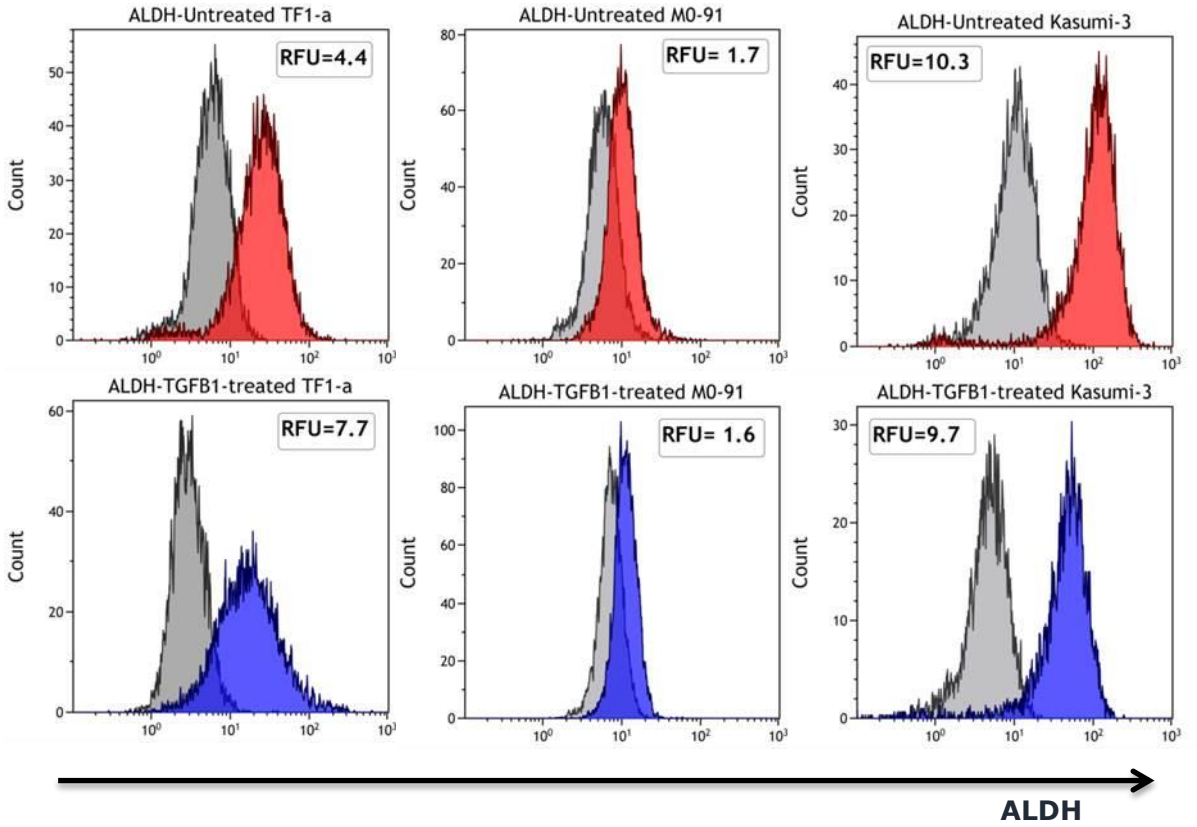



**Figure 3.11: ALDH expression modulation by TGFβ1 treatment in TF1-a, M0-91, and Kasumi-3 cells.** The cell lines were cultured with 4ng/ml of TGFβ1 for 3 days. DEAB controls (grey histograms) were used as negative control to calculate the RFU of the untreated (red histograms) and the treated (blue histograms) cells. The charts are representative examples of three independent experiments for TF1a and two for M0-91 and Kasumi-3 that showed similar results.

To sum up, it is clear from the above results that TF1-a was the most suitable AML cell line for the dormancy model. This was due to several features characterizing TF1-a from the other 3 candidates such as the most primitive immunophenotyping (CD34+CD38-ALDH$^{Int}$ CD117$^{low}$), the highly significant inhibition of proliferation in response to TGFβ1 treatment without deteriorating cellular viability ($p< 0.001$), the significant increase in Ki-67 negative cells ($p< 0.01$), the significant reduction in the marker of proliferation CD71 ($p< 0.05$), and the significant upregulation of the marker of stemness ALDH ($p< 0.05$). Therefore, TF1a was selected for in-depth investigations to model dormancy in leukaemia cells with stemness characteristics. It is worth mentioning that no molecular feature in TF1-a was considered for investigation that can charecterize this cells among the other 3 candidate AML cell lines for modelling dormancy in AML .

### 3.2.10. TGFβ1-treated TF1-a cells showed additional feature of dormancy

It has been reported that as the cells enter the cell cycle from quiescence, their RNA content increases (Ladd, Pyatt *et al.* 1997). Therefore, cells with lower RNA content might be in G0 phase of the cell cycle if compared to their proliferating counterparts. In the current study, the total RNA content was assessed in TF1a cells using the nanodrop following RNA extraction. In comparison to proliferating counterparts, TF1a cells induced to dormancy by TGFβ1 treatment showed a

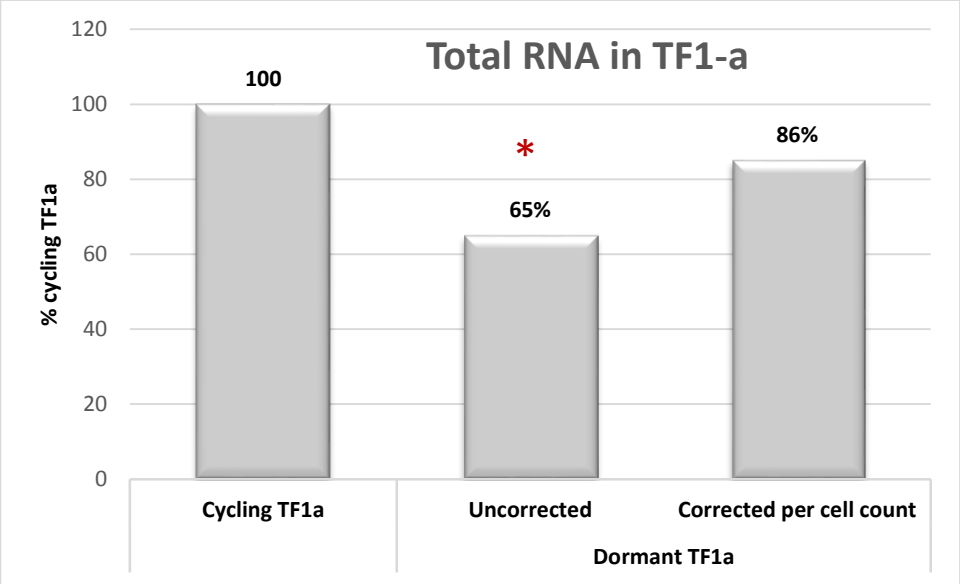



**Figure 3.12: Total RNA content in TF1-a before (Cycling TF1-a) and after (Dormant TF1-a) 3 days culture with 4ng/ml of TGFβ1.** The percentages represent the mean figure for 3 independent biological replicates. (*: $p < .05$).

decline in total RNA content from a mean value of 1181.1 ng/ml to 768.7 ng/ml (35% decrease) ($p<0.05$) which represented a decrease from a mean value of 45 ng/ml to 30 ng/ml (14% decrease) 10^5 cells (figure 3.12). However, the corrected figure per cell count was statistically non-significant.

### 3.2.11. TGFβ1 treatment up-regulates stemness-related markers in TF1-a cells

The effect of the TGFβ1 treatment on the expression of the marker of stemness (CD34) and the enzyme protein (ALDH) was studied by flow cytometry. Furthermore, immunofluorescence study was used to investigate the effect of the treatment on FOXO3a subcellular localization. FOXO3a is a member of a family of transcription factors that are believed to cooperate with TGFβ1 in maintaining leukaemia initiating cells (Naka, Hoshii *et al.* 2010). Moreover, FOXO3a was found to act as a tumour suppressor by regulating cell cycle progression (Schmidt, Fernandez de Mattos *et al.* 2002).

#### 3.2.11.1. CD34 expression modulation by TGFβ1 on TF1-a cells

CD34 expression showed a remarkable increase in TF1-a cells in response to culture with 4ng/ml TGFβ1. It increased from approximately half of the cells to up to 90% after treatment (figure 3.13; panels A, B, and C). In dual-staining for CD34 and Ki-67, CD34+ subpopulation showed higher Ki-67 staining than the CD34- subpopulation of untreated TF1-a cells (figure 3.13; panels A) whilst the reverse was true for CD71 expression when the untreated CD34+ TF1-a cells demonstrated lower CD71 expression than that for the untreated CD34- TF1-a cells (figure 3.13; panel B). Nevertheless, both TF1-a subpopulations expressed similar overall Ki-67 and CD71 expression responses following TGFβ1 treatment.

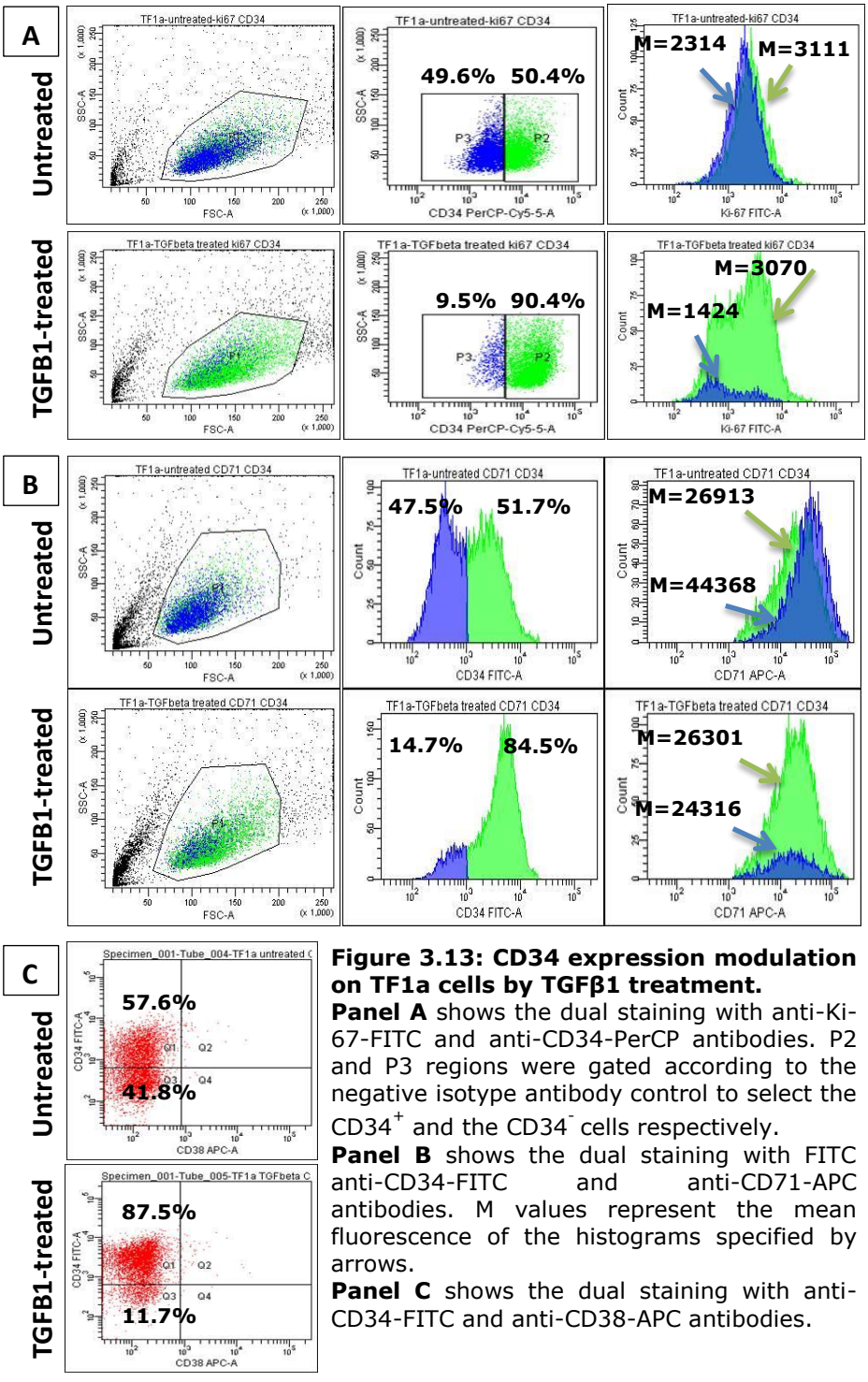



**Figure 3.13: CD34 expression modulation on TF1a cells by TGFβ1 treatment.**
**Panel A** shows the dual staining with anti-Ki-67-FITC and anti-CD34-PerCP antibodies. P2 and P3 regions were gated according to the negative isotype antibody control to select the $CD34^{+}$ and the $CD34^{-}$ cells respectively.
**Panel B** shows the dual staining with FITC anti-CD34-FITC and anti-CD71-APC antibodies. M values represent the mean fluorescence of the histograms specified by arrows.
**Panel C** shows the dual staining with anti-CD34-FITC and anti-CD38-APC antibodies.

3.2.11.2. FOXO3a subcellular localization modulation by TGFβ1 in TF1-a cells

The function of the transcription factor FOXO3a is linked to stemness and/or cell cycle control in HSCs and LSCs and is believed to be regulated by its subcellular localization (Naka, Hoshii *et al.* 2010). It is activated by phosphorylation inside the nucleus where it regulates several target genes, whereas it will be inactivated in response to various extracellular stimuli by translocation into the cytoplasm ((Sakoe, Sakoe *et al.* 2010) and references therein). Importantly, the active FOXO3a was reported to maintain leukemic cells through TGFβ1 pathway-related regulatory interaction (Naka, Hoshii *et al.* 2010).

In this study, TGFβ1 treatment relocated FOXO3a in TF1a cells; mostly cytoplasmic FOXO3a in untreated cells was translocated to be mostly nuclear in response to 3 days culture with 4ng/ml TGFβ1 (figure 3.14). Nuclear localization of FOXO3a might indicate its activation.

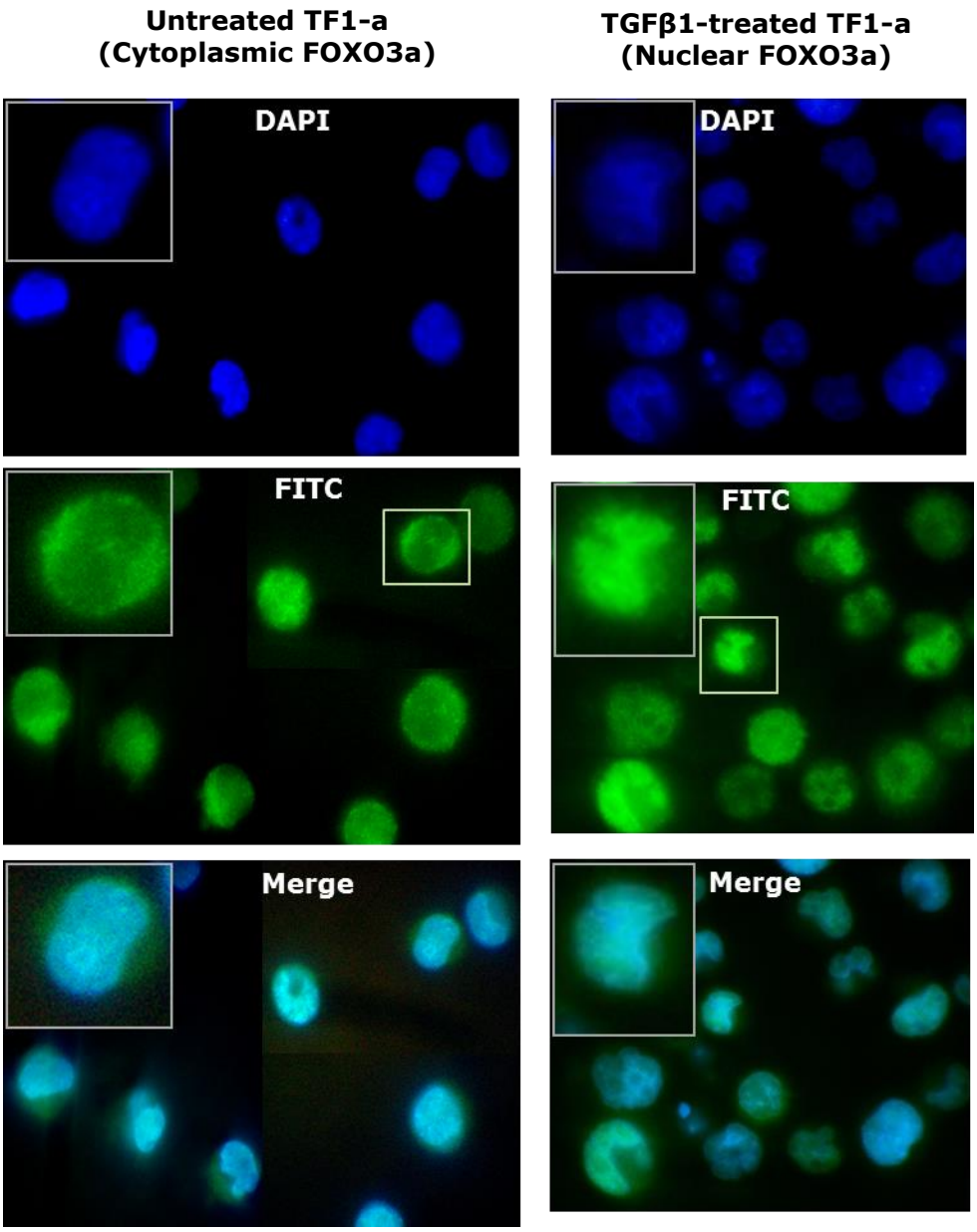



**Figure 3.14: Immunofluorescence microscopy for the subcellular localization of FOXO3a protein in TF1-a cells.** The left panel shows that FOXO3a is mainly cytoplasmic in the untreated (proliferating) TF1-a cells, while a considerable nuclear translocation can be noticed in response to 3 days treatment with 4ng/ml of TGFβ1 (right panel). The pictures are a representative example of two independent experiments that showed similar results

## 3.3. Discussion

The current scientific knowledge supports that the leukemic clone arranged in a hierarchal way of differentiation similar to the normal haematopoietic cells ((Mosna and Gottardi 2016) and references therein). In such arrangement, $CD34^+$ AML cells were thought to be the cells that possess the regenerative potential that precipitates relapse in AML (Gerber, Smith *et al.* 2012). In this study, three out of the four selected AML cell lines were positive for the surface marker CD34 in a variable degree of expression (figure 3.2; panel A). This was associated with variable co-expression of the differentiation marker CD38. It is believed that $CD34^+CD38^-$ cells are considered higher in the hierarchy than the $CD34^+CD38^+$ cells; whereas, the $CD34^-CD38^+$ cells come lower than the later (Mosna and Gottardi 2016). Consequently, TF1a seems to express the most primitive phenotype among the 4 studied cell lines while M0-91 was the lowest according to the proposed myeloid differentiation hierarchy.

As regards CD117 expression, Kasumi-3 was the only cell line that was associated with high expression of this surface receptor protein. M0-91, TF1-a, and KG-1a, on the other hand, showed low CD117 expression. It has been suggested that $CD117^{low}$ cells which are positive for CD34 are more primitive and possess stronger repopulating potential both *in vitro* and *in vivo* than those with double positivity for these two stem cell markers (Blair and Sutherland 2000). Consequently, TF1a and KG1a could be regarded, phenotypically, more primitive than Kasumi-3.

In normal haematopoiesis the loss of ALDH activity is an early indicator of differentiation and it has been reported to happen in $CD34^+$ primitive normal haematopoietic cells just shortly after the acquisition of the $CD38^+$ phenotype(Christ, Lucke *et al.* 2007). In contrast, recent evidence support the fact that ALDH activity in leukaemia stem cells from AML and CML patients showed a considerable variability and not all LSCs where positive to the ALDH1A1 gene

coding for ALDH expression (Bogen, Buske *et al.* 2017). Nevertheless, the AML cells with intermediate ALDH expression ($CD34^{+}$ $CD38^{-}$ $ALDH^{Int}$) were reported to be responsible for tumour relapse as this subclone of leukemic cells was found to be highly represented in minimal residual disease samples following chemotherapy in AML (Gerber, Smith *et al.* 2012). Interestingly, TF1a showed an intermediate activity of the enzyme ALDH which was between the $ALDH^{Low}$ cells (KG1-a and M0-91) and the $ALDH^{High}$ cells Kasumi-3.

In this study, it was an essential differential point to test the four candidates AML cell lines for their response to the inhibitory signals of TGFβ1 in order to choose which one is suitable for further investigations. Both TF1-a and M0-91 were previously reported to express a positive response to the inhibitory signals of the exogenous TGFβ1 (Hu, Moscinski *et al.* 1998, Scandura, Boccuni *et al.* 2004); whereas no previous reports have investigated the effect of this cytokine on the proliferation of Kasumi-3 and KG-1a leukaemia cells. In agreement with the reported inhibitory role of TGFβ1, the proliferation of the four studied cell lines was inhibited by TGFβ1 treatment but with a variable degree of significance (figure 3.3). KG-1a cell line, for instance, showed the lowest and statistically non-significant growth inhibition if compared to the other cell lines, therefore, it was excluded from further investigations. On the other hand Kasumi-3, TF1-a, and M0-91 were significantly inhibited by 3 days culture with 4ng/ml of TGFβ1.

In this study, serum-free medium (SFM) culture system was investigated in maintaining the 3 AML cell lines M0-91, TF1-a and Kasumi-3. Indeed, SFM *in vitro* culture has been occasionally previously used in AML cell line (Bruserud, Gjertsen *et al.* 2000). In contrast, SFM was primarily the culture of choice for primary (native) normal and malignant haematopoietic cells as these cells showed better survival in published works (Levesque, O'Loughlin *et al.* 2001) and in our lab also. Indeed, the SFM; Stemspan, which was employed in this study, has been widely

used for the *in vitro* maintenance of HSCs (Lechman, Gentner *et al.* 2012) and primary AML cells with minimal influence on cellular viability and characteristics (Houtenbos, Westers *et al.* 2003). Importantly, several *in vitro* systems have considered serum withdrawal for modelling dormancy in primary non-transformed cells (Coller, Sang *et al.* 2006, Oki, Nishimura *et al.* 2014). Experiments in this study, nevertheless, consistently uncovered that serum withdrawal was associated with poor survival of the 3 investigated AML cell lines. Clearly, M0-91 was addicted to the presence of serum in the culture medium when the survival of this cell line, remarkably, deteriorated in the Stemspan medium (figure 3.3; panel A). Similarly, TF1-a and Kasumi-3 cells showed a significant reduction in viability (confirmed by AnnexinV/PI assay (figure 3.4)) despite the continuous proliferation of these cells in SFM (figure 3.3; panels B and C). Consequently, the conclusion was that the SFM was not suitable for the *in vitro* maintenance of the candidates AML-cell lines and hence the ordinary SCM was used as the standard culture system for the *in vitro* modelling of dormancy.

TGFβ1 was reported to play a key role in proliferation inhibition in AML cells (Hu, Moscinski *et al.* 1998, Scandura, Boccuni *et al.* 2004), in haematopoietic stem cells (Fortunel, Hatzfeld *et al.* 2000, Fortunel, Hatzfeld *et al.* 2000), and in dormancy regulation in cancer cells (Bui, Laurent *et al.* 2015). This study demonstrates the role of TGFβ1 in inducing quiescence in 4 AML cell lines, namely; TF1-a, KG1-a, Kasumi-3, and M0-91.

Indeed, various mechanisms were suggested to explain the escape of leukaemic cells from the inhibitory signals of TGFβ1 such as the mutation in the TGFβ signalling pathway members and the disruption of this pathway by oncoproteins, such as EVI1 (Kurokawa, Mitani *et al.* 1998, Dong and Blobe 2006). Kasumi-3, for example, showed the lowest significant growth inhibition (figure 3.3) which might be explained by the fact that it has a high EVI1 expression which is believed to

block the inhibitory effect of TGFβ1 by forming complexes with the Smad3 member of the TGFβ1 canonical pathway (Kurokawa, Mitani *et al.* 1998, Kurokawa, Mitani *et al.* 1998). Moreover, Kasumi-3 baseline proliferation rate was considerably slow, if compared to the other 3 growth factor-independent AML cell lines, which might be related to several factors; Kasumi-3 was found to have considerable endogenous angiopoietin production, a cytokine believed to contribute to quiescence in EVI1high leukaemia cells (Ichihara, Kaneda *et al.* 2011). Furthermore, EVI1 overexpression in Kasumi-3 was found to interfere with cellular proliferation and accumulating cells within the G0/1 phase of the cell cycle (Karakaya, Herbst *et al.* 2012). More importantly, the suggested role of endogenous TGFβ1 in the cell cycle arrest of $CD117^{high}$ human BM $CD34^{+}CD38^{-}$ cells (Morita, Yamamoto *et al.* 2003) might also explain the slow proliferation of Kasumi-3 as it possesses a high CD117 expression. Consequently, the survival of Kasumi-3 in a very low proliferation resulted in a negligible additional growth inhibition by the exogenous TGFβ1 used in this study; making Kasumi-3 not the best choice for the proposed *in vitro* dormancy model that largely rely on the significant contrast in the rate of proliferation and dormancy markers expression between untreated cells and their counterparts cultured with TGFβ1.

As regards M0-91 cells, this cell line was the only one that showed statistically significant increase in the CDKI p57 (figure 3.8). However, the p57 upregulation by TGFβ1 seems to be transient as it was only significant within up to 4 hours of treatment if compared to 24 of TGFβ1 treatment when it declined back to nearly the starting level before treatment. Furthermore, M0-91 cells showed a very rapid baseline proliferation rate with an approximate doubling time of 18 hours. Moreover, despite the statistically significant growth inhibition by TGFβ1 treatment, M0-91 continued to show a considerable increase in cell count to a mean value of approximately 15 x 10^5 cells/ml from initially seeded cell count at 2 x 10^5 cells/ml; which is approximately 3 doubling times (figure 3.3). This

was associated with both slight increase in the proportion of Ki-67 negative cells (figure 3.9) and a non-significant decrease in CD71 expression (figure 3.10). By considering the CD34 negativity of M0-91, however, TGFβ1 inhibitory effect seems to cover a wide range of AML cells regardless their CD34 status. Collectively, M0-91 features of proliferation and dormancy markers expressions post-TGFβ1 treatment were inferior to that of TF1-a cells for the *in vitro* model of dormancy in AML.

TF1-a cells showed the most significant ($p<0.001$) growth inhibition by TGFβ1 treatment. This was in agreement with Xiaotang Hu *et al.* findings, who reported a dose-dependent growth inhibition in TF1-a after TGFβ1 treatment when the maximal inhibition was obtained at concentrations of 1–10 ng/ml (Hu, Moscinski *et al.* 1998). TF1-a proliferation inhibition, in this study, was also associated with the largest increase in the proportion of Ki-67 negative cells (cells in the G0 phase of the cell cycle) if compared to Kasumi-3 and M0-91. Similarly, the decline in the proliferation marker CD71 was mostly on TF1-a cells.

Treatment with TGFβ1 clearly resulted in leukaemia cells growth inhibition without affecting cell viability as there was no increase in early and late apoptotic cells in all treated AML cell lines. This was consistent with the finding of Batard P. *et al.* (2000) who reported that TGFβ1 reversibly inhibits growth without inducing detectable cell death in $CD34^+$ haematopoietic umbilical cord progenitors (Batard, Monier *et al.* 2000). Indeed, TGFβ1 was found to exert an anti-apoptotic effect in AML cells against chemotherapeutic agents such as AraC (Tabe, Shi *et al.* 2013).

The modulation of the stem cell markers CD34 and ALDH in TF1-a cells by TGFβ1 could reflect the pleiotropic effect of this cytokine. The significant upregulation of CD34 on TF1-a cells was consistent with previously reported findings. Indeed, it has been reported that TGFβ1 maintains human $CD34^+$ haematopoietic progenitors in a state of non-differentiation and that depletion of TGFβ1 stimulates

differentiation in association with CD34 reduction (Pierelli, Marone *et al.* 2002). Moreover, it was reported that TF1 cells (the mother cell line of TF1-a) showed an increase in CD34 expression following TGFβ1 treatment at a concentration of 5ng/ml (Marone, Scambia *et al.* 2002, Pierelli, Marone *et al.* 2002). Similarly, it has been found that TGFβ1 up-regulated CD34 expression on $CD34^+$ cells isolated from the umbilical cord (Batard, Monier *et al.* 2000).

For the best of our knowledge, no previous study reported the induction of ALDH by TGFβ1 in AML cells. This finding might uncover an additional role for TGFβ1 in driving resistance feature in AML cells as ALDH expression was linked to drug resistance in cancer stem cells (Huang, Tsai *et al.* 2013, Januchowski, Wojtowicz *et al.* 2013, Raha, Wilson *et al.* 2014). For example, it has been reported recently that a drug-tolerant subpopulation of gastric cancer cells showed high ALDH expression that protects them from the toxic effects of the increased reactive oxygen species (ROS) levels by chemotherapy (Raha, Wilson *et al.* 2014).

To sum up, as a model for studying dormancy in AML, TF1-a cells appears to be the most suitable among the 4 candidates cell lines in terms of the degree of growth inhibition, the cell viability after treatment, the reduction of the proliferation marker Ki-67 and CD71 in addition to the up-modulation of the markers of stemness, CD34, ALDH, and FOXO3a. Nevertheless and despite the significant growth inhibition, about half of the treated TF1-a cells retained the expression of Ki-67 which might suggest the heterogeneity of myeloid leukemic cells in their response to TGFβ1 inhibitory stimuli or it might highlight the need for further *in vitro* conditioning to augment the TGFβ1 effect on leukaemia cell proliferation.

# CHAPTER FOUR
# mTOR PATHWAY INHIBITION AUGMENTS THE TGFB1-DEPENDENT DORMANCY FEATURES IN TF1-a LEUKAEMIA CELLS

## 4.1. Background

TF1-a cells induced to dormancy by TGFβ1 continued to show significant proliferation and Ki-67 positivity. This drove us to search for further *in vitro* conditioning to potentiate the TGFβ1 effect by mimicking the bone marrow endosteal niche features regulating AML dormancy.

Accumulating data have demonstrated that leukaemia cells which are responsible for relapse AML, similar to the HSCs, reside in a low perfusion microenvironment in the endosteal region of the bone marrow (Ishikawa, Yoshida *et al.* 2007, Winkler, Barbier *et al.* 2010, Kunisaki, Bruns *et al.* 2013, Morrison and Scadden 2014, Itkin, Gur-Cohen *et al.* 2016). The scarcity of nutrients in the poorly-perfused niche could contribute to leukaemia cell dormancy and resistance to chemotherapy as they survive in a low metabolic state that protects them from chemotherapeutic agents targeting metabolically active cells (Ishikawa, Yoshida *et al.* 2007).

The mTOR (mammalian target of Rapamycin) pathway is believed to be constitutionally active in cycling cancer cells and is largely regulated by the level of the extracellular nutrients (Zoncu, Efeyan *et al.* 2011). Moreover, it has been reported that mTOR pathway regulates several cellular functions including nutrient uptake (Chen, Liu *et al.* 2008); hence it is regarded as a nutrients sensor pathway in cancer and other cells (Fingar and Blenis 2004, Jewell and Guan 2013, Blagosklonny 2014).

More importantly, mTOR inhibition by Rapamycin was used as a strategy for the *in vitro* maintenance of the haematopoietic stem cells (Huang, Nguyen-McCarty *et al.* 2012) and, recently, for the *in vitro* induction of stemness characteristics in T-cells (Scholz, Jandus *et al.* 2016). Furthermore, it has been reported that mTOR-inhibited leukaemia cell lines (Pallis, Burrows *et al.* 2013) and prostatic cancer cells (Kim, Jung *et al.* 2013) showed feature of dormancy and resistance to

chemotherapy. Finally, a combination of mTOR inhibition with TGFβ1 was reported to potentiate the inhibitory effect of TGFβ1 in transformed cells (Law, Chytil *et al.* 2002).

Therefore, we aimed to investigate inhibiting the mTOR pathway by Rapamycin to mimic the scarcity of nutrients that characterises the LICs endosteal niche in an attempt to mimic the bone marrow microenvironment that surrounding dormant leukaemia initiating cells.

This chapter will demonstrate the added benefit of the mTOR pathway inhibition to the TGFβ1-dependent induction of dormancy model in the selected leukaemia cell line TF1-a.

## 4.2. Results

### 4.2.1. The mTOR inhibition by Rapamycin augments TF1-a growth inhibition by TGFβ1 without detrimentally affecting cellular viability

In our lab, Rapamycin in a dose of 100mM was optimised to model dormancy in the leukaemia cell line KG-1a (Pallis, Burrows *et al.* 2013). Consequently, this dose was chosen in this study to treat TF1-a cells. Culturing TF1-a cells with the two inhibitors together (TGFβ1 and Rapamycin) resulted in a highly significant growth inhibition which was synergistic (CDI=0.9) and statistically significant if compared to the growth inhibition following TF1-a cultured with TGFβ1 alone (figure 4.1). The inhibition of TF1-a proliferation by inhibiting the mTOR pathway only, nevertheless, was not superior and statistically non-significant to the growth inhibition of this cell line by TGFβ1.

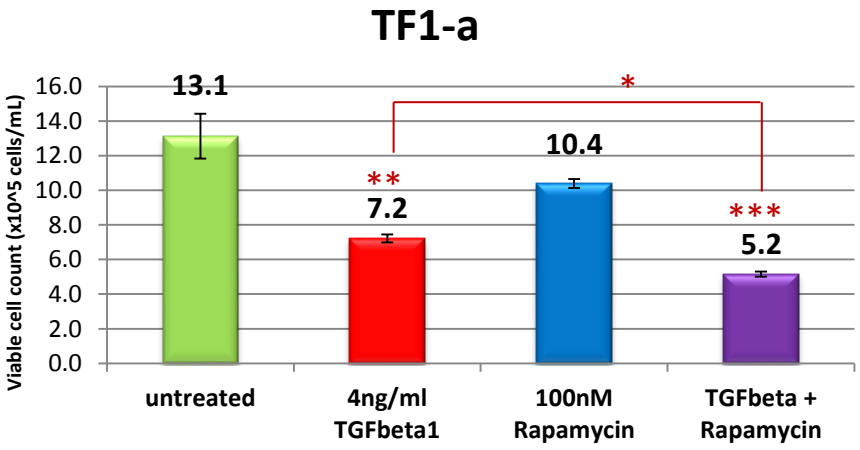



**Figure 4.1: The inhibitory effect of TGFβ1+Rapamycin combination on the TF1-a cell line growth.** The cells were seeded at a concentration of 2x10^5 cells/mL and incubated for 72 hrs. The columns represent mean values of three independent experiments (*: $p < .05$; **: $p < .01$; ***: $p < .001$). The error bars represent +/- 1SD.

The effect of Rapamycin treatment on TF1-a was validated by measuring the expression of the mTOR pathway downstream effector phosphorylated ribosomal protein S6 (p-rpS6) using flow cytometry. Rapamycin has remarkably inhibited the mTOR pathway at the dose of 100mM which was confirmed by the significant

decline in the level of the p-rpS6 in TF1-a cells cultured with Rapamycin if compared to the untreated counterparts; from 35.4 to 1.6 RFU ($p < .001$) (figure 4.2).

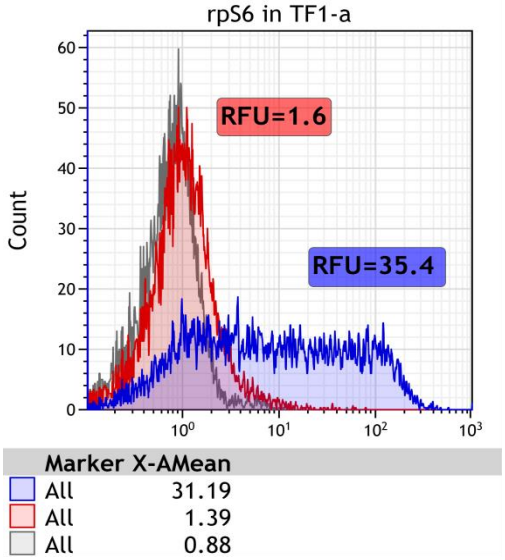



**Figure 4.2: The expression of the phosphorylated ribosomal protein S6 (rpS6) in TF1-a cells** cultured in the presence (red histogram) or absence (blue histogram) of 100mM of Rapamycin. Cells treated with Rapamycin + U0126 ERK-inhibitor (grey histogram) was used as a negative control to determine the minimal baseline expression of rpS6. This figure is an example of 3 biological replicates showed similar results.

More importantly, the addition of mTOR inhibition by Rapamycin to potentiate the TGFβ1 treatment showed no detrimental effect on TF1-a cells viability as the Annexin V-PI flow cytometry result illustrates (figure 4.3). It is clear that the proportion of viable TF1-a cells (Annexin V and PI double negative events) was similar in TF1-a cells cultured with each of the two inhibitors alone or in combination if compared to the untreated counterparts (90.41%, 92.43%, 91.04%, and 93.25% for untreated, TGFβ1-treated, Rapamycin-treated, and TGFβ1+Rapamycin-treated TF1-a cells respectively). Interestingly, it could be noticed that the treated TF1-a cells showed a slight increase in viable cell count which was associated with a slight decrease in apoptotic and dead cells if compared to the untreated cells (figure 4.3).

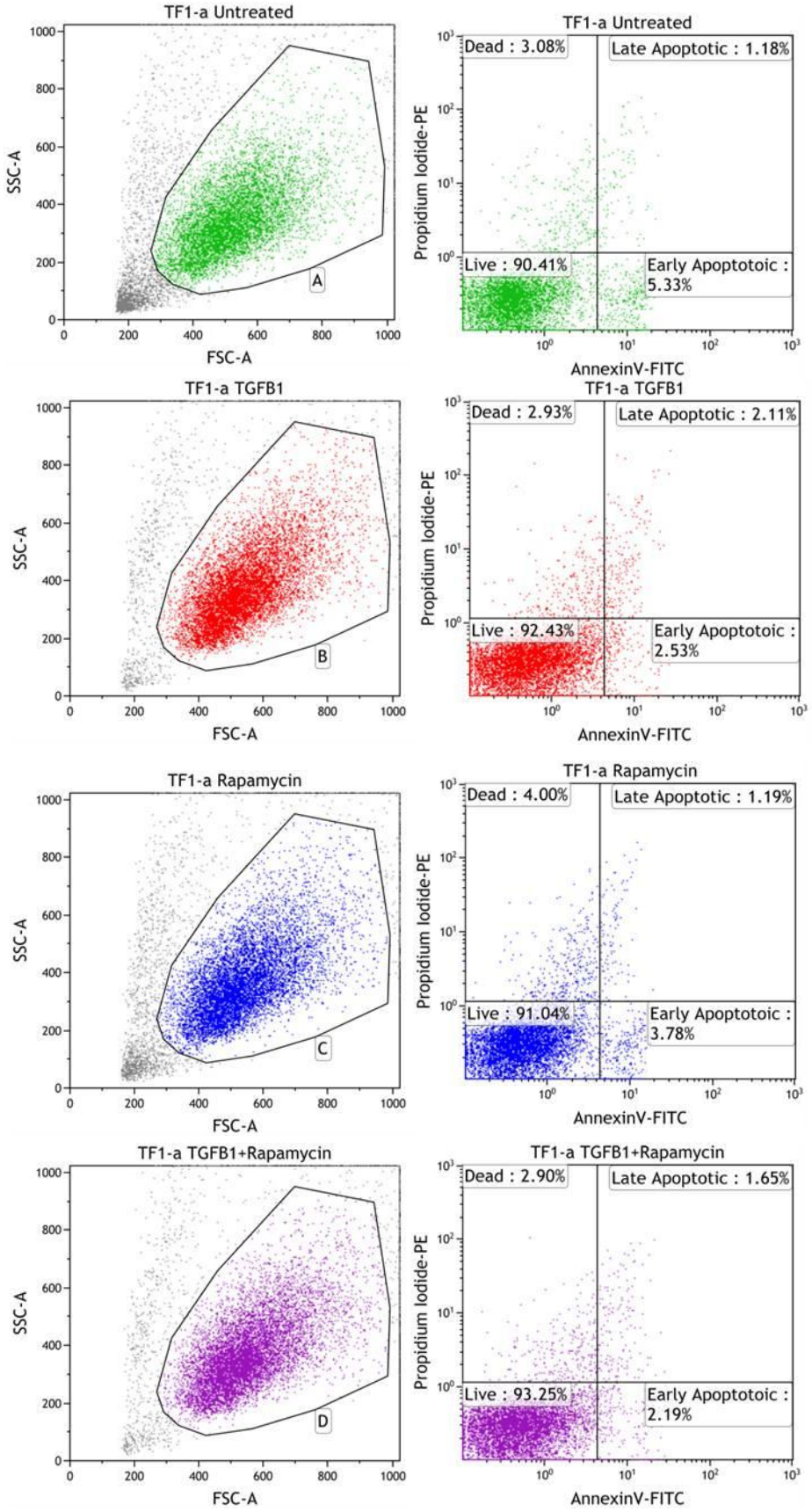



**Figure 4.3: TF1-a cells viability after 3 days culture with 4ng/ml of TGFβ1 or 100nM of Rapamycin or both.** The cells were probed with AnnexinV and Propidium Iodide at the end of the incubation period and subjected to flow cytometric analysis. The plots are representative examples of two independent experiments that showed similar results.

### 4.2.2. Combining mTOR inhibition with TGFβ1 enhances features of dormancy in TF1a cells

Despite the significant improvement in growth inhibition of TF1-a cells by the combination of mTOR inhibition and TGFβ1, it was crucial to ensure that the presence of the two growth inhibitors together did not alter features of dormancy on which TF1-a cells has been selected among the other 3 AML cell lines. Therefore, Ki-67 and CD71 expression in addition to the total RNA contents in TF1-a cell line were investigated following the addition of rapamycin to TGFβ1 treatment.

#### 4.2.2.1. CD71 expression modulation on TF1-a cells induced to dormancy by TGFβ1 and Rapamycin

In line with the trend of growth inhibition (section 5.2.1), the expression of CD71 on TF1-a cells showed a significant decline after culture with TGFβ1 or TGFβ1 + Rapamycin (from 48 to 32 RFU and to 29 RFU mean values respectively ($p < .01$)) (figure 4.4). Rapamycin alone, however, has non-significantly lowered the CD71 expression on TF1-a cell surface when it was used by its own (figure 4.4). The effect of the combination treatment on CD71 expression was additive in nature if compared to the effect of each agent alone (CDI=1).

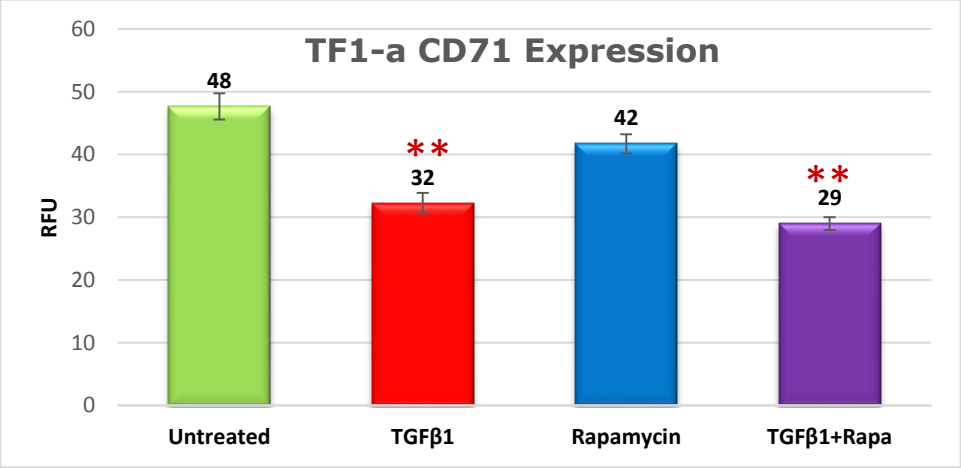



**Figure 4.4: The effect of TGFβ1 and Rapamycin treatment on the CD71 expression on TF1-a cells surface membrane.** The cells were seeded at a concentration of 2x10^5 cells/mL and incubated for 72 hrs. The columns represent mean values of three independent experiments (**: $p < .01$). The error bars represent +/- 1SD.

#### 4.2.2.2. Ki-67 expression modulation in TF1-a cells induced to dormancy by TGFβ1 and Rapamycin

The marked and significant increase in Ki-67 negative (dormant) TF1-a cells which was found following TGFβ1 treatment (section 3.2.8.1), was augmented by combining it with the mTOR inhibition by Rapamycin. In one experiment, for example, the proportion of Ki-67 negative TF1-a cells was increased from 6% in untreated cells to 50% after 3 days culture with the two inhibitors. However, the effect of the combination treatment on Ki-67 expression was additive in nature if compared to the effect of each agent alone (CDI=1). Notably, TGFβ1 treatment was the main player in this context as Rapamycin treatment alone showed a smaller increase in Ki-67 negative cells if compared to TGFβ1 treatment alone (from 6% to 18% and from 6% to 42% respectively) (figure 4.5).

#### 4.2.2.3. Total RNA concentration modulation in TF1-a cells induced to dormancy by TGFβ1 and Rapamycin

It was evident that TF1-a cells induced to dormancy have shown less total RNA content after TGFβ1 treatment (section 3.2.10). The decrease, nevertheless, was statistically non-significant, if corrected to the cell count, which could reflect the need for a further conditioning as dormant cells are supposed to survive with the minimal metabolic activity which is logically associated with low RNA contents.

Mimicking the scarcity of nutrients by inhibiting the mTOR pathway was associated with a marked decrease in the amount of the total RNA inside the TF1-a cells as proven by the nanodrop measurement of total RNA concentration extracted from the cell lysate. This decrease was statistically significant when corrected for the number of cells harvested if the mTOR inhibition was used in combination with TGFβ1 treatment (from 45 ng/ml to 30 ng/ml mean values of RNA for each 10^5 TF1-a cells ($p < .05$)) (figure 4.6). The effect of the combination treatment on the total RNA concentration was additive in nature if compared to the effect of each dormancy inducer alone (CDI=1).

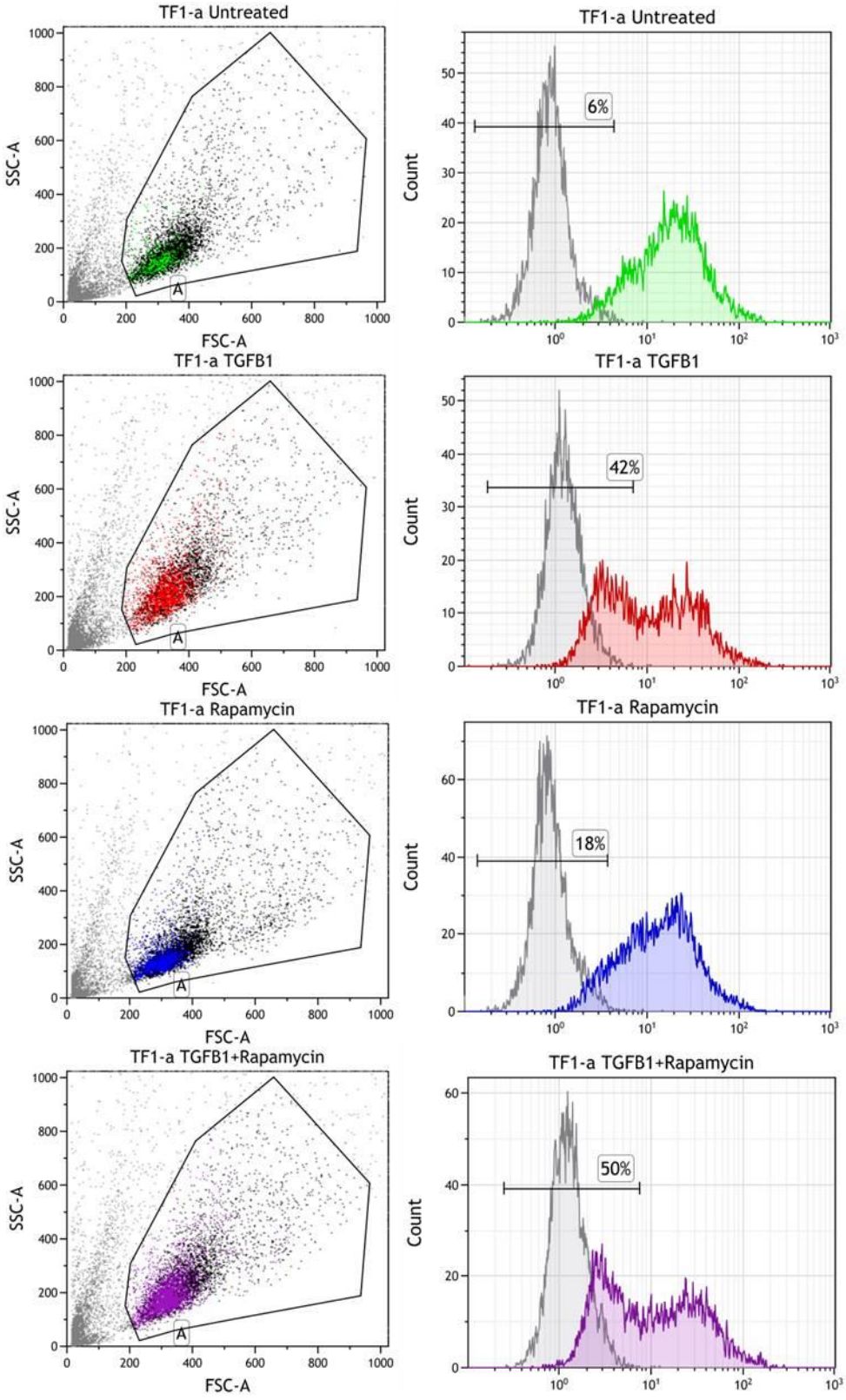



**Figure 4.5: Ki-67 expression in TF1-a cells induced to dormancy.** The histograms show untreated TF1-a cells (green histogram) and TF1-a cells treated with 4ng/ml of TGFβ1 (red histogram) or 100nM Rapamycin (blue histogram) or both (purple histogram) for 3 days. FITC Mouse IgG1 isotype control (grey histograms) was used as a reference to determine the Ki-67 negative cells (the percentages on the histograms). The figure is a representative example of 3 biological replicates that showed similar results.

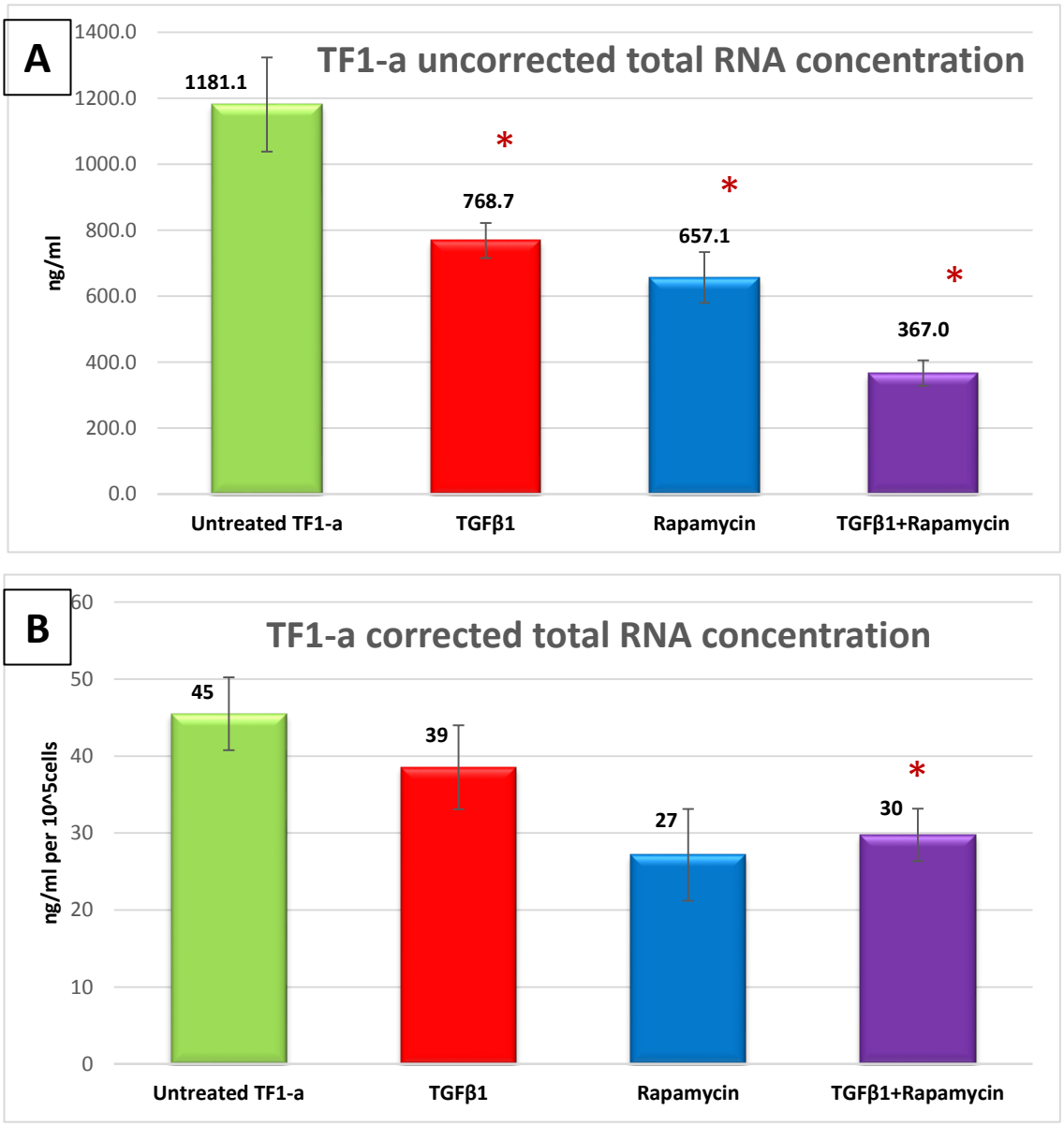



**Figure 4.6: Total RNA content in TF1-a cells induced to dormancy.** The figure shows total RNA in cells before (cycling TF1-a) and after (dormant TF1-a) 3 days culture with 4ng/ml of TGFβ1 or 100nM of rapamycin or Both. Panel A shows the total RNA concentration extracted from the whole TF1-a cells harvested at the end of the incubation time; whereas panel B illustrates the same figures of total RNA concentrations corrected by the cell count. The columns represent mean values of three independent experiments. The error bars represent

### 4.2.3. TF1-a cells induced to dormancy did not show signs of differentiation

It is believed that cellular proliferation potential decreases in the haematopoietic cells hierarchy as they differentiate. Therefore, it was vital to exclude the possibility of induction of differentiation, following the *in vitro* conditioning of TF1-a cells by TGFβ1 and/or rapamycin, as a cause for the inhibition of proliferation.

Following culture with TGFβ1 and/or the mTOR pathway inhibitor Rapamycin, TF1-a has maintained the primitive morphology with no signs of differentiation; this was confirmed by investigating the TF1-a cells morphology in smears stained with Wright-Giemsa stain.

In response to culture with the two inhibitors, TF1-a cells became smaller in size, less in nuclear convolutions with more conspicuous nucleoli, and lower in the amount of the cytoplasmic and cytoplasmic basophilia; the decrease in cytoplasmic basophilia could reflect the decrease in RNA content (section 4.2.2.3). Furthermore, there were no morphological features indicating differentiation such as nuclear lobation, chromatin condensation, and cytoplasmic granulation or vaculation which could be seen in differentiated haematopoietic or AML cells (figure 4.7).

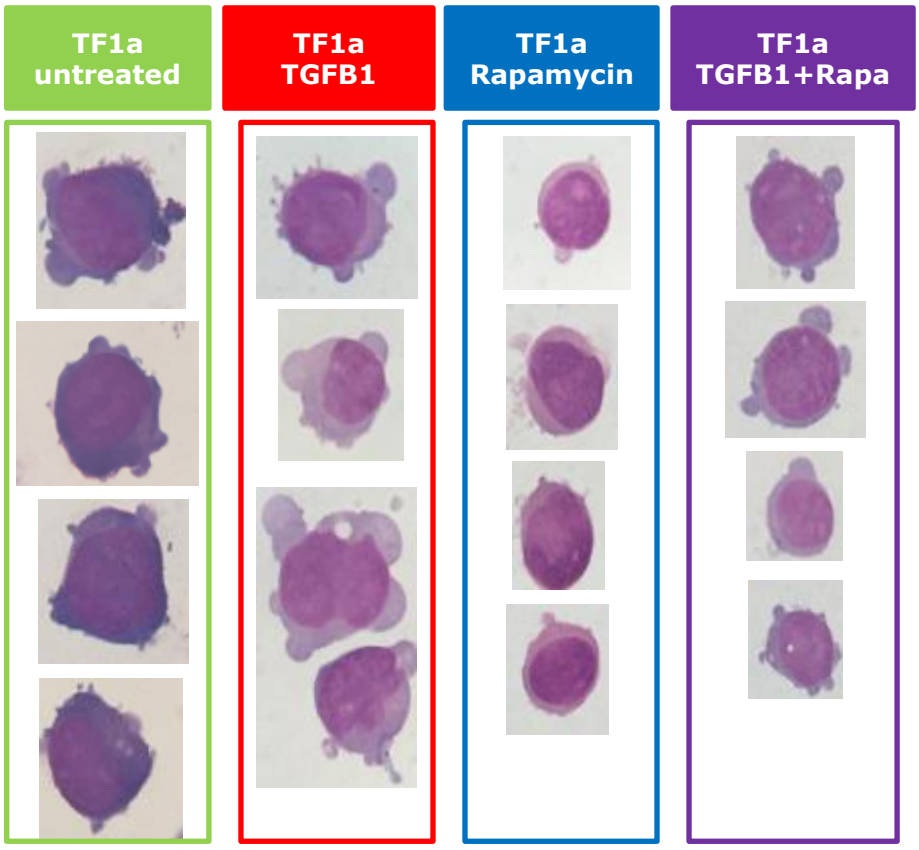



**Figure 4.7: TF1-a Cell line Morphology before (Cycling TF1-a) and after (Dormant TF1-a) 3 days culture with 4ng/ml of TGFβ1 or 100nM of rapamycin or Both.** Air-dried smears of TF1-a cells of each condition were staining with Wright-Geimsa stain and examined and pictured using Olympus fluorescence microscope adjusted as a light microscope. Images were processed with Image J software.

## 4.3. Discussion

Among the many features that contribute to the maintenance of dormancy in haematopoietic stem cells and leukaemia initiating cells and besides the excess of TGFβ1, the low perfusion was frequently reported to characterize this sub-compartment of the bone marrow (Kunisaki, Bruns *et al.* 2013, Itkin, Gur-Cohen *et al.* 2016). Indeed, it has been suggested that the cells' potential to proliferate varies between those cells live in the highly perfused perisinusoidal BM niche, where the proliferating HSCs and leukaemia cells localize, from those live in the limitedly-perfused endosteal niche, where the dormant HSCs and LICs resides. Moreover, the low perfusion in the endosteal region makes the HSCs and LICs adapted to live in a low nutrient microenvironment with inhibited activity of the nutrient sensor pathway the mTOR pathway.

The data in this chapter clearly demonstrates the usefulness of adding the mTOR pathway inhibitor rapamycin to the exogenous TGFβ1 in inducing dormancy in TF1-a cells. These leukaemia cells showed further statistically significant reduction in proliferation, CD71 expression, and total RNA contents; with an additional increase in Ki-67 negative cells following 3 days culture with TGFβ1 and rapamycin.

The selected dose of rapamycin was sufficient to reduce the expression of the constitutively active protein p-rpS6 to the minimum indicating that TF1-a cells survived with very low mTOR activity. Interestingly, this condition had no detrimental consequences on the viability of TF1-a cells. Indeed, TF1-a cells showed a slight increase in the proportion of the viable cells if compared to the untreated counterparts. It has been reported that the undifferentiated AML cells, unlike the differentiated ones, are not dependent for their survival on the presence of the mTORC1 complex activity (rapamycin main mTOR complexes target) (Hoshii, Tadokoro *et al.* 2012). This could explain the survival of the

undifferentiating TF1-a cells in culture with the mTORC1 inhibitor rapamycin if the stemness features of this cell line have been taken into consideration. Moreover, mTORC2 complex, which is reported to be involved in cellular survival (Li, Kim *et al.* 2014) has been found to remain active in cells treated with rapamycin that mainly attenuating the mTORC1 complex activity (Li, Kim *et al.* 2014).

More importantly, the addition of mTOR pathway inhibition to TGFβ1 potentiated the dormancy feature of TF1-a cells. This was especially true in regards to the total RNA contents which showed significant reduction (section 4.2.2.3). Nevertheless, the effect of rapamycin alone was inferior to TGFβ1 alone in terms of inhibiting TF1-a proliferation and suppressing the expression of the cell cycle markers Ki-67 and CD71; this highlights the fact that TGFβ1 was the main player in inducing features of dormancy in TF1-a cells.

To conclude, the results of chapters three and four paved the way for the establishment of the *in vitro* dormancy model in AML cells with features of stemness. This achieved by the *in vitro* culturing of TF1-a cells with 4ng/ml of TGFβ1 and 100nM of rapamycin for 3 days. Dormant TF1-a cells were subjected, thereafter, to two lines of investigations. The first one was to study its molecular signature by whole human genome gene expression profiling (GEP) to identify the group of genes differentially upregulated in dormant TF1-a cells in comparison to their cycling counterparts (chapter five). The second line of investigations was to study TF1-a cells surviving a prolonged sub-lethal genotoxicity using one of the commonly used antileukaemic drugs etoposide before comparing its molecular signature to the molecular signature of TF1-a induced to dormancy in attempt to investigate the induction of molecular dormancy in these cells (chapter seven).

# CHAPTER FIVE

# MOLECULAR SIGNATURE OF DORMANCY IN THE $CD34^{+}CD38^{-}$ ACUTE MYELOID LEUKAEMIA CELLS TF1-a

## 5.1. Background

Dormant AML cells have been identified in the bone marrow (BM) endosteal region which is characterised by an excess of TGFβ1 and a shortage of nutrients. We developed and characterized an *in vitro* model of AML cell dormancy by exploiting these features. TF1-a cells were selected for this purpose as they showed significant inhibition of proliferation with features of dormancy in response to 72 hours culture with TGFβ1 and mTOR pathway inhibition; the later mimics major effects of nutrient scarcity (chapter 3 and 4).

The dormancy-induced TF1-a cells were subjected to molecular characterization to provide, for the first time, whole human genome molecular signature of human CD34+ CD38- AML cells with feature of dormancy and stemness using Affymetrix microarrays technology.

This chapter will aim to present and discuss the GEP results including the microarrays data analysis and identification of the genes and signalling pathways of interest. The laboratory investigations using qPCR on selected genes of the molecular signature, for the purpose of validating the microarrays results, will also be discussed.

## 5.2. Results

### 5.2.1. MiniGEP by qPCR for optimizing the time point for the GEP of Affymetrix Microarrays Experiments

Before testing the global gene expression profile (GEP) using the Affymetrix microarray technology, we sought to select a time point for the duration of the TGFβ1 and rapamycin treatment. This was important because the high cost of the microarray experiments prohibited inclusion of different time points. Short term *in vitro* treatment (2 hours) was considered as an option due to the previously published work reporting the upregulation of p57 in leukaemia cells in response to short term culture with TGFβ1 (Scandura, Boccuni *et al.* 2004); this was also confirmed by the molecular work conducted in this study (section 3.2.7). Prolonged *in vitro* treatment (72 hours), however, was included as a closer simulation of the *in vivo* adaptive response of the LICs. These cells are believed to live in the endosteal niche with prolonged exposure to the dormancy regulators TGFβ1 and shortage of nutrients. Moreover, 24 hours of treatment was added for the purpose of comparison and to track and confirm the consistency of the effect of treatment during the period between the short and prolonged treatment. Consequently, 3 durations of treatments were selected for a qPCR-based preliminary investigation; 2 hours, 24 hours, and 72 hours.

In addition to p57, we selected 5 other genes to optimize the treatment duration. These comprised of CD34, BTG2, ATG5, STK11, and E2F4 genes; collectively the 6 genes made what was called a mini-gene expression profile (miniGEP). CD34 was included as a positive control because of a previous study which confirmed the up-regulation of this gene by TGFβ1 in TF1 leukaemia cells (the mother cells of TF1-a) (Marone, Scambia *et al.* 2002), which was also supported by the CD34 receptor up-regulation that was detected in the current model (section 3.5.1). We were particularly interested to include BTG2, because of unpublished observations

in the department (in leukaemia cells) and a previous report showing that it was upregulated in normal cells induced to dormancy as well as in cells with damaged DNA (Zhou, Chou *et al.* 2006).

STK11 (also known as LKB1), E2F4 and the autophagy-related gene ATG5 were included due to previous reports suggesting their role in dormancy and cell cycle regulation (Liu, Wu *et al.* 2009, Gan, Hu *et al.* 2010, Nakada, Saunders *et al.* 2010, Chaterjee and van Golen 2011, Litovchick, Florens *et al.* 2011, Sosa, Bragado *et al.* 2014, Mao, Zhang *et al.* 2015).

E2F4 is one of the downstream effectors that dephosphorylated RB (retinoblastoma) protein and is reported to be part of the 'DREAM' (DP, RB, E2F, and MuvB) complex. Indeed, quiescence has been reported to be highly dependent on the highly conserved function of proteins forming the DREAM complex including E2F4 (Sadasivam and DeCaprio 2013). This complex act by suppressing cell cycle-dependent genes (Litovchick, Florens et al. 2011).

LKB1 was found to play a central role in HSCs maintenance. In an *in vivo* mouse model, LKB1 knock-out resulted in increase HSCs proliferation and then exhaustion of HSCs reserve with the development of pancytopenia. Indeed, LKB1 appears to acts through its role as a regulator of cellular energy metabolism in eukaryotic cells that involved in the cellular response to nutrient signals with the involvement of AMPK-related kinases and mTORC1 functions (Gurumurthy, Xie et al. 2010). Importantly, LKB1 was reported to play a tumour suppression activity in AML through the repression of mTOR pathway-dependent oncogenic mRNA translation (Green, Chapuis et al. 2010).

ATG5 is one of the genes of regulating autophagy; a lysosomal degradation pathway in eukaryotic cells. Indeed, there is growing interest in the last decade in investigating the role of genes regulating autophagy in the maintenance of cancer stem cells. Indeed, there is evidence supporting the activation of autophagy genes

in dormant cancer and non-transformed cells under nutrient deprivation microenvironment. This suggesting that autophagy might play a role in the survival of these cells under shortage of energy through directing cellular machinery to alternative sources of energy (Sosa, Bragado et al. 2014). Importantly, recent evidence has come to confirm the role of ATG5, one of the key autophagy-related proteins, in the development of AML in a mouse model (Liu, Chen et al. 2016). Although this finding does not necessarily indicate the role of ATG5 in dormancy in AML, we were interested to including an autophagy-related gene with an importance in AML in the list of the miniGEP.

Three of the miniGEP genes (ATG5, STK11, and E2F4) showed no increase in expression in response to culture with TGFβ1 and/or rapamycin for any of the 3 tested durations (figure 5.1); therefore, they could not help in selecting the most suitable treatment duration. On the other hand, P57, BTG2, and CD34 displayed a general up-regulation pattern in response to the combination of dormancy inducers (figure 5.1). As regards P57, it showed significant upregulation in TF1-a cells after 72 hours culture with TGFβ1 and rapamycin if compared to 24 hours of treatment or to treatment with each of the two dormancy inducers separately. Moreover, CD34 and BTG2 showed an interesting stepwise increase with the duration of treatment. Therefore, despite all the variability - between genes, between rapamycin and TGFβ1, between time points as well as inter-assay variation, on balance it seemed reasonable to select 72 hours for the GEP experiments as we were trying to model a sustained rather than a transient state of dormancy. This was also consistent with the previously discussed features of dormancy (Ki-67, CD71, and total RNA contents) in TF1-a cells treated for 72 hours (section 4.2.2).

Consequently, 72 hours of continuous treatment with 4ng/ml of TGFβ1 and 100nM of rapamycin was selected to investigate the TF1-a leukaemia cell dormancy signature by Affymetrix microarray technology for the entire human genome.

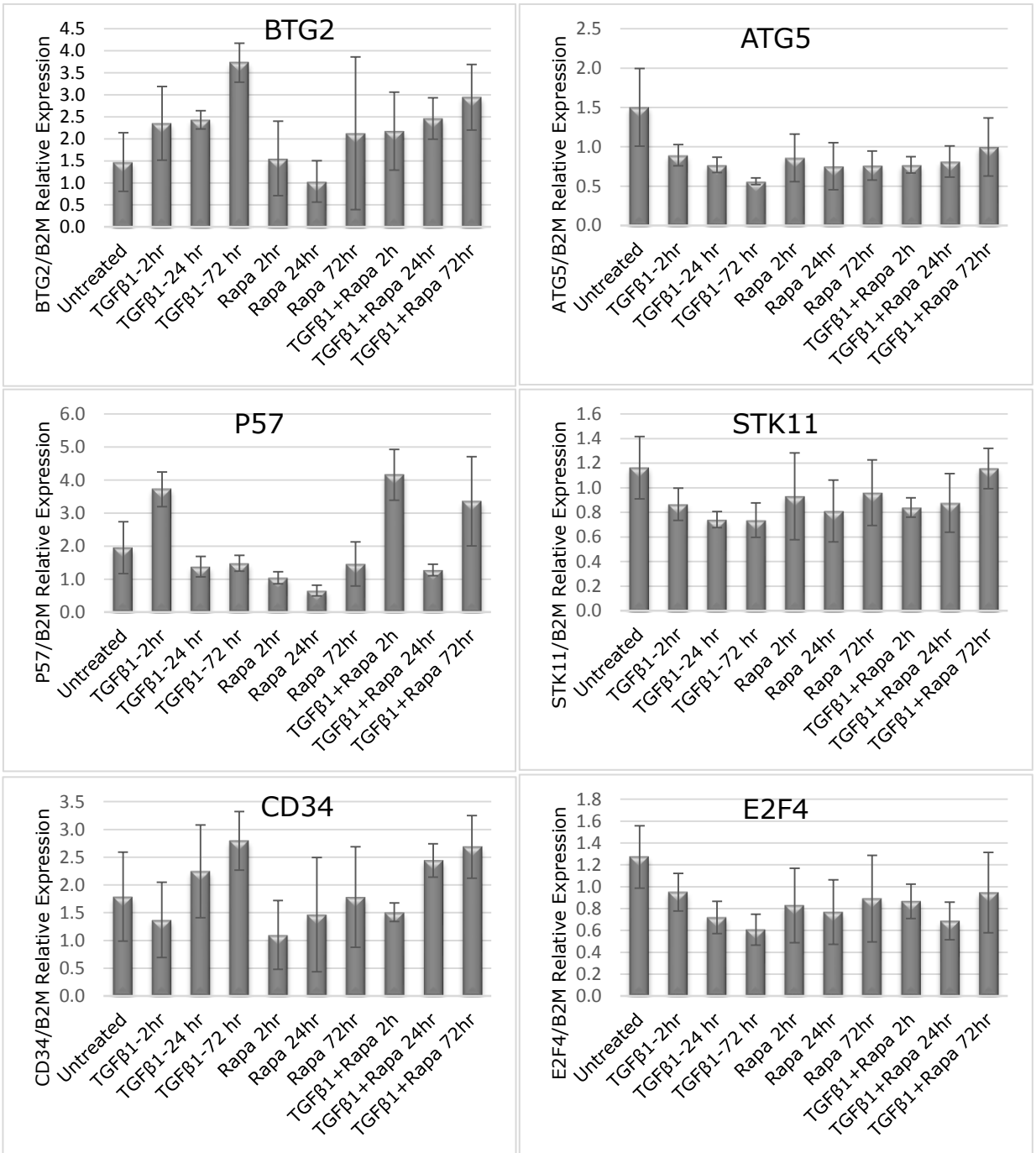



**Figure 5.1: The Expression of the 6 selected genes in TF1-a cells for the miniGEP.** All cells were seeded at a concentration of 2x10^5 cells/ml and incubated for 2hr, 24hr, or 72hr with or without TGFβ1, rapamycin, or both at a dose of 4ng/ml for TGFβ1 and 100nM for rapamycin. The columns represent mean values of three independent experiments. The error bars represent +/- 1SD.

### 5.2.2. Investigating the molecular signature of dormant TF1-a cells using whole human gene expression profiling

Whole human genome GEP using the Affymetrix strips (HuGene2.1ST) was conducted on three independent biological replicates of RNA preps obtained from untreated TF1-a cells and TF1-a cells induced to dormancy by 72 hours culture with TGFβ1 and rapamycin (dormant TF1-a). This was accompanied by testing the RNA preps of TF1-a cells cultured with each of the two dormancy inducers separately.

Once reads were obtained from the microarray chips, normalization steps were performed using Partek Genomics Suite 6.6. Software. This software facilitates generating the lists of differentially expressed genes through comparing different intensity signals between two samples (in this case the expression levels of untreated TF1-a cells with that of TF1-a cells induced to dormancy).

5.2.2.1 Selecting the genes of interest in the dormancy signature of TF1-a cells.

The GEP strips have been manufactured to produce data covering >33500 coding transcripts. Many of these transcripts showed up or down regulation with variable degrees of fold change and statistical significance (figure 5.2; panel B). To meet the aim of this study, nevertheless, we focused on genes significantly differentially upregulated by more than 2 fold with false discovery rate (FDR)-adjusted p-value (<0.05) in dormant TF1-a cells in comparison to their untreated counterparts (figure 5.2; panel B). Employing the FDR in selecting the significant p-value was recommended in order to exclude any possible false positives that might accompany simultaneous calculating of large numbers of hypotheses in the microarray data analysis (Pawitan, Michiels *et al.* 2005).

This refining process resulted in 240 genes only (table 5.1), which were subjected to detailed analysis by researching literature to identify their functional and biological importance.

Using the same previously discussed selecting criteria, there were 136 significantly downregulated genes (figure 5.2; panel B). Those genes, however, were not subjected to the same comprehensive analysis that was performed on the upregulated genes. This was because we aimed, in the first place, to investigate genes in the dormancy signature that might be involved in the initiation or maintenance of dormancy in TF1-a cells. This was an attempt to identify candidate targets for breaking dormancy and eradicating LICs, in addition to the main goal of this study of comparing the dormancy signature to the molecular signature of TF1-a cells subjected to sub-lethal genotoxicity (chapters seven and eight).

As regards the significantly down regulated genes and similar to the upregulated ones, TGFB1 was the main player in term of the number of down regulated genes and the extent of their downregulation if compared to rapamycin treatment (figure 5.4). This could be related to the pleotropic effect of TGFB1 which is known to be involved in many biological processes including inhibition of proliferation. In contrast, rapamycin is a specific synthetic inhibitor of the mTORC1 component in the mTOR pathway that largely acts to shut down protein synthesis. Therefore, one would expect produce a narrower spectrum of affected genes.

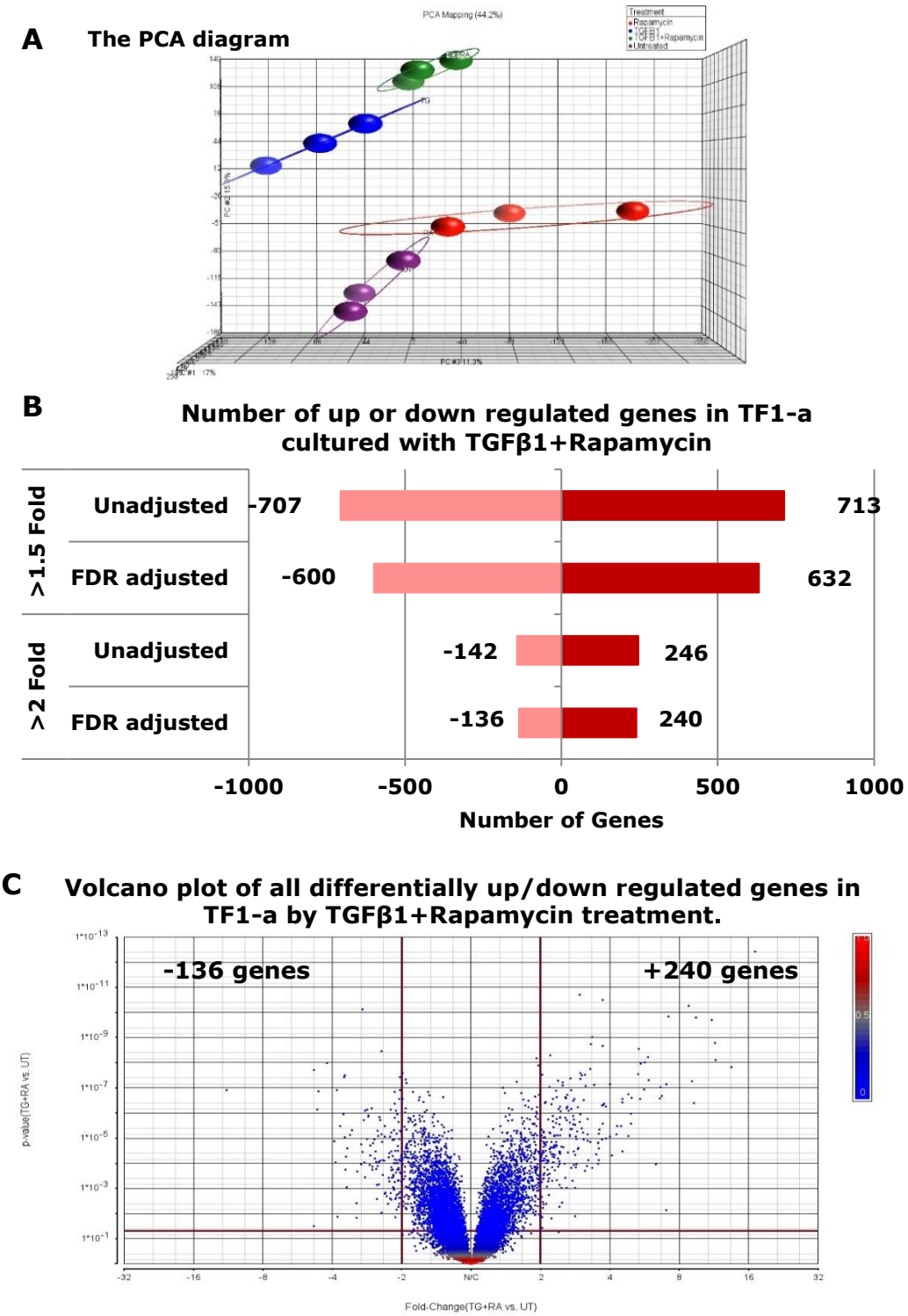



**Figure 5.2: Genes of interest selected in the dormant TF1-a cells. Panel A:** Principal Component Analysis (PCA) clusters the 12 samples TF1-a cells based on the global signal of each sample. The purple dots represent the Untreated TF1-a cells whereas the red, blue, and green dots represent TF1-a cells treated with rapamycin, TGFβ1, or both respectively **Panel B:** Bar diagram distribute the number of genes, that were differentially up (dark red) or down (pink) regulated in TF1-a cultured for 3 days with 4ng/ml of TGFβ1 and 100nM of rapamycin in comparison to their untreated counterparts, according to fold change and unadjusted or FDR-adjusted p-value (<0.05). **Panel C:** The volcano scatter-plot illustrates all differentially up/down regulated genes in dormant TF1-a cells distributed according to the statistical significance (Y axis) and fold change (X axis). Each dot represents a gene. The vertical lines represent the 2 fold change cut-off limit and the horizontal line represent the selected p value for the list of genes of interest.

**Table 5.1: The 240 genes significantly upregulated in dormant TF1-a cells.** (NB: the 86 genes uniquely upregulated by TGFβ1 and rapamycin combination are highlighted in red). * FC: fold change.

| | Gene Symbol | FC* | | Gene Symbol | FC | | Gene Symbol | FC |
|---|---|---|---|---|---|---|---|---|
| **1** | SPP1 | 17.1 | **81** | ANGPTL2 | 2.9 | **161** | LOC100133920 | 2.3 |
| **2** | TMC7 | 13.5 | **82** | PRSS1 | 2.9 | **162** | KLHL41 | 2.3 |
| **3** | ABCC3 | 11.5 | **83** | VDR | 2.9 | **163** | GRAMD2 | 2.3 |
| **4** | PTPRU | 11.4 | **84** | MYOM1 | 2.9 | **164** | CLU | 2.3 |
| **5** | MYLK | 11 | **85** | SP7 | 2.8 | **165** | SCARA3 | 2.3 |
| **6** | FLJ35282(DMRTA1) | 9.5 | **86** | SLC22A23 | 2.8 | **166** | RGS10 | 2.3 |
| **7** | HTN3 | 9.3 | **87** | QPCT | 2.8 | **167** | IL16 | 2.3 |
| **8** | ALOX5AP | 9.1 | **88** | SYNPO2 | 2.8 | **168** | CD34 | 2.3 |
| **9** | PLXNC1 | 8.8 | **89** | GAL | 2.8 | **169** | YPEL3 | 2.3 |
| **10** | ITGB3 | 7.2 | **90** | GRAP2 | 2.8 | **170** | ALOX12 | 2.3 |
| **11** | ADAMTS10 | 7.1 | **91** | CEP112 | 2.8 | **171** | KLHL24 | 2.2 |
| **12** | RGS9 | 6.7 | **92** | ITGAV | 2.8 | **172** | GOLGA6L5 | 2.2 |
| **13** | PTH2 | 6.6 | **93** | EBI3 | 2.8 | **173** | KIAA1161 | 2.2 |
| **14** | SMAD7 | 6.6 | **94** | CMTM1 | 2.8 | **174** | C7orf41 | 2.2 |
| **15** | CCL2 | 6.3 | **95** | ITGA6 | 2.8 | **175** | SERPINF1 | 2.2 |
| **16** | IL3RA | 5.9 | **96** | RSPH1 | 2.8 | **176** | SLC35D2 | 2.2 |
| **17** | SYTL5 | 5.9 | **97** | PROCR | 2.8 | **177** | LOC642361 | 2.2 |
| **18** | IL3RA | 5.7 | **98** | CRLF2 | 2.7 | **178** | BMF | 2.2 |
| **19** | CNN1 | 5.6 | **99** | KIAA1109 | 2.7 | **179** | ACSM3 | 2.2 |
| **20** | CNR1 | 5.5 | **100** | GRK5 | 2.7 | **180** | MEF2A | 2.2 |
| **21** | MMP2 | 5.4 | **101** | C19orf77 | 2.7 | **181** | EEPD1 | 2.2 |
| **22** | CNR1 | 5.4 | **102** | ABAT | 2.7 | **182** | ARHGAP6 | 2.2 |
| **23** | MYO7A | 5.3 | **103** | BHLHE40 | 2.7 | **183** | KIAA1107 | 2.2 |
| **24** | CHST15 | 5 | **104** | BMPR2 | 2.7 | **184** | TPM1 | 2.2 |
| **25** | ITGB4 | 4.9 | **105** | PLD4 | 2.7 | **185** | RASA4 | 2.2 |
| **26** | RASGRP1 | 4.9 | **106** | CDKN2B | 2.7 | **186** | CD207 | 2.2 |
| **27** | NTRK3 | 4.8 | **107** | TCP11L2 | 2.7 | **187** | TSPAN9 | 2.2 |
| **28** | CPNE2 | 4.8 | **108** | GYPB | 2.6 | **188** | CNR1 | 2.2 |
| **29** | CYTIP | 4.5 | **109** | RD3L | 2.6 | **189** | INPPL1 | 2.2 |
| **30** | SLC4A1 | 4.5 | **110** | GPRC5B | 2.6 | **190** | EPHA4 | 2.2 |
| **31** | UNC5B | 4.5 | **111** | MEIS1 | 2.6 | **191** | ITGB5 | 2.2 |
| **32** | ITGA3 | 4.5 | **112** | ASAP2 | 2.6 | **192** | RD3 | 2.2 |
| **33** | SLC2A12 | 4.3 | **113** | TM6SF1 | 2.6 | **193** | HBE1 | 2.1 |
| **34** | LURAP1L | 4.3 | **114** | PLEKHH2 | 2.6 | **194** | PNMT | 2.1 |
| **35** | HAVCR2 (TIM-3) | 4.1 | **115** | MMRN1 | 2.6 | **195** | LOC401321 | 2.1 |
| **36** | IDS | 4 | **116** | RASA4B | 2.6 | **196** | ENPP6 | 2.1 |
| **37** | SMAD6 | 4 | **117** | CCBP2 | 2.6 | **197** | S100A13 | 2.1 |
| **38** | NKD1 | 3.9 | **118** | FAM214A | 2.6 | **198** | ADC | 2.1 |
| **39** | VASH1 | 3.8 | **119** | CORO6 | 2.5 | **199** | SFXN3 | 2.1 |

| | Gene Symbol | FC* | | Gene Symbol | FC | | Gene Symbol | FC |
|---|---|---|---|---|---|---|---|---|
| **40** | SPRY3 | 3.8 | **120** | GPR37 | 2.5 | **200** | USP18 | 2.1 |
| **41** | ENKUR | 3.8 | **121** | GFOD1 | 2.5 | **201** | BAMBI | 2.1 |
| **42** | SKIL | 3.7 | **122** | GLIPR1 | 2.5 | **202** | TRPC3 | 2.1 |
| **43** | CD44 | 3.7 | **123** | PPBP | 2.5 | **203** | KIAA0355 | 2.1 |
| **44** | ECM1 | 3.7 | **124** | C15orf65 | 2.5 | **204** | TGFB1 | 2.1 |
| **45** | SPRY3 | 3.7 | **125** | IGFBP5 | 2.5 | **205** | Sep-04 | 2.1 |
| **46** | GSN | 3.7 | **126** | TNNI3 | 2.5 | **206** | HIVEP2 | 2.1 |
| **47** | SERPINE1 | 3.6 | **127** | KCNH3 | 2.4 | **207** | RAB30 | 2.1 |
| **48** | CLCA1 | 3.6 | **128** | MICAL3 | 2.4 | **208** | SEPT5-GP1BB | 2.1 |
| **49** | EPHB6 | 3.6 | **129** | GPR153 | 2.4 | **209** | TMEM158 | 2.1 |
| **50** | SIGLEC6 | 3.6 | **130** | GPR56 | 2.4 | **210** | MYEOV | 2.1 |
| **51** | FBXO32 | 3.6 | **131** | HRC | 2.4 | **211** | CMTM3 | 2.1 |
| **52** | DMTN | 3.6 | **132** | MRAP2 | 2.4 | **212** | THBS3 | 2.1 |
| **53** | DUSP21 | 3.5 | **133** | BTBD19 | 2.4 | **213** | EFHB | 2.1 |
| **54** | PTHLH | 3.5 | **134** | CTSE | 2.4 | **214** | OPTN | 2.1 |
| **55** | SLC37A1 | 3.4 | **135** | BTG2 | 2.4 | **215** | KLRC3 | 2.1 |
| **56** | FMNL3 | 3.3 | **136** | SLC46A3 | 2.4 | **216** | IL10RB-AS1 | 2.1 |
| **57** | PLCL1 | 3.3 | **137** | IGSF3 | 2.4 | **217** | C1orf116 | 2.1 |
| **58** | BMPER | 3.3 | **138** | OR6C76 | 2.4 | **218** | TMPRSS11B | 2.1 |
| **59** | CTTNBP2 | 3.3 | **139** | ARID5B | 2.4 | **219** | MYH9 | 2.1 |
| **60** | ENC1 | 3.3 | **140** | ANGPT2 | 2.4 | **220** | ME3 | 2.1 |
| **61** | LOC100507003 | 3.2 | **141** | MFGE8 | 2.4 | **221** | PERP | 2.1 |
| **62** | RGS1 | 3.2 | **142** | LRRC32 | 2.4 | **222** | MC4R | 2.1 |
| **63** | FHOD3 | 3.2 | **143** | IL6ST | 2.4 | **223** | LTBP1 | 2.1 |
| **64** | CREB3L3 | 3.2 | **144** | TP53INP1 | 2.4 | **224** | RTN1 | 2 |
| **65** | ITGA11 | 3.2 | **145** | FRY | 2.4 | **225** | GPR183 | 2 |
| **66** | SERPINI1 | 3.1 | **146** | KRT79 | 2.4 | **226** | RHOB | 2 |
| **67** | C15orf26 | 3.1 | **147** | ZMAT3 | 2.4 | **227** | STX1A | 2 |
| **68** | AQP1 | 3.1 | **148** | NRP2 | 2.3 | **228** | P2RY14 | 2 |
| **69** | OLFM2 | 3.1 | **149** | CPEB4 | 2.3 | **229** | LOC221272 | 2 |
| **70** | RUNX2 | 3.1 | **150** | FOLR1 | 2.3 | **230** | SLFN5 | 2 |
| **71** | PHOSPHO1 | 3.1 | **151** | NEB | 2.3 | **231** | HIC1 | 2 |
| **72** | HDAC5 | 3 | **152** | PPAPDC1A | 2.3 | **232** | STX11 | 2 |
| **73** | SYNJ2 | 3 | **153** | SPRY4 | 2.3 | **233** | GOLGA6L10 | 2 |
| **74** | ABHD2 | 3 | **154** | ASIC3 | 2.3 | **234** | HPGD | 2 |
| **75** | MAGI3 | 3 | **155** | LTBP3 | 2.3 | **235** | ATP8B4 | 2 |
| **76** | ALAS2 | 3 | **156** | MED12L | 2.3 | **236** | GOLGA6L10 | 2 |
| **77** | PAPSS2 | 3 | **157** | LINC00642 | 2.3 | **237** | PROS1 | 2 |
| **78** | LMO7 | 3 | **158** | LOC285972 | 2.3 | **238** | MAGED2 | 2 |
| **79** | CD3G | 2.9 | **159** | C3 | 2.3 | **239** | SFRP4 | 2 |
| **80** | CALCOCO1 | 2.9 | **160** | GOLGA6L4 | 2.3 | **240** | GOLGA6L10 | 2 |

5.2.2.2. Partek Genomics Suite software-based analysis of the dormancy signature of TF1-a cells.

The data generated from the GEP chips were imported into the Partek Genomics Suite 6.6 (PGS) software for further analysis focusing on the 240 genes found to be differentially upregulated in TF1-a cells induced to dormancy. To start, the principle component analysis (PCA) was generated for the 12 TF1-a RNA samples. The PCA is a mathematical algorithm that has been utilized to visually assess similarities and differences between samples of all tested conditions with very high number of tested variables (such as in GEP experiments) and assesses the ability of grouping these samples (Ringner 2008). In this study the PCA figure showed a clear grouping of the three replicates of each condition of TF1-a cells (figure 5.3; panel A). The gap was particularly wide between TF1-a cells cultured with TGFβ1 and rapamycin (purple balls) and untreated TF1-a cells (green balls) which indicates the obvious effect of treatment.

Moreover, the Venn diagram (figure 5.3; panel B), which was used here to compare between the three types of treatments, showed that most of the 240 genes (149 out of 240 genes) were commonly upregulated by the effect of TGFβ1 or TGFβ1 and rapamycin treatment whereas rapamycin treatment, individually, has increased the expression of 5 genes only out of the 240 genes. Interestingly, however, the combination of TGFβ1 and rapamycin have significantly increased the expression of 86 genes which were only upregulated if the two dormancy inducers were used together (figure 5.3; panel B). In addition, the treatment combination clustered a group of genes which were functionally enriched in a specific biological processes in response to the treatment combination only if compared to individual treatment with TGFβ1 or rapamycin (figure 5.3; panel C). This might reflect that leukaemia cell responses to TGFβ1 could be altered by the low nutrients environment which was modelled here by mTOR pathway inhibition.

Despite the presence of these 86 genes that were unique for the combination of two dormancy inducers, we considered all the 240 genes to be potentially important for representing the dormancy signature in TF1-a cells. This was mainly based on two facts. First, TGFβ1-only treatment induced significant inhibition of proliferation and features of dormancy in TF1-a cells (chapter 3), therefore excluding genes that were common between TGFβ1-only and TGFβ1+rapamycin treatments is not preferable at this level of investigation. By doing this we might exclude biologically important genes. Second, in the current model of dormancy, we presented that TGFβ1 + rapamycin combination induced significant dormancy features in TF1-a cells. Therefore, we believe all genes upregulated in this *in vitro* conditioning strategy (the 240 genes) are of value for further investigation as potential targets in AML.

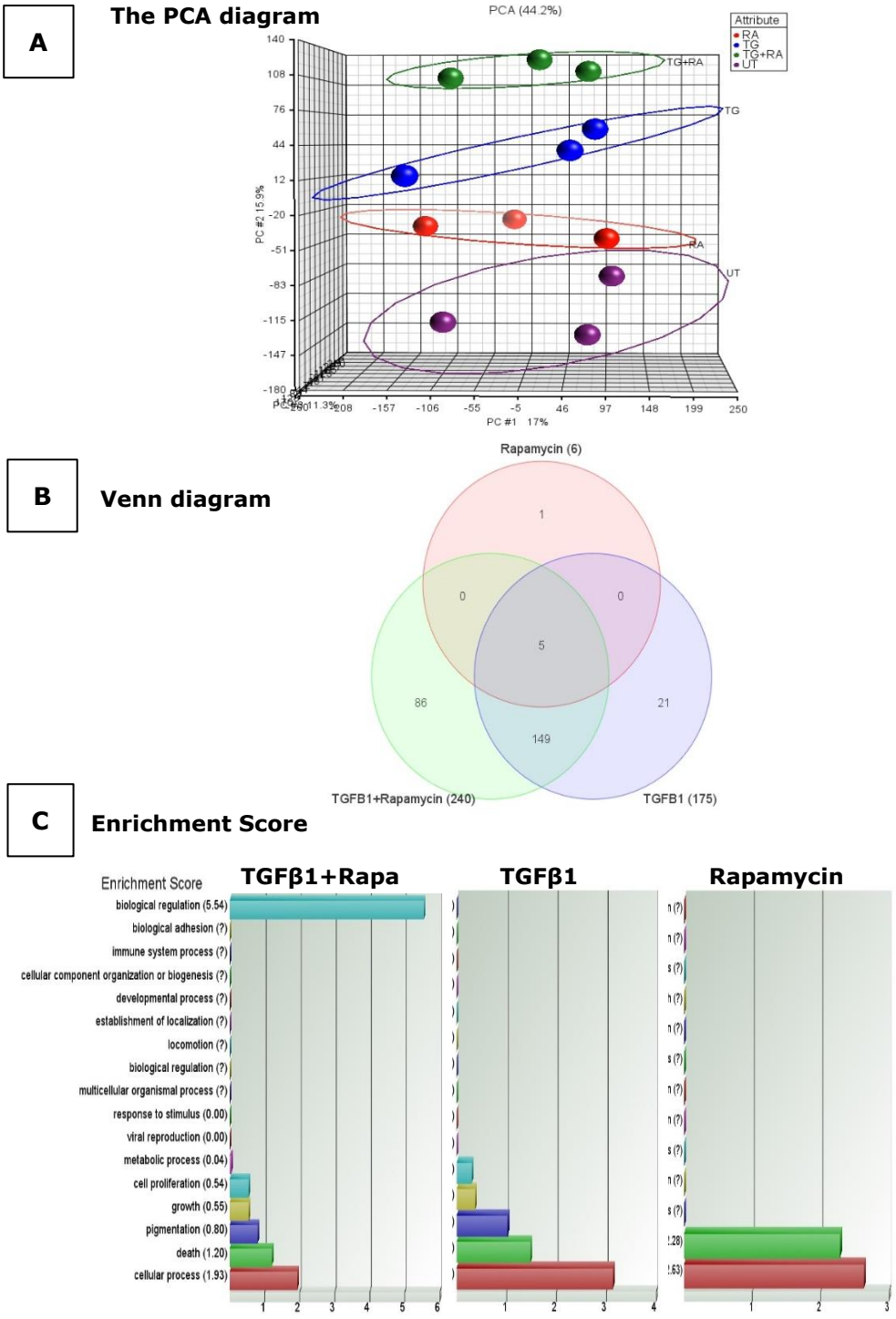



**Figure 5.3: Analysis of the 240 upregulated genes GEP of TF1-a cells cultured with TGFβ1 and/or Rapamycin**. **Panel A:** Principal Component Analysis (PCA) clusters the 12 samples TF1-a cells based on the 240 genes signal of each sample. The purple dots represent the Untreated TF1-a cells whereas the red, blue, and green dots represent TF1-a cells treated with rapamycin, TGFβ1, or both respectively. **Panel B:** The Venn diagram which compares the three conditions of TF1-a cells in regards to the top 240 differentially upregulated genes of the dormancy signature. **Panel C:** The Enrichment score of the 240 differentially up-regulated genes in TF1a Cells due to the three different treatment conditions. The four figures were generated using Partek Genomics Suite 6.6 software.

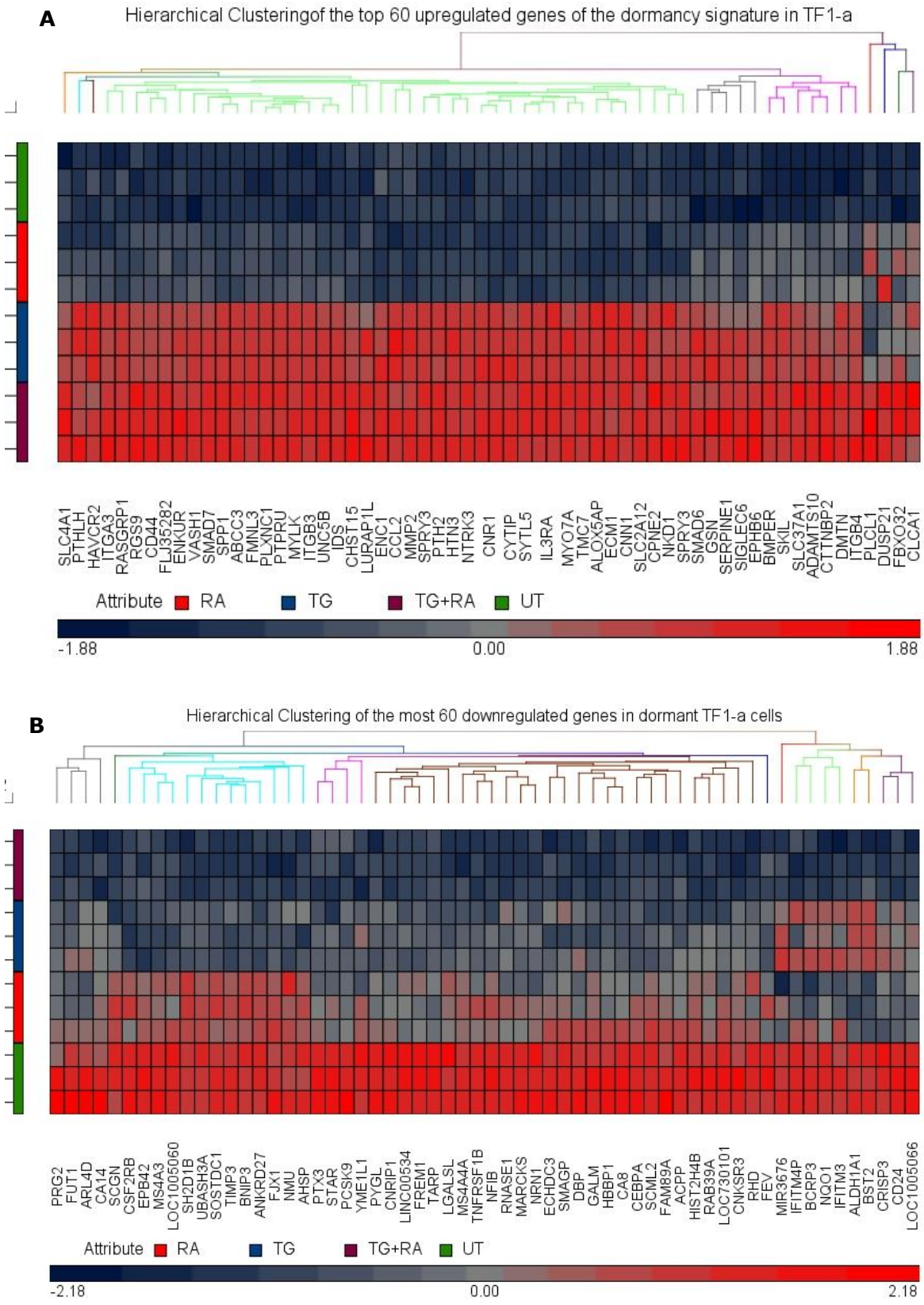



**Figure 5.4: The heat maps of the molecular signature of the TF1-a cells induced to dormancy. Panel A:** illustrates the top 60 genes of the 240 most upregulated genes in TF1-a induced to dormancy. **Panel B:** illustrates the top 60 genes of the 136 most downregulated genes in TF1-a induced to dormancy. The figures were generated using Partek Genomics Suite 6.6 software. UT: untreated, TG: TGFβ1, RA: rapamycin.

5.2.2.3. Analysis of the biological processes/ signalling pathways significantly enriched in the dormancy signature of TF1-a cells.

Partek Genomic Suite 6.6 (PGS) software facilitates mapping of the detected genes based on their gene ontology (GO) categories into their relevant biological process, molecular function and cellular localization. To emphasize the biological meaning of the dormancy signature, however, we focused on investigating the biological processes or signalling pathways involved by conducting the 'enrichment analyses' on the 240 genes upregulated in the dormancy signature of TF1-a cells. This analysis helps to discover possible association and interactions among the detected differentially expressed genes. Moreover, the Kyoto Encyclopaedia of Genes and Genomes (KEGG) database (KEGG-pathway) was also utilized to obtain a comprehensive understanding about the biological processes or signalling pathways mostly enriched in dormant TF1-a signature.

Indeed, enrichment analysis was able to give information about 195 genes only out of the 240 genes. Among the long list of biological processes/signalling pathways annotated by KEGG-pathway database, the 195 genes were grouped into 56 significantly enriched distinct biologically relevant groups (table 5.2). Many genes were classified within more than one group due to the possible multi-functionality of these genes. For instance, GPR56 was grouped in the G-protein coupled receptor protein signalling pathway and in the cell adhesion protein group of genes.

**Table 5.2: Significantly enriched biological processes/signalling pathways in the dormancy signature of TF1-a cells cultured with TGFβ1 and rapamycin.** Note: The groups presented in this table were restricted to the groups contained a minimum of 2 genes.

| Signalling Pathway/Biological process | Enrichment Score | Enrichment p value | Genes in list in group | Genes not in list in group | GO ID |
|---|---|---|---|---|---|
| Integrin-mediated signalling pathway | 14.43 | 0.00 | 8 | 55 | 7229 |
| Cell adhesion | 13.41 | 0.00 | 21 | 536 | 7155 |
| Response to laminar fluid shear stress | 10.48 | 0.00 | 3 | 3 | 34616 |
| Negative regulation of cell migration | 10.03 | 0.00 | 6 | 51 | 30336 |
| Positive regulation of endothelial cell migration | 9.60 | 0.00 | 4 | 16 | 10595 |
| Negative regulation of blood vessel endothelial cell migration | 8.72 | 0.00 | 3 | 7 | 43537 |
| Leukocyte migration | 8.49 | 0.00 | 7 | 99 | 50900 |
| Cellular component organization or biogenesis | 8.41 | 0.00 | 15 | 440 | 7596 |
| Positive regulation of angiogenesis | 8.02 | 0.00 | 5 | 48 | 45766 |
| Negative regulation of low density lipoprotein particles receptor biosynthesis process | 7.87 | 0.00 | 2 | 1 | 45715 |
| Negative regulation of pathway-restricted SMAD protein phosphorylation | 7.87 | 0.00 | 2 | 1 | 60394 |
| Positive regulation of Apoptosis | 7.71 | 0.00 | 8 | 150 | 43065 |
| Negative regulation of transforming growth factor beta receptor signalling pathway | 7.59 | 0.00 | 4 | 29 | 30512 |
| Osteoblast differentiation | 6.75 | 0.00 | 4 | 37 | 1649 |
| Tens fibre cell differentiation | 6.68 | 0.00 | 2 | 6 | 70306 |
| Negative regulation of insulin-like growth factor receptor signalling pathway | 6.68 | 0.00 | 3 | 22 | 30514 |
| Positive regulation of endothelial cell proliferation | 6.48 | 0.00 | 4 | 40 | 1938 |
| Chemotaxis | 6.09 | 0.00 | 6 | 112 | 6953 |
| Negative regulation of BMP signalling pathway | 5.90 | 0.00 | 3 | 22 | 30514 |
| Negative regulation of smooth muscle migration | 5.68 | 0.00 | 2 | 6 | 14912 |
| Regulation of transport | 5.68 | 0.00 | 2 | 6 | 51049 |
| Negative regulation of Apoptosis | 5.50 | 0.00 | 8 | 216 | 43066 |
| Mitotic cell cycle G1/S transition checkpoint | 5.43 | 0.00 | 2 | 7 | 31575 |
| Muscle contraction | 5.40 | 0.03 | 3 | 58 | 1503 |
| Positive regulation of cell proliferation | 5.32 | 0.00 | 10 | 324 | 8264 |
| Positive regulation of cell adhesion | 5.28 | 0.01 | 3 | 28 | 30155 |
| Response to wounding | 5.23 | 0.01 | 4 | 58 | 9611 |
| Positive regulation of vascular endothelial growth factor production | 4.85 | 0.01 | 2 | 10 | 10575 |
| Axon guidance | 4.69 | 0.01 | 9 | 302 | 7411 |
| Regulation of smooth muscle contraction | 4.69 | 0.01 | 2 | 11 | 6940 |
| Aging | 4.67 | 0.01 | 5 | 106 | 7568 |
| Negative regulation of cell proliferation | 4.65 | 0.01 | 9 | 304 | 8285 |
| Positive regulation of osteoblastic differentiation | 4.63 | 0.01 | 3 | 36 | 45669 |
| Positive regulation of protein kinase B signalling cascade | 4.43 | 0.01 | 3 | 39 | 51897 |
| Osteoblast development | 4.41 | 0.01 | 2 | 13 | 2076 |
| Cell cycle arrest | 4.37 | 0.01 | 5 | 117 | 7050 |
| Bmp signalling pathway | 4.30 | 0.01 | 3 | 41 | 30509 |
| Negative regulation of sequence-specific DNA binding transcription factor activity | 4.13 | 0.02 | 3 | 44 | 43433 |
| Response to vitamin D | 4.05 | 0.02 | 2 | 16 | 33280 |
| Positive regulation of endothelial to mesenchymal transition | 4.05 | 0.02 | 2 | 16 | 10718 |
| Multi-cellular organismal development | 4.05 | 0.02 | 18 | 903 | 7275 |
| Protein localization at cell surface | 4.05 | 0.02 | 2 | 16 | 34394 |
| Positive regulation of pathway-restricted SMAD protein phosphorylation | 4.05 | 0.02 | 2 | 16 | 10662 |
| Intracellular signal transduction | 3.88 | 0.02 | 8 | 290 | 35556 |

| Signalling Pathway/Biological process | Enrichment Score | Enrichment p value | Genes in list in group | Genes not in list in group | GO ID |
|---|---|---|---|---|---|
| Response to electrical stimulus | 3.85 | 0.02 | 2 | 18 | 51602 |
| Tissue regeneration | 3.76 | 0.02 | 2 | 19 | 42246 |
| Negative regulation of DNA replication | 3.65 | 0.02 | 2 | 18 | 8156 |
| Wnt receptor signalling pathway | 3.51 | 0.03 | 4 | 99 | 16055 |
| Transforming growth factor beta receptor signalling pathway | 3.44 | 0.03 | 3 | 58 | 7179 |
| Response to electrical stimulus | 3.36 | 0.03 | 2 | 24 | 9314 |
| Regulation of signal transduction | 3.36 | 0.03 | 2 | 24 | 9966 |
| Positive regulation of bone mineralization | 3.22 | 0.04 | 2 | 26 | 30501 |
| Immune response | 3.18 | 0.04 | 8 | 334 | 6955 |
| Response to hypoxia | 3.17 | 0.04 | 5 | 162 | 1666 |
| G-protein coupled receptor protein signalling pathway | 3.15 | 0.04 | 8 | 336 | 7186 |
| Cytokine mediated-signalling pathway | 2.89 | 0.04 | 5 | 154 | 19221 |

#### 5.2.2.4. Functional analysis of the TF1-a dormancy signature

In addition to the PGS and KEGG-pathway analysis in studying the genes forming the dormancy signature of TF1-a cells, we conducted a deeper investigation in an aim to find correlation between the detected genes, dormancy regulation and LIC maintenance. This was specifically important because these analysis tools did not provide information on all the 240 genes. Published reports discussing genes implicated in dormancy or cell cycle regulation in AML or LICs maintenance, therefore, were researched. As a result, three functionally relevant groups of genes were identified among the 240 differentially upregulated genes in dormant TF1-a cells. These were adhesion-related, tumour suppressors/inhibitors of proliferation, and stemness and inhibition of differentiation-related genes (figure 5.5).

Indeed, five of the top ten upregulated genes were adhesion-related genes. These were SPP1, MYLK, PLXNC1, and ITGB3 which showed 17.2, 11, 8.8, 7.8 fold increase respectively (figure 5.4). In addition, PTPRU (11.4 fold upregulation), which could be classified among the tumour suppressers, is also reported to play a role in adhesion of gastric (Liu, Zhu *et al.* 2014) and glioma (Zhu, Liu *et al.* 2014) cells. Interestingly, the most upregulated gene in the dormant TF1-a cells was secretin phosphoprotein 1 (SPP1) that codes for osteopontin (OPN) expression. Osteopontin was implicated in the leukaemia cell-bone marrow (BM)

niche interaction that regulates leukaemia cell dormancy (Boyerinas, Zafrir *et al.* 2013).

In addition, the molecular signature of dormant TF1-a cells showed significant representation of 2 more functionally related groups of genes. Firstly, several tumour suppressor genes were identified such as PTPRU, HTN3, CDKN2B, BTG2 (figure 5.5). These showed 11.4, 9.3, 2.7, and 2.4 fold increase respectively. Secondly, TGFβ1 and rapamycin treatment were found to upregulate stemness genes and genes involved in inhibition of differentiation such as ABCC3, CD123, TIM-3, and MEIS1 which showed 11.5, 5.9, 4.1, and 2.6 fold increase respectively (figure 5.5).

Finally and expectedly, several SMAD-signalling pathway genes were identified to form the dormancy signature of dormant TF1-a cells. Among these genes the TGFβ1 gene itself was upregulated by 2.1 fold (table 5.1) which might indicate an added role for the endogenous TGFβ1 to the used exogenous TGFβ1 in regulating TF1-a cells dormancy.

Further research on the proteins coded by the adhesion-related genes using the KEGG-pathway has detected that many of these proteins are involved in various cell-cell, cell-proteins and cell-extracellular matrix (ECM) interactions as well as genes positively regulating adhesion. Furthermore, some of these proteins mainly function as part of the ECM such as OPN and thrombospondin (THBS) which are coded by SPP1 and THBS3 respectively. Many others, on the other hand, are expressed on the cell membrane including various integrins and CD44 proteins (figure 5.6).

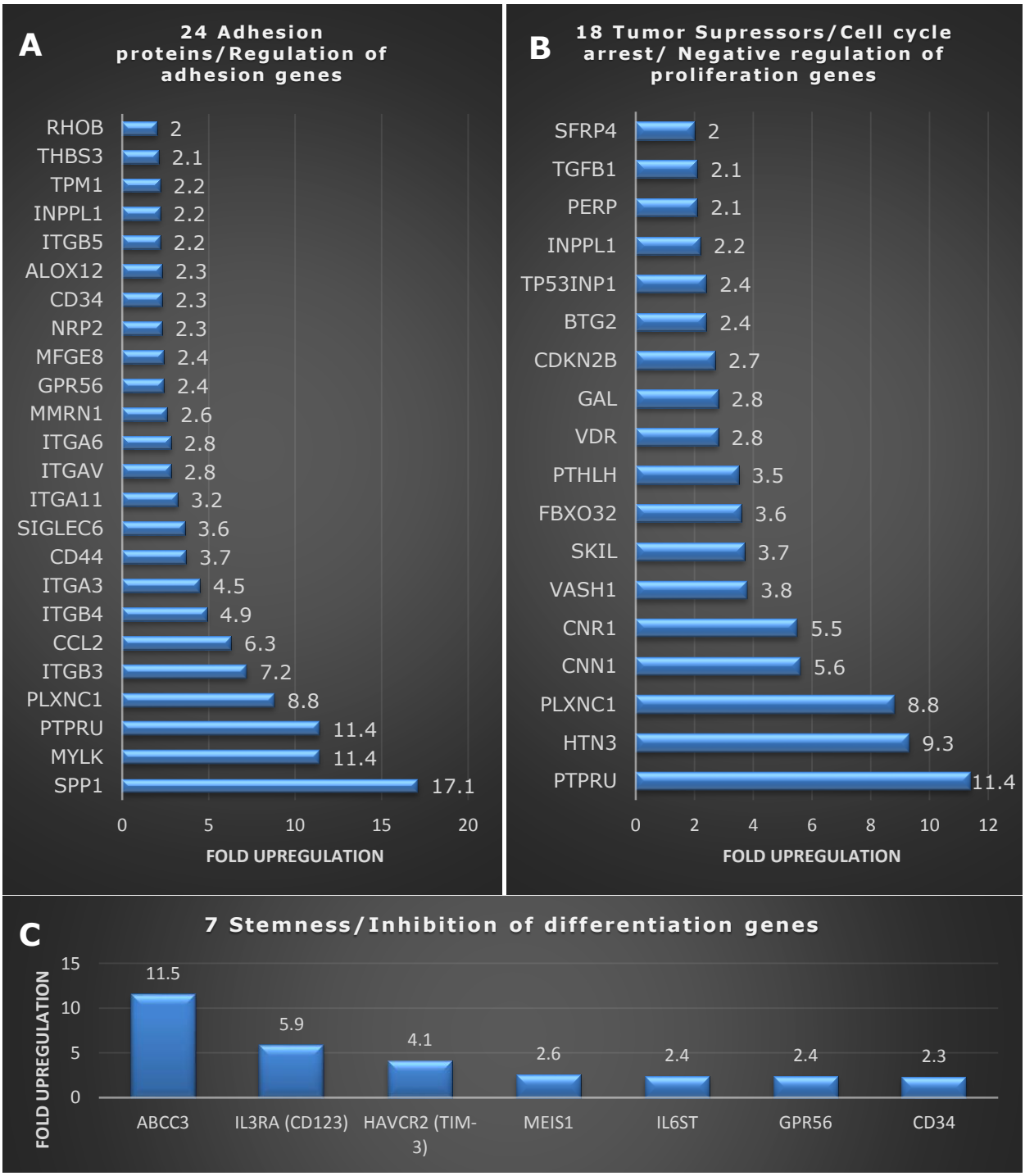



**Figure 5.5: The three biologically related groups of genes markedly represented in the dormancy signature of dormant TF1-a cells.** Panel A illustrates 24 genes involved in cellular adhesion. Panel B shows 18 genes considered to play a role in inhibition of proliferation, tumour suppression and cell cycle arrest. Panel C display 6 genes believed to be expressed in stem cells and genes inhibiting cellular differentiation. Data obtained from the microarray experiments, using Partek Genomic Suite 6.6 software, which represent the mean values for fold upregulation of three independent replicates.

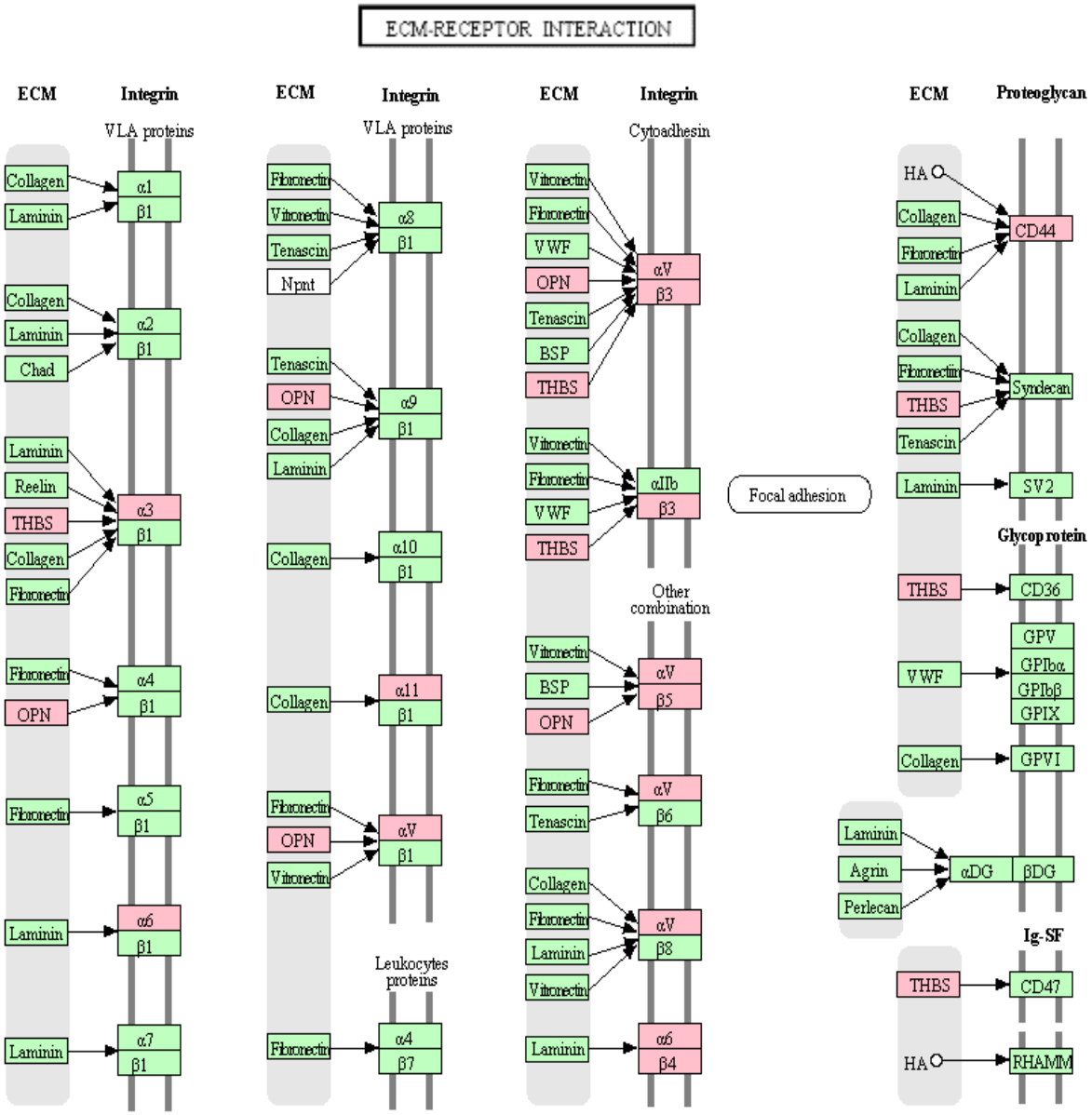



**Figure 5.6: The possible interactions of some of the detected adhesion-related genes products in the TF1-a dormancy signature.** Proteins highlighted in pink colour are coded by genes found differentially up-regulated in TF1-a cells cultured with TGFβ1 and rapamycin. Some of these proteins can be part of the extracellular matrix (ECM) such as osteopontin (OPN) and thrombospondin (THBS) whereas many others are expressed on the cell membrane including various integrins and CD44. The figure generated using the KEGG-pathway database (pathway code: hsa04512).

### 5.2.3. Validation of the GEP microarray results using qPCR

In order to confirm the accuracy of the Affymetrix microarray results we selected 7 adhesion-related genes as representatives to validate the GEP data. All tested genes showed a similar pattern of upregulation to those resulted from the GEP experiments (figure 5.7). Because the qPCR results were consistent and in line with the GEP results and due to cost reasons we did not carry out further validation.

Interestingly, qPCR results showed that SPP1 and ITGA3 have displayed a switching on from negligible expression in the dormancy signature rather than a real upregulation which was the case in the other 5 tested adhesion-related genes (figure 5.7). Consequently, these two genes and their related proteins could be considered as potential candidate markers of dormancy in this model.

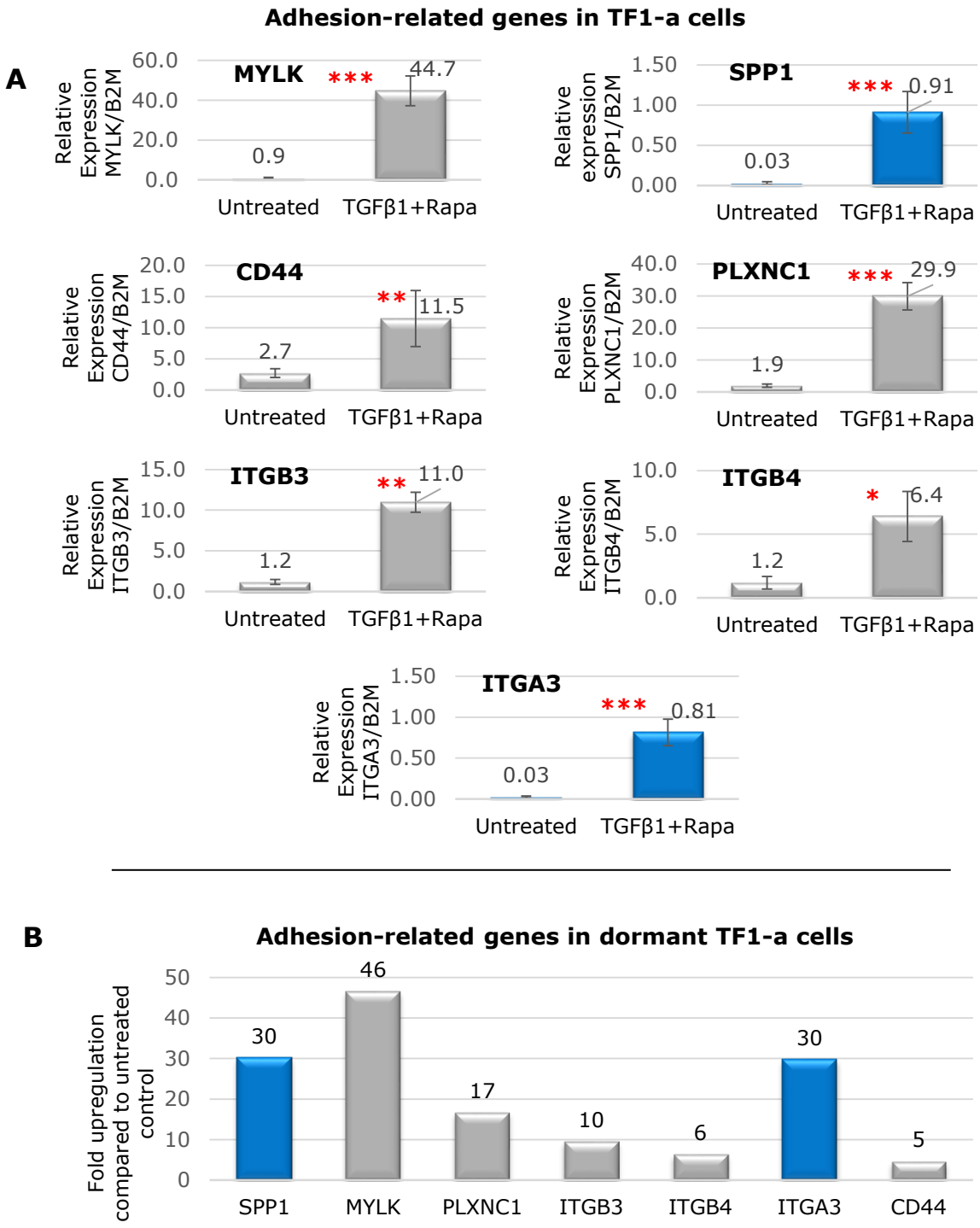



**Figure 5.7: The qPCR validation of the top 7 adhesion-related genes in TF1-a cells.** **Panel A** shows the qPCR results of each gene in untreated TF1-a cells and the treated with TGFB1 and rapamycin counterparts. The house keeping gene β2M expression was used as comparator in measuring the relative expression of each gene. **Panel B** illustrates the fold upregulation of each gene based on panel A results. SPP1 and ITGA3 genes were highlighted in blue as they showed switching on from negligible expression rather than an upregulation which was the case in the other 5 genes. The columns represent mean values of three independent experiments. The error bars represent +/- 1SD. *= p value<0.05, **= p value<0.01, ***= p value<0.001

## 5.3. Discussion

Mammalian cells are believed to exit the cell cycle into the G0-phase (dormant) in response to extracellular environment factors such as shortage of nutrients (Oki, Nishimura *et al.* 2014). This state of dormancy is an important feature of normal and malignant stem cells including LICs in AML. LICs that survive in a dormant state have not been well characterized because it is difficult to isolate these cells from clinical samples or murine leukaemia models due to their rarity and lack of viable cell markers effectively identifying the G0-phase of the cell cycle. In this study we demonstrated a whole human genome molecular signature of dormancy in human CD34+CD38- leukaemia cells.

### 5.3.1. MiniGEP of the dormant TF1-a cells

Three of the 6 genes selected for the qPCR experiments to investigate the most suitable duration of treatment showed no increase in expression in TF1-a cells induced to dormancy. These were STK11 (LKB1), E2F4 and ATG5. E2F4 is one of the downstream effector for dephosphorylated RB protein and is reported to be part of the 'DREAM' complex that represses gene expression in dormant cells (Litovchick, Florens *et al.* 2011). In cancer cells, however, the role of this complex is not well understood as perturbation of its quiescence-regulation function is likely due to mutations in cancer cells (Sadasivam and DeCaprio 2013). This might explain the lack of increase expression of the gene coding for the E2F4 protein in the dormant AML cells TF1-a.

Similarly, LKB1 is a known dormancy regulator in normal HSCs (Gan, Hu *et al.* 2010) and exerts a tumour suppression activity in AML cells (Green, Chapuis *et al.* 2010). However, its role in dormancy regulation of cancerous haematopoietic cells such as in AML cells is not well documented. Therefore, lack of up-regulation of this gene in dormant TF1-a cells could be attributed to the heterogeneity and multiple mutations that characterize the AML cells. On the other hand, the other 3 genes, namely CD34, p57 and BTG2 showed a clear increase in expression in

response to the dormancy treatment which guided us to select the 72 hours of treatment. As regards CD34 and p57, this upregulation came in line with the published effect of TGFβ1 on these two genes. BTG2, on the other hand highlights an interesting finding pending the results of the GEP to validate this response.

### 5.3.2. The functional importance of the genes of TF1-a dormancy signature in AML biology

The resulted 240 genes (table 5.1), which were selected using the 2 fold as a cut-off point, were subjected to thorough research in the up-to-date literature to identify their functional and biological importance. It is important to remember however that the degree of fold change does not always reflect the biological significance of the genes (McCarthy and Smyth 2009). This is because by choosing 2 fold as a cut-off point we might exclude biologically meaningful target genes. For instance, CD47 gene showed a 1.7 fold increase in dormant TF1-a's which was statistically significant (p 0.00002); CD47 is a promising potential therapeutic target under current investigation to eradicate leukaemia and other cancer cells ((Kong, Gao *et al.* 2016) and references therein).

Among the 240 genes forming the TF1-a cell dormancy signature, genes related to cellular adhesion were markedly presented (section 5.2.2.4). Indeed, five of the top ten upregulated genes were linked to leukaemia or other cell adhesion (figure 5.5). These were SPP1 (OPN-coding gene), MYLK, PLXNC1 and ITGB3 as well as PTPRU which was classified with the tumour suppressors but has been reported to play a role in cell adhesion. Moreover, the adhesion genes were not restricted to those genes presented in figure 5.7. For example, one of the G-protein signalling pathway genes (GPR56) was reported to play a vital role in HSCs and leukaemia stem cells adhesion in the bone marrow (Saito and Morishita 2015).

Osteopontin (OPN) is one of the most abundant secretory phosphoproteins produced mainly by the osteoblasts in the endosteal region believed to host the LICs (Sodek, Chen *et al.* 1995). It can function as adhesion protein, cytokine or

chemokine and is implicated in HSC migration and self-renewal (Nilsson, Johnston *et al.* 2005). Cells interact with extracellular OPN through many surface receptors including several α and β integrins as well as CD44 which has been implicated to play a key role in HSC and LIC homing and dormancy ((Zoller 2015) and references therein). The role of OPN in HSC and solid tumour proliferation and migration has been extensively investigated (Carlinfante, Vassiliou *et al.* 2003, Nilsson, Johnston *et al.* 2005, Haylock and Nilsson 2006, Lee, Wang *et al.* 2007, Grassinger, Haylock *et al.* 2009, Mi, Guo *et al.* 2009). In AML, importantly, OPN was reported as a serum protein marker of poor survival (Lee, Tien *et al.* 2008) and SPP1 (OPN-coding gene) as a potential therapeutic target (Powell, Thomas *et al.* 2009) in AML patients. Similarly, high OPN mRNA levels were found to be associated with poor overall survival and event free survival in intermediate-risk AML patients (Liersch, Gerss *et al.* 2012). Moreover, osteopontin was implicated in leukaemia cell-bone marrow niche interaction that regulates lymphoblastic cell dormancy. It was reported that these cells produce OPN and interact with extracellular OPN within the malignant BM. This interaction results in leukemic blasts exiting the cell cycle (becoming dormant) which renders them resistant to chemotherapy (Boyerinas, Zafrir *et al.* 2013).

Whereas little is known regarding the role of many of the other adhesion genes in AML which makes them novel candidates for investigations, some were recently reported to play a key role in other types of malignancy such as MYLK in breast cancer (Sundararajan, Gengenbacher *et al.* 2015) and PLXNC1 in melanoma (Chen, Soong *et al.* 2013). ITGB3, on the other hand, was reported to be a potential target to eliminate AML cells by interfering with the interaction with the BM niche, particularly as it has been found that genetic inactivation of this gene was associated with no impairment in normal haematopoiesis in an *in vivo* model (Miller, Al-Shahrour *et al.* 2013).

As regards the tumour suppressor genes, we were able to identify several genes in the dormancy signature of TF1-a cells including BTG2, PTPRU and CDKN2B

(figure 5.5). The known growth inhibitory influence of these genes could cooperate with the previously discussed adhesion-related genes for the maintenance of dormancy in leukaemia cells. BTG2 is a known anti-proliferative gene that plays a key role in B-cell malignancies and normal B-cell development (Tijchon, van Emst *et al.* 2016). It has been also implicated as a tumour suppressor gene in many solid malignancies ((Mao, Zhang *et al.* 2015) and references therein). Similarly, PTPRU (protein tyrosine phosphatase receptor-type U) has been reported to exert a growth inhibitory effect that involves the β-catenin signalling pathway in colonic and gastric cancer cells (Liu, Zhu *et al.* 2014). Interestingly, other member of the same family (PTPN13) were recently reported to play a role in maintaining HSC quiescence and their cross talk with the BM niche (Lopez-Ruano, Prieto-Bermejo *et al.* 2015). The role of BTG2 and PTPRU in AML, however, has not been adequately investigated which could make them novel targets in dormant leukaemia cells.

In contrast CDKN2B (the cyclin dependent kinase inhibitor p15) has been extensively investigated in AML and other types of leukaemia and myelodysplasia. This transcription factor, which is known to be epigenetically regulated (Hong, Li *et al.* 2016), has been recently reported to be frequently mutated and have a poor prognostic impact in AML (Achille, Othus *et al.* 2016, De Braekeleer, Douet-Guilbert *et al.* 2016) and in ALL (Mai, Liu *et al.* 2016). Interestingly, a recent report showed that CDKN2B silencing was mediated by CD93 which in turn acts to distinguish a proliferating (non-dormant) leukaemia stem cells (LSCs) sub-population from the CD34+CD38- dormant LSCs (Iwasaki, Liedtke *et al.* 2015). Consequently, targeting CDKN2B might be a promising strategy for breaking dormancy in AML.

The dormancy signature came to support the marked overexpression of several important stemness and inhibition of differentiation related genes including CD34, CD123, TIM-3, ABCC3, MEIS1, IL6ST and GPR56. Among these genes, ABCC3 was one of the top 3 upregulated genes in dormant TF1-a (table 5.1). This gene is

known to be associated with multi-drug resistance and poor prognosis in AML (Muller, Asher *et al.* 2008, Giannoudis, Davies *et al.* 2014, Bartholomae, Gruhn *et al.* 2016). It was classified with other stemness-related genes because it is known to be highly expressed in normal and leukemic CD34+ stem cells in comparison to differentiated counterparts (Giannoudis, Davies *et al.* 2014). However, it has been also reported to exert a tumour suppression activity as the loss of this gene found to promote tumour formation (Wiel, Gras *et al.* 2016).

Tim-3 (also known as HAVCR2), CD123 (also known as IL3RA) and GPR56 genes are of particular importance in LIC as these stemness markers have recently been found to be specifically expressed in leukaemia stem cells while they are absent in normal haematopoietic stem cells. (Kikushige, Shima *et al.* 2010, Kikushige and Miyamoto 2015, Kikushige, Miyamoto *et al.* 2015, Al-Mawali, Gillis *et al.* 2016, Bonifant, Szoor *et al.* 2016, Pabst, Bergeron *et al.* 2016). This makes them promising therapeutic targets in AML.

In line with the above discussed stemness-related genes, TF1-a cell stemness features were confirmed at the protein expression level. This was confirmed immunophenotypically by overexpression of CD34 and ALDH and by immunofluorescence study through nuclear translocation of FOXO3a (sections 3.2.9 and 3.2.11). It is worth to mention, however, that the CD34 receptor expression is known to be regulated at the transcriptional level therefore the GEP results came in agreement with the phenotypic findings. On the other hand, the regulation of FOXO3a is more complex and believed to be mainly by post-translational modification and ubiquitination regulation that control the movement of this transcription protein between the nucleus and the cytoplasm.

The discussed upregulated genes of the dormancy signature of dormant TF1-a cells highlight the important features of this *in vitro* system in modelling dormancy in LIC.

# CHAPTER SIX
# INVESTIGATION OF OSTEOPONTIN AND ITS RECEPTORS IN AML CELLS

## 6.1. Background

OPN is a secretory phosphoglycoprotein with pleotropic biological effects produced by a variety of cells including osteoblasts which are considered as one of the major sources of this protein in the BM. OPN can bind to various integrins through an arginine-glycine-aspartate–mediated interaction and to CD44 through a non-arginine-glycine-aspartate–mediated interaction (Stier, Ko *et al.* 2005). Extracellular OPN expression has been detected to be highly restricted to the endosteal region of normal murine BM (Nilsson, Johnston *et al.* 2005). In this area of the BM, it can function as adhesion protein, cytokine or chemokine and is implicated in HSC migration and self-renewal (Nilsson, Johnston *et al.* 2005) and HSCs pool regulation (Stier, Ko *et al.* 2005). One of the most important pieces of early evidence of the role of exogenous OPN in HSC proliferation inhibition was demonstrated by Nilsson *et al* (2005). In this study, HSCs isolated from OPN-wild mice infused with Bromodeoxyuridine (BrdU), a live nuclear dye labelling proliferating cells, showed 60% proliferation in comparison to 100% of the HSC counterparts in $OPN^{-/-}$ mice. This was supported by inhibition of growth of $CD34^{+}CD38^{-}$ human HSCs isolated from human umbilical cord *in vitro* cultured with exogenous OPN. Interestingly, in these *in vitro* experiments the proliferation of HSCs was inhibited by thrombin-cleaved OPN whereas the full length OPN showed nonsignificant effects on HSC growth (Nilsson, Johnston *et al.* 2005). This might suggest an *in vivo* activation step is necessary for the OPN to exert its inhibitory function. A similar inhibitory role for extracellular OPN on leukaemia cells was investigated recently by Boyerinas *et al* (2013). These researchers were able to demonstrate that *in vivo* neutralization of OPN in a mouse ALL model increases the proliferation of the leukaemia cells and enhances the therapeutic effect of Ara-C in reducing the minimal residual disease (MRD) burden (Boyerinas, Zafrir *et al.* 2013).

In addition to its expression and function in the extracellular compartment, OPN was detected intracellularly where it has been reported to have a distinct structure and function in dendritic cells (Shinohara, Kim *et al.* 2008). In this case OPN was found to be translated from a different start codon of the same OPN mRNA (Shinohara, Kim *et al.* 2008). This might be relevant to our dormancy model as CD44 was one of the significantly upregulated genes in dormant TF1-a cells (table 5.1). Moreover, in macrophages, endogenous OPN is found to be involved in modulating CD44-dependent chemotaxis (Zhu, Suzuki *et al.* 2004). Furthermore, it has been recently reported that intracellular OPN–deficient natural killer (NK) cells showed increased apoptosis, defective maturation, and reduced ability to generate memory-like NK cells that respond to mouse cytomegalovirus (Leavenworth, Verbinnen *et al.* 2015). Finally, a study has confirmed a distinct role for intracellular OPN in the regulation of innate immunity using OPN-deficient mouse model (Zhao, Zhang *et al.* 2016).

The role of intracellular OPN in dormancy or proliferation has not yet been well investigated and, despite the role of extracellular OPN in dormancy and proliferation in HSCs and ALL cells discussed above, its role in AML cells has not been previously investigated. Therefore, in this study, we subjected OPN to two lines of investigations; firstly the *in vitro* role of exogenous OPN (as a cytokine) on TF1-a proliferation was investigated and secondly the expression of OPN protein and one of the OPN principal receptors (CD44) was studied in bone marrow biopsies of AML patient by immunohistochemistry. It is worth mentioning that the *in vitro* experiments investigating OPN in AML cells (section 6.2.1) were carried out before the results of the GEP were obtained.

## 6.2. Results

### 6.2.1. Investigating the role of osteopontin in the *in vitro* dormancy induction of TF1-a cells

Declaration: Most of the data presented in this section (section 6.2.1) were generated by Nikita Dutta (MSc student) under my co-supervision.

In this part of the study we sought to investigate two areas linked to OPN in AML; firstly, the protein expression of OPN ligands in primary AML cells and in TF1-a cells. Secondly, the role of OPN as an exogenous cytokine in inducing inhibition of proliferation and dormancy features in TF1-a cells. No previous studies had investigated the effect of OPN on myeloid leukaemia cells despite the strong evidence of roles in HSCs (Nilsson, Johnston *et al.* 2005, Stier, Ko *et al.* 2005) which encouraged us to explore this area of research.

Initially, TF1-a cells were investigated for the expression of the OPN-related receptors. OPN had been found to bind to multiple integrins receptors such as , αvβ3, α9β1, αvβ5, αvβ1, αvβ6, α4β1, α5β1 and α4β7, in addition to CD44 ((Haylock and Nilsson 2006)and references therein). Firstly, we aimed to explore which of these putative OPN ligands were expressed in primary AML samples by investigating the Cancer Genomic Atlas (TCGA) database (available at the TCGA portal (https://tcga-data.nci.nih.gov/docs/publications/tcga/)). Table 6.1 provides information about the selected receptors for flow cytometry investigation based on Affymetrix data of leukaemia patients obtained from the TCGA database. An expression level of 2000 MAS5 output intensity units was considered as the lower limit for positive expression (Dr. J Payton, depositor, personal communication). It was clear that the genes regulating the receptors ITGA4, ITGB1 and CD44 have the highest expression levels at approximately 21000, 20000, and 60000 respectively. In addition, ITGAV, ITGA5 and ITGA9 exceeded the lower limit and hence they were also included for the flow cytometry study.

**Table 6.1: Osteopontin-related receptor genes expression in leukaemia patients according to The Cancer Genomic Atlas database.**

| Gene symbol | MAS5 intensity value | Antibody used for the flow cytometry assay |
|---|---|---|
| ITGAV | 5015.4 | Anti-Integrin αv |
| ITGA4 | 21883 | Anti-CD49d (BD Pharmingen 560972) |
| ITGA5 | 5000 | Anti-CD49e (BD Pharmingen 555617) |
| ITGA8 | 443.162 | |
| ITGA9 | 2353.13 | Anti-α9β1 (abdserotec MCA1585T) |
| ITGB1 | 20786.6181 | |
| ITGB3 | 1175.437 | |
| ITGB5 | 1000.73 | |
| ITGB6 | 113.56 | |
| ITGB7 | 1064.21 | |
| CD44 | 60000 | Anti-CD44 (abdserotec MCA89F) |

The flow cytometry investigation resulted in three of the studied receptors showing high expression on the surface of TF1-a cells. These were CD49d, CD44, and CD49e; whereas TF1-a cells showed low expression of α9β1 and αv OPN receptors (figure 6.1).

The effect of exogenous OPN on the proliferation of TF1-a cells was studied by culturing the cells for 3 days with full-length OPN or with Thrombin-cleaved OPN (which is reported to be more active than the full length form (Nilsson, Johnston *et al.* 2005, Grassinger, Haylock *et al.* 2009)). The doses of OPN and Thrombin

were selected based on previously published studies (Mi, Oliver *et al.* 2007, Boyerinas, Zafrir *et al.* 2013).

There was no significant inhibition of proliferation of TF1-a cells in response to OPN treatment (figure 6.2). Similarly, the attempt to detect an OPN effect on TF1-a cell proliferation by culturing these cells with OPN on fibronectin-coated or hyaluronic acid-coated surfaces was unsuccessful (figure 6.3). Fibronectin is a major component of the ECM and it has been reported that leukaemia cells tend to be more resistant to chemotherapy when they interact with fibronectin via VLA-4 (α4β1) and VLA-5 (α5β1) receptors (Matsunaga, Takemoto *et al.* 2003, Singh, Erb *et al.* 2013). Therefore, and based on this evidence, this assay was carried out to assess if OPN decreases TF1-a cell proliferation in the presence of fibronectin, possibly by interacting with either of these integrins which were found to be highly expressed on TF1-a cells (figure 6.1). Hyaluronic acid, on the other hand, was used because it is a major ligand of CD44 and adhesion of CD44 to hyaluronic acid is found to play a role in HSC homing and promotes HSC quiescence in the bone marrow (Avigdor, Goichberg *et al.* 2004, Zoller 2015). None of these attempts of *in vitro* culture of TF1-a cells with OPN have resulted in recognizable effect on the rate of cell growth.

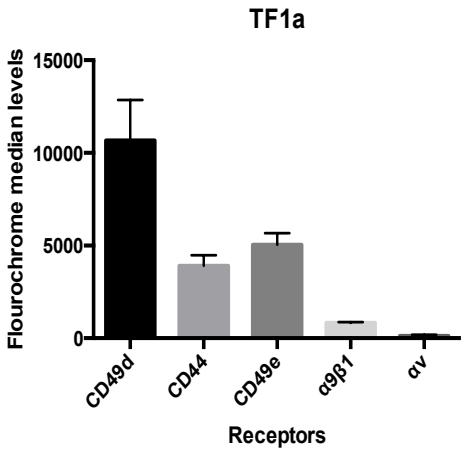



**Figure 6.1: The expression of OPN receptors on TF1-a cells** Untreated TF1-a cells were probed with the appropriate antibodies against each of the five receptor proteins before analysis by flow cytometry. Isotype-matched antibodies were used to identify the positive cells. The columns represent mean values of three independent experiments. The error bars represent +1SD.

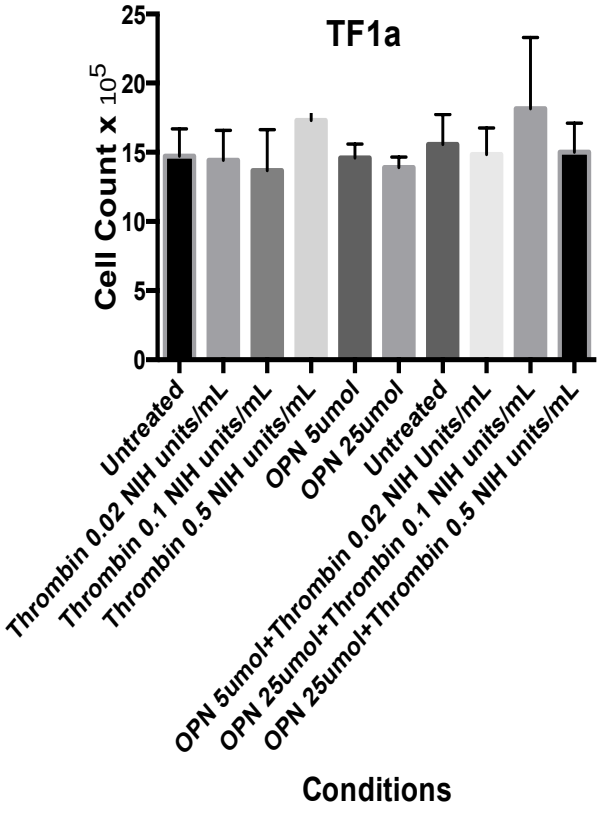



**Figure 6.2: TF1-a cells proliferation in response to OPN treatment.** TF1-a cells were cultured for 3 days with or without OPN and/or Thrombin at the mentioned concentrations before counting viable cells by FSCs/FACS method. The columns represent mean values of three independent experiments. The error bars represent +1SD.

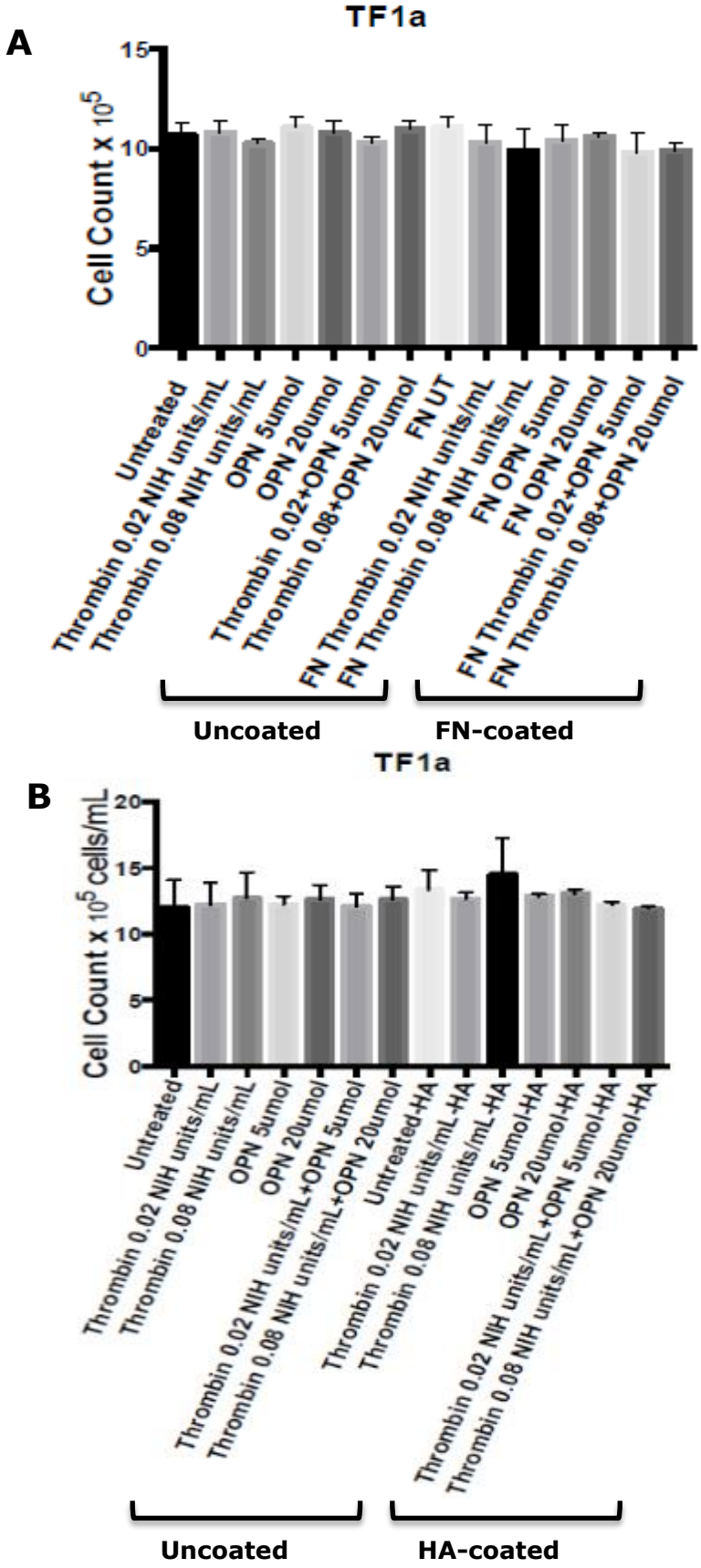



**Figure 6.3: TF1-a cell proliferation in response to OPN treatment in fibronectin or hyaluronic acid coated plates.** TF1-a cells were cultured for 3 days with or without OPN and/or Thrombin at the mentioned concentrations in 96-wells plates coated with fibronectin (FN) **(Panel A)** or hyaluronic acid (HA) **(Panel B)** before counting viable cells by FSCs/FACS method. The columns represent mean values of three independent experiments. The error bars represent +1SD.

### 6.2.2. Immunocytochemistry study of BM biopsies of AML patients

Expression of OPN, CD44 (one of the principal OPN receptors in leukaemia cell) and the cell cycle marker Ki-67 were investigated retrospectively by IHC staining of BM biopsies from 7 AML patients. OPN expression has been documented in the BM near the bone trabeculae and is linked to osteoblastic activation (Nilsson, Johnston *et al.* 2005, Stier, Ko *et al.* 2005). This region is also known as the endosteal region (Islam, Glomski *et al.* 1990). Liersch et al (2012) have investigated the expression of OPN in BM biopsies and they detected its expression in the cytoplasm of the BM haematopoietic cells including normal and leukaemia cells (Liersch, Gerss *et al.* 2012). However, these investigator did not focus on the anatomical localization of the extracellular OPN and the OPN-positive AML cells. Furthermore, they did not comment on the expression of this protein in the other haematopoietic cells in the BM. As the endosteal region harbours the dormant LICs, we were interested to discover whether this region is enriched for OPN-positive AML cells. It was also important to document intracellular and extracellular OPN, given that there are functional distinctions between the two (Shinohara, Kim *et al.* 2008).

Among the list of putative OPN-receptors (Haylock and Nilsson 2006) CD44 was selected for the IHC investigation. CD44 is the OPN receptor that was reported to act as a potential therapeutic target to eliminate leukaemia stem cells in mouse model (Jin, Hope *et al.* 2006). Moreover, CD44 was reported to play a vital role in HSCs and LSCs homing in the endosteal region (Erb, Megaptche *et al.* 2014, Szmigielska-Kaplon, Szemraj *et al.* 2014). In addition, the CD44 gene was one of the significantly upregulated gene in the TF1-a dormancy signature. Therefore CD44 expression in the BM biopsies of AML patients was investigated.

For this purpose, we obtained presentation (pre-therapeutic) and follow up (during therapy) BM biopsies for 7 AML patients (table 6.2 for the detailed clinical

characteristics). The main purpose of investigating these biopsies was to explore the expression of OPN and CD44 proteins in the leukaemia cells in their anatomical localization inside the BM whilst paying attention to cells near the para-trabecular region of the BM. Normal BM biopsies, unfortunately, could not be included as controls for the selected target proteins. However, no-primary-antibody controls were used as negative controls to validate the IHC staining. These controls were prepared in parallel to the test slides and subjected to all steps of the IHC staining, including the addition of the detection polymer and DAB stain, except adding the primary antibodies.

Prior to the IHC studies, sections from the 14 BM biopsies were stained with haematoxylin and eosin (H&E) stain for morphological examination to confirm the putative diagnosis and to have a background about the extent and distribution of the leukaemia cells infiltration in the BM (figure 6.4). Morphology of all presentation biopsies was consistent with the diagnosis of AML. The proportion of leukaemia cells were variable among the 7 patients, but in all of the cases they constituted the majority of the cellular marrow. The follow-up biopsies, on the other hand, showed considerably variable number of leukemic blasts where in some patients (figure 6.4) a marked reduction in blasts was noted whereas others showed little difference in comparison to presentation biopsies counterparts (appendix A5).

## Table 6.2: The clinical characteristics of the 14 BM biopsies of the 7 AML patients.

| Code | age | gender | immunophenotyping | cytogenetics | molecular genetics | type and duration of induction treatment | disease status at time of biopsy |
|---|---|---|---|---|---|---|---|
| **1P** | 67 | F | 31% CD34, CD117pos, aberrant CD7, cytCD79a | 46XXdel(2)(q11 q21),der(7)t(1; 7)(q2q22),add( 11)(q2)[9] | FLT3 ITD | presentation | presentation |
| **1T** | 67 | F | No data | Abnormal as previous, but donor cells also present | No data | post-transplant | incomplete engraftment and disease progression |
| **2P** | 45 | M | CD34neg/CD11 7neg, 54% CD64+ monocytes consistent with CMML in transformation | NORMAL | NORMAL | presentation | Presentation. AML, consistent with transformed MDS or CMML. Longstanding monocytosis |
| **2T** | 45 | M | No data | No data | No data | post one cycle chemo | probable residual disease |
| **3P** | 78 | M | 36% CD34+, CD117+, aberrant CD7 | NORMAL | all neg. | presentation | presentation |
| **3T** | 78 | M | 69% CD34+, CD117+, aberrant CD7 | No data | No data | post 4 cycles low dose ara C | resistant disease |
| **4P** | 83 | F | CD34neg, CD117pos, aberrant CD7 | NORMAL | FLT3 ITD | presentation | presentation |
| **4T** | 83 | F | No data | No data | No data | post 2 cycles low dose araC | partial response |
| **5P** | 9 | M | No data | NORMAL | No data | No data | relapse |
| **5T** | 9 | M | No data | No data | No data | chemo (no details) | remission |
| **6P** | 25 | F | 44% CD34+ | minus 7 (9/10) | all neg. | presentation | presentation, biopsy suggests AML on an MDS background |
| **6T** | 25 | F | No data | Normal, no sign of chr 7 abn. by FISH | No data | post FLAG-Ida | normal regenerating marrow |
| **7P** | 60 | F | 20% CD34+, aberrant cytCD79a | NORMAL | FLT3ITD | presentation | presentation |
| **7T** | 60 | F | 1% CD34, 1% CD34, poor sample (clotted) | No data | No data | post chemo (AML17), falling counts | 20% CD34 by histo. Relapse |

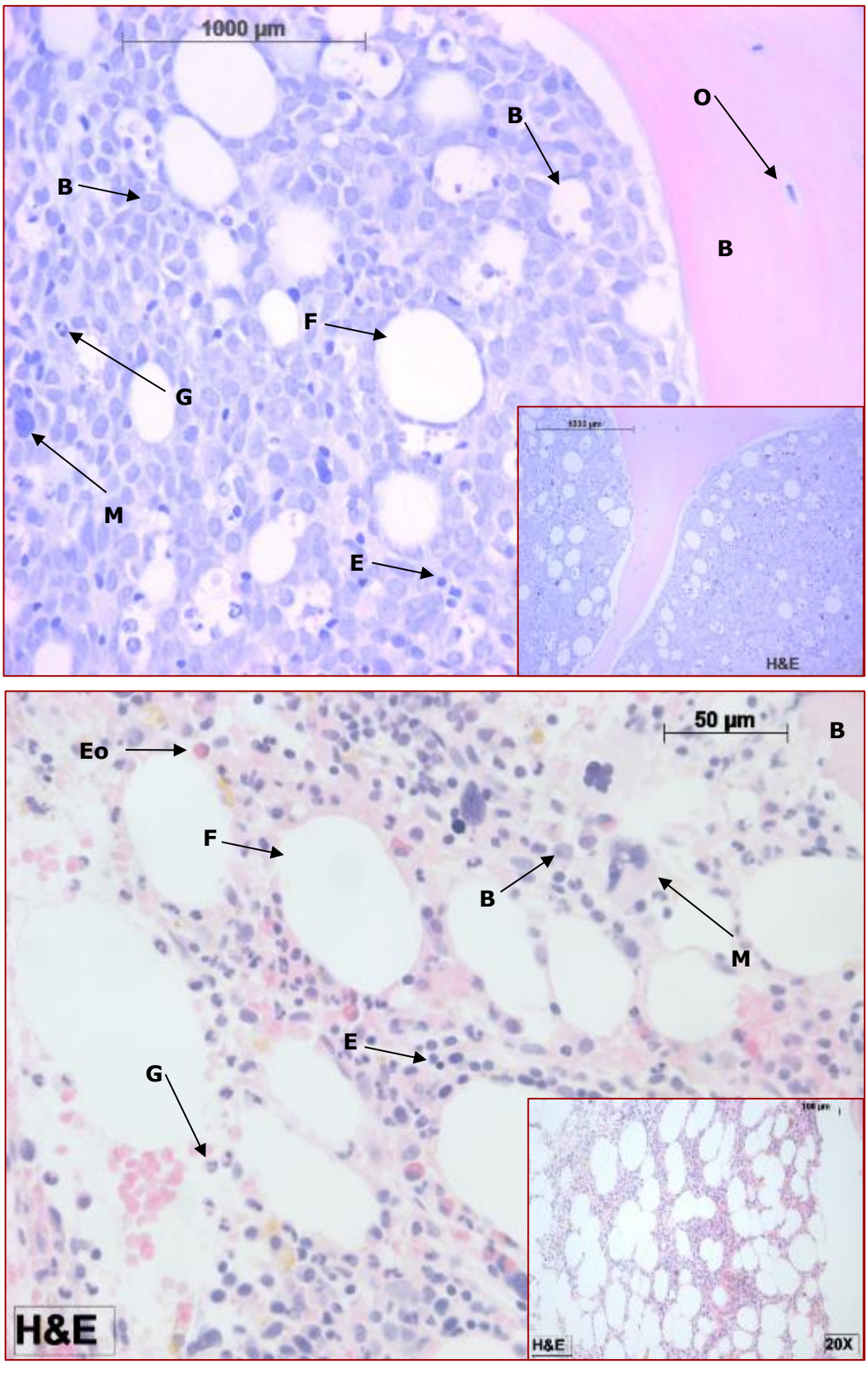



**Figure 6.4: BM biopsies of AML patient number one stained with H&E. The** pictures show that leukemic blasts constituted the majority of the BM cells in the presentation biopsy (upper) whereas they displayed significant reduction after treatment in the follow-up biopsy (lower) which was associated with regeneration of normal BM cellular components. BT, bone trabeculae; M, megakaryocyte; E, erythrocyte; B, Blast; F, fat cell; G, granulocyte; Eo, eosinophil; O, osteocyte.

#### 6.2.2.1. Osteopontin expression detection by Immunohistochemistry of BM biopsies of AML patients

The next step following the H&E staining was to investigate the expression of OPN in BM biopsies of the AML patients. Two concentrations for the anti-OPN antibody were selected for optimization; 1:250 and 1:500, based on the manufacturer instruction and previously published reports. Both concentrations resulted in comparable staining intensity with a slightly stronger signal obtained from the 1:250 dilution. Therefore, this dilution was used for all experiments thereafter.

Despite the variability in the intensity of the staining, most of the leukemic blasts were OPN-positive in the 7 studied presentation BM biopsies. Signals were, mostly, associated with the cytoplasm of leukemic blasts. In some cases, however, the inter-cellular spaces showed positive OPN staining particularly in regions where leukemic blasts become adjacent to the bone trabeculae. Interestingly in term of the amount of staining, two of the studied patients showed differential OPN expression in the cytoplasm of leukemic blasts which were adjacent to the bone trabeculae in comparison to those relatively far from this area of the BM (figure 6.5). The other 5 cases, nevertheless, showed a similar degree of cytoplasmic OPN expression regardless the anatomical localization of the leukaemia cells (appendix A5).

In contrast to its expression in AML cells, OPN expression in other cellular components was generally weak or negative. Exceptionally, the megakaryocytes showed constant high cytoplasmic OPN expression in almost all the studied cases. OPN staining in post-therapeutic biopsies with marked reduction in blasts count showed similar pattern of expression in all types of marrow cells (figure 6.6).

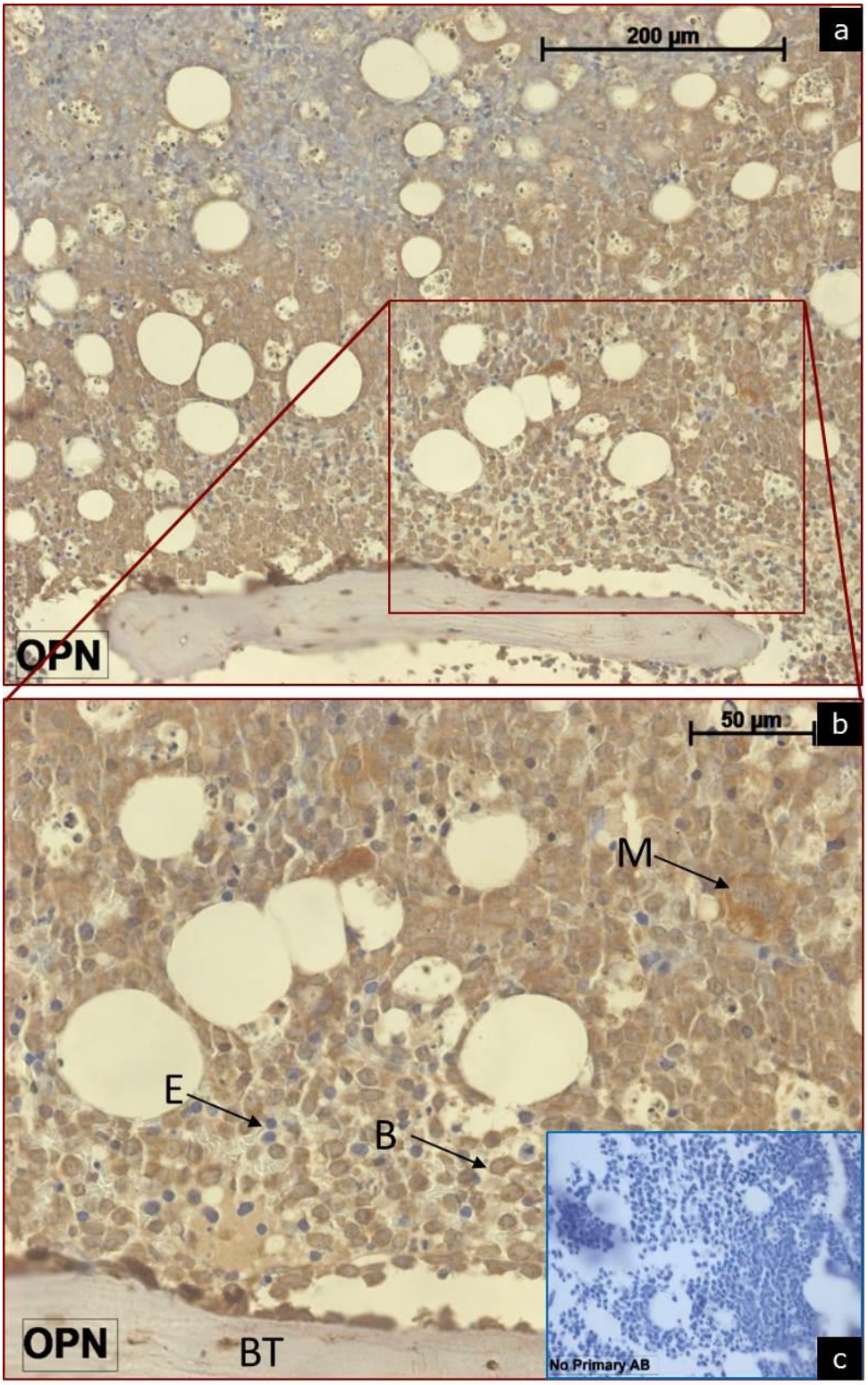



**Figure 6.5: Immunohistochemistry of OPN Expression in BM biopsies of AML patients.** Microscopy pictures for one of the two AML patients (patient number 4) that showed preferential OPN expression in blasts adjacent to the bone trabeculae in comparison to those relatively far from this area of the BM. Picture b displays a zooming into this area to illustrate the cytoplasmic expression of OPN in the leukemic blasts. No primary antibody negative controls (picture c) were prepared to validate the IHC staining. B, blast; E, erythrocyte; M, megakaryocyte; BT, bone trabeculae.

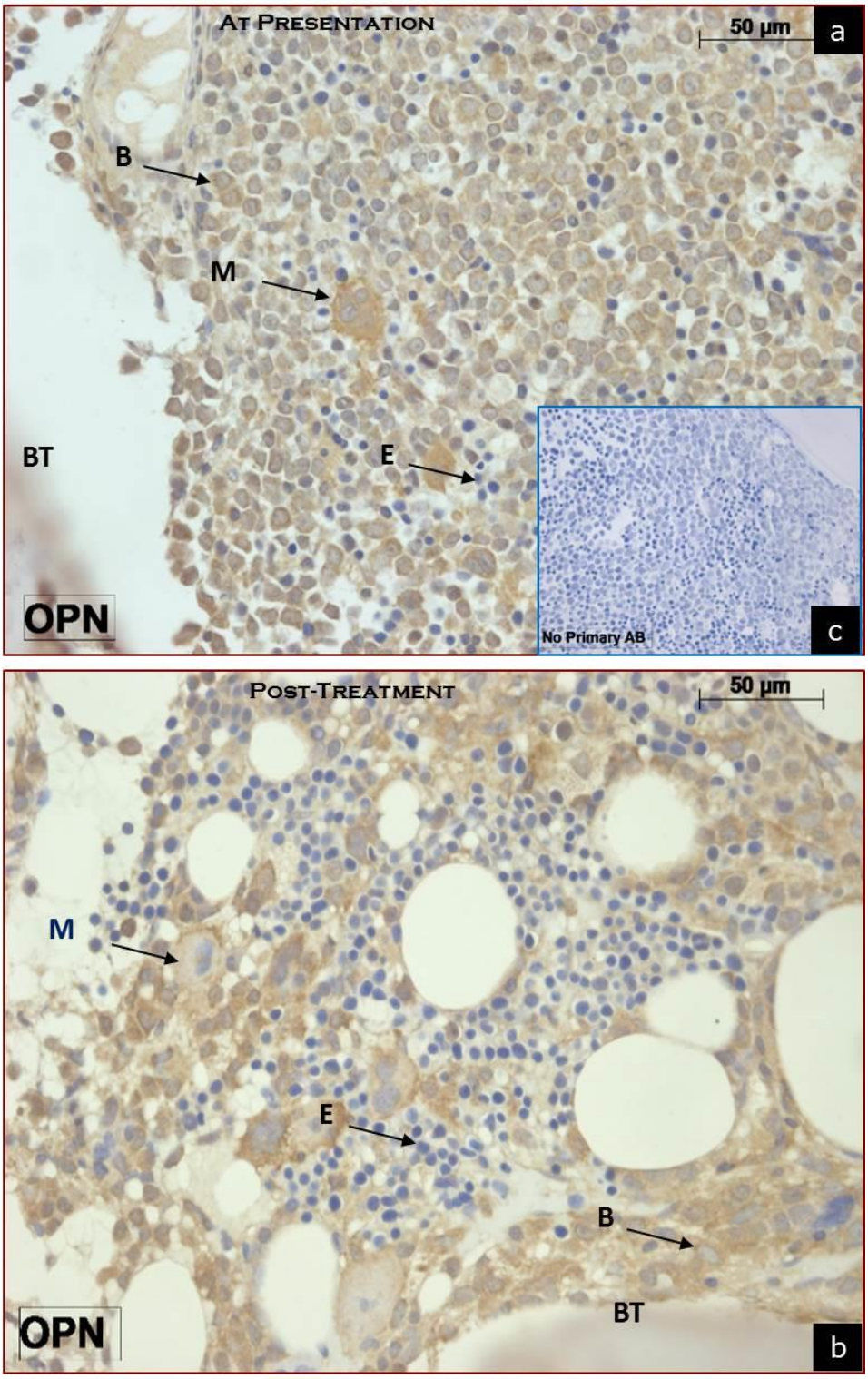



**Figure 6.6: Immunohistochemistry of OPN Expression in BM biopsies of AML patients.** The pictures compare OPN expression in presentation (picture a) and post-treatment (picture b) BM biopsies for the same patient (patient number 5). Notably, despite the signs of marrow regeneration post treatment, which is represented by the active erythropoiesis and megakaryopoiesis, significant residual leukemic blasts can be seen near the bone trabeculae and these blasts retain the OPN expression. No primary antibody negative control (pictures c) were used to validate the IHC staining. B, blast; E, erythrocyte; M, megakaryocyte; BT, bone trabeculae.

#### 6.2.2.2. CD44 investigation by Immunohistochemistry of BM biopsies of AML patients

Alongside OPN assessment by IHC, the expression of the transmembrane receptor CD44 was investigated in the 14 BM core biopsies of the 7 AML patients. Based on the manufacturer recommendations and published works, two dilutions for the anti-CD44 antibody were optimized; 1:100 and 1:200. The later dilution was then selected as both concentrations showed a similar staining intensity.

Leukemic cells displayed variable degree of CD44 expression among the 7 AML patients. While some cases showed marked membranous CD44 staining in the majority of leukemic blasts, others showed less than 10% of the blasts with strong CD44 expression (figure 6.7). As regards the normal BM cellular components, the megakaryocytes were consistently negative for CD44 expression whereas cells belonging to erythroid and granulocytic series were positive for CD44 expression in almost all the studied biopsies (figure 6.7). Importantly, there was no paratrabecular preference in the distribution of CD44 expression in the surface of the leukaemia cells i.e no indication that OPN and CD44 expression co-vary (figures 6.7 and appendix A5).

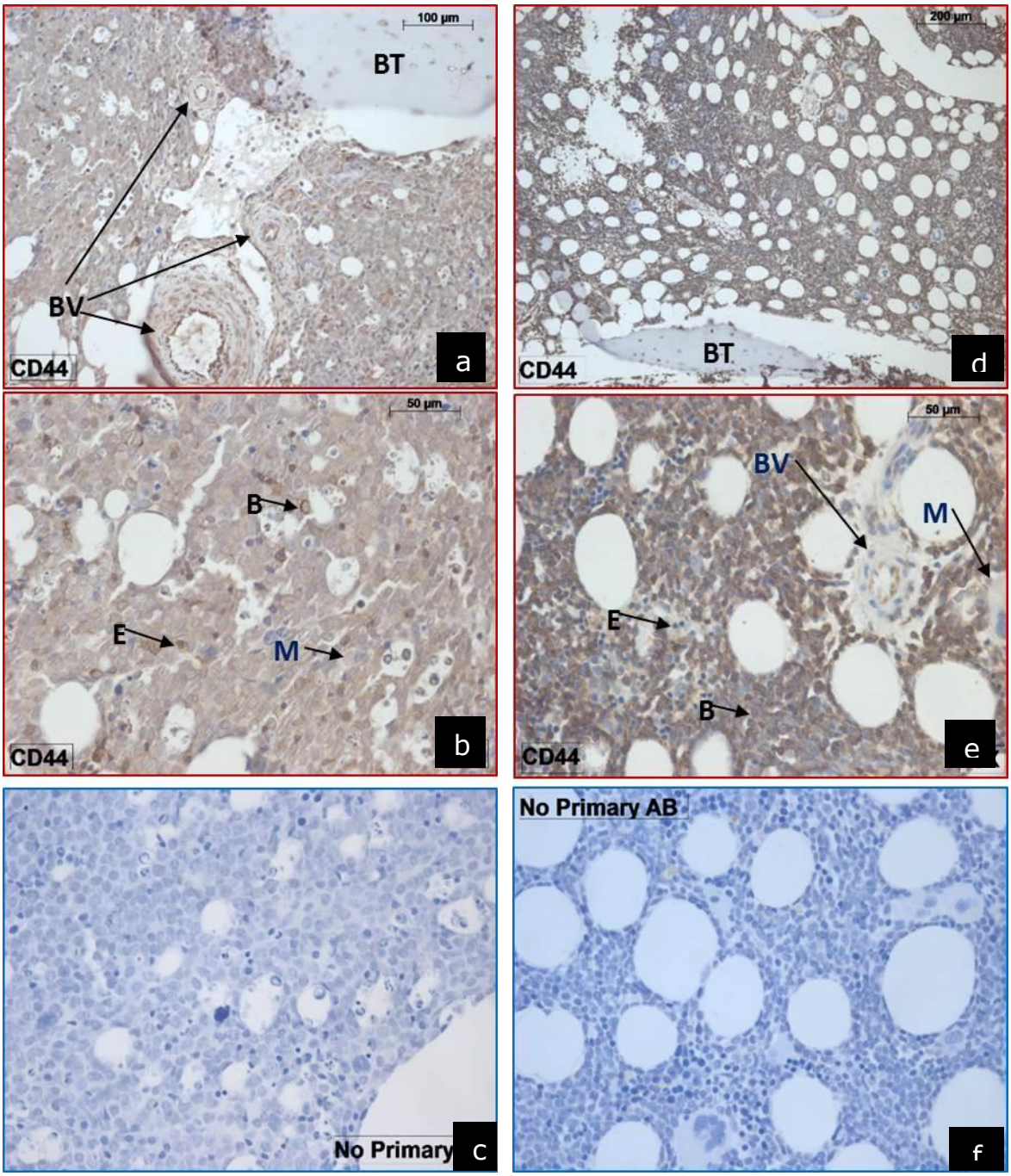



**Figure 6.7: Immunohistochemistry study of CD44 expression in BM biopsies of AML patients.** CD44 expression in patient 1 (pictures a-c) and patient 7 (pictures d-f) contrasting marked memberanous staining in the majority of blasts (d-e) with strong staining in less than 10% of blasts (a-b). Of note, there was no differential increase in CD44 expression in blasts adjacent to the bone trabeculae in comparison to those relatively far from this area of the BM. Moreover, the non-malignant cellular components of the BM such as the erythroid and granulocytic cells showed CD44 staining. No primary antibody negative controls (pictures c and f) were used to validate the IHC staining. B, blast; E, erythrocyte; M, megakaryocyte; N, neutrophil; BT, bone trabeculae; BV, blood vessel.

6.2.2.3. Ki-67 investigation by Immunohistochemistry of BM biopsies of AML patients

The expression of the proliferation marker Ki-67 in the AML patient BM biopsies was investigated by immunohistochemistry. This was to evaluate the distribution of the cycling (Ki-67 positive) and the dormant (Ki-67 negative) leukaemia cells in relation to the endosteal region of the BM. In addition, it was useful to compare the pattern of expression of this cell cycle marker with the OPN expression pattern which might explore any possible correlation. For these purposes, all presentation and treatment BM biopsies were included except the presentation biopsy of patient number 4 (4P) due to the inadequacy of the available biopsy sections.

In addition to the visual microscopical examination of the IHC-stained biopsy sections for the Ki-67 expression, the expression of this nuclear protein was subjected to a scoring system to facilitate the assessment of the extent and distribution of dormant and cycling leukaemia cells in the studied BM biopsies. The Ki-67 expression, calculated as Ki-67 index using IHC of tissue biopsy sections, is a widely used and standardized as a predictive and prognostic marker in solid malignancies such as breast cancer (Niikura, Sakatani *et al.* 2016) whereas its use in leukaemia patients is limited. Finally, despite all biopsies being stained for Ki-67 expression, the analysis is shown for the presentation biopsies only as the treatment biopsies were found to have variable degree of normal BM cells regeneration which is associated with significant Ki-67 expression that made the distinction between normal and malignant blasts unreliable.

The presentation biopsies showed variable proportions of cycling (Ki-67 positive) leukaemia cells (figure 6.8). The Ki-67 index ranged from as little as 25% for patient number 1 (1P) to as high as 60% for patient number 2 (2P). The other cases showed that almost half of the leukaemia cells were Ki-67 positive. Consequently, the Ki-67 negative (dormant) AML cells also varied in number among the studied biopsies. These could be either differentiated non-cycling

leukaemia cells or dormant leukaemia initiating cells which could not be distinguished at this level of investigation.

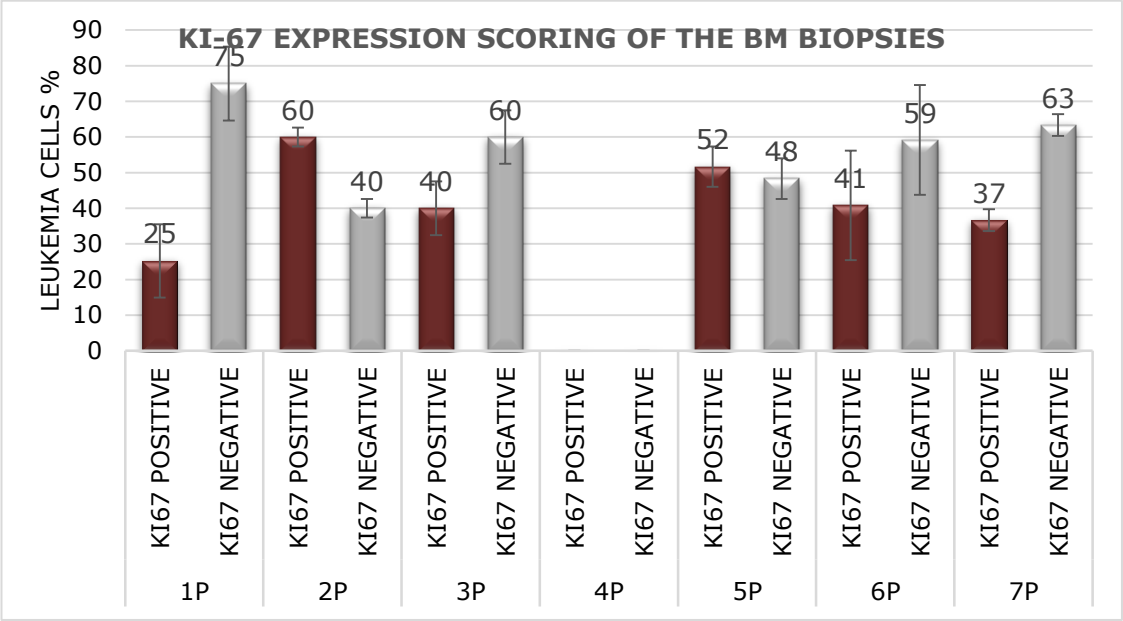



**Figure 6.8: KI67 expression scoring of the BM biopsies of the AML patients.** At least 500 leukaemia cells from up to 6 high power fields (chosen to adequately represent all BM areas infiltrated by leukaemia cells) were counted using ImageJ software and classified into Ki67-positive or Ki67-negative according to the presence or absence of the DAB stain. The brown bars represent the mean value of the proportion of Ki67-positive leukaemia cells and the grey bars represent the Ki67-negative ones for each BM biopsy. 1P: presentation BM biopsy of patient number one. Similarly, 2P, 3P, 4P, 5P, 6P AND 7P refer to the relevant patient's biopsy code accordingly. Patient number 4 was not investigated due to insufficiency of the presentation biopsy sections.

Importantly, the anatomical localization of the dormant leukaemia cells showed no specific relation to the endosteal region. They were distributed throughout the BM areas regardless their distance from the bone trabeculae (Figure 6.9). In general, two pattern of Ki67-positive cells distribution were noticed. In some cases Ki-67 positive leukaemia cells were arranged as agglomerates that resulted in BM fields with high proportion and others with low proportion of stained leukaemia cells. In other cases the Ki-67 positive and negative cells were distributed homogenously in areas of leukaemia infiltration (appendix A5 shows the detailed IHC pictures of all studied cases).

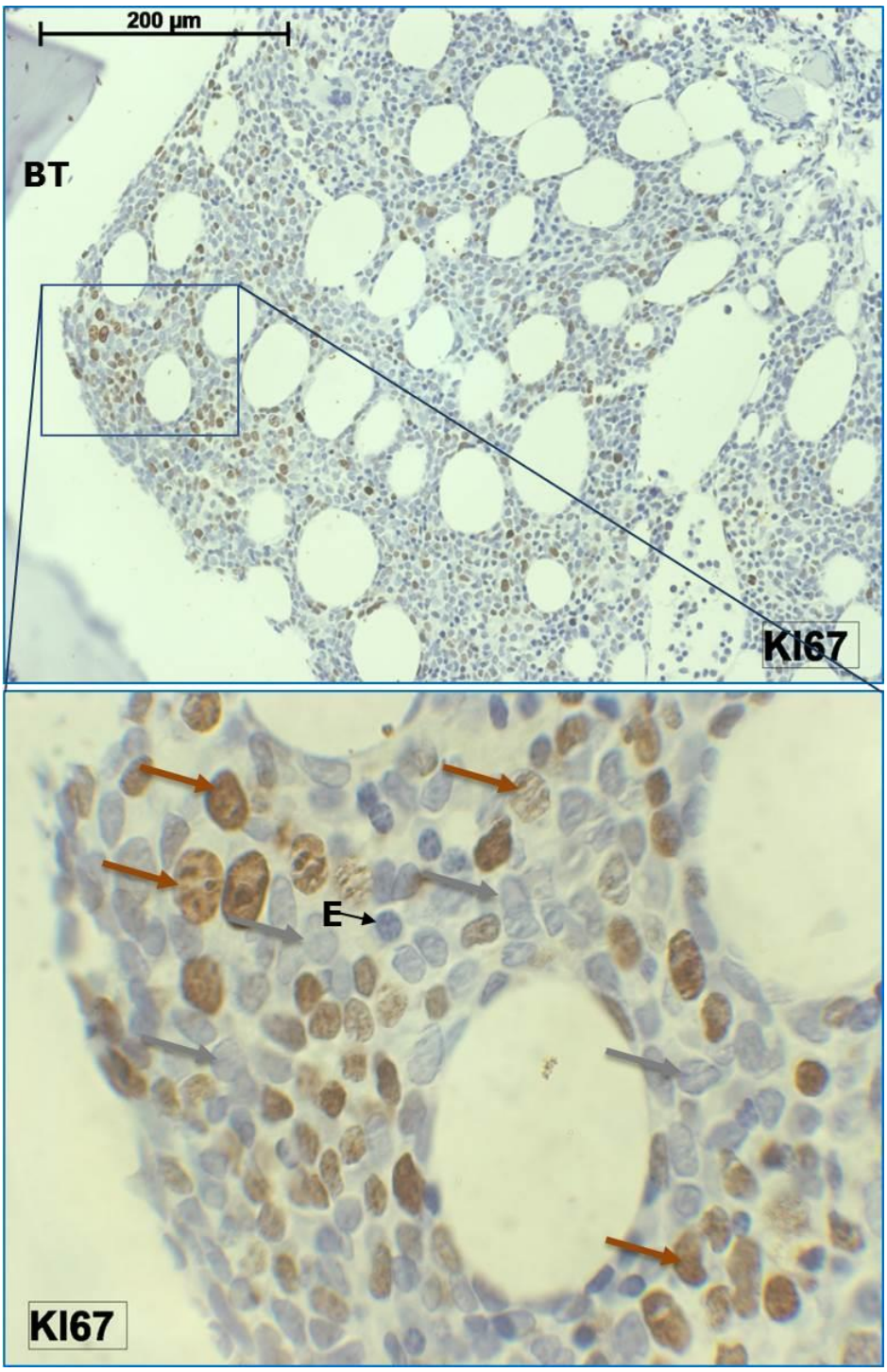



**Figure 6.9: Immunohistochemistry of Ki-67 Expression in BM biopsy of AML patient.** The lower picture is a magnification of small area of the upper picture and both taken for the presentation biopsy of patient number 3 (3P). It shows the distribution of Ki-67 positive (brown arrows) and the Ki-67 negative (grey arrows) leukaemia cells in areas close to the bone trabeculae (BT). It is clear that the leukaemia cells constituted most of the nuclear component of this BM with occasional small non-cycling erythroid cells (E) among the malignant cells. It is noticeable, also, that the Ki-67 staining was varied in the Ki-67 positive cells which might reflect the variation in the quantity of Ki-67 protein in different stages of the cell cycle.

## 6.3. Discussion

### 6.3.1. comparison between OPN receptors expression on primary AML cells with that on TF1-a cells.

To determine the likelihood of TF1-a dormancy signature findings being widely applicable to AML cases we sought to compare the findings of GEP data from TCGA database with that of GEP of dormant TF1-a cells in this study. In this context, it was clear that two of the OPN receptors (ITGAV and CD44) which were highly expressed in primary samples, according to the TCGA database, were significantly upregulated in dormant TF1-a cells. On the other hand, two other receptors, ITGA9 and ITGB1, which were significantly expressed on AML cells by the TCGA database showed slight and non-significant increase in the dormancy model. The heterogeneity of primary samples, however, not necessarily conferring the sensitivity needed for looking at dormant subset within niche. The ITGA4 receptor which was significantly upregulated in primary AML cells and was the most expressed receptor on untreated TF1-a cells by flow cytometry (figure 6.1), showed a down regulation in the dormancy signature by 1.9 fold (table 6.3) suggesting that it might not play a specialized role in dormancy. Finally, ITGB3 and ITGB5 which were non-significantly expressed in AML patients according to the TCGA database displayed a marked upregulation in the TF1-a dormancy signature. TF1-a ITGB3 expression was measured subsequently in the department (by Grace Brindle; B.Med.Science student) which showed a positive expression on these cells (mean value of approximately 1500 MFI of 3 independent experiments). Furthermore, it showed significant expression up-modulation on dormant TF1-a cells by flow cytometry ($p=0.01$) compared to untreated counterparts (data not shown). The gene coding for this integrin receptor was the most upregulated one in dormant TF1-a cells (table 5.1).

**Table 6.3: Comparison between OPN receptors genes expression in leukaemia cells from two sources; the TCGA data base and dormant TF1-a cells.** Note: OPN receptor protein expression by flow cytometry (FC) in untreated TF1-a cells also included.*

| | Receptor symbol | Primary AML cells (TCGA GEP intensity value) | Dormant TF1-a (GEP fold change) | Untreated TF1-a (FC intensity value) |
|---|---|---|---|---|
| 1 | ITGAV | 5015.4 | 2.8 | 100 |
| 2 | ITGA4 | 21883 | -1.9 | 11000 |
| 3 | ITGA5 | 5000 | 1.4 | 5000 |
| 4 | ITGA8 | 443.162 | -1.1 | |
| 5 | ITGA9 | 2353.13 | 1.2 | 1000 |
| 6 | ITGB1 | 20786.6181 | 1.2 | 1000 |
| 7 | ITGB3 | 1175.437 | 7.2 | 1500 |
| 8 | ITGB5 | 1000.73 | 2.2 | |
| 9 | ITGB6 | 113.56 | 1.1 | |
| 10 | ITGB7 | 1064.21 | -1.02 | |
| 11 | CD44 | 60000 | 3.7 | 4000 |

*negative values indicate down regulation, values highlighted in red are statistically significant (chapter five).

### 6.3.2. Lack of an inhibitory effect for exogenous osteopontin as a cytokine on TF1-a cells proliferation

The *in vitro* attempts to inhibit the proliferation of TF1-a cells by exogenous OPN were unsuccessful in this study (section 6.2.3.1). This was in agreement with a previous study by Boyerinas et. al. (2013) who despite the solid evidence they demonstrated regarding the role of OPN in the *in vivo* dormancy regulation in ALL, they reported no *in vitro* effect of exogenous OPN on ALL cells proliferation (Boyerinas, Zafrir *et al.* 2013). In addition, the inhibitory effect of OPN on HSCs

proliferation was reported due to the thrombin-cleaved OPN rather than the full length one (Nilsson, Johnston *et al.* 2005). In this study both full-length and thrombin-cleaved OPN were unable to induce groth inhibition in TF1-a cells. This might explained by the assumption that the main role of OPN is centralized around creating a sub-compartment inside the BM through anchoring the leukaemia cells to the extra cellular matrix near the endosteal region promoting other environmental factors, such as shortage of nutrients and excess of TGFβ1, to exert their dormancy effects. Moreover, expression of receptors does not necessarily mean it binds to its ligands as adhesion depends on a range of factors such as glycosylation and receptor density (Hanke, Hoffmann *et al.* 2014).

### 6.3.3. Myeloid Leukaemia cells in the bone marrow biopsies of AML patients were positive for expression of osteopontin and CD44

The IHC study of the BM biopsies was associated with some limitations (out side our control) such as the inability to provide a normal BM biopsies as controls. Moreover, the timing of obtaining the treatment biopsies, in relation to the treatment protocol, could not be taken in consideration; therefore, it was difficult to establish patterns. In addition, the number of sections available per biopsy were also too limited to allow including other adhesion related proteins which might be of importance. The available biopsies, nevertheless, provided sufficient materials for the main purpose of study which was exploring the OPN and CD44 expression in leukaemia cells near the bone marrow trabeculae.

The IHC study of BM biopsies of the 7 AML patients confirmed the expression of OPN in the cytoplasm of AML cells and in the intercellular space between these malignant cells near the bone trabeculae. Similarly in acute lymphoblastic leukaemia (ALL), the para-trabecular BM had been reported to be rich in OPN which is believed to be produced by both the osteoblastic endosteal cells and by the leukemic cells near the endosteum (Boyerinas, Zafrir *et al.* 2013). In the

current study, BM biopsies of two AML patients at presentation were in line with this finding. The other 5 AML patients displayed a uniformly distributed expression of OPN in the cytoplasm of leukemic cells and in the extracellular compartments irrespective to the distance of the leukemic cells to the bone trabeculae. This was in agreement with a previous report investigating the expression of OPN in BM biopsies of a cohort of 84 AML patient at presentation (pre-treatment) (Liersch, Gerss *et al.* 2012). The normal control BM biopsies in that study showed a weak OPN expression which was limited to few positive cells near the endosteal region. Unfortunately, we were unable to include normal BM biopsies to compare the OPN expression with that of AML patients.

By taking deeper examination, the localization of OPN expression in the cytoplasm of the leukaemia cells was, sometimes, stronger than its expression in the extracellular space separating the leukaemia cells. Indeed, OPN is believed to exerts a wide range of intra as well as extra cellular roles in normal and malignant cells of various tissues ((Inoue and Shinohara 2011) and references therein). For instance, intracellular OPN has been found to play a key role in CD44-hyaluronan-ERM complex function in human fibroblasts (Zohar, Suzuki *et al.* 2000). Hence, our findings provide a basis for continued investigation of the intracellular role of OPN in leukaemia cells dormancy.

Interestingly, the megakaryocytes showed a consistent cytoplasmic expression of OPN in almost all the studied BM biopsies (appendix A5). In certain occasions, this expression was stronger in megakaryocytes of the presentation biopsies if compared to the treatment biopsies of the same patients (figure 6.6). There is little known about the role of OPN produced by the megakaryocytes, however it has been reported that the megakaryocytes exert a vital role in maintaining homeostatic quiescence of HSCs through a TGFβ1-mediated mechanism (Zhao, Perry *et al.* 2014). Taking this fact in association with our result that the OPN gene

was the most upregulated gene by TGFβ1 in the TF1-a dormancy signature, it might suggest future research into a possible role of OPN in the cross-talk between leukaemia cells and the megakaryocytes.

Studying the expression of CD44 in the BM biopsies of the 7 AML patients demonstrated a variable degree of expression among the investigated cases in term of the number of positive cells and the intensity of the staining. This variation might be due to the large number of splice variants of CD44 or it might reflect the heterogeneity of AML cells and this requires further investigation. It has been reported that the CD44 gene has 20 exons and that nine of these 20 exons encode for the CD44H variant (the haematopoietic standard membranous molecule). One exon control the synthesis of a short cytoplasmic variant of CD44 whereas the rest of exons can be expressed in variable combination inserted at the proximal end of the membranous CD44 to give different CD44 variants (Bendall, Bradstock *et al.* 2000). It has been found that in addition to the CD44H, several other variants of CD44 carrying the exons v6, v8, v9 and v10 have been detected in a number of AML cell lines and normal blood mononuclear cells (Dougherty, Landorp *et al.* 1991). In this study, we used a polyclonal anti-CD44 antibody for the IHC experiments. This helped us to detect a wider possible range of CD44 variants on the surface of the leukaemia and normal BM cells but it also carried the drawback of the heterogeneity of CD44 staining intensity.

Unlike OPN, CD44 showed significant membranous expression in normal haematopoietic cells belonging mainly to the erythrocytic or granulocytic series of the studied BM biopsies. Indeed, it has been found that CD44 has a wide range of expression on normal and malignant haematopoietic cells making it a non-specific therapeutic target (Zoller, Fohr *et al.* 1998, Megaptche, Erb *et al.* 2014) despite its reported role as a therapeutic target in eliminating LSCs (Jin, Hope *et al.* 2006). Importantly, there was no discrepancy between the expression of OPN and CD44

in the leukaemia cells of the studied BM biopsies. In other ward, all cases that showed CD44 expression in the BM blasts were also positive for OPN in these leukaemia cells. This finding could be explained in light with the fact that OPN can play a role in inducing CD44 expression in malignant cells (Marroquin, Downey *et al.* 2004).

Finally, the result of investigating the expression of Ki-67 by IHC in the BM biopsies highlights the complexity of the distribution of dormant and proliferating leukaemia cells in the BM. It was clear that Ki-67 positive cells can be seen in any anatomical area of the BM. Furthermore, there was no clear correlation between the Ki-67 and OPN expression. Nevertheless, in order to have a clearer picture for analysis, it might be useful to conduct a longitudinal IHC study to investigate Ki-67 expression together with a leukaemia-specific stemness marker to track the residual dormant leukaemia cells at the minimal residual disease (MRD)-negative stage of remission post-chemotherapy.

# CHAPTER SEVEN

# INVESTIGATION OF $CD34^{+}CD38^{-}$ ACUTE MYELOID LEUKAEMIA TF1-a CELLS SUBJECTED TO PROLONGED SUB-LETHAL GENOTOXIC STRESS

## 7.1. Background

AML cells which are identified in the bone marrow (BM) endosteal region are likely to survive chemotherapy for several reasons including the low concentration of the drug delivered to this poorly perfused area of the BM. Consequently, the fate of these cancer cells might differ from others residing in the highly perfused peri-sinusoidal niche due to the sub-lethal concentrations of chemotherapeutic drugs. In fact, little is known regarding the molecular changes in those AML cells surviving genotoxic stress.

To investigate the AML cells surviving genotoxic stress, we developed and characterized an *in vitro* model of prolonged sub-lethal genotoxicity in AML cells by utilizing the TF1-a cells treated with etoposide for 6 days. The molecular signature of TF1-a cells under this conditioning was characterized using GEP of the whole human genome and was compared to that of the dormancy-induced TF1-a cells (chapter five) in an aim to identify genes commonly up-regulated in both scenarios that might be considered as possible drivers of dormancy in AML cells residing in a sub-lethal genotoxic environment.

Etoposide is a DNA topoisomerase II inhibitor that induces apoptosis in AML cells (Siitonen, Alaruikka *et al.* 1999). Etoposide is a known inducer of genotoxicity represented by DNA double strands breaks (DSB) in normal and cancer cells (Vock, Lutz *et al.* 1998, Karpinich, Tafani *et al.* 2002). In this context etoposide mimics the genotoxicity of ionizing radiation (IR) which has been reported to induce dormancy-like gene expression in a human diploid fibroblasts cell line (Zhou, Chou *et al.* 2006). Although we have considered using AraC or daunorubicin, etoposide was selected for this study principally because the precedent established in the previously mentioned study of cells acquiring features of dormancy when they survive treatment with an inducer of severe (double strand break-inducing) genotoxic stress.

This chapter will present and discuss the steps of establishing the *in vitro* genotoxicity model in TF1-a cells and the process of characterizing these cells by GEP including the microarray data analysis and the identification of genes and signalling pathways of interest. The laboratory investigations using qPCR on selected genes commonly up-regulated between the dormancy and the genotoxicity molecular signatures, for the purpose of validating the microarrays results, will also be presented.

## 7.2. Results

### 7.2.1. Selection of etoposide treatment dose and duration in TF1-a cells

In the treatment of AML patients, etoposide is administered for a duration of 5 days continuous therapy as 10+3+5 or 8+3+5 ADE regimes (10 or 8 days Ara-C + 3 days and 5 days of daunorubicin and etoposide respectively) (Burnett, Russell *et al.* 2013). In an aim to mimic this in vivo duration of treatment, we optimized a sub-lethal dose of etoposide to treat the AML cell line TF1-a for 6 days of treatment. To avoid the confounding effect of overcrowding and consumption of nutrients that can occur if cells are cultured continuously for more than 3 days, the 6 days of treatment was modelled by sub-culturing the cells at day 3 at the starting concentration prior to the second 3 days of treatment. Therefore, titrated doses of etoposide ranged from 31.25-8000 nM and were used to treat TF1-a cells in cell suspension medium for 3 consecutive days as basis for the 6 days of etoposide treatment. TF1-a cell growth showed a clear dose dependent decline in response to etoposide treatment when almost all the cells were killed by 8000nM of etoposide whereas little effect was noticed when the cells were cultured with a low concentration of the chemotherapeutic agent for the duration of treatment (figure 7.1,panel A). The etoposide dose that kills 20% of the TF1-a cells (IC20) was selected using GraphPad Prism-7 software which was equal to approximately 205nM. IC50 (the dose of etoposide that kills 50% of TF1-a cells) was also determined and used as a control that shows stronger etoposide genotoxicity effect (figure 7.1, panel A) for the validation experiments. Both IC20 and IC50 doses of etoposide resulted in statistically significant decrease in the viable cell count of TF1-a cells after 6 days of treatment (figure 7.1, panel B).

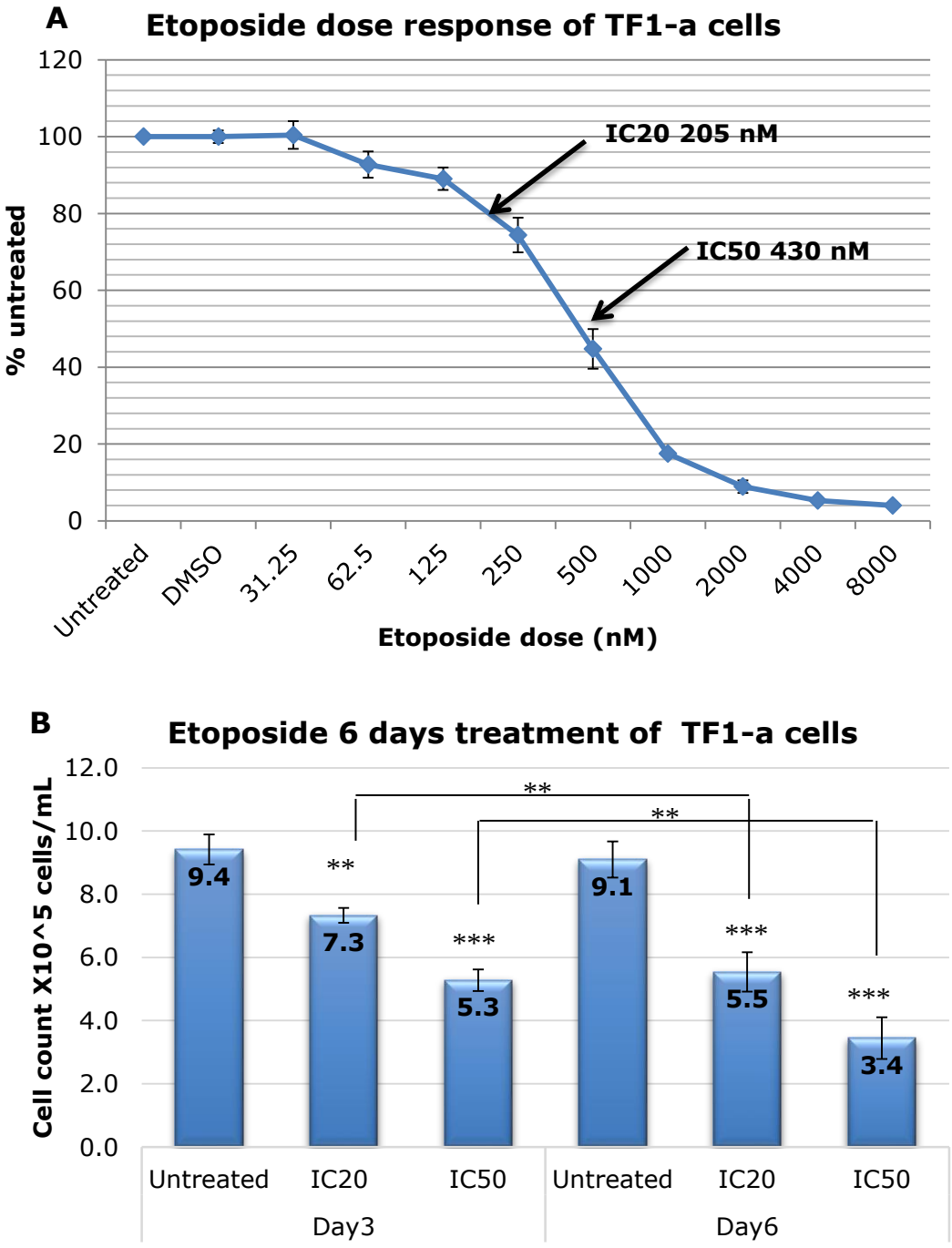



**Figure 7.1: Etoposide treatment optimization for TF1-a cells. Panel A** illustrates etoposide dose response assay. TF1-a cells were cultured for 3 days with escalating doses of etoposide in a 96 well plate. Untreated TF1-a cells were cultured in the same conditions as a control. The doses of etoposide that killed 20% or 50% of the cells (IC20 and IC50 respectively) were selected using GraphPad Prism-7 software for future experiments. **Panel B** shows the cell count of TF1-a cultured for up to 6 days with etoposide at both IC20 and IC50 doses selected from panel A. Cells were counted by FSCc/7AAD method. Values of the curve or the columns represent the mean values of 3 (panel A) or 4 (panel B) biologically independent replicates and the error bars represent +/- 1SD. **: $p<0.01$, ***: $p<0.001$.

### 7.2.2. Validating the genotoxicity in the Etoposide-treated TF1-a cells

The dose response assays give little clue as to the health of the survivor cells. In order to confirm lethality in some cells and at the same time to show whether the etoposide-treated survivor TF1-a cells are undergoing severe damage and early signs of apoptosis under the stressful conditions exemplified by the genotoxic effect of etoposide, we investigated the expression of 3 markers of apoptosis; namely, Annexin V, activated Caspase-3 and C-PARP by flow cytometry. In addition, the expression of the phosphorylated γH2AX, which is a marker of DNA DSBs, was also tested by flow cytometry in TF1-a cells cultured with 6 days of etoposide at the two selected doses (205nM and 430nM for the IC20 and IC50 respectively).

#### 7.2.2.1. Annexin-V assay

Etoposide-treated TF1-a cells showed statistically significant increases in the proportion of Annexin-V-positive cells, from a mean value of 9% in untreated to 18% in etoposide IC20-treated and 23% in etoposide IC50-treated TF1-a cells (figure 7.2; Panel A). Nevertheless, most survivor cells appeared healthy with double negative expression for both Annexin V and PI.

#### 7.2.2.2. γH2AX assay

Etoposide-treated TF1-a cells showed statistically significant increase in the proportion of phosphorylated γH2AX-positive cells, from a mean value of 2% in untreated to 6% in etoposide IC20-treated and 9% in etoposide IC50-treated TF1-a cells (figure 7.2; panel B). The majority of the cells surviving etoposide, however, were negative for γH2AX expression.

#### 7.2.2.3. C-PARP

Etoposide-treated TF1-a cells showed an increase in the proportion of C-PARP-positive cells, from a mean value of 5% in untreated to 8% in etoposide IC20-treated and 11% ($p<0.01$) in etoposide IC50-treated TF1-a cells (figure 7.2; panel

C). The majority of the cells surviving etoposide, however, were negative for C-PARP expression.

7.2.2.4. Activated Caspase-3 assay

Etoposide-treated TF1-a cells showed an increase in the proportion of aCaspase-3-positive cells, from a mean value of 7% in untreated to 9% in etoposide IC20-treated and 18% ($p<0.01$) in etoposide IC50-treated TF1-a cells (figure 7.2; panel D). The majority of the cells surviving etoposide, however, were negative for aCaspase-3 expression.

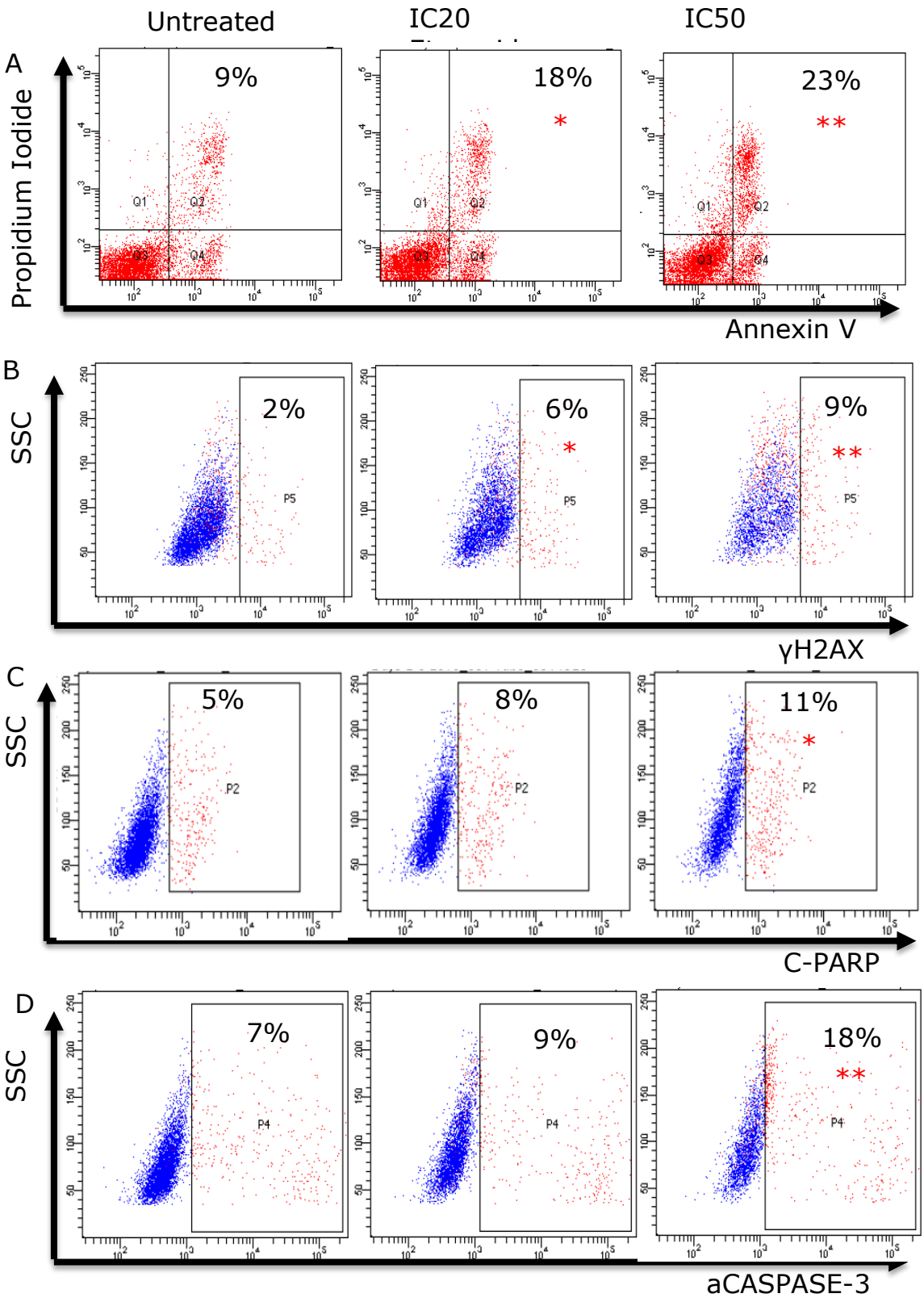



**Figure 7.2: Validation of genotoxicity in etoposide-treated TF1-a cells.** TF1-a cells were cultured for 6 days with or without etoposide at two doses (IC20 and IC50). The cells were then harvested and labelled with 4 apoptosis/DNA damage markers; namely, Annexin V **(panel A)**, γH2AX **(panel B)**, C-PARP **(panel C)** and aCASPASE-3 **(panel D)**. The fluorescence of these markers were then measured by flow cytometry and the proportions of marker positive cells were identified. The figures are representative examples of 3 biologically independent experiments that showed similar results. *=p value<0.05, **=p value<0.01.

### 7.2.3. Tracking TF1-a cellular division using PKH26 viability dye

The TF1-a cells treated with etoposide were labelled with the tracking dye PKH26 with the aim of investigating the effect of the treatment on the proliferation of this cell line and whether a sub-population of cells could be identified that could be sorted for a more refined model. PKH26 is a hydrophobic molecule that has been shown to be stably combined into cell membrane lipids by phase-partitioning without contaminating neighbouring cells. Division of the PKH26-labelled cells results in a 50% dilution of the fluorescence intensity in daughter cells (Horan and Slezak 1989).

As expected, the TF1-a cells cultured with etoposide showed slower proliferation in comparison to the untreated cells. This was confirmed by the fact that the etoposide-treated cells retained more PKH26 stain than the untreated counterparts after 6 days of culture; 21, 27 and 36 RFU for the untreated, IC20-treated and IC50-treated cells respectively (figure 7.3). Nevertheless, the cells proliferated as a single population in all the tested conditions and there was no sub-population that could be sorted using the PKH26 labelling.

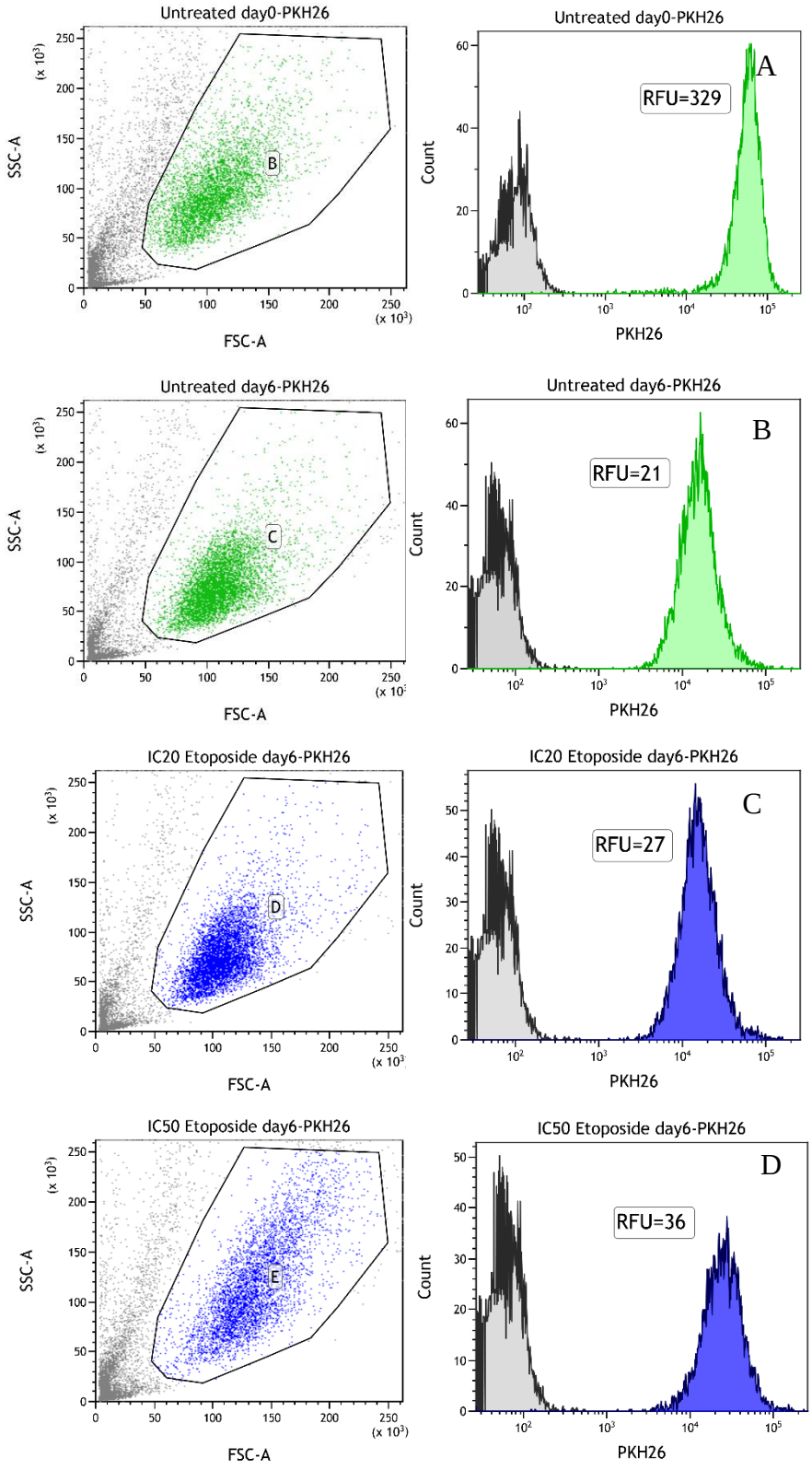



**Figure 7.3: Tracking of TF1-a cell division by PKH26 labelling.** TF1-a cells were labelled with PKH26 dye at day0 (histogram A) and then cultured for 6 days without (histogram B) or with etoposide at two doses; IC20 (histogram C) and IC50 (histogram D). The PKH26 fluorescence then measured by flow cytometry and the relative fluorescence unit (RFU) values for each condition were calculated in relation to the background fluorescence of unlabelled TF1-a cells (grey histograms). The figure is a representative example of 2 biologically independent experiments that showed similar results.

### 7.2.4. Molecular signature of the Etoposide-treated TF1-a cells

Whole human genome GEP using the Affymetrix strips (HuGene2.1ST) was conducted on three independent biological replicates of untreated TF1-a cells and TF1-a cells surviving a prolonged sub-lethal genotoxicity using 6 days culture with etoposide.

Once reads were obtained from the microarray chips, normalization steps were performed using Partek Genomics Suite 6.6. Software (figure 7.4). The list of differentially up/down regulated genes were generated through comparing different intensity signals between the expression levels of untreated TF1-a cells with that of TF1-a cells cultured with etoposide at IC20 dose.

#### 7.2.4.1 Selecting the genes of interest in the genotoxicity signature of TF1-a cells.

The GEP data generated for the genotoxicity signature showed a relatively low extent of up/down regulation of genes where the most significantly up regulated gene was increased by 2.7 fold and the most significantly down regulated one was decreased by -2.5 fold (table 7.1). Furthermore, when we used the FDR-based p-value adjustment and 2fold limit to filter genes significantly differentially up/down regulated, the number of genes obtained was limited to 10 up regulated and zero downregulated genes only. Lowering the threshold to 1.5 resulted in the number of upregulated genes increasing to 20 whereas the downregulated ones remained zero. Employing the FDR in selecting the significant p-value aims to exclude any possible false positives that might accompany simultaneous calculating of large numbers of hypotheses in the microarray data analysis (Pawitan, Michiels *et al.* 2005). Accepting that any positive results would have to be carefully validated by other means, and aiming to expand the number of genes for further study, we re-analysed the data without the FDR filtration step to include all significantly altered genes with more than a 1.5 fold change with $p<0.05$. This resulted in 88

significantly upregulated genes and 25 significantly down regulated genes (figure 7.5 and table 7.1). All further analysis of the genotoxicity signature is based on this list of genes.

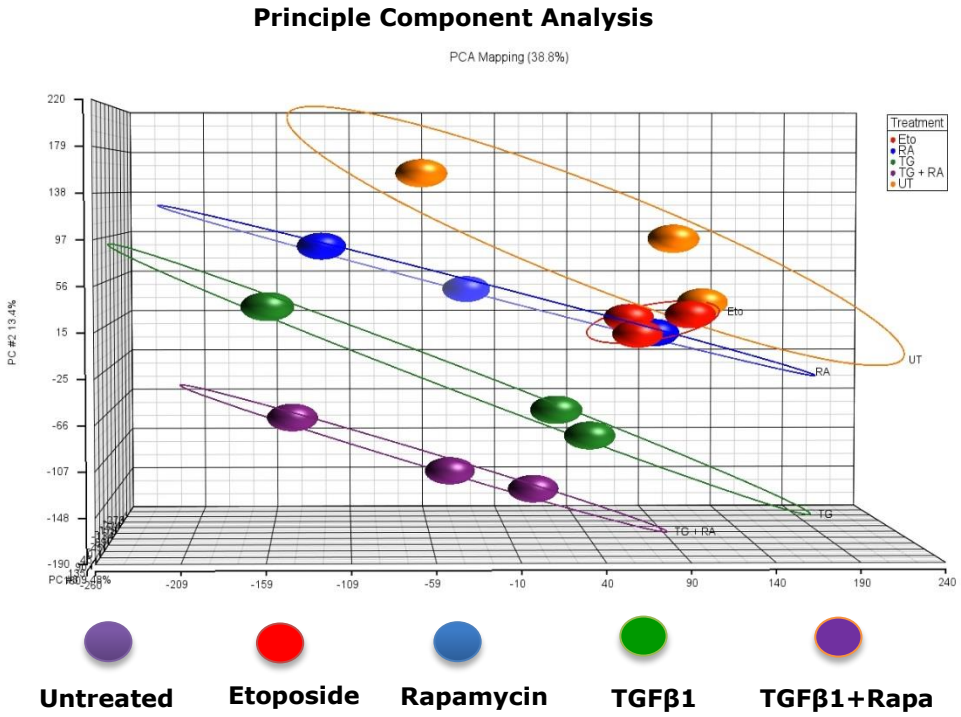



**Figure 7.4:** Principal Component Analysis (PCA) of the 15 samples of TF1-a cells based on the global signal of each sample.

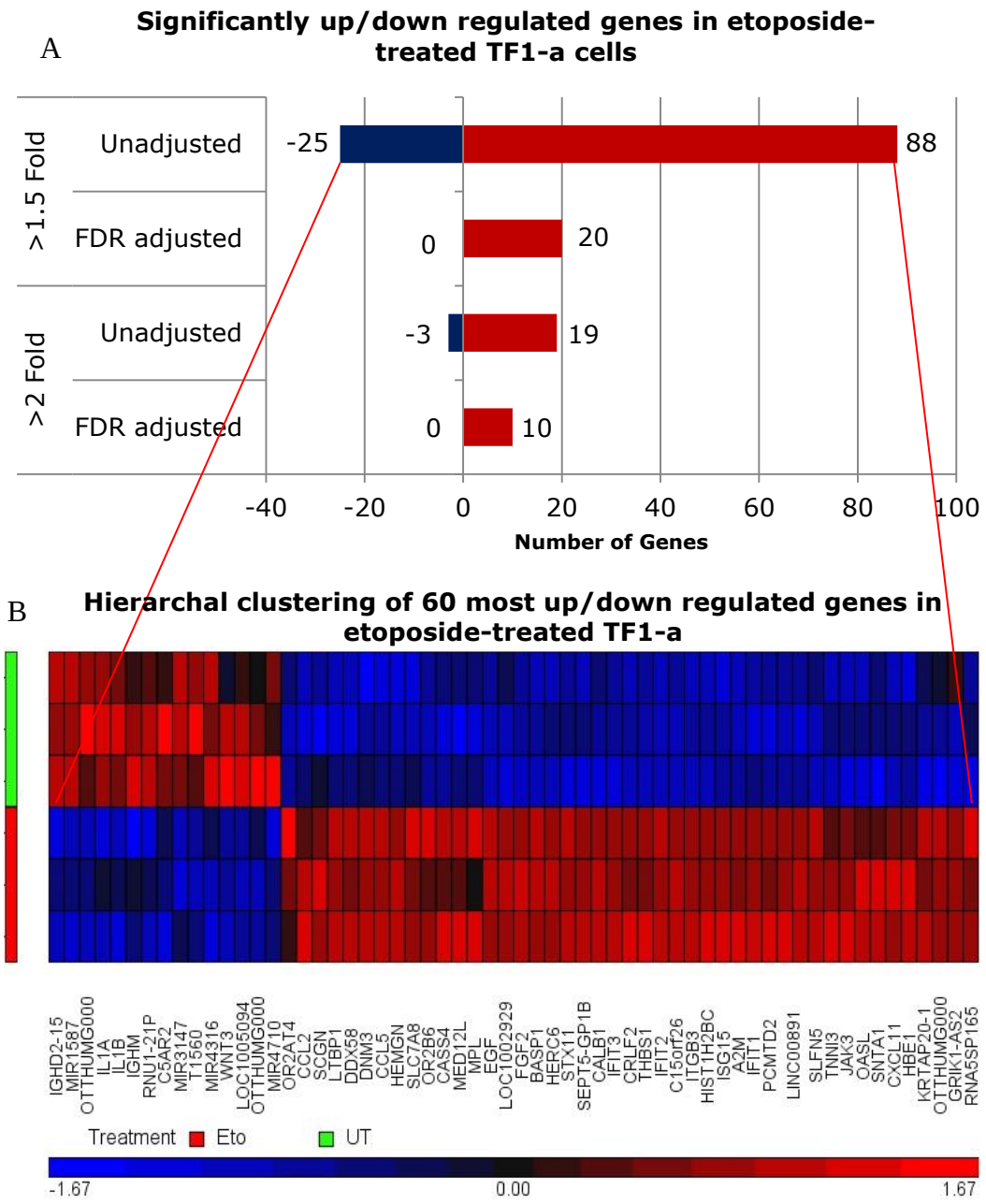



**Figure 7.5: Molecular signature of TF1-a cells surviving etoposide treatment. Panel A** illustrates the number of genes that were differentially up (red columns) or down (blue columns) regulated in TF1-a cells cultured for 6 days with etoposide at IC20 in comparison to their untreated counterparts distributed according to degree of fold change with or without FDR- adjustment. **Panel B** shows the heat map of the 60 most up/down regulated genes in the TF1-a genotoxicity signature including 45 out of the 88 most upregulated genes and 15 out of the 25 most downregulated. The heat map was generated using Partek Genomics Suite 6.6 software. UT: untreated, Eto: etoposide-treated.

**Table 7.1: The 88 significantly up regulated and 25 significantly downregulated genes by at least 1.5 fold in TF1-a cells which survived prolonged sub-lethal etoposide-mediated genotoxic stress**. (Note: The 20 genes that showed significant p-value after FDR filtration are highlighted in red).

| | Gene Symbol | Fold-Change | | Gene Symbol | Fold-Change | | Gene Symbol | Fold-Change |
|---|---|---|---|---|---|---|---|---|
| **1** | **IFIT3** | 2.7 | **39** | EGF | 1.7 | **77** | **FLJ35282** | 1.6 |
| **2** | THBS1 | 2.6 | **40** | PCMTD2 | 1.7 | **78** | **TMPRSS11F** | 1.5 |
| **3** | OR2B6 | 2.4 | **41** | TNNI3 | 1.7 | **79** | AQP1 | 1.5 |
| **4** | **IFIT2** | 2.4 | **42** | DDX58 | 1.7 | **80** | C1orf116 | 1.5 |
| **5** | **C15orf26** | 2.3 | **43** | ESPT5 | 1.7 | **81** | HLA-DRA | 1.5 |
| **6** | **HEMGN** | 2.3 | **44** | KRTAP20-1 | 1.7 | **82** | HIST2H4B | 1.5 |
| **7** | CALB1 | 2.3 | **45** | HBE1 | 1.7 | **83** | **GRAP2** | 1.5 |
| **8** | IFIT1 | 2.3 | **46** | MPL | 1.7 | **84** | ZEB2 | 1.5 |
| **9** | **LINC00891** | 2.2 | **47** | **EPSTI1** | 1.7 | **85** | TP53INP2 | 1.5 |
| **10** | **ITGB3** | 2.1 | **48** | IL16 | 1.7 | **86** | CALCOCO1 | 1.5 |
| **11** | **LINC00891** | 2.1 | **49** | SNORA38B | 1.6 | **87** | TAS2R30 | 1.5 |
| **12** | **A2M** | 2.1 | **50** | **HERC5** | 1.6 | **88** | SEMA7A | 1.5 |
| **13** | CCL2 | 2.1 | **51** | BTG2 | 1.6 | | | |
| **14** | ISG15 | 2.1 | **52** | GSERG1 | 1.6 | **1** | MIR3147 | -2.4 |
| **15** | SLC7A8 | 2.0 | **53** | ITGA11 | 1.6 | **2** | MIR1587 | -2.2 |
| **16** | RNA5SP165 | 2.0 | **54** | MIR4502 | 1.6 | **3** | T1560 | -1.8 |
| **17** | CRLF2 | 2.0 | **55** | PLEK | 1.6 | **4** | IL1A | -1.8 |
| **18** | **CCL5** | 1.9 | **56** | HLA-DRA | 1.6 | **5** | MIR4316 | -1.8 |
| **19** | **OASL** | 1.9 | **57** | BAMBI | 1.6 | **6** | OTTHUMG000 | -1.7 |
| **20** | CASS4 | 1.9 | **58** | MEG3 | 1.6 | **7** | RNU1-21P | -1.7 |
| **21** | CXCL11 | 1.9 | **59** | VNN1 | 1.6 | **8** | MIR4710 | -1.7 |

| | Gene Symbol | Fold-Change | | Gene Symbol | Fold-Change | | Gene Symbol | Fold-Change |
|---|---|---|---|---|---|---|---|---|
| **22** | **LTBP1** | 1.9 | **60** | TP53INP1 | 1.6 | **9** | IL1B | -1.7 |
| **23** | OR2AT4 | 1.9 | **61** | RNA5SP279 | 1.6 | **10** | WNT3 | -1.7 |
| **24** | LOC10029292 | 1.9 | **62** | BMP8A | 1.6 | **11** | C5AR2 | -1.6 |
| **25** | HIST1HCBC | 1.8 | **63** | ALAS2 | 1.6 | **12** | LOC10050945 | -1.6 |
| **26** | MED12L | 1.8 | **64** | RASGRP3 | 1.6 | **13** | OTTHUMG000 | -1.6 |
| **27** | **HERC6** | 1.8 | **65** | VSIG4 | 1.6 | **14** | IGHM | -1.6 |
| **28** | **SLFN5** | 1.8 | **66** | IRI6 | 1.6 | **15** | IGHD2-15 | -1.6 |
| **29** | GRIK1-AS2 | 1.8 | **67** | EFNB2 | 1.6 | **16** | BHLHA15 | -1.6 |
| **30** | FGF2 | 1.8 | **68** | KIT | 1.6 | **17** | KGFLP1 | -1.6 |
| **31** | OTTHUMG000 | 1.8 | **69** | LINC00910 | 1.6 | **18** | DKFZP434K02 | -1.6 |
| **32** | STX11 | 1.8 | **70** | SERPINI1 | 1.6 | **19** | MIR769 | -1.5 |
| **33** | JAK3 | 1.8 | **71** | HIST1H3H | 1.6 | **20** | SPRR2A | -1.5 |
| **34** | DNM3 | 1.8 | **72** | TXK | 1.6 | **21** | GRM6 | -1.5 |
| **35** | SCGN | 1.8 | **73** | MIR4633 | 1.6 | **22** | DDIT3 | -1.5 |
| **36** | **SNTA1** | 1.8 | **74** | PSORS1C2 | 1.6 | **23** | TRBV5-3 | -1.5 |
| **37** | **DSERG1** | 1.8 | **75** | NCCRP1 | 1.6 | **24** | HPN-AS1 | -1.5 |
| **38** | BASP1 | 1.7 | **76** | ITGA6 | 1.6 | **25** | LIN00167 | -1.5 |

### 7.2.4.2. Analysis of the biological processes/ signalling pathways significantly enriched in the genotoxicity signature of TF1-a cells.

Partek Genomic Suite 6.6 software facilitates mapping of the detected genes based on their gene ontology (GO) categories into their relevant biological process, molecular function and cellular localization using the KEGG-data base annotation codes. To emphasize the biological meaning of the genes of the etoposide-dependent genotoxicity signature, however, we focused on investigating the biological processes/signalling pathways induced in TF1-a by conducting an 'enrichment analyses' on the 88 upregulated genes.

The enrichment analysis was able to give information about 64 genes out of the 88 genes significantly up-regulated by more than 1.5 fold (table 7.1). Among the long list of biological processes/signalling pathways annotated by KEGG-pathway database, the 64 genes were grouped into more than 56 significantly enriched distinct biologically relevant groups (appendix A6). Many genes could be assigned to more than one biological process. For instance, IFIT1, IFIT2 and IFIT3 genes which were enriched in the type 1 interferon-mediated signalling pathway were also enriched in cellular response to virus and in negative regulation of protein binding biological processes. Indeed, signalling pathways with the highest enrichment scores (ES) in the etoposide-treated TF1-a cells (at 21.64 and 15.65 ESs) included these 3 genes as well as other interferon-related genes such as IFI6, ISG15 and OASL (table 7.1).

In addition, the GEP analysis of TF1-a cells cultured in prolonged sub-lethal genotoxic environment revealed that adhesion-related genes were significantly represented. Six genes were enriched in this category including ITGB3, ITGA11, PLEK, ITGA6 and SEMA7A. This biological category was the fourth most enriched group in etoposide-treated TF1-a cells at 12.45 ES (appendix A6). In response to sub-lethal etoposide, TF1-a cells upregulated genes functioning in several

immune-linked biological processes/signalling pathways such as immune response, chronic inflammatory process, leukocytes migration and macrophage chemotaxis.

In addition, genes significantly enriched in the genotoxicity model include CCL5 and FGF2, which were enriched within the negative regulation of cell death group (5.78 ES), in addition BTG2 and JAK3, were enriched within the positive regulation of anti-apoptosis category (4.65 ES) (appendix A6). Finally, other functionally related genes were known to be involved in platelet activation and blood coagulation including THBS1, ITGB3, A2M, EGF, MPL, PLEK, SLC7A8, HBE1 and ITGA6 (table 7.1).

### 7.2.5. Molecular features of dormancy in the CD34+CD38- Acute Myeloid Leukaemia TF1-a Cells subjected to prolonged sub-lethal genotoxic stress

One of the main aims of the current study was to investigate the hypothesis of induction of dormancy in AML cells under prolonged sub-lethal genotoxic stress. For this purpose we sought to investigate the presence of molecular features of dormancy in the TF1-a cells cultured for 6 days with etoposide at IC20 concentration. This was essentially achieved by intersecting the differentially upregulated genes in TF1-a cells induced to dormancy (i.e. the 240 genes signature of dormancy discussed in section 5.2.2.1) with the signature of the etoposide-treated counterparts (section 7.2.4.1) using the Partek Genomic Suite 6.6 software.

#### 7.2.5.1 Partek Genomics Suite software-based analysis to select the genes of interest in TF1-a cells

Employing the 2fold upregulation as a minimum level for selecting the genes in the etoposide treated cells omitted all genes but 2 (C15orf26 and ITGB3). Even when broadening the selection criteria to include those upregulated by at least 1.5fold (retaining the FDR-based-analysis) six genes only were commonly upregulated in both TF1-a cells induced to dormancy by TGFβ1+rapamycin and TF1-a cells treated with etoposide. These were, in order of statistical significance, C15orf26, ITGB3, SLFN5, GRAP2, LTBP1, and FLJ35282 (also known as DMRTA1) which were significantly upregulated by 2.3, 2.1, 1.8, 1.5, 1.9, and 1.6 respectively. Excluding the FDR from the filtration process resulted in 31 genes that were significantly upregulated by at least 1.5 fold (figures 7.6 and 7.7).

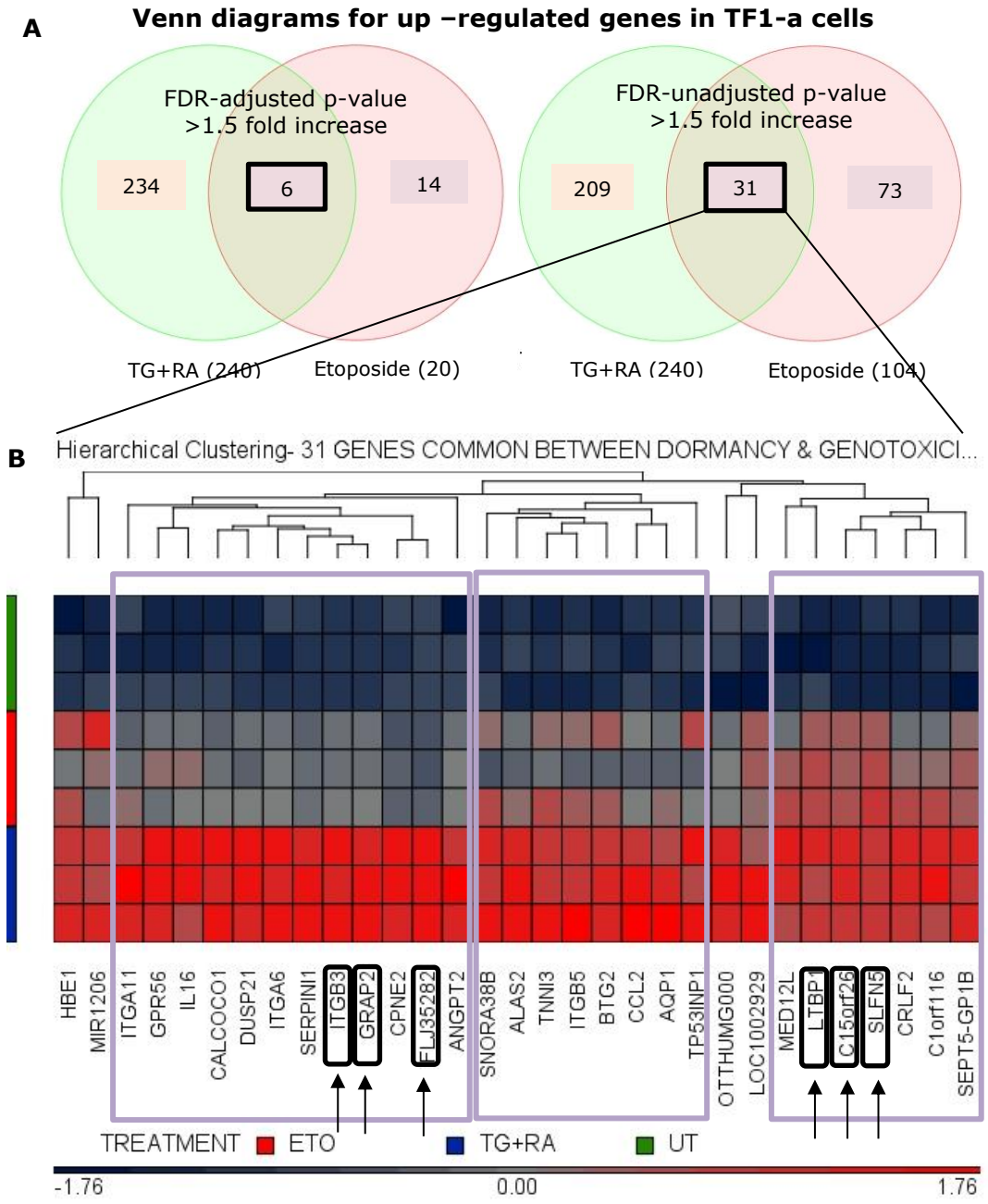



**Figure 7.6: Genes commonly upregulated between the dormancy and genotoxicity signature of TF1-a cells. Panel A:** Venn diagrams show the number of genes commonly upregulated by at least 1.5fold between the dormancy and the genotoxicity signatures with FDR-adjusted (left venn diagram) or unadjusted (right venn diagram) p-value respectively. **Panel B:** Heat map of the most 31 commonly significantly upregulated genes by at least 1.5fold increase in both TF1-a induced to dormancy by TGFβ1 and rapamycin and TF1-a cells surviving sub-lethal genotoxicity with etoposide. The three purple boxes indicate the three main clusters of genes. The 6 genes significantly upregulated with FDR-adjusted p-value were indicated with black arrows. The figures was generated using Partek Genomics Suite 6.6 software. UT: untreated, Eto: etoposide, TG+RA: TGFβ1 and rapamycin.

Focusing on these 31 significantly upregulated genes (figure 7.7), 2 of the top upregulated genes in the dormancy model were among the top 3 upregulated genes in TF1-a cells under genotoxic stress; these were ITGB3 and CCL2. On the other hand, DMRTA1 which was the sixth highest upregulated gene in dormant TF1-a cells (at 9.5 fold increase) was significantly increased by only 1.6fold change in response to the genotoxicity conditioning of TF1-a cells. The remaining genes generally showed a narrow range of difference in the level of upregulation ranging between 0.3-2 fold differences between the two conditions. An exception for that was the gene CPNE2 which was upregulated by 5.3fold in dormant TF1-a cells in comparison to only 1.5fold increase in the genotoxicity model (figure 7.7).

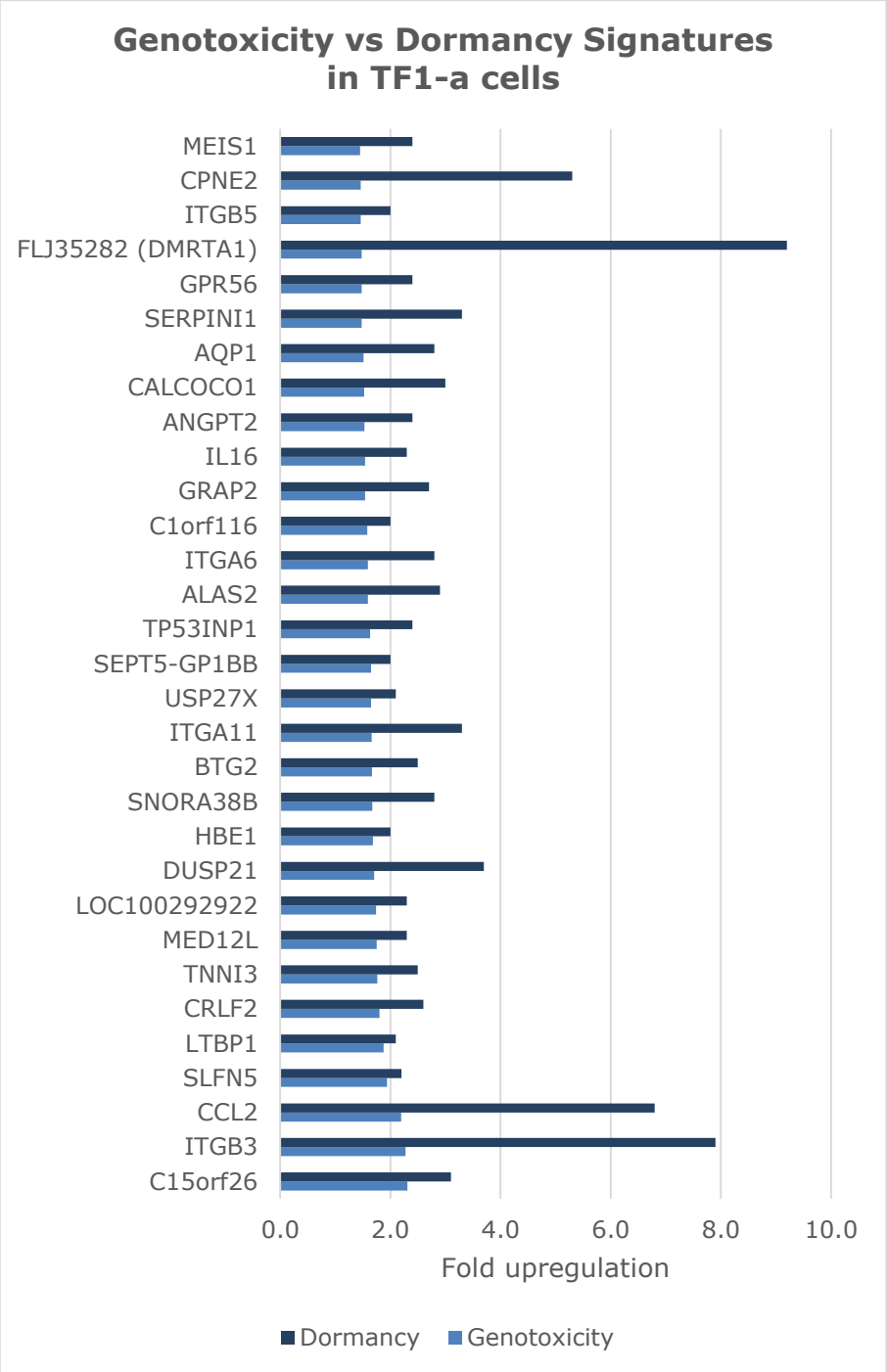



**Figure 7.6:** The 31 genes significantly upregulated by at least 1.5 fold change with FDR unadjusted p value in TF1-a under prolonged sub-lethal genotoxic stress with comparison to the degree of upregulation of the same genes in the dormancy signature of TF1-a cells. Data obtained from the microarray experiments, using Partek Genomic Suite 6.6 software, which represent the mean values for fold upregulation of three independent replicates.

7.2.5.2. Validation of the GEP microarray expression of the 4 genes using qPCR

The GEP results were validated by selecting the top 4 genes, in term of the statistical significance, out of the 6 significantly upregulated genes common in the two models (dormancy and genotoxicity) for investigation by qPCR; these were C15orf26, ITGB3, SLFN5 and GRAP2. The housekeeping gene B2M was used as a standard for the relative quantification of the target genes expression.

All the tested genes showed similar trend of increase in expression to that obtained in the GEP data with some degree of difference in the level of fold increase and the statistical significance (figure 7.8).

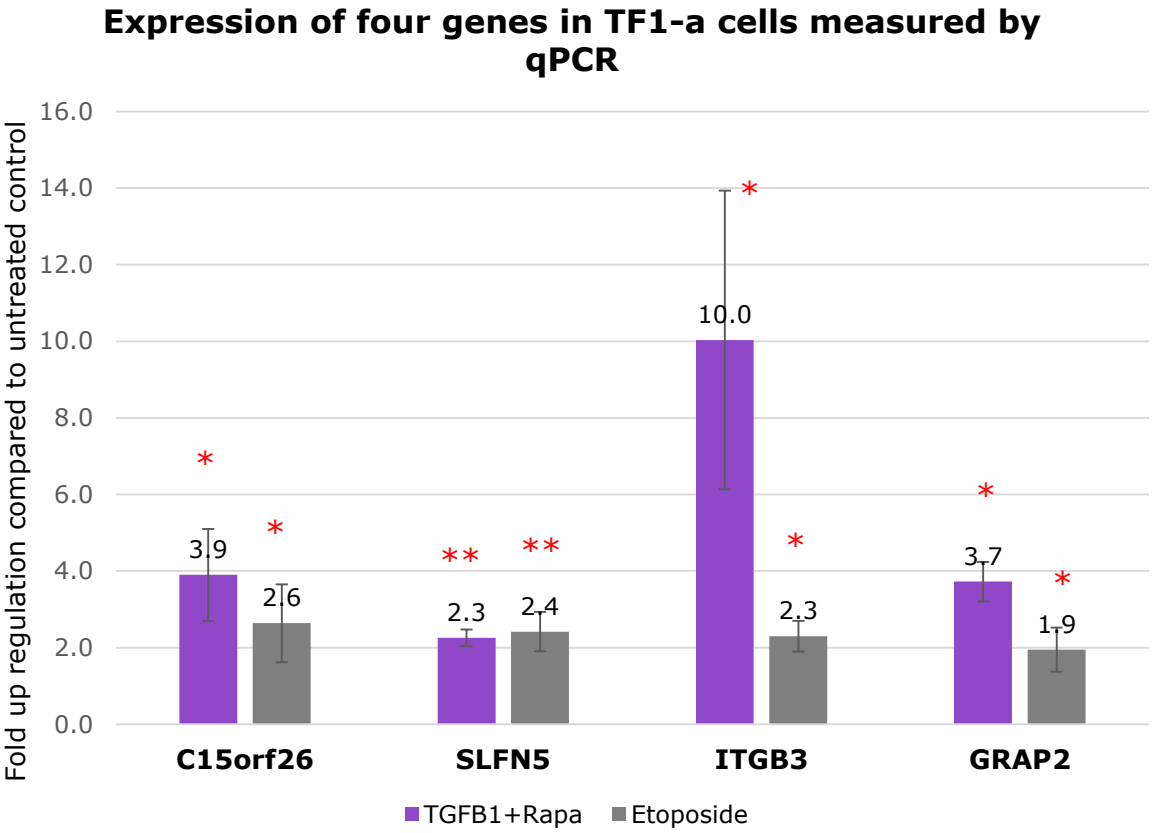



**Figure 7.7: The qPCR validation of the expression of 4 significantly commonly upregulated genes in the genotoxicity and dormancy signatures of TF1-a cells.** Columns represent mean values of three biological replicates for all conditions except for C15orf26, SLFN5 and GRAP2 expression in etoposide treated TF1-a cells which represent mean values of five replicates. The error bars represent +/- 1SD. The statistical significance was measured in comparison to untreated controls. *= p value<0.05, **= p value<0.01.

## 7.3. Discussion

### 7.3.1. Selecting the etoposide IC20 for modelling sub-lethal genotoxicity in TF1-a cells

Among the tested doses of etoposide, the day 3 IC20 (equivalent to 6 day IC40) was selected for the in vitro sub-lethal genotoxicity model. This was mainly in order to meet the main aim of this study which is to investigate the molecular signature of leukaemia cells surviving a genotoxic environment rather than dying in it. The day 3 IC50 dose of etoposide (equivalent to 6 day IC70), on the other hand, was selected as a positive control in preliminary experiments as it showed stronger genotoxicity in TF1-a cells (figure 7.2) when larger number of cells at this dose of treatment showed higher number of apoptosis marker-positive cells.

The endosteal region is likely to be characterized by a low perfusion status due to the abundance of the thick-walled blood vessels such as the arterioles at the expense of the fenestrated thin-walled sinusoids. In other words, cells residing in the endosteal region will be exposed to lower concentrations of chemotherapeutic drugs. Consequently, we chose the IC20 as an approximation of leukaemia cell response within this BM environment. In addition, in this genotoxicity model we were trying to balance stress with low level of apoptosis so that dying cells do not contaminate the GEP. To the best of our knowledge, no previous reports modelled and studied the sub-lethal genotoxicity effect on the molecular signature of AML cells. Studying leukaemia cells in such conditions can give an insight into the possible cellular adaptive molecular mechanisms which could help in targeting the cells which are responsible for relapse in AML.

### 7.3.2. Molecular signature of TF1-a cells under a prolonged sub-lethal genotoxic stress

We sought to molecularly characterize AML cells with stemness characteristics (modelled by TF1-a cells) surviving a prolonged sub-lethal genotoxic environment

(modelled by 6 days of etoposide treatment at the IC20 dose) by GEP. It was evident that applying the FDR to select the list of significantly differentially deregulated genes resulted in excluding the majority of the upregulated and all the downregulated genes. This was mainly due to the low consistency of the triplicates of the etoposide-treated TF1-a samples which resulted in a low number of altered genes after FDR filtration. In addition, it was noticeable that the selected dose of etoposide resulted in a relatively low fold change in the up/down regulated genes (ranged between 2.7 to -2.4 fold change respectively) (table 7.1). Unfortunately, it was not possible to include the higher etoposide dose, the IC50-treated TF1-a cells, in the GEP study due to cost reasons. With hindsight, including this condition would have provided a stronger genotoxic effect that might help explaining the findings of the IC20 genotoxicity signature. Consequently, we decided to select the differentially deregulated genes in the TF1-a cells cultured with etoposide that showed at least 1.5 fold change with FDR-unadjusted p value. Employing the FDR in selecting the significant p-value was recommended in order to exclude any possible false positives that might accompany simultaneous calculating of large numbers of hypotheses in the microarray data analysis (Pawitan, Michiels *et al.* 2005). Although excluding the FDR filtration was not ideal, it at least provides a basis for validating the most promising changes.

The sub-lethal genotoxicity signature contained deregulated genes attributed to various biological processes in the AML cells. The top upregulated genes were mainly categorized within the type 1 interferon-mediated signalling pathway. Specifically, these were genes that code for interferon-inducible proteins including IFIT3, IFIT2 and IFIT1 (type 1 interferon-inducible protein with tetratricopeptide repeat 3, 2 and 1 respectively). These proteins are involved in various sensor and effector functions. For example, it has been reported that they inhibit translation at the eIF3 (eukaryotic initiation factor 3) translation initiation complex ((Diamond 2014) and references therein). Furthermore, the deregulation of interferon

pathway has been previously reported in HeLa cells in response to various genotoxic treatments. This was exemplified by the activation of IRF3 (interferon regulatory factor 3) through its phosphorylation (Kim, Kim *et al.* 1999).

In AML, Rig-G (the alternative name for IFIT3) was found to be upregulated in the promyelocytic leukaemia cell line NB4 in response to ATRA treatment (Yu, Tong *et al.* 1997). More importantly, Rig-G was reported to exert a key role in regulating the anti-proliferative proteins p21 and p27 in leukaemia cells (Xiao, Li *et al.* 2006). Both the anti-proliferative and the inhibition of translation roles of these genes might be involve in explaining the proliferation inhibition of TF-1a cells in response to etoposide treatment (figure 7.3).

The etoposide-treated AML cells showed an increase in the expression of genes involved in the immune response, chemotaxis, chronic inflammation and defence response to external insults. This reflects the adaptive mechanisms through which the leukemic cells re-programme their molecular machinery to survive external stress. In addition, genes classified as anti-apoptotic or as negative regulators of cell death participated in forming the molecular signature of AML cells surviving prolonged sub-lethal etoposide-mediated genotoxic stress.

Collectively, these results suggest pathways utilised in response of leukemic cells to sub-lethal genotoxicity that require future validation by qPCR and protein analysis as well. Furthermore, they demonstrate that etoposide-treated AML cells upregulate genes that largely influence other haematopoietic and non-hematopoietic cellular components of the bone marrow such as genes involved in macrophage chemotaxis, platelet activation, blood vessel endothelial cells migration and others (appendix A6). This observation supports the notion that cancer cells, including AML cells, are believed to create their own niche through producing aberrant external signals to their neighbours (Schepers, Campbell *et al.* 2015).

### 7.3.3. Induction of dormancy in the CD34+CD38- Acute Myeloid Leukaemia Cells TF1-a subjected to prolonged sub-lethal genotoxic stress

In the current study we sought to investigate whether feature of dormancy were induced in the genotoxicity model at the molecular level by comparing the molecular signature of dormancy in TF1-a cells with that of the etoposide-treated counterparts. In this context, 31 genes showed similar trend of upregulation in the genotoxicity model out of the 240 genes of the dormancy signature. However, the extent of this upregulation was lower with less consistency than that of the dormancy genes. Importantly, these were common observations and were applicable to all the genotoxicity signature genes. Consequently, we sought to subject these genes to investigation as potentially important features of dormancy in TF1-a cells under genotoxic stress.

Among these 31 genes, there were genes involved in adhesion, stemness and tumour suppression. The adhesion-related genes included ITGB3, ITGA11, ITGA6, GPR56 and ITGB6. The upregulation of these genes in AML cells under sub-lethal genotoxic stress is worth further investigation. This is because validating such response in primary AML cells in vivo would make these molecules potential therapeutic targets to eradicate residual AML cells. For example, ITGB3 was reported to be a potential target to eliminate AML cells by interfering with the interaction with the BM niche (Miller, Al-Shahrour et al. 2013). This might be of importance specifically in elderly AML patients who are treated with lower doses of chemotherapeutic agents due to the common existence of comorbidities. Finally, the qPCR validation experiments came to confirm the trend of upregulation of the 4 selected genes (figure 7.8). Indeed, ITGB3 was selected among these genes as a consistently upregulated gene common in both models for further deeper functional investigation in AML cells (discussed further in chapter 8).

SLFN5 (schlafen family member 5) gene was one of the top upregulated genes in the genotoxicity model as well as being part of the dormancy signature in TF1-a cells induced to dormancy. Interestingly the word 'schlafen' is a Germany word that means 'sleeping' which refers to the cell cycle arrest that was demonstrated upon ectopic expression of the prototypic family member SLFN1 in NIH-3T3 fibroblast cells. The SLFN family in human includes five members of proteins that have been found to play roles in the biology of many haematopoietic cells, including monocytes, dendritic cells and T cells (Puck, Aigner et al. 2015). SLFN5 , in particular, is believed to exert a role in inhibition of cellular proliferation (Mavrommatis, Fish et al. 2013). This anti-proliferative role of SLFN5 might play a role in the inhibition of proliferation that was observed in TF1-a cells in response to both cytokine and chemotherapy treatment. No previous reports, however, studied this possible role of this novel gene in AML cells neither in dormancy nor in the post chemotherapy contexts.

Similarly the C15orf26 (chromosome 15 open reading frame 26 also known as CFAP161 which stands for cilia and flagella associated protein 161) was the top upregulated gene in the genotoxicity model if compared to the dormancy signature and there is no data link this novel gene with AML cells in both scenarios (genotoxicity and dormancy). The other open reading frame gene was C1orf116 (chromosome 1 open reading frame 116) which was increased in TF1-a cells under the effect of both cytokine induced dormancy and the etoposide induced genotoxicity. This gene also lack a specific determined function in AML and other cancer cell biology.

GRAP2 (GRB2-related adapter protein 2), also known as GADS (GRB2-related adaptor downstream of SHC), is an adaptor protein whose is mainly expressed in hematopoietic tissues, including BM, lymph node, and spleen (Liu, Berry et al. 2001). Although GRAP2 has a major role in T-cell biology and T-cell receptor

signalling (Watanabe, Harada et al. 2006, Zhang, Parker et al. 2011, Rohr, Guo et al. 2016), it was reported to play critical roles in antigen-receptor signalling and receptor tyrosine kinase-mediated signalling in other hematopoietic lineages such as B-ALL cells (Gillis, Berry et al. 2013). Importantly, in AML cells, GRAP2 was reported to increase the FLT3-ITD receptor activity which results in enhanced phosphorylation of many target proteins, including AKT, ERK1/2, p38 and STAT5 (Chougule, Cordero et al. 2016). No evidence was found that could link GRAP2 with dormancy or response to genotoxicity in AML cells, however.

Finally, the TF1-a cells that survived the genotoxic environment had upregulated the chemoattractant gene CCL2 (C-C motif chemokine ligand 2) which is also known as monocyte chemoattractant ligand 1 (MCP1). In this study CCL2 was not included in the qPCR validation experiments as it did not pass the FDR-filtration step despite the fact it showed significant upregulation in the genotoxicity model ($p=0.0039$). Nevertheless, because CCL2 were one of the top 3 upregulated genes, by considering fold change (figure 7.7), we have reviewed the role of this gene in AML cells. It has been reported that AML cells create a resistance microenvironment through many mechanisms including the inhibition of the T-cell immunity. CCL2 upregulation has been reported to be involved in this mechanism. Indeed, anti-CCL2 antibody-treated mice that bearing AML cells decreased the tumour burden, augmented anti-leukemic T-cell responses, and improved survival rate compared to untreated mice (Driss, Quesnel et al. 2015).

# CHAPTER EIGHT
# GENERAL DISCUSSIONS, CONCLUSIONS AND FUTURE WORK

## 8.1. Study aims and objectives

The aims of this study were:

1. To establish an *in vitro* culture system that mimics features of the LIC niche to model dormancy in AML by primarily using TGFβ1 with or without the mTOR pathway inhibitor, rapamycin to treat a $CD34^+$ AML cell line.
2. To characterize the dormant AML cells using whole-human genome gene expression profiling to study the molecular signature of AML cells induced to dormancy.
3. To model and molecularly characterize AML cells surviving prolonged sub-lethal genotoxic stress and compare their molecular signature with that of the dormant counterparts.

## 8.2. Establishing dormancy model in AML by mimicking the LICs niche using TGFβ1+rapamycin *in vitro* treatment of TF1-a AML cell line.

The maintenance of active haematopoiesis throughout the individual life is the result of endogenous features of the HSCs and exogenous signals from their specialized niche. This indispensable relation for a healthy body in a physiological BM condition is a major problem in a BM harbouring AML cells retaining the leukaemia re-initiation potential as these cells can hijack these exogenous signals to survive. One of the most important products of this LIC-niche relation, which is also considered as a key factor for the survival of these cells, is the induction of dormancy. Consequently, relapse rates in AML remains high due to the escape of these rare dormant LICs the frontline chemotherapeutic treatment. Knowledge in the underlying mechanism of dormancy regulation in LICs is limited due to the difficulty in isolating these cells from clinical samples. Thus, we sought to establish a model of dormancy in AML cells with stemness features in aim to move this knowledge forward.

Following a thorough research on the up-to-date knowledge on the reported possible regulators of dormancy in HSCs and LICs, we investigated 4 AML cell lines for *in vitro* modelling of dormancy in AML, namely KG1-a, TF1-a, Kasumi-3 and M0-91. By exploiting the bone marrow (BM) micro-environmental factors that constitute the LICs niche, we were able to induce dormancy in the TF1-a AML cell line in suspension culture using 4ng/ml of TGFβ1 and 100nM of the mTOR pathway inhibitor rapamycin (mTOR pathway inhibition mimics major effects of nutrient scarcity). It was clear that TGFβ1 was the main player in this context. TF1-a cells cultured for 3 days with TGFβ1 with/without rapamycin showed significant inhibition of proliferation with features of dormancy and stemness without affecting their viability.

### 8.2.1. A comparison of the current study with previous studies investigating dormancy signature

Accepting the limitations of *in vitro* biological systems in simulating the *in vivo* microenvironment, this model can be considered as a robust one if compared to other attempts to study dormancy for several reasons. Firstly, this model is based on, and aimed to mimic, the up-to-date reported *in vivo* criteria of the LICs niche regulating dormancy (reviewed in sections 1.8 and 1.9). Secondly, it followed an integrated approach in selecting the candidate AML cell line to mimic the LICs as close as possible through paying attention to the features of stemness in these cell lines. Finally, it is considered as the first *in vitro* model of dormancy in human AML cells that showed largely consistent results using accessible resources exemplified by TF1-a cell line in ordinary culture system cultured with TGFβ1 and rapamycin. In this culture system, TF1-a cells showed significant inhibition of proliferation with features of dormancy including the increase in Ki-67 negative (dormant) cells, inhibition of proliferation marker CD71 and significant decrease in total RNA content in comparison to their proliferating counterparts (chapters 3 and 4). This model can be used as a platform for deeper studying and comparing different molecular pathways and proteins linked to dormancy in AML.

The study of dormancy as a biological phenomenon has been a focus of interest and extensive study by many researchers using various cellular systems that investigated the GEP of dormancy signature in different normal and transformed cells of mouse (Venezia, Merchant et al. 2004, Forsberg, Passegue et al. 2010, Oki, Nishimura et al. 2014, Subramaniam, Sreenivas et al. 2014) or human origin. In comparison to our study, many of these *in vitro* systems, and others not included in the table, were dependent on serum withdrawal to induce and characterize dormant cells. This approach ignores the effect of this type of conditioning on the cell viability which might biased the underlying mechanism of

inhibition of proliferation. In contrast in the current study, the viability of TF1-a cells induced to dormancy was a priority besides other features of dormancy.

The two studies that investigated and molecularly characterized primary human $CD34^+$ $CD38^-$ AML (Gal, Amariglio et al. 2006, Won, Kim et al. 2015) have ignored two essential factors if compared to the current study. Firstly, they did not pay attention to features of dormancy in the tested primary AML cells; they used the stemness phenotype as a surrogate for dormancy. Secondly, they characterized these cells suspended in ordinary in vitro culture medium which is considerably different from the *in vivo* microenvironment from which these cells survive. To illustrate, in our lab, we found that primary AML cells of patients that showed significant OPN expression in their BM biopsies by IHC studying showed significant OPN expression in mononuclear cells isolates only after culturing them with TGFβ1 (data not shown). This observation reflects the importance of modifying the *in vitro* culture system to create an *ex vivo* one closer to the *in vivo* environment. Indeed, nowadays many *ex vivo* culture models have been established for such purpose including using feeder cells co-cultured with AML cells (for example the murine cell line MS5 which we have used in previous, unpublished, dormancy modelling studies) and 3D culture systems. Nevertheless, using a pre-defined cytokine or extracellular protein in such models can be more helpful to explain the possible underlying mechanisms of the obtained results and building on that for more targeted investigations.

Another major difference between these two studies and the current study is the number of genes tested. In comparison to the global human genome tested in this study which covers more than 33500 coding transcripts, Gal H et. al. (2006) investigated 22215 genes in their study whilst Won et al. (2015) investigated only a pre-defined set of 84 genes related to pluripotent stem cell biology. However, some interesting findings were commonly noticed among these two and the

current study. For instance, ITGB3 has been found within the significantly upregulated gene in CD34+CD38- leukaemia cells in comparison to CD34+CD38+ ones (Gal, Amariglio et al. 2006). ITGB3 was one of genes forming the dormancy TF1-a signature (chapter 5) and also the signature of TF1-a cells surviving the genotoxic environment (chapter 7). Indeed, we are currently subjecting this gene to deeper functional investigations in the department to validate its role in AML.

Only one of the 9 reviewed dormancy studies has targeted to mimic the *in vivo* environment by modelling two physiological factors suggested to play a role in regulating dormancy in prostatic cancer cells; the increase in osmotic pressure of the medium and decrease in cell density (Bui, Laurent et al. 2015). This interesting approach highlights the fact that dormancy regulation is a multifactorial process that can be modified by many biological, chemical and physical signals from the surrounding niche. Interestingly, in this study SMAD-signalling pathway (the canonical pathway of TGFβ1) has been identified as a major player in regulating dormancy in prostatic cancer cells. Of this pathway SMAD6, SMAD7, BMP1, BMP2, GDF11 and ID1 were significantly upregulated in dormant prostatic cell line. Comparatively, in our study, 6 members of this pathway were among the significantly up-regulated genes in TF1-a dormancy signature, namely SMAD7, SMAD6, BMPER, BMPR2, LTBP1 and TGFβ1. In addition, TGFβ1 and other members of the SMAD signalling pathway were frequently reported to be markedly modulated in the dormancy signature of other studies (Coller, Sang et al. 2006, Subramaniam, Sreenivas et al. 2014, Bui, Laurent et al. 2015, Won, Kim et al. 2015). Indeed, such a common finding supports the importance of this pathway in regulating dormancy and also highlights the fact that any improvement in the knowledge in how this pathway regulates dormancy in LICs will be of benefit not only in AML but in other cancers with BM metastasis such as prostatic cancer. This is because the BM niche is a recognized 'soil' for the metastatic cancer cells that

are responsible for relapse in several solid tumours including prostatic, breast and lung cancers (Kaplan, Psaila et al. 2006, Psaila, Kaplan et al. 2006).

## 8.3. Molecular signature of dormancy in the CD34+ CD38- AML cells TF1-a showed a marked presentation of the adhesion-related genes

In the current study we demonstrated that dormant TF1-a cells showed up-regulation of many genes despite the significant decrease in total RNA content. This indicates that dormancy is an active process in which the leukaemia cell re-shapes its transcriptome to prioritize new functions over others. Therefore, dormancy is not merely an inhibition of proliferation or exit from the cell cycle (Coller, Sang et al. 2006) but it is a phenomenon associated with various active biological processes which were proved to be significantly presented in the molecular signature of the dormant TF1-a cells in the current study.

Adhesion was found to be one of the markedly represented biological process in dormant TF1-a. This finding came in line with the fact that adhesion is considered as an important phenomenon for securing homing of the dormant stem cells in their niche. To illustrate, it has been shown that proliferating long term HSC (LT-HSC) display a dramatic impairment of their engraftment and reconstitution ability if compared to dormant counterparts (Glimm, Oh et al. 2000). This appears to be due to the increase adhesiveness of dormant HSC to stromal cells (Passegue, Wagers et al. 2005). Moreover and with the help of microarray analysis, it has been reported that migratory molecules are important for establishing dormancy in mouse HSC (Venezia, Merchant et al. 2004).

Indeed, the adhesion-related genes were, also, repeatedly represented in the molecular signature of other previously reported dormancy models. For instance,

Subramaniam et al (2013) reported that ITGB5, ITGA2b and ITGFG1 were induced in dormant myoblasts. Also, Weirenga et al (2014) reported that ITGA5, ITGB5, ITGAM and ITGAX were up-modulated in HSC by hypoxia (one of the possible regulator of dormancy in HSC). Finally, the adhesion gene MYLK was reported in two previous studies to be part of the transcriptional programme that is involved in dormancy initiation (Liu, Adler et al. 2007) and dormancy maintenance (Coller, Sang et al. 2006) of primary human fibroblasts.

In the current study, cell mechanisms related to adhesion were the top two significantly enriched biological processes in dormant TF1-a. Also, five of the top ten upregulated genes were adhesion-related genes: SPP1, MYLK, PLXNC1, PTPRU and ITGB3. Among these genes, ITGB3 has been a focus of extensive recent research in various malignancies as a protein involved in tumour invasiveness, adhesion to microenvironment, maintenance of stemness and drug resistance (Cao, Fan et al. 2015, Bae, Hong et al. 2016, Chen, Wei et al. 2016, Hong, Park et al. 2016, Wei, Yang et al. 2016). In AML using a small hairpin RNA (an artificial RNA molecule that can be utilized to silence target gene expression), ITGB3 has recently been reported to selectively affect AML stem cells as compared to normal counterparts. ITGB3 knockdown resulted in impairment of LSC homing, downregulation of LSC transcriptional programme, and induced differentiation of this cell (Miller, Al-Shahrour et al. 2013). Further, this group of researchers were able to investigate the downstream effectors of ITGB3 in AML cells both *in vitro* and *in vivo*. They demonstrated that ITGB3 exerts its function through the phosphorylation of the intracellular kinase SYK and they found that activated SYK rescued the effects of ITGB3 knockdown. In other recent work, ITGB3 was found to be an important component of the molecules involved in the leukaemia cell/microenvironment interaction that was found to be responsible for resistance of AML cells to the chemotherapeutic agent sorafenib (Yi, Zeng et al. 2016). Due to this large body of evidence and due to the significant up-regulation of ITGB3

the dormant TF1-a cells and also in TF1-a cells surviving the sub-lethal genotoxicity, we are currently subjecting this gene and its product to a deeper functional study.

Nevertheless, little is known about the direct role of ITGB3, and other adhesion related genes discovered in the dormant TF1-a cells, in regulating dormancy and cell cycle. Indeed, further investigations using a selective target gene knockout approach and cell cycle analysis may be required to establish or exclude any possible role of these adhesion-related genes in dormancy regulation. The TF1-a dormancy signature, also, included the up-modulation of CDKN2B (p15) which is a known regulator of cell cycle, as well as many tumour suppressor genes such as PTPRU that could play a key role in dormancy regulation in AML. The identification of these genes suggests novel possible mehcanisms or dormancy regulation in LIC for further investigations in AML (figure 8.1).

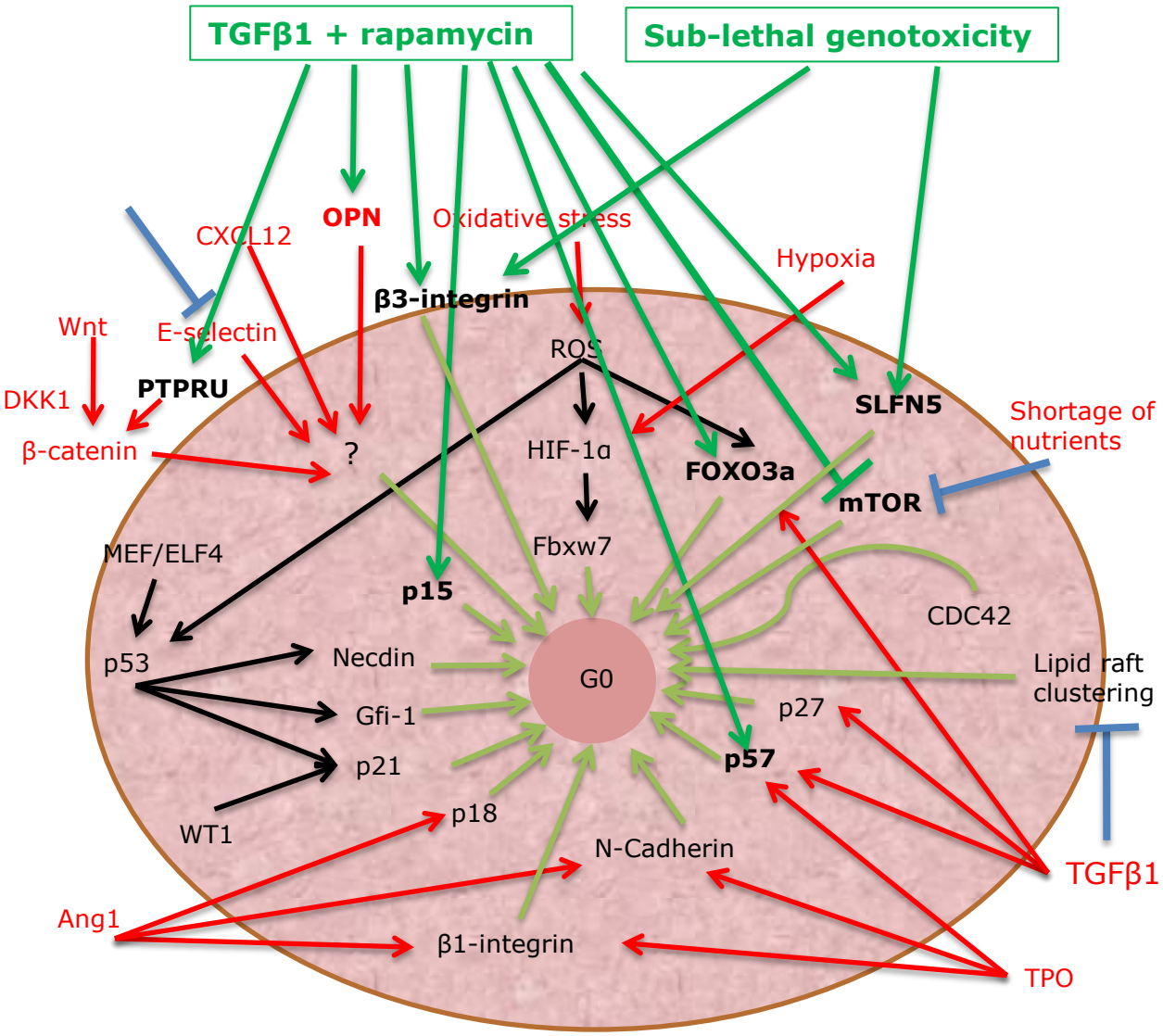



**Figure 8.1: Suggested regulatory mechanisms of dormancy in LIC according to the TF1-a dormancy and genotoxicty models**. Arrows highlighted in dark green in this schematic diagram represent possible mechanisms of dormancy regulation according to the dormancy signature generated from TF1-a cells cultured with TGFβ1+ the mTOR pathway inhibitor rapamycin and from TF1-a cells survived prolonged sub-lethal genotoxicity by etoposide treatment. The rest of information are replicate of figure 1.4.

## 8.5. Induction of dormancy in the response of AML cells to sub-lethal genotoxic insult

In this study we established and validated a model of AML cells surviving a prolonged sub-lethal genotoxicity through culturing the AML cell line, TF1-a, in etoposide-containing culture medium for 6 days. The transcriptome of these cells, thereafter, was subjected to whole human GEP study in aim to identify the genes significantly over-transcribed in response to etoposide treatment. Indeed, the research on the molecular characterization of AML or other cancer cells in response to chemotherapy has been a frequent point of interest for many researchers. For instance, Oyan *et al* (2009) studied the global GEP of primary AML cells obtained from the peripheral blood of untreated patients and up to 24 hours post conventional treatment with a combination of cytarabine and anthracycline (Oyan, Anensen et al. 2009). Similarly, Ruthe *et al* (2010) have modelled and molecularly characterized AML cells under genotoxicity using murine AML cell lines resistant to AraC derived from mother AraC- sensitive murine cell lines B117P and B140P. What makes our approach novel, however, is that it was designed to mimic the under-perfused BM niche that harbours the LICs which is characterized by sub-optimal delivery of the chemotherapeutics. In fact, little is known about the molecular changes in these rare sub-set of AML cells. In addition and from the clinical point of view, it is known that in many occasions the oncologists elect to administer a sub-optimal doses of chemotherapeutic drugs in AML patients with co-morbidities and in elderly patients with AML who are unable to tolerate a full therapeutic doses. Thus, the model presented in this study can, also, mimic such clinical scenarios and the knowledge obtained from the current model might have both biological and clinical implications.

The analysis of the molecular signature of TF1-a surviving 6 days of etoposide (TF1-a-Eto) was focused on the aim of this study which was to identify the common molecular features between these cells and the TF1-a cells induced to dormancy by TGFβ1 and rapamycin (dormant TF1-a). In this context, 35% of the

genes significantly upregulated in the TF1-a-Eto cells were also significantly upregulated in the dormant counterparts (31 out of 88 genes) (will be called the common signature thereafter). Although most of these genes are not necessarily indicate dormancy features in TF1-a-Eto cells, they are of biological importance as they reflect the adaptive behaviour of these cells to prolonged sub-lethal genotoxicity. Therefore, they might have a potential therapeutic role in AML.

The notion of dormancy induction by genotoxic stress has been supported by findings from previous studies. Indeed, beside the identified protective mechanisms that have been suggested as a response of cancer cells to external insults, induction of quiescence is believed to enable the survival of LSCs over the other possible outcomes: senescence, cell death, transformation and premature differentiation (Suda, Takubo et al. 2011). In support of this hypothesis, Ishikawa and colleagues (2007) developed a primary human AML xenotransplantation model using new-born non obese diabetic/severe combined immune-deficient/interleukin2rγ null (NOD/SCID/IL2rγ) mice and they demonstrated that CD34+ CD38- leukaemia cells reside within the osteoblast-rich area of the BM where they survive the Ara-C-induced apoptosis. Interestingly and using a cell cycle study, they found that these residual AML cells following Ara-C treatment were dormant and downregulated the proliferation gene CCNA1 if compared to the CD34+ CD38+ leukaemia cells counterparts (Ishikawa, Yoshida et al. 2007). Furthermore, Zhou T. and colleagues (2006) using telomerase-expressing human diploid fibroblast cell lines subjected to ionizing radiation (IR) insults, identified that these cells showed synchronization behind the G1 checkpoint in a G0-like state of quiescence with prominent induction of genes of G0 quiescence like GAS1 and BTG2(Zhou, Chou et al. 2006). IR-induced DNA damage was also reported to result in impaired G1 arrest of p21-/- mouse embryo fibroblasts in comparison to p21+/+ cells. This evidence highlights the role of the up-regulation of the CDKI p21 as a checkpoint response to safeguard genomic integrity by quiescence induction (Brugarolas, Bronson et al. 1998). Similarly, Cuadrado et al. (2009)

reported the role of the other CDKI p27 in the induction of quiescence in response to DNA damage. They used Doxorubicin to induce DNA double strands breaks in the human lung cancer cell line A549 and concluded that p27 stabilization is required for cell cycle arrest in response to DNA damage (Cuadrado, Gutierrez-Martinez et al. 2009). Finally, a recent interesting abstract submitted for oral presentation at the last annual ASH meeting (December 2016), Cihangir Duy and colleagues used an *in vivo* model of genotoxicity in AML by treating primary AML cells engrafted in mice with functionally therapeutic doses of AraC. They concluded that AML cells after chemotherapy can persist in a reversible senescent-like dormant state with leukaemia repopulation ability proved by *in vivo* transplantation mouse model. Indeed, such findings highlight the fluidity of the term "dormancy" in cancer cells in comparison to "quiescence" in non-transformed somatic cells. Whilst the latter is describing the G0 phase of the cell cycle, which most evidence supports is regulated by the CDKI including p21, p27 and p57, the former might include several cell cycle arrest states including G0, G1 or senescence. Also, it might include what we are describing in the current study which are cells with features of persistent cell cycle arrest that is functionally meaningful, in modelling survivor cells that might cause relapse.

The common signature of these survivor TF1-a cells included genes that can be classified as tumour suppressors or having anti-proliferative potential such as CDKN2B (p15) (section 5.3.2), SLFN5 (section 7.3.3) and BTG2. These genes might explain the inhibition of proliferation in TF1-a-Eto cells and hence can be considered a link between dormancy and genotoxicity in AML cells. This makes them candidates for future research to establish any possible association between these genes and regulation of dormancy or cell cycle control in AML cells surviving genotoxicity (figure 8.1).

## 8.6. Conclusions

In the current study we established an *in vitro* model of dormant AML cells with stemness features using the $CD34^+$ $CD38^-$ TF1-a AML cell lines treated for 72 hours with TGFβ1 and the mTOR inhibitor rapamycin. This model provided a source of dormancy-enriched cells and minimized the difficulties and limitations in obtaining these cells from clinical samples from patients. It also provided and will provide a relatively constant model for repetition and comparison of different experimental conditioning to test different pathways, markers, effects of chemotherapeutic agents and the damage response to them in the context of dormant leukaemia stem cells.

Using whole human genome Affymetrix microarray strips (HuGene2.1ST) to compare the differentially regulated genes in dormancy-induced TF1a cells to their proliferating (untreated) counterparts, we identified 240 genes which are significantly up-regulated by at least twofold including genes involved in adhesion, stemness, chemoresistance, tumour suppression and genes involved in canonical cell cycle regulation. The most upregulated gene was osteopontin (17.1 fold). Immunocytochemistry of BM biopsies from AML patients confirmed high levels of osteopontin in the cytoplasm of blasts near the paratrabecular BM. Osteopontin and other genes identified in this model, including well-characterised genes (e.g. CD44, CD47, CD123, ABBC3 and CDKN2B) as well as little-known ones (e.g. PTPRU, ITGB3 and BTG2), are potential therapeutic targets and are candidates for further investigations in AML.

Finally, we demonstrated that the dormant TF1-a cells and their counterparts that survived the prolonged sub-lethal genotoxic stress by culture for 6 days with etoposide, had a common molecular signature included several novel genes (e.g. SLFN5, ITGB3 and BTG2) which could reflect a possible dormancy-like adaptive response of AML cells surviving sub-optimal concentration of chemotherapeutic agents.

## 8.7. Limitations of the study

This study was conducted with some potential limitations which are worth to be addressed. First, the model of dormancy in AML relied on AML cell lines which were growth factors-independent in proliferation. In fact, their self-tendency to proliferate could be an obstacle against achieving a complete dormancy status. To illustrate, despite the significant inhibition of proliferation and the significant increase in Ki-67 negative (dormant) AML cells, TF1-a cells continued to show significant growth. Indeed, the attempt to use primary AML cells were experimentally not possible for the *in vitro* modelling of dormancy due to the limited survival of these cells that limited their reproducibility. Therefore, our model requires a validation in a well-designed *in vivo* system of AML that was not possible to provide during this study. Nevertheless, it has been argued that dormancy in cancer cells is more complex and difficult to describe if compared to quiescence of non-transformed cells (discussed in section 1.4) which supports the validity of the findings of the TF1-a cells dormancy model.

Second, the process of obtaining BM biopsies of AML patients was not ideal to meet the goal of this study. This was due to the limited number of sections per biopsy, shortage of clinical data clarifying the immunophenotyping, molecular features, chemotherapeutic agents used in the treatment and the MRD status of the patients. Also, it was not possible to provide normal BM biopsies to achieve a better evaluation of the proteins of interest. Therefore, it would be of importance to conduct a longitudinal studies in collaboration with the clinical haematologists in pre-treatment and followup investigations of BM biopsies and other clinical samples from AML patients.

Third, the high cost of the GEP study was a limiting factor prevented including more conditions of TF1-a cells or including other cell lines that showed fewer features of dormancy such as Kasumi-3 and M0-91. Indeed, it could be useful if we could include TF1-a under higher etoposide treatment (IC50) or TF1-a cells in

different time points of dormancy induction conditioning. These additional conditions might have guided us to a better understanding of the most important genes in the resulted molecular signatures.

## 8.8. Future directions

Despite the above-discussed limitations, the results of this study opned the doors to many important future directions of investigations. Firstly, we will be focused on selecting genes for further functional validation such as ITGB3 which was commonly upregulated in AML cells under dormancy or genotoxic environment. Indeed ITGB3 and other novel genes identified in this study are candidates for investigations to establish their possible direct link with dormancy regulation in response to both combination of TGFβ1 and rapamycin or to etoposide treatment in an attempt to find targets to stimulate dormant AML cells to cycling and hence eradication by chemotherapy.

Secondly, investigations can be directed to study the effect of principal chemotherapeutic agents such as AraC and daunorubicin on dormancy-induced AML cells such as the dormant TF1-a cells cultured with the combination of TGFβ1 and rapamycin or primary AML cells under similar *in vitro* conditioning. The damage response of these cells induced to dormancy in comparison to their proliferating counterparts could help to identify the mechanism of resistance of these cells to treatment.

Finally, in vivo murine models of AML can be utilized to validate the most important gene among the novel genes identified in this study through knock-out models or *in vivo* neutralization assays and *in vivo* tracking of dormant AML cells. This carry a potentially significant impact on advancing the current therapeutic regimens in AML.

# REFERENCES


**Achille, N. J.**, M. Othus, K. Phelan, S. Zhang, K. Cooper, J. E. Godwin, F. R. Appelbaum, J. P. Radich, H. P. Erba, S. Nand and N. J. Zeleznik-Le **(2016)**. "Association between early promoter-specific DNA methylation changes and outcome in older acute myeloid leukemia patients." Leuk Res 42: 68-74.

**Al-Mawali, A.**, D. Gillis and I. Lewis **(2016)**. "Immunoprofiling of leukemic stem cells CD34+/CD38-/CD123+ delineate FLT3/ITD-positive clones." J Hematol Oncol 9(1): 61.

**Anthony, B. A.** and D. C. Link **(2014)**. "Regulation of hematopoietic stem cells by bone marrow stromal cells." Trends Immunol 35(1): 32-37.

**Arai, F.**, A. Hirao, M. Ohmura, H. Sato, S. Matsuoka, K. Takubo, K. Ito, G. Y. Koh and T. Suda **(2004)**. "Tie2/angiopoietin-1 signaling regulates hematopoietic stem cell quiescence in the bone marrow niche." Cell 118(2): 149-161.

**Arber, D. A.**, A. Orazi, R. Hasserjian, J. Thiele, M. J. Borowitz, M. M. Le Beau, C. D. Bloomfield, M. Cazzola and J. W. Vardiman **(2016)**. "The 2016 revision to the World Health Organization classification of myeloid neoplasms and acute leukemia." Blood 127(20): 2391-2405.

**Avigdor, A.**, P. Goichberg, S. Shivtiel, A. Dar, A. Peled, S. Samira, O. Kollet, R. Hershkoviz, R. Alon, I. Hardan, H. Ben-Hur, D. Naor, A. Nagler and T. Lapidot **(2004)**. "CD44 and hyaluronic acid cooperate with SDF-1 in the trafficking of human CD34+ stem/progenitor cells to bone marrow." Blood 103(8): 2981-2989.

**Bae, G. Y.**, S. K. Hong, J. R. Park, O. S. Kwon, K. T. Kim, J. Koo, E. Oh and H. J. Cha **(2016)**. "Chronic TGFbeta stimulation promotes the metastatic potential of lung cancer cells by Snail protein stabilization through integrin beta3-Akt-GSK3beta signaling." Oncotarget 7(18): 25366-25376.

**Bain, B. J. (2003)**. Leukaemia diagnosis. Oxford, UK, Blackwell Publishing Ltd.

**Barbier, V.**, I. G. Winkler and J. P. Levesque **(2012)**. "Mobilization of hematopoietic stem cells by depleting bone marrow macrophages." Methods Mol Biol 904: 117-138.

**Bartholomae, S.**, B. Gruhn, K. M. Debatin, M. Zimmermann, U. Creutzig, D. Reinhardt and D. Steinbach **(2016)**. "Coexpression of Multiple ABC-Transporters is Strongly Associated with Treatment Response in Childhood Acute Myeloid Leukemia." Pediatr Blood Cancer 63(2): 242-247.

**Batard, P.**, M. N. Monier, N. Fortunel, K. Ducos, P. Sansilvestri-Morel, T. Phan, A. Hatzfeld and J. A. Hatzfeld **(2000)**. "TGF-(beta)1 maintains hematopoietic immaturity by a reversible negative control of cell cycle and induces CD34 antigen up-modulation." J Cell Sci 113 ( Pt 3): 383-390.

**Bendall, L. J.**, K. F. Bradstock and D. J. Gottlieb **(2000)**. "Expression of CD44 variant exons in acute myeloid leukemia is more common and more complex than that observed in normal blood, bone marrow or CD34+ cells." Leukemia 14(7): 1239-1246.

**Bhatia, M.**, D. Bonnet, B. Murdoch, O. I. Gan and J. E. Dick **(1998)**. "A newly discovered class of human hematopoietic cells with SCID-repopulating activity." Nat Med 4(9): 1038-1045.

**Bhola, N. E.**, J. M. Balko, T. C. Dugger, M. G. Kuba, V. Sanchez, M. Sanders, J. Stanford, R. S. Cook and C. L. Arteaga **(2013)**. "TGF-beta inhibition enhances chemotherapy action against triple-negative breast cancer." J Clin Invest 123(3): 1348-1358.

**Blagosklonny, M. V. (2014)**. "Koschei the immortal and anti-aging drugs." Cell Death Dis 5: e1552.

**Blair, A.**, D. E. Hogge and H. J. Sutherland **(1998)**. "Most acute myeloid leukemia progenitor cells with long-term proliferative ability in vitro and in vivo have the phenotype CD34(+)/CD71(-)/HLA-DR." Blood 92(11): 4325-4335.

**Blair, A.** and H. J. Sutherland **(2000)**. "Primitive acute myeloid leukemia cells with long-term proliferative ability in vitro and in vivo lack surface expression of c-kit (CD117)." Exp Hematol 28(6): 660-671.

**Blank, U.** and S. Karlsson **(2015)**. "TGF-beta signaling in the control of hematopoietic stem cells." Blood 125(23): 3542-3550.

**Bogen, A.**, C. Buske, W. Hiddemann, S. K. Bohlander and O. Christ **(2017)**. "Variable aldehyde dehydrogenase activity and effects on chemosensitivity of primitive human leukemic cells." Exp Hematol 47: 54-63.

**Bonifant, C. L.**, A. Szoor, D. Torres, N. Joseph, M. P. Velasquez, K. Iwahori, A. Gaikwad, P. Nguyen, C. Arber, X. T. Song, M. Redell and S. Gottschalk **(2016)**. "CD123-Engager T Cells as a Novel Immunotherapeutic for Acute Myeloid Leukemia." Mol Ther.

**Bonnet, D.** and J. E. Dick **(1997)**. "Human acute myeloid leukemia is organized as a hierarchy that originates from a primitive hematopoietic cell." Nat Med 3(7): 730-737.

**Boyerinas, B.**, M. Zafrir, A. E. Yesilkanal, T. T. Price, E. M. Hyjek and D. A. Sipkins **(2013)**. "Adhesion to osteopontin in the bone marrow niche regulates lymphoblastic leukemia cell dormancy." Blood 121(24): 4821-4831.

**Brugarolas, J.**, R. T. Bronson and T. Jacks **(1998)**. "p21 is a critical CDK2 regulator essential for proliferation control in Rb-deficient cells." J Cell Biol 141(2): 503-514.

**Brunet, A.**, L. B. Sweeney, J. F. Sturgill, K. F. Chua, P. L. Greer, Y. Lin, H. Tran, S. E. Ross, R. Mostoslavsky, H. Y. Cohen, L. S. Hu, H. L. Cheng, M. P. Jedrychowski, S. P. Gygi, D. A. Sinclair, F. W. Alt and M. E. Greenberg **(2004)**. "Stress-dependent regulation of FOXO transcription factors by the SIRT1 deacetylase." Science 303(5666): 2011-2015.

**Bruns, I.**, D. Lucas, S. Pinho, J. Ahmed, M. P. Lambert, Y. Kunisaki, C. Scheiermann, L. Schiff, M. Poncz, A. Bergman and P. S. Frenette **(2014)**. "Megakaryocytes regulate hematopoietic stem cell quiescence through CXCL4 secretion." Nat Med 20(11): 1315-1320.

**Bruserud, O.**, B. T. Gjertsen and H. L. von Volkman **(2000)**. "In vitro culture of human acute myelogenous leukemia (AML) cells in serum-free media: studies of native AML blasts and AML cell lines." J Hematother Stem Cell Res 9(6): 923-932.

**Bui, A. T.**, F. Laurent, M. Havard, F. Dautry and T. Tchenio **(2015)**. "SMAD signaling and redox imbalance cooperate to induce prostate cancer cell dormancy." Cell Cycle 14(8): 1218-1231.

**Burnett, A. K. (2006)**. Acute myeloid leukaemia. Oxford, UK, Blackwell Publishing Ltd.

**Burnett, A. K.**, N. H. Russell, R. K. Hills, A. E. Hunter, L. Kjeldsen, J. Yin, B. E. Gibson, K. Wheatley and D. Milligan **(2013)**. "Optimization of chemotherapy for younger patients with acute myeloid leukemia: results of the medical research council AML15 trial." J Clin Oncol 31(27): 3360-3368.

**Caceres-Cortes, J. R. (2013)**. "Blastic leukaemias (AML): a biologist's view." Cell Biochem Biophys 66(1): 13-22.

**Calvi, L. M.**, G. B. Adams, K. W. Weibrecht, J. M. Weber, D. P. Olson, M. C. Knight, R. P. Martin, E. Schipani, P. Divieti, F. R. Bringhurst, L. A. Milner, H. M. Kronenberg and D. T. Scadden **(2003)**. "Osteoblastic cells regulate the haematopoietic stem cell niche." Nature 425(6960): 841-846.

**Calvi, L. M.** and D. C. Link **(2014)**. "Cellular complexity of the bone marrow hematopoietic stem cell niche." Calcif Tissue Int 94(1): 112-124.

**Cao, L.**, X. Fan, W. Jing, Y. Liang, R. Chen, Y. Liu, M. Zhu, R. Jia, H. Wang, X. Zhang, Y. Zhang, X. Zhou, J. Zhao and Y. Guo **(2015)**. "Osteopontin promotes a cancer stem cell-like phenotype in hepatocellular carcinoma cells via an integrin-NF-kappaB-HIF-1alpha pathway." Oncotarget 6(9): 6627-6640.

**Carlinfante, G.**, D. Vassiliou, O. Svensson, M. Wendel, D. Heinegard and G. Andersson **(2003)**. "Differential expression of osteopontin and bone sialoprotein in bone metastasis of breast and prostate carcinoma." Clin Exp Metastasis 20(5): 437-444.

**Chaterjee, M.** and K. L. van Golen **(2011)**. "Breast cancer stem cells survive periods of farnesyl-transferase inhibitor-induced dormancy by undergoing autophagy." Bone Marrow Res 2011: 362938.

**Chatterjee, M.** and K. L. van Golen **(2011)**. "Farnesyl transferase inhibitor treatment of breast cancer cells leads to altered RhoA and RhoC GTPase activity and induces a dormant phenotype." Int J Cancer 129(1): 61-69.

**Chen, C.**, Y. Liu, R. Liu, T. Ikenoue, K. L. Guan, Y. Liu and P. Zheng **(2008)**. "TSC-mTOR maintains quiescence and function of hematopoietic stem cells by repressing mitochondrial biogenesis and reactive oxygen species." J Exp Med 205(10): 2397-2408.

**Chen, X.**, L. Wei and S. Zhao **(2016)**. "miR-338 inhibits the metastasis of lung cancer by targeting integrin beta3." Oncol Rep 36(3): 1467-1474.

**Chen, Y.**, J. Soong, S. Mohanty, L. Xu and G. Scott **(2013)**. "The neural guidance receptor Plexin C1 delays melanoma progression." Oncogene 32(41): 4941-4949.

**Chougule, R. A.**, E. Cordero, S. A. Moharram, K. Pietras, L. Ronnstrand and J. U. Kazi **(2016)**. "Expression of GADS enhances FLT3-induced mitogenic signaling." Oncotarget 7(12): 14112-14124.

**Christ, O.**, K. Lucke, S. Imren, K. Leung, M. Hamilton, A. Eaves, C. Smith and C. Eaves **(2007)**. "Improved purification of hematopoietic stem cells based on their elevated aldehyde dehydrogenase activity." Haematologica 92(9): 1165-1172.

**Coller, H. A. (2007)**. "What's taking so long? S-phase entry from quiescence versus proliferation." Nat Rev Mol Cell Biol 8(8): 667-670.

**Coller, H. A.**, L. Sang and J. M. Roberts **(2006)**. "A new description of cellular quiescence." PLoS Biol 4(3): e83.

**Conway O'Brien, E.**, S. Prideaux and T. Chevassut **(2014)**. "The epigenetic landscape of acute myeloid leukemia." Adv Hematol 2014: 103175.

**Cuadrado, M.**, P. Gutierrez-Martinez, A. Swat, A. R. Nebreda and O. Fernandez-Capetillo **(2009)**. "p27Kip1 stabilization is essential for the maintenance of cell cycle arrest in response to DNA damage." Cancer Res 69(22): 8726-8732.

**Cui, X. Y.**, G. Skretting, Y. Jing, H. Sun, P. M. Sandset and L. Sun **(2013)**. "Hypoxia influences stem cell-like properties in multidrug resistant K562 leukemic cells." Blood Cells Mol Dis 51(3): 177-184.

**Darzynkiewicz, Z.**, F. Traganos and M. R. Melamed **(1980)**. "New cell cycle compartments identified by multiparameter flow cytometry." Cytometry 1(2): 98-108.

**David Brown**, K. G., Yasodha Natkunam and Roger Warnke **(2006)**. "Bone Marrow Diagnosis: an illustrated guide."

**De Braekeleer, M.**, N. Douet-Guilbert and E. De Braekeleer **(2016)**. "Prognostic impact of p15 gene aberrations in acute leukemia." Leuk Lymphoma: 1-9.

**Diamond, M. S. (2014)**. "IFIT1: A dual sensor and effector molecule that detects non-2'-O methylated viral RNA and inhibits its translation." Cytokine Growth Factor Rev 25(5): 543-550.

**Ding, L.**, T. L. Saunders, G. Enikolopov and S. J. Morrison **(2012)**. "Endothelial and perivascular cells maintain haematopoietic stem cells." Nature 481(7382): 457-462.

**Dohner, H.**, E. Estey, D. Grimwade, S. Amadori, F. R. Appelbaum, T. Buchner, H. Dombret, B. L. Ebert, P. Fenaux, R. A. Larson, R. L. Levine, F. Lo-Coco, T. Naoe, D. Niederwieser, G. J. Ossenkoppele, M. Sanz, J. Sierra, M. S. Tallman, H. F. Tien, A. H. Wei, B. Lowenberg and C. D. Bloomfield **(2017)**. "Diagnosis and management of AML in adults: 2017 ELN recommendations from an international expert panel." Blood 129(4): 424-447.

**Dohner, H.**, E. H. Estey, S. Amadori, F. R. Appelbaum, T. Buchner, A. K. Burnett, H. Dombret, P. Fenaux, D. Grimwade, R. A. Larson, F. Lo-Coco, T. Naoe, D. Niederwieser, G. J. Ossenkoppele, M. A. Sanz, J. Sierra, M. S. Tallman, B. Lowenberg, C. D. Bloomfield and L. European **(2010)**. "Diagnosis and management of acute myeloid leukemia in adults: recommendations from an

international expert panel, on behalf of the European LeukemiaNet." Blood 115(3): 453-474.

**Dohner, H.**, D. J. Weisdorf and C. D. Bloomfield **(2015)**. "Acute Myeloid Leukemia." N Engl J Med 373(12): 1136-1152.

**Dombret, H.** and C. Gardin **(2016)**. "An update of current treatments for adult acute myeloid leukemia." Blood 127(1): 53-61.

**Dong, H. Y.**, S. Wilkes and H. Yang **(2011)**. "CD71 is selectively and ubiquitously expressed at high levels in erythroid precursors of all maturation stages: a comparative immunochemical study with glycophorin A and hemoglobin A." Am J Surg Pathol 35(5): 723-732.

**Dong, M.** and G. C. Blobe **(2006)**. "Role of transforming growth factor-beta in hematologic malignancies." Blood 107(12): 4589-4596.

**Dougherty, G. J.**, P. M. Landorp, D. L. Cooper and R. K. Humphries **(1991)**. "Molecular cloning of CD44R1 and CD44R2, two novel isoforms of the human CD44 lymphocyte "homing" receptor expressed by hemopoietic cells." J Exp Med 174(1): 1-5.

**Driss, V.**, B. Quesnel and C. Brinster **(2015)**. "Monocyte chemoattractant protein 1 (MCP-1/CCL2) contributes to thymus atrophy in acute myeloid leukemia." Eur J Immunol 45(2): 396-406.

**Ema, H.** and T. Suda **(2012)**. "Two anatomically distinct niches regulate stem cell activity." Blood 120(11): 2174-2181.

**Erb, U.**, A. P. Megaptche, X. Gu, M. W. Buchler and M. Zoller **(2014)**. "CD44 standard and CD44v10 isoform expression on leukemia cells distinctly influences niche embedding of hematopoietic stem cells." J Hematol Oncol 7: 29.

**Essers, M. A.** and A. Trumpp **(2010)**. "Targeting leukemic stem cells by breaking their dormancy." Mol Oncol 4(5): 443-450.

**Fingar, D. C.** and J. Blenis **(2004)**. "Target of rapamycin (TOR): an integrator of nutrient and growth factor signals and coordinator of cell growth and cell cycle progression." Oncogene 23(18): 3151-3171.

**Forsberg, E. C.**, E. Passegue, S. S. Prohaska, A. J. Wagers, M. Koeva, J. M. Stuart and I. L. Weissman **(2010)**. "Molecular signatures of quiescent, mobilized and leukemia-initiating hematopoietic stem cells." PLoS One 5(1): e8785.

**Fortunel, N.**, P. Batard, A. Hatzfeld, M. N. Monier, B. Panterne, J. Lebkowski and J. Hatzfeld **(1998)**. "High proliferative potential-quiescent cells: a working model to study primitive quiescent hematopoietic cells." J Cell Sci 111 ( Pt 13): 1867-1875.

**Fortunel, N.**, J. Hatzfeld, L. Aoustin, P. Batard, K. Ducos, M. N. Monier, A. Charpentier and A. Hatzfeld **(2000)**. "Specific dose-response effects of TGF-beta1 on developmentally distinct hematopoietic stem/progenitor cells from human umbilical cord blood." Hematol J 1(2): 126-135.

**Fortunel, N.**, J. Hatzfeld, S. Kisselev, M. N. Monier, K. Ducos, A. Cardoso, P. Batard and A. Hatzfeld **(2000)**. "Release from quiescence of primitive human

hematopoietic stem/progenitor cells by blocking their cell-surface TGF-beta type II receptor in a short-term in vitro assay." Stem Cells 18(2): 102-111.

**Fortunel, N. O.**, A. Hatzfeld and J. A. Hatzfeld **(2000)**. "Transforming growth factor-beta: pleiotropic role in the regulation of hematopoiesis." Blood 96(6): 2022-2036.

**Frenette, P. S.**, S. Pinho, D. Lucas and C. Scheiermann **(2013)**. "Mesenchymal stem cell: keystone of the hematopoietic stem cell niche and a stepping-stone for regenerative medicine." Annu Rev Immunol 31: 285-316.

**Gal, H.**, N. Amariglio, L. Trakhtenbrot, J. Jacob-Hirsh, O. Margalit, A. Avigdor, A. Nagler, S. Tavor, L. Ein-Dor, T. Lapidot, E. Domany, G. Rechavi and D. Givol **(2006)**. "Gene expression profiles of AML derived stem cells; similarity to hematopoietic stem cells." Leukemia 20(12): 2147-2154.

**Gallacher, L.**, B. Murdoch, D. M. Wu, F. N. Karanu, M. Keeney and M. Bhatia **(2000)**. "Isolation and characterization of human CD34(-)Lin(-) and CD34(+)Lin(-) hematopoietic stem cells using cell surface markers AC133 and CD7." Blood 95(9): 2813-2820.

**Gan, B.**, J. Hu, S. Jiang, Y. Liu, E. Sahin, L. Zhuang, E. Fletcher-Sananikone, S. Colla, Y. A. Wang, L. Chin and R. A. Depinho **(2010)**. "Lkb1 regulates quiescence and metabolic homeostasis of haematopoietic stem cells." Nature 468(7324): 701-704.

**Gerber, J. M.**, B. D. Smith, B. Ngwang, H. Zhang, M. S. Vala, L. Morsberger, S. Galkin, M. I. Collector, B. Perkins, M. J. Levis, C. A. Griffin, S. J. Sharkis, M. J. Borowitz, J. E. Karp and R. J. Jones **(2012)**. "A clinically relevant population of leukemic CD34(+)CD38(-) cells in acute myeloid leukemia." Blood 119(15): 3571-3577.

**Gerdes, J.**, H. Lemke, H. Baisch, H. H. Wacker, U. Schwab and H. Stein **(1984)**. "Cell cycle analysis of a cell proliferation-associated human nuclear antigen defined by the monoclonal antibody Ki-67." J Immunol 133(4): 1710-1715.

**Giannoudis, A.**, A. Davies, R. J. Harris, C. M. Lucas, M. Pirmohamed and R. E. Clark **(2014)**. "The clinical significance of ABCC3 as an imatinib transporter in chronic myeloid leukaemia." Leukemia 28(6): 1360-1363.

**Gillis, L. C.**, D. M. Berry, M. D. Minden, C. J. McGlade and D. L. Barber **(2013)**. "Gads (Grb2-related adaptor downstream of Shc) is required for BCR-ABL-mediated lymphoid leukemia." Leukemia 27(8): 1666-1676.

**Glimm, H.**, I. H. Oh and C. J. Eaves **(2000)**. "Human hematopoietic stem cells stimulated to proliferate in vitro lose engraftment potential during their S/G(2)/M transit and do not reenter G(0)." Blood 96(13): 4185-4193.

**Godley, L. A.**, J. Cunningham, M. E. Dolan, R. S. Huang, S. Gurbuxani, M. E. McNerney, R. A. Larson, H. Leong, Y. Lussier, K. Onel, O. Odenike, W. Stock, K. P. White and M. M. Le Beau **(2011)**. "An integrated genomic approach to the assessment and treatment of acute myeloid leukemia." Semin Oncol 38(2): 215-224.

**Gothot, A.**, R. Pyatt, J. McMahel, S. Rice and E. F. Srour **(1997)**. "Functional heterogeneity of human CD34(+) cells isolated in subcompartments of the G0 /G1 phase of the cell cycle." Blood 90(11): 4384-4393.

**Graham, S. M.**, H. G. Jorgensen, E. Allan, C. Pearson, M. J. Alcorn, L. Richmond and T. L. Holyoake **(2002)**. "Primitive, quiescent, Philadelphia-positive stem cells from patients with chronic myeloid leukemia are insensitive to STI571 in vitro." Blood 99(1): 319-325.

**Grassinger, J.**, D. N. Haylock, M. J. Storan, G. O. Haines, B. Williams, G. A. Whitty, A. R. Vinson, C. L. Be, S. Li, E. S. Sorensen, P. P. Tam, D. T. Denhardt, D. Sheppard, P. F. Choong and S. K. Nilsson **(2009)**. "Thrombin-cleaved osteopontin regulates hemopoietic stem and progenitor cell functions through interactions with alpha9beta1 and alpha4beta1 integrins." Blood 114(1): 49-59.

**Green, A. S.**, N. Chapuis, T. T. Maciel, L. Willems, M. Lambert, C. Arnoult, O. Boyer, V. Bardet, S. Park, M. Foretz, B. Viollet, N. Ifrah, F. Dreyfus, O. Hermine, I. C. Moura, C. Lacombe, P. Mayeux, D. Bouscary and J. Tamburini **(2010)**. "The LKB1/AMPK signaling pathway has tumor suppressor activity in acute myeloid leukemia through the repression of mTOR-dependent oncogenic mRNA translation." Blood 116(20): 4262-4273.

**Gur-Cohen, S.**, T. Itkin, S. Chakrabarty, C. Graf, O. Kollet, A. Ludin, K. Golan, A. Kalinkovich, G. Ledergor, E. Wong, E. Niemeyer, Z. Porat, A. Erez, I. Sagi, C. T. Esmon, W. Ruf and T. Lapidot **(2015)**. "PAR1 signaling regulates the retention and recruitment of EPCR-expressing bone marrow hematopoietic stem cells." Nat Med 21(11): 1307-1317.

**Gurumurthy, S.**, S. Z. Xie, B. Alagesan, J. Kim, R. Z. Yusuf, B. Saez, A. Tzatsos, F. Ozsolak, P. Milos, F. Ferrari, P. J. Park, O. S. Shirihai, D. T. Scadden and N. Bardeesy **(2010)**. "The Lkb1 metabolic sensor maintains haematopoietic stem cell survival." Nature 468(7324): 659-663.

**Hanke, M.**, I. Hoffmann, C. Christophis, M. Schubert, V. T. Hoang, A. Zepeda-Moreno, N. Baran, V. Eckstein, P. Wuchter, A. Rosenhahn and A. D. Ho **(2014)**. "Differences between healthy hematopoietic progenitors and leukemia cells with respect to CD44 mediated rolling versus adherence behavior on hyaluronic acid coated surfaces." Biomaterials 35(5): 1411-1419.

**Haylock, D. N.** and S. K. Nilsson **(2006)**. "Osteopontin: a bridge between bone and blood." Br J Haematol 134(5): 467-474.

**Ho, T. C.**, M. LaMere, B. M. Stevens, J. M. Ashton, J. R. Myers, K. M. O'Dwyer, J. L. Liesveld, J. H. Mendler, M. Guzman, J. D. Morrissette, J. Zhao, E. S. Wang, M. Wetzler, C. T. Jordan and M. W. Becker **(2016)**. "Evolution of acute myelogenous leukemia stem cell properties after treatment and progression." Blood 128(13): 1671-1678.

**Hoang, V. T.**, E. C. Buss, W. Wang, I. Hoffmann, S. Raffel, A. Zepeda-Moreno, N. Baran, P. Wuchter, V. Eckstein, A. Trumpp, A. Jauch, A. D. Ho and C. Lutz **(2015)**. "The rarity of ALDH(+) cells is the key to separation of normal versus leukemia stem cells by ALDH activity in AML patients." Int J Cancer 137(3): 525-536.

**Holyoake, T.**, X. Jiang, C. Eaves and A. Eaves **(1999)**. "Isolation of a highly quiescent subpopulation of primitive leukemic cells in chronic myeloid leukemia." Blood 94(6): 2056-2064.

**Hong, Q.**, Y. Li, X. Chen, H. Ye, L. Tang, A. Zhou, Y. Hu, Y. Gao, R. Chen, Y. Xia and S. Duan **(2016)**. "CDKN2B, SLC19A3 and DLEC1 promoter methylation alterations

in the bone marrow of patients with acute myeloid leukemia during chemotherapy." Exp Ther Med 11(5): 1901-1907.

**Hong, S. K.**, J. R. Park, O. S. Kwon, K. T. Kim, G. Y. Bae and H. J. Cha **(2016)**. "Induction of integrin beta3 by sustained ERK activity promotes the invasiveness of TGFbeta-induced mesenchymal tumor cells." Cancer Lett 376(2): 339-346.

**Horan, P. K.** and S. E. Slezak **(1989)**. "Stable cell membrane labelling." Nature 340(6229): 167-168.

**Hoshii, T.**, Y. Tadokoro, K. Naka, T. Ooshio, T. Muraguchi, N. Sugiyama, T. Soga, K. Araki, K. Yamamura and A. Hirao **(2012)**. "mTORC1 is essential for leukemia propagation but not stem cell self-renewal." J Clin Invest 122(6): 2114-2129.

**Houtenbos, I.**, T. M. Westers, A. G. Stam, T. D. de Gruijl, R. J. Scheper, G. J. Ossenkoppele and A. A. van de Loosdrecht **(2003)**. "Serum-free generation of antigen presenting cells from acute myeloid leukaemic blasts for active specific immunisation." Cancer Immunol Immunother 52(7): 455-462.

**Hu, J.**, H. Nakhla and E. Friedman **(2011)**. "Transient arrest in a quiescent state allows ovarian cancer cells to survive suboptimal growth conditions and is mediated by both Mirk/dyrk1b and p130/RB2." Int J Cancer 129(2): 307-318.

**Hu, X.**, L. C. Moscinski, B. J. Hill, Q. Chen, J. Wu, A. B. Fisher and K. S. Zuckerman **(1998)**. "Characterization of a unique factor-independent variant derived from human factor-dependent TF-1 cells: a transformed event." Leuk Res 22(9): 817-826.

**Huang, C. P.**, M. F. Tsai, T. H. Chang, W. C. Tang, S. Y. Chen, H. H. Lai, T. Y. Lin, J. C. Yang, P. C. Yang, J. Y. Shih and S. B. Lin **(2013)**. "ALDH-positive lung cancer stem cells confer resistance to epidermal growth factor receptor tyrosine kinase inhibitors." Cancer Lett 328(1): 144-151.

**Huang, J.**, M. Nguyen-McCarty, E. O. Hexner, G. Danet-Desnoyers and P. S. Klein **(2012)**. "Maintenance of hematopoietic stem cells through regulation of Wnt and mTOR pathways." Nat Med 18(12): 1778-1785.

**Ichihara, E.**, K. Kaneda, Y. Saito, N. Yamakawa and K. Morishita **(2011)**. "Angiopoietin1 contributes to the maintenance of cell quiescence in EVI1(high) leukemia cells." Biochem Biophys Res Commun 416(3-4): 239-245.

**Inoue, M.** and M. L. Shinohara **(2011)**. "Intracellular osteopontin (iOPN) and immunity." Immunol Res 49(1-3): 160-172.

**Iriuchishima, H.**, K. Takubo, S. Matsuoka, I. Onoyama, K. I. Nakayama, Y. Nojima and T. Suda **(2011)**. "Ex vivo maintenance of hematopoietic stem cells by quiescence induction through Fbxw7α overexpression." Blood 117(8): 2373-2377.

**Ishikawa, F., S.** Yoshida, Y. Saito, A. Hijikata, H. Kitamura, S. Tanaka, R. Nakamura, T. Tanaka, H. Tomiyama, N. Saito, M. Fukata, T. Miyamoto, B. Lyons, K. Ohshima, N. Uchida, S. Taniguchi, O. Ohara, K. Akashi, M. Harada and L. D. Shultz (2007). "Chemotherapy-resistant human AML stem cells home to and engraft within the bone-marrow endosteal region." Nat Biotechnol 25(11): 1315-1321.

**Islam, A.**, C. Glomski and E. S. Henderson **(1990)**. "Bone lining (endosteal) cells and hematopoiesis: a light microscopic study of normal and pathologic human bone marrow in plastic-embedded sections." Anat Rec 227(3): 300-306.

**Itkin, T.**, S. Gur-Cohen, J. A. Spencer, A. Schajnovitz, S. K. Ramasamy, A. P. Kusumbe, G. Ledergor, Y. Jung, I. Milo, M. G. Poulos, A. Kalinkovich, A. Ludin, O. Kollet, G. Shakhar, J. M. Butler, S. Rafii, R. H. Adams, D. T. Scadden, C. P. Lin and T. Lapidot **(2016)**. "Distinct bone marrow blood vessels differentially regulate haematopoiesis." Nature 532(7599): 323-328.

**Iwasaki, M.**, M. Liedtke, A. J. Gentles and M. L. Cleary **(2015)**. "CD93 Marks a Non-Quiescent Human Leukemia Stem Cell Population and Is Required for Development of MLL-Rearranged Acute Myeloid Leukemia." Cell Stem Cell 17(4): 412-421.

**Jaiswal, S.**, P. Fontanillas, J. Flannick, A. Manning, P. V. Grauman, B. G. Mar, R. C. Lindsley, C. H. Mermel, N. Burtt, A. Chavez, J. M. Higgins, V. Moltchanov, F. C. Kuo, M. J. Kluk, B. Henderson, L. Kinnunen, H. A. Koistinen, C. Ladenvall, G. Getz, A. Correa, B. F. Banahan, S. Gabriel, S. Kathiresan, H. M. Stringham, M. I. McCarthy, M. Boehnke, J. Tuomilehto, C. Haiman, L. Groop, G. Atzmon, J. G. Wilson, D. Neuberg, D. Altshuler and B. L. Ebert **(2014)**. "Age-related clonal hematopoiesis associated with adverse outcomes." N Engl J Med 371(26): 2488-2498.

**Jakubowiak, A.**, C. Pouponnot, F. Berguido, R. Frank, S. Mao, J. Massague and S. D. Nimer **(2000)**. "Inhibition of the transforming growth factor beta 1 signaling pathway by the AML1/ETO leukemia-associated fusion protein." J Biol Chem 275(51): 40282-40287.

**Jan, M.**, M. P. Chao, A. C. Cha, A. A. Alizadeh, A. J. Gentles, I. L. Weissman and R. Majeti **(2011)**. "Prospective separation of normal and leukemic stem cells based on differential expression of TIM3, a human acute myeloid leukemia stem cell marker." Proc Natl Acad Sci U S A 108(12): 5009-5014.

**Januchowski, R.**, K. Wojtowicz and M. Zabel **(2013)**. "The role of aldehyde dehydrogenase (ALDH) in cancer drug resistance." Biomed Pharmacother 67(7): 669-680.

**Jewell, J. L.** and K. L. Guan **(2013)**. "Nutrient signaling to mTOR and cell growth." Trends Biochem Sci 38(5): 233-242.

**Jin, L.**, K. J. Hope, Q. Zhai, F. Smadja-Joffe and J. E. Dick **(2006)**. "Targeting of CD44 eradicates human acute myeloid leukemic stem cells." Nat Med 12(10): 1167-1174.

**Jordan, C. T. (2002)**. "Unique molecular and cellular features of acute myelogenous leukemia stem cells." Leukemia 16(4): 559-562.

**Jordan, C. T.**, G. Yamasaki and D. Minamoto **(1996)**. "High-resolution cell cycle analysis of defined phenotypic subsets within primitive human hematopoietic cell populations." Exp Hematol 24(11): 1347-1355.

**Kansal, R. (2016).** "Acute myeloid leukemia in the era of precision medicine: recent advances in diagnostic classification and risk stratification." Cancer Biol Med 13(1): 41-54.

**Kaplan, R. N.**, B. Psaila and D. Lyden **(2006)**. "Bone marrow cells in the 'pre-metastatic niche': within bone and beyond." Cancer Metastasis Rev 25(4): 521-529.

**Karakaya, K.**, F. Herbst, C. Ball, H. Glimm, A. Kramer and H. Loffler **(2012)**. "Overexpression of EVI1 interferes with cytokinesis and leads to accumulation of cells with supernumerary centrosomes in G0/1 phase." Cell Cycle 11(18): 3492-3503.

**Karpinich, N. O.**, M. Tafani, R. J. Rothman, M. A. Russo and J. L. Farber **(2002)**. "The course of etoposide-induced apoptosis from damage to DNA and p53 activation to mitochondrial release of cytochrome c." J Biol Chem 277(19): 16547-16552.

**Khwaja, A.**, M. Bjorkholm, R. E. Gale, R. L. Levine, C. T. Jordan, G. Ehninger, C. D. Bloomfield, E. Estey, A. Burnett, J. J. Cornelissen, D. A. Scheinberg, D. Bouscary and D. C. Linch **(2016)**. "Acute myeloid leukaemia." Nat Rev Dis Primers 2: 16010.

**Kikushige, Y.** and K. Akashi **(2012)**. "TIM-3 as a therapeutic target for malignant stem cells in acute myelogenous leukemia." Ann N Y Acad Sci 1266: 118-123.

**Kikushige, Y.** and T. Miyamoto **(2015)**. "Identification of TIM-3 as a Leukemic Stem Cell Surface Molecule in Primary Acute Myeloid Leukemia." Oncology 89 Suppl 1: 28-32.

**Kikushige, Y.**, T. Miyamoto, J. Yuda, S. Jabbarzadeh-Tabrizi, T. Shima, S. Takayanagi, H. Niiro, A. Yurino, K. Miyawaki, K. Takenaka, H. Iwasaki and K. Akashi **(2015)**. "A TIM-3/Gal-9 Autocrine Stimulatory Loop Drives Self-Renewal of Human Myeloid Leukemia Stem Cells and Leukemic Progression." Cell Stem Cell 17(3): 341-352.

**Kikushige, Y.**, T. Shima, S. Takayanagi, S. Urata, T. Miyamoto, H. Iwasaki, K. Takenaka, T. Teshima, T. Tanaka, Y. Inagaki and K. Akashi **(2010)**. "TIM-3 is a promising target to selectively kill acute myeloid leukemia stem cells." Cell Stem Cell 7(6): 708-717.

**Kim, J. K.**, Y. Jung, J. Wang, J. Joseph, A. Mishra, E. E. Hill, P. H. Krebsbach, K. J. Pienta, Y. Shiozawa and R. S. Taichman **(2013)**. "TBK1 regulates prostate cancer dormancy through mTOR inhibition." Neoplasia 15(9): 1064-1074.

**Kim, T.**, T. Y. Kim, Y. H. Song, I. M. Min, J. Yim and T. K. Kim **(1999)**. "Activation of interferon regulatory factor 3 in response to DNA-damaging agents." J Biol Chem 274(43): 30686-30689.

**Kim, Y. M.**, C. H. Jung, M. Seo, E. K. Kim, J. M. Park, S. S. Bae and D. H. Kim **(2015)**. "mTORC1 phosphorylates UVRAG to negatively regulate autophagosome and endosome maturation." Mol Cell 57(2): 207-218.

**Klapper, W.**, E. Hoster, O. Determann, I. Oschlies, J. van der Laak, F. Berger, H. W. Bernd, J. Cabecadas, E. Campo, S. Cogliatti, M. L. Hansmann, P. M. Kluin, R. Kodet, Y. A. Krivolapov, C. Loddenkemper, H. Stein, P. Moller, T. E. Barth, K. Muller-Hermelink, A. Rosenwald, G. Ott, S. Pileri, E. Ralfkiaer, G. Rymkiewicz, J. H. van Krieken, H. H. Wacker, M. Unterhalt, W. Hiddemann, M. Dreyling and M. C. L. N. European **(2009)**. "Ki-67 as a prognostic marker in mantle cell lymphoma-consensus guidelines of the pathology panel of the European MCL Network." J Hematop 2(2): 103-111.

**Kong, F.**, F. Gao, H. Li, H. Liu, Y. Zhang, R. Zheng, Y. Zhang, J. Chen, X. Li, G. Liu and Y. Jia **(2016)**. "CD47: a potential immunotherapy target for eliminating cancer cells." Clin Transl Oncol.

**Konopleva, M.**, S. Konoplev, W. Hu, A. Y. Zaritskey, B. V. Afanasiev and M. Andreeff **(2002)**. "Stromal cells prevent apoptosis of AML cells by up-regulation of anti-apoptotic proteins." Leukemia 16(9): 1713-1724.

**Kozlowski, R.**, I. A. Reilly, D. Sowter, R. A. Robins and N. H. Russell **(1988)**. "Transferrin receptor expression of AML blasts is related to their proliferative potential." Br J Haematol 69(2): 275-280.

**Krause, D. S.**, D. T. Scadden and F. I. Preffer **(2013)**. "The hematopoietic stem cell niche--home for friend and foe?" Cytometry B Clin Cytom 84(1): 7-20.

**Kunisaki, Y.**, I. Bruns, C. Scheiermann, J. Ahmed, S. Pinho, D. Zhang, T. Mizoguchi, Q. Wei, D. Lucas, K. Ito, J. C. Mar, A. Bergman and P. S. Frenette **(2013)**. "Arteriolar niches maintain haematopoietic stem cell quiescence." Nature 502(7473): 637-643.

**Kurokawa, M.**, K. Mitani, Y. Imai, S. Ogawa, Y. Yazaki and H. Hirai **(1998)**. "The t(3;21) fusion product, AML1/Evi-1, interacts with Smad3 and blocks transforming growth factor-beta-mediated growth inhibition of myeloid cells." Blood 92(11): 4003-4012.

**Kurokawa, M.**, K. Mitani, K. Irie, T. Matsuyama, T. Takahashi, S. Chiba, Y. Yazaki, K. Matsumoto and H. Hirai **(1998)**. "The oncoprotein Evi-1 represses TGF-beta signalling by inhibiting Smad3." Nature 394(6688): 92-96.

**Ladd, A. C.**, R. Pyatt, A. Gothot, S. Rice, J. McMahel, C. M. Traycoff and E. F. Srour **(1997)**. "Orderly process of sequential cytokine stimulation is required for activation and maximal proliferation of primitive human bone marrow CD34+ hematopoietic progenitor cells residing in G0." Blood 90(2): 658-668.

**Lainey, E.**, M. Sebert, S. Thepot, M. Scoazec, C. Bouteloup, C. Leroy, S. De Botton, L. Galluzzi, P. Fenaux and G. Kroemer **(2012)**. "Erlotinib antagonizes ABC transporters in acute myeloid leukemia." Cell Cycle 11(21): 4079-4092.

**Lane, S. W.**, D. T. Scadden and D. G. Gilliland **(2009)**. "The leukemic stem cell niche: current concepts and therapeutic opportunities." Blood 114(6): 1150-1157.

**Lapidot, T.**, C. Sirard, J. Vormoor, B. Murdoch, T. Hoang, J. Caceres-Cortes, M. Minden, B. Paterson, M. A. Caligiuri and J. E. Dick **(1994)**. "A cell initiating human acute myeloid leukaemia after transplantation into SCID mice." Nature 367(6464): 645-648.

**Larsson, J.** and S. Karlsson **(2005)**. "The role of Smad signaling in hematopoiesis." Oncogene 24(37): 5676-5692.

**Law, B. K.**, A. Chytil, N. Dumont, E. G. Hamilton, M. E. Waltner-Law, M. E. Aakre, C. Covington and H. L. Moses **(2002)**. "Rapamycin potentiates transforming growth factor beta-induced growth arrest in nontransformed, oncogene-transformed, and human cancer cells." Mol Cell Biol 22(23): 8184-8198.

**Leavenworth, J. W.**, B. Verbinnen, Q. Wang, E. Shen and H. Cantor **(2015)**. "Intracellular osteopontin regulates homeostasis and function of natural killer cells." Proc Natl Acad Sci U S A 112(2): 494-499.

**Lechman, E. R.**, B. Gentner, P. van Galen, A. Giustacchini, M. Saini, F. E. Boccalatte, H. Hiramatsu, U. Restuccia, A. Bachi, V. Voisin, G. D. Bader, J. E. Dick and L. Naldini **(2012)**. "Attenuation of miR-126 activity expands HSC in vivo without exhaustion." Cell Stem Cell 11(6): 799-811.

**Lee, C. Y.**, H. F. Tien, H. A. Hou, W. C. Chou and L. I. Lin **(2008)**. "Marrow osteopontin level as a prognostic factor in acute myeloid leukaemia." Br J Haematol 141(5): 736-739.

**Lee, J. L.**, M. J. Wang, P. R. Sudhir, G. D. Chen, C. W. Chi and J. Y. Chen **(2007)**. "Osteopontin promotes integrin activation through outside-in and inside-out mechanisms: OPN-CD44V interaction enhances survival in gastrointestinal cancer cells." Cancer Res 67(5): 2089-2097.

**Levesque, M. C.**, C. W. O'Loughlin and J. B. Weinberg **(2001)**. "Use of serum-free media to minimize apoptosis of chronic lymphocytic leukemia cells during in vitro culture." Leukemia 15(8): 1305-1307.

**Li, J., S. G.** Kim and J. Blenis **(2014)**. "Rapamycin: one drug, many effects." Cell Metab 19(3): 373-379.

**Liersch, R.**, J. Gerss, C. Schliemann, M. Bayer, C. Schwoppe, C. Biermann, I. Appelmann, T. Kessler, B. Lowenberg, T. Buchner, W. Hiddemann, C. Muller-Tidow, W. E. Berdel and R. Mesters **(2012)**. "Osteopontin is a prognostic factor for survival of acute myeloid leukemia patients." Blood 119(22): 5215-5220.

**Litovchick, L.**, L. A. Florens, S. K. Swanson, M. P. Washburn and J. A. DeCaprio **(2011)**. "DYRK1A protein kinase promotes quiescence and senescence through DREAM complex assembly." Genes Dev 25(8): 801-813.

**Liu, H.**, A. S. Adler, E. Segal and H. Y. Chang **(2007)**. "A transcriptional program mediating entry into cellular quiescence." PLoS Genet 3(6): e91.

**Liu, M.**, H. Wu, T. Liu, Y. Li, F. Wang, H. Wan, X. Li and H. Tang **(2009)**. "Regulation of the cell cycle gene, BTG2, by miR-21 in human laryngeal carcinoma." Cell Res 19(7): 828-837.

**Liu, Q.**, L. Chen, J. M. Atkinson, D. F. Claxton and H. G. Wang **(2016)**. "Atg5-dependent autophagy contributes to the development of acute myeloid leukemia in an MLL-AF9-driven mouse model." Cell Death Dis 7(9): e2361.

**Liu, Q.**, M. Wang, Y. Hu, H. Xing, X. Chen, Y. Zhang and P. Zhu **(2014)**. "Significance of CD71 expression by flow cytometry in diagnosis of acute leukemia." Leuk Lymphoma 55(4): 892-898.

**Liu, S. K.**, D. M. Berry and C. J. McGlade **(2001)**. "The role of Gads in hematopoietic cell signalling." Oncogene 20(44): 6284-6290.

**Liu, Y.**, S. E. Elf, Y. Miyata, G. Sashida, Y. Liu, G. Huang, S. Di Giandomenico, J. M. Lee, A. Deblasio, S. Menendez, J. Antipin, B. Reva, A. Koff and S. D. Nimer **(2009)**. "p53 regulates hematopoietic stem cell quiescence." Cell Stem Cell 4(1): 37-48.

**Liu, Y.**, Z. Zhu, Z. Xiong, J. Zheng, Z. Hu and J. Qiu **(2014)**. "Knockdown of protein tyrosine phosphatase receptor U inhibits growth and motility of gastric cancer cells." Int J Clin Exp Pathol 7(9): 5750-5761.

**Lopez-Ruano, G.**, R. Prieto-Bermejo, T. L. Ramos, L. San-Segundo, L. I. Sanchez-Abarca, F. Sanchez-Guijo, J. A. Perez-Simon, J. Sanchez-Yague, M. Llanillo and A. Hernandez-Hernandez **(2015)**. "PTPN13 and beta-Catenin Regulate the Quiescence of Hematopoietic Stem Cells and Their Interaction with the Bone Marrow Niche." Stem Cell Reports 5(4): 516-531.

**Lowenberg, B.**, W. van Putten, M. Theobald, J. Gmur, L. Verdonck, P. Sonneveld, M. Fey, H. Schouten, G. de Greef, A. Ferrant, T. Kovacsovics, A. Gratwohl, S. Daenen, P. Huijgens, M. Boogaerts, G. Dutch-Belgian Hemato-Oncology Cooperative and R. Swiss Group for Clinical Cancer **(2003)**. "Effect of priming with granulocyte colony-stimulating factor on the outcome of chemotherapy for acute myeloid leukemia." N Engl J Med 349(8): 743-752.

**Lutz, C.**, V. T. Hoang, E. Buss and A. D. Ho **(2013)**. "Identifying leukemia stem cells--is it feasible and does it matter?" Cancer Lett 338(1): 10-14.

**Mai, H.**, X. Liu, Y. Chen, C. Li, L. Cao, X. Chen, S. Chen, G. Liu and F. Wen **(2016)**. "Hypermethylation of p15 gene associated with an inferior poor long-term outcome in childhood acute lymphoblastic leukemia." J Cancer Res Clin Oncol 142(2): 497-504.

**Mao, B.**, Z. Zhang and G. Wang **(2015)**. "BTG2: a rising star of tumor suppressors (review)." Int J Oncol 46(2): 459-464.

**Mao, J. H.**, I. J. Kim, D. Wu, J. Climent, H. C. Kang, R. DelRosario and A. Balmain **(2008)**. "FBXW7 targets mTOR for degradation and cooperates with PTEN in tumor suppression." Science 321(5895): 1499-1502.

**Marone, M.**, G. Scambia, G. Bonanno, S. Rutella, D. de Ritis, F. Guidi, G. Leone and L. Pierelli **(2002)**. "Transforming growth factor-beta1 transcriptionally activates CD34 and prevents induced differentiation of TF-1 cells in the absence of any cell-cycle effects." Leukemia 16(1): 94-105.

**Marroquin, C. E.**, L. Downey, H. Guo and P. C. Kuo **(2004)**. "Osteopontin increases CD44 expression and cell adhesion in RAW 264.7 murine leukemia cells." Immunol Lett 95(1): 109-112.

**Martelli, M. P.**, V. Pettirossi, C. Thiede, E. Bonifacio, F. Mezzasoma, D. Cecchini, R. Pacini, A. Tabarrini, R. Ciurnelli, I. Gionfriddo, N. Manes, R. Rossi, L. Giunchi, U. Oelschlagel, L. Brunetti, M. Gemei, M. Delia, G. Specchia, A. Liso, M. Di Ianni, F. Di Raimondo, F. Falzetti, L. Del Vecchio, M. F. Martelli and B. Falini **(2010)**. "CD34+ cells from AML with mutated NPM1 harbor cytoplasmic mutated nucleophosmin and generate leukemia in immunocompromised mice." Blood 116(19): 3907-3922.

**Massague, J. (2000)**. "How cells read TGF-beta signals." Nat Rev Mol Cell Biol 1(3): 169-178.

**Masuda, S.**, M. Li and J. C. Izpisua Belmonte **(2013)**. "Niche-less maintenance of HSCs by 2i." Cell Res 23(4): 458-459.

**Matsumoto, A.** and K. I. Nakayama **(2013).** "Role of key regulators of the cell cycle in maintenance of hematopoietic stem cells." Biochim Biophys Acta 1830(2): 2335-2344.

**Matsumoto, A.**, S. Takeishi, T. Kanie, E. Susaki, I. Onoyama, Y. Tateishi, K. Nakayama and K. I. Nakayama **(2011)**. "p57 is required for quiescence and maintenance of adult hematopoietic stem cells." Cell Stem Cell 9(3): 262-271.

**Matsunaga, T.**, N. Takemoto, T. Sato, R. Takimoto, I. Tanaka, A. Fujimi, T. Akiyama, H. Kuroda, Y. Kawano, M. Kobune, J. Kato, Y. Hirayama, S. Sakamaki, K. Kohda, K. Miyake and Y. Niitsu **(2003)**. "Interaction between leukemic-cell VLA-4 and stromal fibronectin is a decisive factor for minimal residual disease of acute myelogenous leukemia." Nat Med 9(9): 1158-1165.

**Mavrommatis, E.**, E. N. Fish and L. C. Platanias **(2013)**. "The schlafen family of proteins and their regulation by interferons." J Interferon Cytokine Res 33(4): 206-210.

**McCarthy, D. J.** and G. K. Smyth **(2009)**. "Testing significance relative to a fold-change threshold is a TREAT." Bioinformatics 25(6): 765-771.

**Megaptche, A. P.**, U. Erb, M. W. Buchler and M. Zoller **(2014)**. "CD44v10, osteopontin and lymphoma growth retardation by a CD44v10-specific antibody." Immunol Cell Biol 92(8): 709-720.

**Mendez-Ferrer, S.**, T. V. Michurina, F. Ferraro, A. R. Mazloom, B. D. Macarthur, S. A. Lira, D. T. Scadden, A. Ma'ayan, G. N. Enikolopov and P. S. Frenette **(2010)**. "Mesenchymal and haematopoietic stem cells form a unique bone marrow niche." Nature 466(7308): 829-834.

**Mi, Z.**, H. Guo and P. C. Kuo **(2009)**. "Identification of osteopontin-dependent signaling pathways in a mouse model of human breast cancer." BMC Res Notes 2: 119.

**Mi, Z.**, T. Oliver, H. Guo, C. Gao and P. C. Kuo **(2007)**. "Thrombin-cleaved COOH(-) terminal osteopontin peptide binds with cyclophilin C to CD147 in murine breast cancer cells." Cancer Res 67(9): 4088-4097.

**Miller, P. G.**, F. Al-Shahrour, K. A. Hartwell, L. P. Chu, M. Jaras, R. V. Puram, A. Puissant, K. P. Callahan, J. Ashton, M. E. McConkey, L. P. Poveromo, G. S. Cowley, M. G. Kharas, M. Labelle, S. Shterental, J. Fujisaki, L. Silberstein, G. Alexe, M. A. Al-Hajj, C. A. Shelton, S. A. Armstrong, D. E. Root, D. T. Scadden, R. O. Hynes, S. Mukherjee, K. Stegmaier, C. T. Jordan and B. L. Ebert **(2013)**. "In Vivo RNAi screening identifies a leukemia-specific dependence on integrin beta 3 signaling." Cancer Cell 24(1): 45-58.

**Moore, K. A.** and I. R. Lemischka **(2006)**. "Stem cells and their niches." Science 311(5769): 1880-1885.

**Morita, N.**, M. Yamamoto and T. Tanizawa **(2003)**. "Correlation of c-kit expression and cell cycle regulation by transforming growth factor-beta in CD34+ CD38- human bone marrow cells." Eur J Haematol 71(5): 351-358.

**Morrison, S. J.** and D. T. Scadden **(2014)**. "The bone marrow niche for haematopoietic stem cells." Nature 505(7483): 327-334.

**Mosna, F.** and M. Gottardi **(2016)**. "Stem Cell Modeling of Core Binding Factor Acute Myeloid Leukemia." Stem Cells Int 2016: 7625827.

**Muller, P.**, N. Asher, M. Heled, S. B. Cohen, A. Risch and D. Rund **(2008)**. "Polymorphisms in transporter and phase II metabolism genes as potential modifiers of the predisposition to and treatment outcome of de novo acute myeloid leukemia in Israeli ethnic groups." Leuk Res 32(6): 919-929.

**Naka, K.**, T. Hoshii, T. Muraguchi, Y. Tadokoro, T. Ooshio, Y. Kondo, S. Nakao, N. Motoyama and A. Hirao **(2010)**. "TGF-beta-FOXO signalling maintains leukaemia-initiating cells in chronic myeloid leukaemia." Nature 463(7281): 676-680.

**Nakada, D.**, T. L. Saunders and S. J. Morrison **(2010)**. "Lkb1 regulates cell cycle and energy metabolism in haematopoietic stem cells." Nature 468(7324): 653-658.

**Nakamura, S.**, L. Tan, Y. Nagata, T. Takemura, A. Asahina, D. Yokota, T. Yagyu, K. Shibata, S. Fujisawa and K. Ohnishi **(2013)**. "JmjC-domain containing histone demethylase 1B-mediated p15(Ink4b) suppression promotes the proliferation of leukemic progenitor cells through modulation of cell cycle progression in acute myeloid leukemia." Mol Carcinog 52(1): 57-69.

**Niikura, N.**, T. Sakatani, N. Arima, Y. Ohi, N. Honma, N. Kanomata, K. Yoshida, T. Kadoya, K. Tamaki, N. Kumaki, T. Iwamoto, T. Sugie and T. Moriya **(2016)**. "Assessment of the Ki67 labeling index: a Japanese validation ring study." Breast Cancer 23(1): 92-100.

**Nilsson, S. K.**, H. M. Johnston, G. A. Whitty, B. Williams, R. J. Webb, D. T. Denhardt, I. Bertoncello, L. J. Bendall, P. J. Simmons and D. N. Haylock **(2005)**. "Osteopontin, a key component of the hematopoietic stem cell niche and regulator of primitive hematopoietic progenitor cells." Blood 106(4): 1232-1239.

**Okabe, M.**, Y. Kunieda, M. Shoji, S. Nakane, M. Kurosawa, J. Tanaka, S. R. Hansen and M. Asaka **(1995)**. "Megakaryocytic differentiation of a leukemic cell line, MC3, by phorbol ester: induction of glycoprotein IIb/IIIa and effects on expression of IL-6, IL-6 receptor, mpl and GATA genes." Leuk Res 19(12): 933-943.

**Oki, T.**, K. Nishimura, J. Kitaura, K. Togami, A. Maehara, K. Izawa, A. Sakaue-Sawano, A. Niida, S. Miyano, H. Aburatani, H. Kiyonari, A. Miyawaki and T. Kitamura **(2014)**. "A novel cell-cycle-indicator, mVenus-p27K-, identifies quiescent cells and visualizes G0-G1 transition." Sci Rep 4: 4012.

**Onoyama, I.** and K. I. Nakayama **(2008)**. "Fbxw7 in cell cycle exit and stem cell maintenance: insight from gene-targeted mice." Cell Cycle 7(21): 3307-3313.

**Oyan, A. M.**, N. Anensen, T. H. Bo, L. Stordrange, I. Jonassen, O. Bruserud, K. H. Kalland and B. T. Gjertsen **(2009)**. "Genes of cell-cell interactions, chemotherapy detoxification and apoptosis are induced during chemotherapy of acute myeloid leukemia." BMC Cancer 9: 77.

**Pabst, C., A.** Bergeron, V. P. Lavallee, J. Yeh, P. Gendron, G. L. Norddahl, J. Krosl, I. Boivin, E. Deneault, J. Simard, S. Imren, G. Boucher, K. Eppert, T. Herold, S. K. Bohlander, K. Humphries, S. Lemieux, J. Hebert, G. Sauvageau and F. Barabe **(2016)**. "GPR56 identifies primary human acute myeloid leukemia cells with high repopulating potential in vivo." Blood 127(16): 2018-2027.

**Pabst, T.**, E. Vellenga, W. van Putten, H. C. Schouten, C. Graux, M. C. Vekemans, B. Biemond, P. Sonneveld, J. Passweg, L. Verdonck, M. C. Legdeur, M. Theobald, E. Jacky, M. Bargetzi, J. Maertens, G. J. Ossenkoppele, B. Lowenberg, G. Dutch-Belgian Hemato-Oncology Cooperative, A. M. L. S. G. German and R. Swiss Collaborative Group for Clinical Cancer **(2012)**. "Favorable effect of priming with granulocyte colony-stimulating factor in remission induction of acute myeloid leukemia restricted to dose escalation of cytarabine." Blood 119(23): 5367-5373.

**Pallis, M.**, F. Burrows, A. Whittall, N. Boddy, C. Seedhouse and N. Russell **(2013)**. "Efficacy of RNA polymerase II inhibitors in targeting dormant leukaemia cells." BMC Pharmacol Toxicol 14: 32.

**Pallis, M.**, T. Harvey and N. Russell **(2016)**. "Phenotypically Dormant and Immature Leukaemia Cells Display Increased Ribosomal Protein S6 Phosphorylation." PLoS One 11(3): e0151480.

**Pallis, M.**, J. Syan and N. H. Russell **(1999)**. "Flow cytometric chemosensitivity analysis of blasts from patients with acute myeloblastic leukemia and myelodysplastic syndromes: the use of 7AAD with antibodies to CD45 or CD34." Cytometry 37(4): 308-313.

**Pallisgaard, N.**, N. Clausen, H. Schroder and P. Hokland **(1999)**. "Rapid and sensitive minimal residual disease detection in acute leukemia by quantitative real-time RT-PCR exemplified by t(12;21) TEL-AML1 fusion transcript." Genes Chromosomes Cancer 26(4): 355-365.

**Papaemmanuil, E.**, H. Dohner and P. J. Campbell **(2016)**. "Genomic Classification in Acute Myeloid Leukemia." N Engl J Med 375(9): 900-901.

**Passegue, E.**, A. J. Wagers, S. Giuriato, W. C. Anderson and I. L. Weissman **(2005)**. "Global analysis of proliferation and cell cycle gene expression in the regulation of hematopoietic stem and progenitor cell fates." J Exp Med 202(11): 1599-1611.

**Patel, J. P.**, M. Gonen, M. E. Figueroa, H. Fernandez, Z. Sun, J. Racevskis, P. Van Vlierberghe, I. Dolgalev, S. Thomas, O. Aminova, K. Huberman, J. Cheng, A. Viale, N. D. Socci, A. Heguy, A. Cherry, G. Vance, R. R. Higgins, R. P. Ketterling, R. E. Gallagher, M. Litzow, M. R. van den Brink, H. M. Lazarus, J. M. Rowe, S. Luger, A. Ferrando, E. Paietta, M. S. Tallman, A. Melnick, O. Abdel-Wahab and R. L. Levine **(2012)**. "Prognostic relevance of integrated genetic profiling in acute myeloid leukemia." N Engl J Med 366(12): 1079-1089.

**Pawitan, Y.**, S. Michiels, S. Koscielny, A. Gusnanto and A. Ploner **(2005)**. "False discovery rate, sensitivity and sample size for microarray studies." Bioinformatics 21(13): 3017-3024.

**Pierelli, L.**, M. Marone, G. Bonanno, S. Rutella, D. de Ritis, S. Mancuso, G. Leone and G. Scambia **(2002)**. "Transforming growth factor-beta1 causes transcriptional activation of CD34 and preserves haematopoietic stem/progenitor cell activity." Br J Haematol 118(2): 627-637.

**Pierre-Louis, O.**, D. Clay, P. Brunet de la Grange, I. Blazsek, C. Desterke, B. Guerton, C. Blondeau, J. V. Malfuson, M. Prat, A. Bennaceur-Griscelli, J. J. Lataillade and M. C. Le Bousse-Kerdiles **(2009)**. "Dual SP/ALDH functionalities refine the human hematopoietic Lin-CD34+CD38- stem/progenitor cell compartment." Stem Cells 27(10): 2552-2562.

**Pietras, E. M.**, M. R. Warr and E. Passegue **(2011)**. "Cell cycle regulation in hematopoietic stem cells." J Cell Biol 195(5): 709-720.

**Polley, M. Y.**, S. C. Leung, D. Gao, M. G. Mastropasqua, L. A. Zabaglo, J. M. Bartlett, L. M. McShane, R. A. Enos, S. S. Badve, A. L. Bane, S. Borgquist, S. Fineberg, M. G. Lin, A. M. Gown, D. Grabau, C. Gutierrez, J. C. Hugh, T. Moriya, Y. Ohi, C. K. Osborne, F. M. Penault-Llorca, T. Piper, P. L. Porter, T. Sakatani, R. Salgado, J. Starczynski, A. V. Laenkholm, G. Viale, M. Dowsett, D. F. Hayes and T. O. Nielsen **(2015)**. "An international study to increase concordance in Ki67 scoring." Mod Pathol 28(6): 778-786.

**Powell, J. A.**, D. Thomas, E. F. Barry, C. H. Kok, B. J. McClure, A. Tsykin, L. B. To, A. Brown, I. D. Lewis, K. Herbert, G. J. Goodall, T. P. Speed, N. Asou, B. Jacob, M. Osato, D. N. Haylock, S. K. Nilsson, R. J. D'Andrea, A. F. Lopez and M. A. Guthridge **(2009)**. "Expression profiling of a hemopoietic cell survival transcriptome implicates osteopontin as a functional prognostic factor in AML." Blood 114(23): 4859-4870.

**Provan D**, G. T., Dokal I and Vos J **(2015)**. Oxford handbook of Clinical Haematology, Oxford Universuty Press.

**Psaila, B.**, R. N. Kaplan, E. R. Port and D. Lyden **(2006)**. "Priming the 'soil' for breast cancer metastasis: the pre-metastatic niche." Breast Dis 26: 65-74.

**Puck, A.**, R. Aigner, M. Modak, P. Cejka, D. Blaas and J. Stockl **(2015)**. "Expression and regulation of Schlafen (SLFN) family members in primary human monocytes, monocyte-derived dendritic cells and T cells." Results Immunol 5: 23-32.

**Quesnel, B. (2013)**. "Tumor dormancy: long-term survival in a hostile environment." Adv Exp Med Biol 734: 181-200.

**Raha, D.**, T. R. Wilson, J. Peng, D. Peterson, P. Yue, M. Evangelista, C. Wilson, M. Merchant and J. Settleman **(2014)**. "The cancer stem cell marker aldehyde dehydrogenase is required to maintain a drug-tolerant tumor cell subpopulation." Cancer Res 74(13): 3579-3590.

**Riether, C.**, C. M. Schurch and A. F. Ochsenbein **(2015)**. "Regulation of hematopoietic and leukemic stem cells by the immune system." Cell Death Differ 22(2): 187-198.

**Ringner, M. (2008)**. "What is principal component analysis?" Nat Biotechnol 26(3): 303-304.

**Rohr, J.**, S. Guo, J. Huo, A. Bouska, C. Lachel, Y. Li, P. D. Simone, W. Zhang, Q. Gong, C. Wang, A. Cannon, T. Heavican, A. Mottok, S. Hung, A. Rosenwald, R. Gascoyne, K. Fu, T. C. Greiner, D. D. Weisenburger, J. M. Vose, L. M. Staudt, W. Xiao, G. E. Borgstahl, S. Davis, C. Steidl, T. McKeithan, J. Iqbal and W. C. Chan **(2016)**. "Recurrent activating mutations of CD28 in peripheral T-cell lymphomas." Leukemia 30(5): 1062-1070.

**Ruscetti, F. W.**, S. Akel and S. H. Bartelmez **(2005)**. "Autocrine transforming growth factor-beta regulation of hematopoiesis: many outcomes that depend on the context." Oncogene 24(37): 5751-5763.

**Russell, N. H. (1992)**. "Autocrine growth factors and leukaemic haemopoiesis." Blood Rev 6(3): 149-156.

**Sadasivam, S.** and J. A. DeCaprio **(2013)**. "The DREAM complex: master coordinator of cell cycle-dependent gene expression." Nat Rev Cancer 13(8): 585-595.

**Saito, Y.**, H. Kitamura, A. Hijikata, M. Tomizawa-Murasawa, S. Tanaka, S. Takagi, N. Uchida, N. Suzuki, A. Sone, Y. Najima, H. Ozawa, A. Wake, S. Taniguchi, L. D. Shultz, O. Ohara and F. Ishikawa **(2010)**. "Identification of therapeutic targets for quiescent, chemotherapy-resistant human leukemia stem cells." Sci Transl Med 2(17): 17ra19.

**Saito, Y.** and K. Morishita **(2015)**. "[Maintenance of leukemic and normal hematopoietic stem cells in bone marrow niches by EVI1-regulated GPR56]." Rinsho Ketsueki 56(4): 375-383.

**Sakoe, Y.**, K. Sakoe, K. Kirito, K. Ozawa and N. Komatsu **(2010)**. "FOXO3A as a key molecule for all-trans retinoic acid-induced granulocytic differentiation and apoptosis in acute promyelocytic leukemia." Blood 115(18): 3787-3795.

**Scandura, J. M.**, P. Boccuni, J. Massague and S. D. Nimer **(2004)**. "Transforming growth factor beta-induced cell cycle arrest of human hematopoietic cells requires p57KIP2 up-regulation." Proc Natl Acad Sci U S A 101(42): 15231-15236.

**Schepers, K.**, T. B. Campbell and E. Passegue **(2015)**. "Normal and leukemic stem cell niches: insights and therapeutic opportunities." Cell Stem Cell 16(3): 254-267.

**Schmid, I. (2007)**. "Combined Flow Cytometric Measurement of Two Cell-Surface Antigens and DNA-RNA Content." CSH Protoc 2007: pdb prot4895.

**Schmidt, M.**, S. Fernandez de Mattos, A. van der Horst, R. Klompmaker, G. J. Kops, E. W. Lam, B. M. Burgering and R. H. Medema **(2002)**. "Cell cycle inhibition by FoxO forkhead transcription factors involves downregulation of cyclin D." Mol Cell Biol 22(22): 7842-7852.

**Scholz, G.**, C. Jandus, L. Zhang, C. Grandclement, I. C. Lopez-Mejia, C. Soneson, M. Delorenzi, L. Fajas, W. Held, O. Dormond and P. Romero **(2016)**. "Modulation of mTOR Signalling Triggers the Formation of Stem Cell-like Memory T Cells." EBioMedicine 4: 50-61.

**Scholzen, T.** and J. Gerdes **(2000)**. "The Ki-67 protein: from the known and the unknown." J Cell Physiol 182(3): 311-322.

**Seedhouse, C. H.**, M. Grundy, P. White, Y. Li, J. Fisher, D. Yakunina, A. V. Moorman, T. Hoy, N. Russell, A. Burnett, M. Pallis and N. National Cancer Research **(2007)**. "Sequential influences of leukemia-specific and genetic factors on p-glycoprotein expression in blasts from 817 patients entered into the National Cancer Research Network acute myeloid leukemia 14 and 15 trials." Clin Cancer Res 13(23): 7059-7066.

**Seedhouse, C. H.**, K. I. Mills, S. Ahluwalia, M. Grundy, S. Shang, A. K. Burnett, N. H. Russell and M. Pallis **(2014)**. "Distinct poor prognostic subgroups of acute myeloid leukaemia, FLT3-ITD and P-glycoprotein-positive, have contrasting levels of FOXO1." Leuk Res 38(1): 131-137.

**Shi, Y.** and J. Massague **(2003)**. "Mechanisms of TGF-beta signaling from cell membrane to the nucleus." Cell 113(6): 685-700.

**Shimobayashi, M.** and M. N. Hall **(2014)**. "Making new contacts: the mTOR network in metabolism and signalling crosstalk." Nat Rev Mol Cell Biol 15(3): 155-162.

**Shinohara, M. L.**, H. J. Kim, J. H. Kim, V. A. Garcia and H. Cantor **(2008)**. "Alternative translation of osteopontin generates intracellular and secreted isoforms that mediate distinct biological activities in dendritic cells." Proc Natl Acad Sci U S A 105(20): 7235-7239.

**Shinohara, M. L.**, J. H. Kim, V. A. Garcia and H. Cantor **(2008)**. "Engagement of the type I interferon receptor on dendritic cells inhibits T helper 17 cell development: role of intracellular osteopontin." Immunity 29(1): 68-78.

**Siitonen, T.**, P. Alaruikka, P. Mantymaa, E. R. Savolainen, T. J. Kavanagh, C. M. Krejsa, C. C. Franklin, V. Kinnula and P. Koistinen **(1999)**. "Protection of acute myeloblastic leukemia cells against apoptotic cell death by high glutathione and gamma-glutamylcysteine synthetase levels during etoposide-induced oxidative stress." Ann Oncol 10(11): 1361-1367.

**Silberstein, L. E.** and C. P. Lin **(2013)**. "A new image of the hematopoietic stem cell vascular niche." Cell Stem Cell 13(5): 514-516.

**Singh, V.**, U. Erb and M. Zoller **(2013)**. "Cooperativity of CD44 and CD49d in leukemia cell homing, migration, and survival offers a means for therapeutic attack." J Immunol 191(10): 5304-5316.

**Sodek, J.**, J. Chen, T. Nagata, S. Kasugai, R. Todescan, Jr., I. W. Li and R. H. Kim **(1995)**. "Regulation of osteopontin expression in osteoblasts." Ann N Y Acad Sci 760: 223-241.

**Sosa, M. S.**, P. Bragado and J. A. Aguirre-Ghiso **(2014)**. "Mechanisms of disseminated cancer cell dormancy: an awakening field." Nat Rev Cancer 14(9): 611-622.

**Sperling, A. S.**, C. J. Gibson and B. L. Ebert **(2017)**. "The genetics of myelodysplastic syndrome: from clonal haematopoiesis to secondary leukaemia." Nat Rev Cancer 17(1): 5-19.

**Steensma, D. P.**, R. Bejar, S. Jaiswal, R. C. Lindsley, M. A. Sekeres, R. P. Hasserjian and B. L. Ebert **(2015)**. "Clonal hematopoiesis of indeterminate potential and its distinction from myelodysplastic syndromes." Blood 126(1): 9-16.

**Stiehl, T.**, N. Baran, A. D. Ho and A. Marciniak-Czochra **(2015)**. "Cell division patterns in acute myeloid leukemia stem-like cells determine clinical course: a model to predict patient survival." Cancer Res 75(6): 940-949.

**Stier, S.**, Y. Ko, R. Forkert, C. Lutz, T. Neuhaus, E. Grunewald, T. Cheng, D. Dombkowski, L. M. Calvi, S. R. Rittling and D. T. Scadden **(2005)**. "Osteopontin is a hematopoietic stem cell niche component that negatively regulates stem cell pool size." J Exp Med 201(11): 1781-1791.

**Subramaniam, S.**, P. Sreenivas, S. Cheedipudi, V. R. Reddy, L. S. Shashidhara, R. K. Chilukoti, M. Mylavarapu and J. Dhawan **(2014)**. "Distinct transcriptional networks in quiescent myoblasts: a role for Wnt signaling in reversible vs. irreversible arrest." PLoS One 8(6): e65097.

**Suda, T.**, K. Takubo and G. L. Semenza **(2011)**. "Metabolic regulation of hematopoietic stem cells in the hypoxic niche." Cell Stem Cell 9(4): 298-310.

**Sugiyama, T.**, H. Kohara, M. Noda and T. Nagasawa **(2006)**. "Maintenance of the hematopoietic stem cell pool by CXCL12-CXCR4 chemokine signaling in bone marrow stromal cell niches." Immunity 25(6): 977-988.

**Sundararajan, V.**, N. Gengenbacher, M. P. Stemmler, J. A. Kleemann, T. Brabletz and S. Brabletz **(2015)**. "The ZEB1/miR-200c feedback loop regulates invasion via actin interacting proteins MYLK and TKS5." Oncotarget 6(29): 27083-27096.

**Sutherland, H. J.**, A. Blair and R. W. Zapf **(1996)**. "Characterization of a hierarchy in human acute myeloid leukemia progenitor cells." Blood 87(11): 4754-4761.

**Szmigielska-Kaplon, A.**, J. Szemraj, K. Hamara, M. Robak, A. Wolska, A. Pluta, M. Czemerska, A. Krawczynska, K. Jamroziak, K. Szmigielska, T. Robak and A. Wierzbowska **(2014)**. "Polymorphism of CD44 influences the efficacy of CD34(+) cells mobilization in patients with hematological malignancies." Biol Blood Marrow Transplant 20(7): 986-991.

**Tabe, Y.**, Y. X. Shi, Z. Zeng, L. Jin, M. Shikami, Y. Hatanaka, T. Miida, F. J. Hsu, M. Andreeff and M. Konopleva **(2013)**. "TGF-beta-Neutralizing Antibody 1D11 Enhances Cytarabine-Induced Apoptosis in AML Cells in the Bone Marrow Microenvironment." PLoS One 8(6): e62785.

**Taussig, D. C.**, J. Vargaftig, F. Miraki-Moud, E. Griessinger, K. Sharrock, T. Luke, D. Lillington, H. Oakervee, J. Cavenagh, S. G. Agrawal, T. A. Lister, J. G. Gribben and D. Bonnet **(2010)**. "Leukemia-initiating cells from some acute myeloid leukemia patients with mutated nucleophosmin reside in the CD34(-) fraction." Blood 115(10): 1976-1984.

**Tesio, M.** and A. Trumpp **(2011)**. "Breaking the cell cycle of HSCs by p57 and friends." Cell Stem Cell 9(3): 187-192.

**Thepot, S.**, E. Lainey, T. Cluzeau, M. Sebert, C. Leroy, L. Ades, M. Tailler, L. Galluzzi, F. Baran-Marszak, H. Roudot, V. Eclache, C. Gardin, S. de Botton, P. Auberger, P. Fenaux, G. Kroemer and S. Boehrer **(2011)**. "Hypomethylating agents reactivate FOXO3A in acute myeloid leukemia." Cell Cycle 10(14): 2323-2330.

**Tijchon, E.**, L. van Emst, L. Yuniati, D. van Ingen Schenau, J. Havinga, J. P. Rouault, P. M. Hoogerbrugge, F. N. van Leeuwen and B. Scheijen **(2016)**. "Tumor suppressors BTG1 and BTG2 regulate early mouse B-cell development." Haematologica 101(7): e272-276.

**Tomita, H.**, K. Tanaka, T. Tanaka and A. Hara **(2016)**. "Aldehyde dehydrogenase 1A1 in stem cells and cancer." Oncotarget 7(10): 11018-11032.

**Venezia, T. A.**, A. A. Merchant, C. A. Ramos, N. L. Whitehouse, A. S. Young, C. A. Shaw and M. A. Goodell **(2004)**. "Molecular signatures of proliferation and quiescence in hematopoietic stem cells." PLoS Biol 2(10): e301.

**Verhagen, H. J.**, M. A. Smit, A. Rutten, F. Denkers, P. J. Poddighe, P. A. Merle, G. J. Ossenkoppele and L. Smit **(2016)**. "Primary acute myeloid leukemia cells with overexpression of EVI-1 are sensitive to all-trans retinoic acid." Blood 127(4): 458-463.

**Viny, A. D.** and R. L. Levine **(2016)**. "Roads Diverge--A Robert Frost View of Leukemia Development." N Engl J Med 374(23): 2282-2284.

**Vock, E. H.**, W. K. Lutz, P. Hormes, H. D. Hoffmann and S. Vamvakas **(1998)**. "Discrimination between genotoxicity and cytotoxicity in the induction of DNA double-strand breaks in cells treated with etoposide, melphalan, cisplatin, potassium cyanide, Triton X-100, and gamma-irradiation." Mutat Res 413(1): 83-94.

**Warr, M. R.**, M. Binnewies, J. Flach, D. Reynaud, T. Garg, R. Malhotra, J. Debnath and E. Passegue **(2013)**. "FOXO3A directs a protective autophagy program in haematopoietic stem cells." Nature 494(7437): 323-327.

**Watanabe, R.**, Y. Harada, K. Takeda, J. Takahashi, K. Ohnuki, S. Ogawa, D. Ohgai, N. Kaibara, O. Koiwai, K. Tanabe, H. Toma, K. Sugamura and R. Abe **(2006)**. "Grb2 and Gads exhibit different interactions with CD28 and play distinct roles in CD28-mediated costimulation." J Immunol 177(2): 1085-1091.

**Wei, W.**, Y. Yang, J. Cai, K. Cui, R. X. Li, H. Wang, X. Shang and D. Wei **(2016)**. "MiR-30a-5p Suppresses Tumor Metastasis of Human Colorectal Cancer by Targeting ITGB3." Cell Physiol Biochem 39(3): 1165-1176.

**Welch, J. S.** and D. C. Link **(2011)**. "Genomics of AML: clinical applications of next-generation sequencing." Hematology Am Soc Hematol Educ Program 2011: 30-35.

**Wiel, C.**, B. Gras, D. Vindrieux, M. Warnier, D. Gitenay, B. Le Calve, M. Ferrand, A. Augert and D. Bernard **(2016)**. "Multidrug resistance protein 3 loss promotes tumor formation by inducing senescence escape." Oncogene 35(12): 1596-1601.

**Wilson, A.** and A. Trumpp **(2006)**. "Bone-marrow haematopoietic-stem-cell niches." Nat Rev Immunol 6(2): 93-106.

**Winkler, I. G.**, V. Barbier, B. Nowlan, R. N. Jacobsen, C. E. Forristal, J. T. Patton, J. L. Magnani and J. P. Levesque **(2012)**. "Vascular niche E-selectin regulates hematopoietic stem cell dormancy, self renewal and chemoresistance." Nat Med 18(11): 1651-1657.

**Winkler, I. G.**, V. Barbier, R. Wadley, A. C. Zannettino, S. Williams and J. P. Levesque **(2010)**. "Positioning of bone marrow hematopoietic and stromal cells relative to blood flow in vivo: serially reconstituting hematopoietic stem cells reside in distinct nonperfused niches." Blood 116(3): 375-385.

**Won, E. J.**, H. R. Kim, R. Y. Park, S. Y. Choi, J. H. Shin, S. P. Suh, D. W. Ryang, M. Szardenings and M. G. Shin **(2015)**. "Direct confirmation of quiescence of CD34+CD38- leukemia stem cell populations using single cell culture, their molecular signature and clinicopathological implications." BMC Cancer 15: 217.

**Wright, N. A. (2012)**. "Stem cell identification--in vivo lineage analysis versus in vitro isolation and clonal expansion." J Pathol 227(3): 255-266.

**Xiao, S.**, D. Li, H. Q. Zhu, M. G. Song, X. R. Pan, P. M. Jia, L. L. Peng, A. X. Dou, G. Q. Chen, S. J. Chen, Z. Chen and J. H. Tong **(2006)**. "RIG-G as a key mediator of the antiproliferative activity of interferon-related pathways through enhancing p21 and p27 proteins." Proc Natl Acad Sci U S A 103(44): 16448-16453.

**Xu, S. P.**, G. P. Sun, Y. X. Shen, W. R. Peng, H. Wang and W. Wei **(2007)**. "Synergistic effect of combining paeonol and cisplatin on apoptotic induction of human hepatoma cell lines." Acta Pharmacol Sin 28(6): 869-878.

**Xu, Y.**, Y. Tabe, L. Jin, J. Watt, T. McQueen, A. Ohsaka, M. Andreeff and M. Konopleva **(2008)**. "TGF-beta receptor kinase inhibitor LY2109761 reverses the anti-apoptotic effects of TGF-beta1 in myelo-monocytic leukaemic cells co-cultured with stromal cells." Br J Haematol 142(2): 192-201.

**Yamazaki, S.**, H. Ema, G. Karlsson, T. Yamaguchi, H. Miyoshi, S. Shioda, M. M. Taketo, S. Karlsson, A. Iwama and H. Nakauchi **(2011)**. "Nonmyelinating Schwann cells maintain hematopoietic stem cell hibernation in the bone marrow niche." Cell 147(5): 1146-1158.

**Yamazaki, S.**, A. Iwama, Y. Morita, K. Eto, H. Ema and H. Nakauchi **(2007)**. "Cytokine signaling, lipid raft clustering, and HSC hibernation." Ann N Y Acad Sci 1106: 54-63.

**Yamazaki, S.**, A. Iwama, S. Takayanagi, K. Eto, H. Ema and H. Nakauchi **(2009)**. "TGF-beta as a candidate bone marrow niche signal to induce hematopoietic stem cell hibernation." Blood 113(6): 1250-1256.

**Yamazaki, S.**, A. Iwama, S. Takayanagi, Y. Morita, K. Eto, H. Ema and H. Nakauchi **(2006)**. "Cytokine signals modulated via lipid rafts mimic niche signals and induce hibernation in hematopoietic stem cells." EMBO J 25(15): 3515-3523.

**Yi, H.**, D. Zeng, Z. Shen, J. Liao, X. Wang, Y. Liu, X. Zhang and P. Kong **(2016)**. "Integrin alphavbeta3 enhances beta-catenin signaling in acute myeloid leukemia harboring Fms-like tyrosine kinase-3 internal tandem duplication mutations: implications for microenvironment influence on sorafenib sensitivity." Oncotarget 7(26): 40387-40397.

**Yu, M.**, J. H. Tong, M. Mao, L. X. Kan, M. M. Liu, Y. W. Sun, G. Fu, Y. K. Jing, L. Yu, D. Lepaslier, M. Lanotte, Z. Y. Wang, Z. Chen, S. Waxman, Y. X. Wang, J. Z. Tan and S. J. Chen **(1997)**. "Cloning of a gene (RIG-G) associated with retinoic acid-induced differentiation of acute promyelocytic leukemia cells and representing a new member of a family of interferon-stimulated genes." Proc Natl Acad Sci U S A 94(14): 7406-7411.

**Zanjani, E. D.**, G. Almeida-Porada, A. G. Livingston, A. W. Flake and M. Ogawa (1998). "Human bone marrow CD34- cells engraft in vivo and undergo multilineage expression that includes giving rise to CD34+ cells." Exp Hematol 26(4): 353-360.

**Zhang, E. Y.**, B. L. Parker and T. M. Yankee **(2011)**. "Gads regulates the expansion phase of CD8+ T cell-mediated immunity." J Immunol 186(8): 4579-4589.

**Zhang, J.**, C. Niu, L. Ye, H. Huang, X. He, W. G. Tong, J. Ross, J. Haug, T. Johnson, J. Q. Feng, S. Harris, L. M. Wiedemann, Y. Mishina and L. Li **(2003)**. "Identification of the haematopoietic stem cell niche and control of the niche size." Nature 425(6960): 836-841.

**Zhang, J.**, C. S. Seet, C. Sun, J. Li, D. You, A. Volk, P. Breslin, X. Li, W. Wei, Z. Qian, N. J. Zeleznik-Le, Z. Zhang and J. Zhang **(2013)**. "p27kip1 maintains a subset of leukemia stem cells in the quiescent state in murine MLL-leukemia." Mol Oncol 7(6): 1069-1082.

**Zhao, K.**, M. Zhang, L. Zhang, P. Wang, G. Song, B. Liu, H. Wu, Z. Yin and C. Gao **(2016)**. "Intracellular osteopontin stabilizes TRAF3 to positively regulate innate antiviral response." Sci Rep 6: 23771.

**Zhao, M.**, J. M. Perry, H. Marshall, A. Venkatraman, P. Qian, X. C. He, J. Ahamed and L. Li **(2014)**. "Megakaryocytes maintain homeostatic quiescence and promote post-injury regeneration of hematopoietic stem cells." Nat Med 20(11): 1321-1326.

**Zhou, T.**, J. W. Chou, D. A. Simpson, Y. Zhou, T. E. Mullen, M. Medeiros, P. R. Bushel, R. S. Paules, X. Yang, P. Hurban, E. K. Lobenhofer and W. K. Kaufmann **(2006)**. "Profiles of global gene expression in ionizing-radiation-damaged human diploid fibroblasts reveal synchronization behind the G1 checkpoint in a G0-like state of quiescence." Environ Health Perspect 114(4): 553-559.

**Zhu, B.**, K. Suzuki, H. A. Goldberg, S. R. Rittling, D. T. Denhardt, C. A. McCulloch and J. Sodek **(2004)**. "Osteopontin modulates CD44-dependent chemotaxis of peritoneal macrophages through G-protein-coupled receptors: evidence of a role for an intracellular form of osteopontin." J Cell Physiol 198(1): 155-167.

**Zhu, Z.**, Y. Liu, K. Li, J. Liu, H. Wang, B. Sun, Z. Xiong, H. Jiang, J. Zheng and Z. Hu **(2014)**. "Protein tyrosine phosphatase receptor U (PTPRU) is required for glioma growth and motility." Carcinogenesis 35(8): 1901-1910.

**Zohar, R.**, N. Suzuki, K. Suzuki, P. Arora, M. Glogauer, C. A. McCulloch and J. Sodek **(2000)**. "Intracellular osteopontin is an integral component of the CD44-ERM complex involved in cell migration." J Cell Physiol 184(1): 118-130.

**Zoller, M. (2015)**. "CD44, Hyaluronan, the Hematopoietic Stem Cell, and Leukemia-Initiating Cells." Front Immunol 6: 235.

**Zoller, M.**, N. Fohr and K. Herrmann **(1998)**. "Treatment of mice with anti-CD44 after allogeneic bone marrow cell transplantation is lethal." J Leukoc Biol 63(2): 175-189.

**Zoncu, R.**, A. Efeyan and D. M. Sabatini **(2011)**. "mTOR: from growth signal integration to cancer, diabetes and ageing." Nat Rev Mol Cell Biol 12(1): 21-35.

**Zou, P.**, H. Yoshihara, K. Hosokawa, I. Tai, K. Shinmyozu, F. Tsukahara, Y. Maru, K. Nakayama, K. I. Nakayama and T. Suda **(2011)**. "p57(Kip2) and p27(Kip1) cooperate to maintain hematopoietic stem cell quiescence through interactions with Hsc70." Cell Stem Cell 9(3): 247-261.

# APPENDICES

# Appendix A1: Immunohistochemistry protocol

## (Protocol for IHC of human bone marrow biopsy (FFPE) sections)

## Procedure:

**Notes: Do not allow sections to dry at any stage of the procedure.**

**Heat slides on a hot plate at $60^0$C for 10 min and then allow for cooling at RT to improve adherence.**

Day One:

**De-paraffinization and rehydration of tissue section**

| | | |
|---|---|---|
| 1- | Dewax in xylene | 5min.s |
| 2- | Dewax in xylene | 5min.s |
| 3- | Rehydrate in 100% ethanol | 5min.s |
| 4- | Rehydrate in 90% ethanol | 5min.s |
| 5- | Rehydrate in 70% ethanol | 5min.s |
| 6- | dH2O | 3min |
| 7- | TBS | 3min |

**Antigen retrieval**

1. Pre-heat water bath with plastic staining dish containing Sodium Citrate Buffer until temperature reaches 95-100 °C.
2. Immerse slides in the staining dish. Place the lid loosely on the staining dish and incubate for 20 min (optimal incubation time should be determined by the user).
3. Turn off water bath and remove the staining dish to room temperature and allow the slides to cool for 10-20 min in running tap water.
4. Rinse sections in TBS for 2x3 min.

*Transfer slides to the staining tray/ humid chamber. Carefully wipe around the tissue section to remove excess buffer and then surround the tissue with barrier pen wait till the marker completely dry (avoid drying of the tissue) apply TBS to cover the tissue.*

**Endogenous peroxidase block**

1. Treat slides with 3% Hydrogen Peroxide for 10 min at RT.
2. Wash in TBS 2x5

**Immunostaining**

Apply 100-500µl diluted Primary Antibody (diluted in **1%BSA in TBS**) to relevant slides and apply the same volume of the AB diluent (**1%BSA in TBS)** to the Negative Control slides. Incubate overnight in the cold room.

Day Two:

1. Wash in TBS 2 x 5.
2. If using **mouse** primary antibodies. Apply 2 or 3 drops of the Mach 4 Mouse Probe solution **(Yellow)** to each slide. Treat ALL slides and incubate for **30 min**. If using rabbit primary antibodies omit this step.
3. Wash in TBS 2 x 5.
4. Apply 2 or 3 drops of Mach 4 HR Polymer solution **(Orange)** to each slide. Treat ALL slides and incubate for **30 min**. *If using rabbit primaries, incubate for 60 min.*
5. Prepare DAB working solution, 1:20 dilution by adding 1 drop DAB per 20-30 drops buffer (abcam ab94665) (keep dark on the ice and used within 6 hours).
6. Wash all slides in TBS 2 x 5.
7. Apply DAB Working solution to ALL slides (at the same time) and notice brownish colour developing up to 5 min.
8. Wash all slides at the same time in TBS 2 x 5.
9. Apply dH2O for 3 min.
10. Sink in Haematoxylin for 3 min. (Mayer's haematoxylin).
11. Transfer into a tap water bath and agitate for a few seconds to remove excess dye. Then rinse thoroughly with tap water (avoid directing water stream onto the tissue sections).

**Dehydration and mounting of tissue section**

1. dH2O 5min
2. Rehydrate in 70% ethanol 5min
3. Rehydrate in 90% ethanol 5min
4. Rehydrate in 100% ethanol 5min
5. xylene 5min
6. xylene 5min
7. Mount sections in DPX and cover with appropriate cover slide, avoid bubbles formation and allow drying completely at RT.

**Buffers Preparation:**

1- TBS (1X) pH 7.6:

Sodium Chloride 8 g

TRIS 2.42 g

dH2O 1000 ml

Dissolve completely then adjust pH using 1N HCL to 7.6

2- Acidic Ag Retrieval Buffer:

Sodium Citrate Buffer (10mM Sodium Citrate, 0.05% Tween 20, pH 6.0):

Tri-sodium citrate (dihydrate) --------- 2.94 g

Distilled water ---------- 1000 ml

Mix to dissolve. Adjust pH to 6.0 with 1N HCl and then add 0.5 ml of Tween 20 and mix well. Store this solution at room temperature for 3 months or at 4 C (cold room) for longer storage.

3- Alkaline Ag Retrieval Buffer:

Tris-EDTA Buffer (10mM Tris Base, 1mM EDTA Solution, 0.05 Tween 20, PH 9.0):

TRIS----------1.21 g

EDTA----------0.37 g

dH2O----------1000 ml

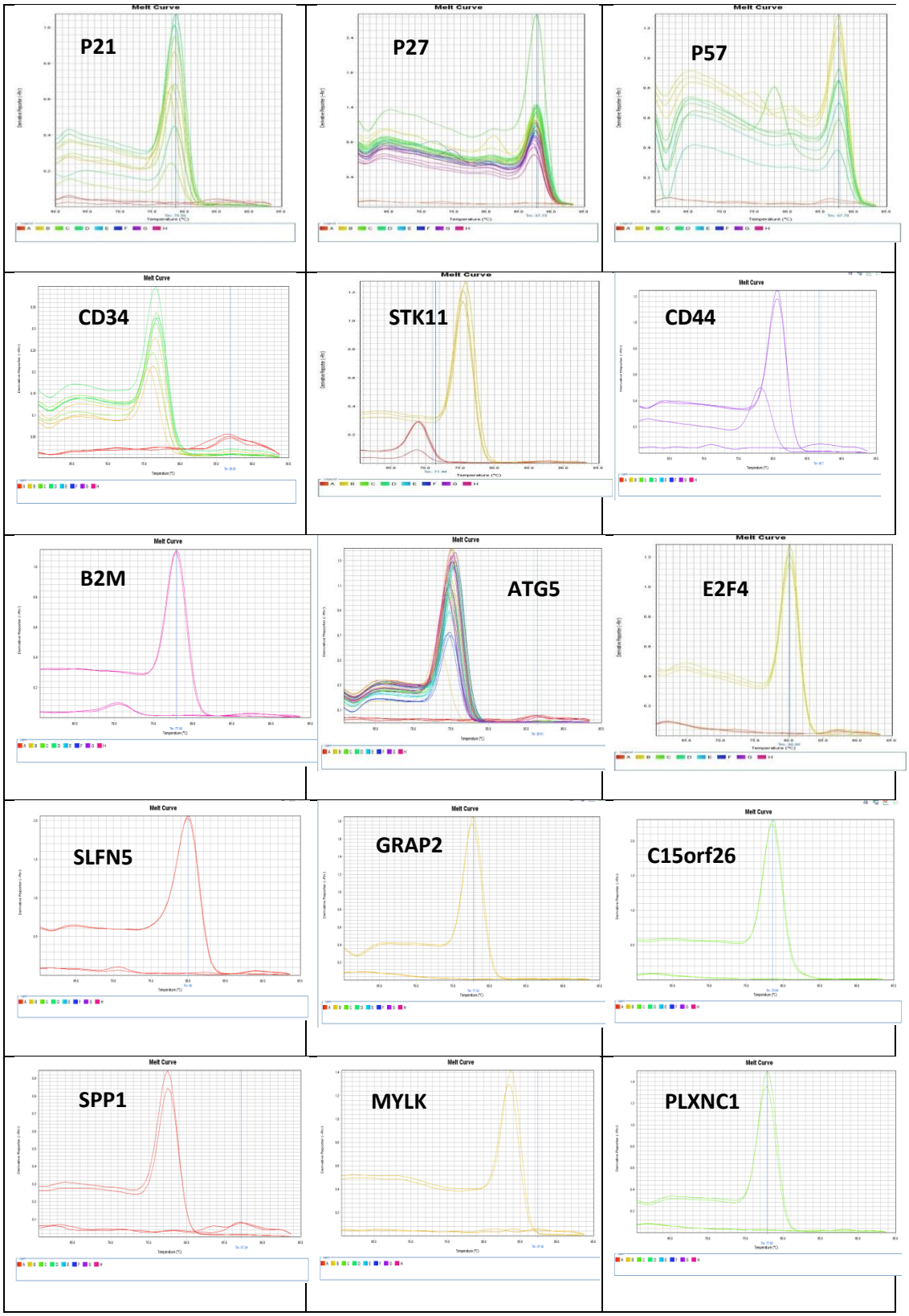
Mix to dissolve, pH usually 9.0. Then add 0.5 ml of Tween 20 and mix well. Store this solution at room temperature for 3 months or at 4 C (cold room) for longer storage.

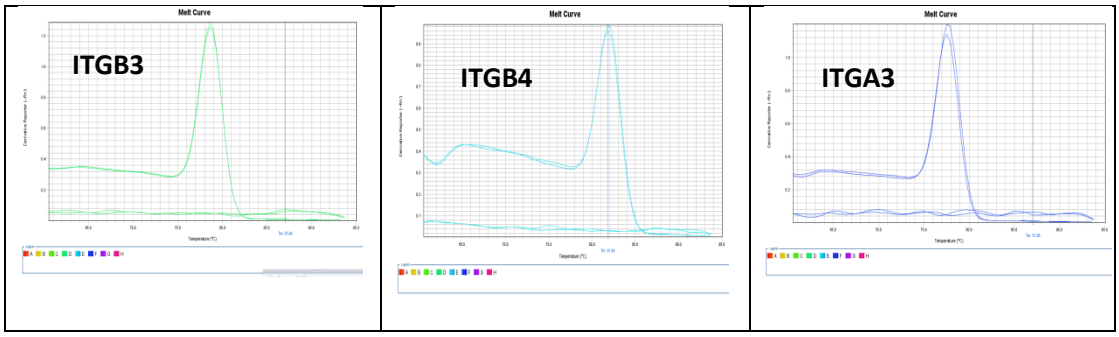
4- 1% BSA in TBS (0.1g BSA dissolved completely in 10ml TBS).

## Appendix A2: List of qPCR primers

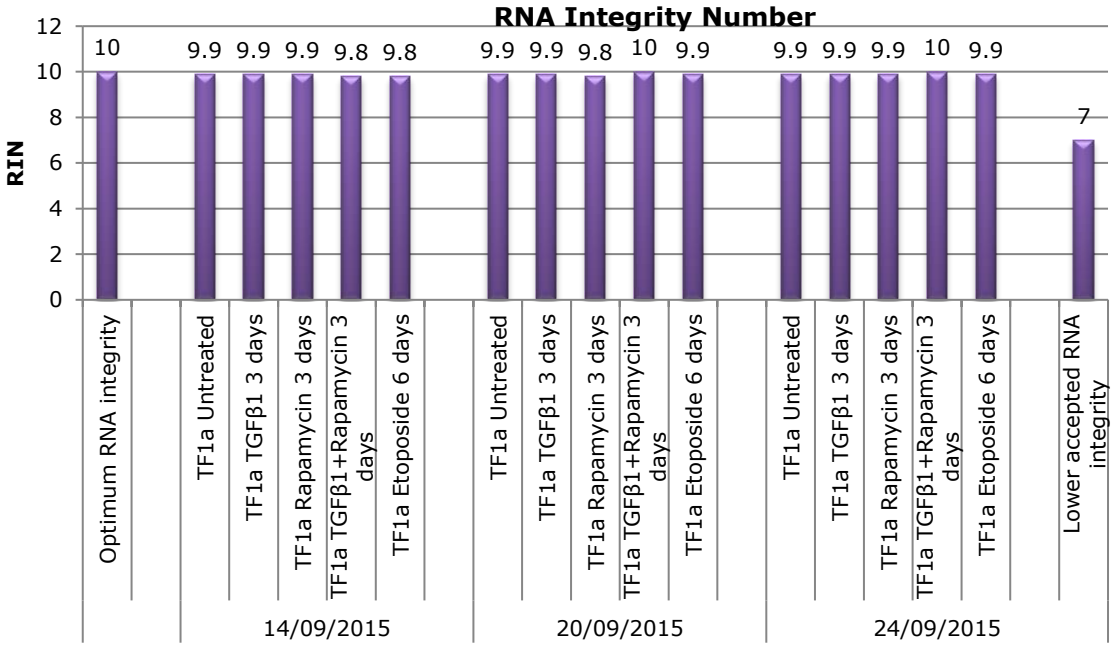
| Target Gene (Transcript) | Qiagen Cat. No. or Primer Sequence | | Product size in bp | Exon/Exon Junction(primer) | Supplier |
|---|---|---|---|---|---|
| P21/CDKN1A | QT00062090 | | 79 | N/A | Qiagen |
| P27/CDKN1B | QT00998445 | | 146 | N/A | Qiagen |
| P57/CDKN1C | QT00018018 | | 146 | N/A | Qiagen |
| CD34 | QT00056497 | | 106 | N/A | Qiagen |
| LKB1/STK11 | QT01008980 | | 91 | N/A | Qiagen |
| BTG2 | QT00240247 | | 84 | N/A | Qiagen |
| E2F4 | QT02308593 | | 109 | N/A | Qiagen |
| ATG5 | QT00073325 | | 105 | N/A | Qiagen |
| β2-microglobulin | F | 5′-GAGTATGCCTGCCGTGTG-3′ | 110 | N/A | Invitrogen |
| | R | 5′-AATCCAAATGCGGCATCT-3′ | | | |
| SPP1(NM_001251830) | F | 5′-AGTTCTGAGGAAAAGCAGCACT-3′ | 102 | 258/259(F) | Invitrogen |
| | R | 5′-GTCCAAGCTTCTGGGGACAA-3′ | | | |
| MYLK(NM_053025) | F | 5′-CTGGCTCCCATTACCTCTGC-3′ | 127 | 1798/1799(R) | Invitrogen |
| | R | 5′-ACGGCAAGCCTTTCCACTTG-3′ | | | |
| PLXNC1(NM_005761) | F | 5′-GAGATACGTGACGGCTTTGCT-3′ | 134 | 3232/3233(F) | Invitrogen |
| | R | 5′-TGGGTGAAGCCACCTGACTC-3′ | | | |
| ITGB3(NM_000212) | F | 5′-AATGGGACACAGCCAACAAC-3′ | 121 | 2321/2322(F) | Invitrogen |
| | R | 5′-ATCGTGGCACAGGCTGATAA-3′ | | | |
| ITGB4(NM_001005619) | F | 5′-TCTCTGGGACCTTGGCAAAC-3′ | 89 | 87/88(F) | Invitrogen |
| | R | 5′-GCAGTAGGCGCAGTCCTTAT-3′ | | | |
| ITGA3(NM_002204) | F | 5′-TGCCTACAACTGGAAAGGAAAC-3′ | 126 | 1136/1137(F) | Invitrogen |
| | R | 5′-CTGCCTACCTGCATCGTGTA-3′ | | | |
| CD44(NM_000610) | F | 5′-CAAGCACAATCCAGGCAACT-3′ | 161 | 1587/1588(F) | Invitrogen |
| | R | 5′-ATGGCTGGTATGAGCTGAGG-3′ | | | |
| SLFN5(NM_144975) | F | 5′-CCAGACCTTTCCAGGTGTCC-3′ | 149 | 1255/1256(R) | Invitrogen |
| | R | 5′-ACCACTCTGTCTGAAAATACTGGA-3′ | | | |
| GRAP2(NM_004810) | F | 5′-ATCTCTGTCAGGCATGAGGATGAC-3′ | 140 | 553/554(F) | Invitrogen |
| | R | 5′-TGTCTGGAGATGGAATTTGTCCT-3′ | | | |
| C15orf26(NM_173528) | F | 5′-CATTTTGAGTGTACACAGAGATGC-3′ | 132 | 419/420(F) | Invitrogen |
| | R | 5′-GATTTCAGGAGGGTCCTGTGG-3′ | | | |

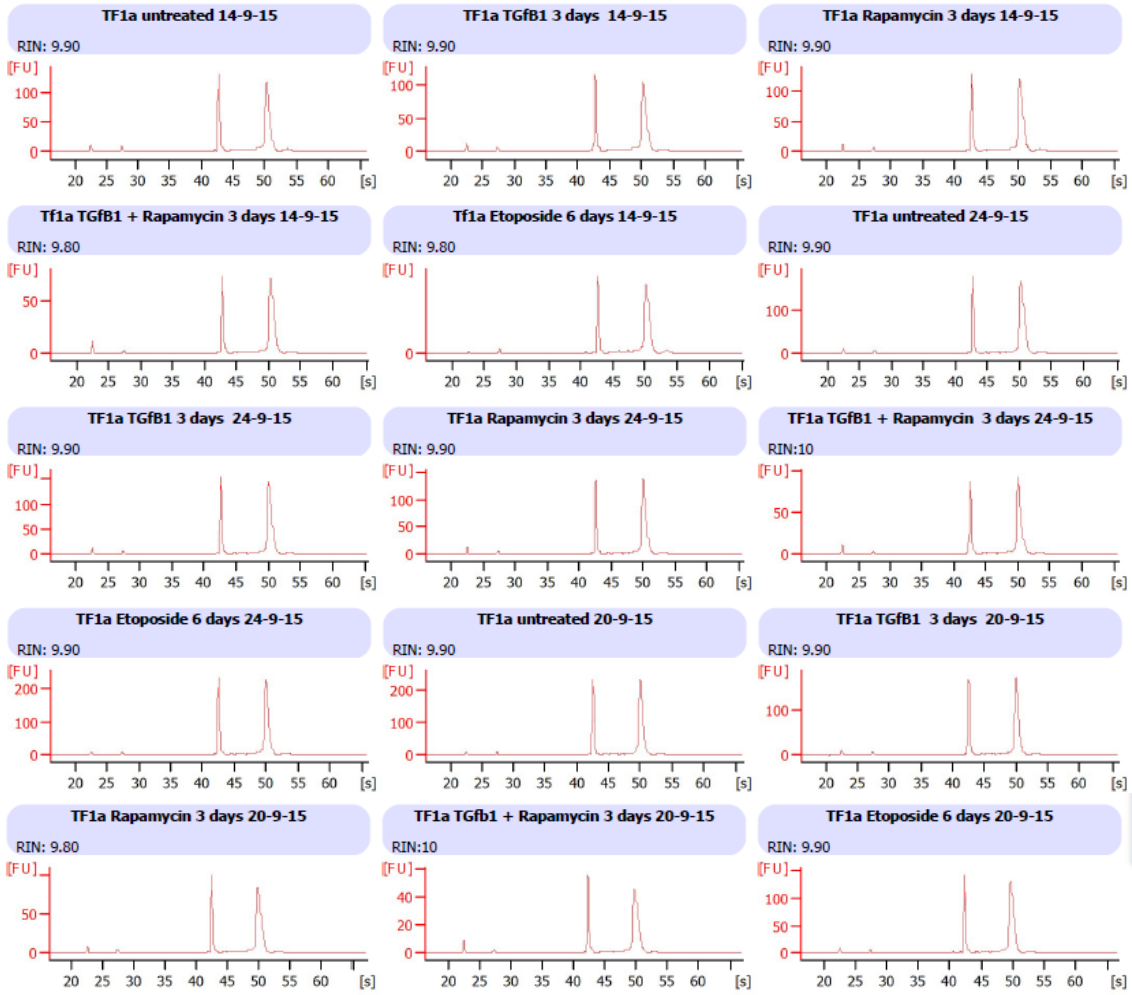
## Appendix A3: Primers melting curves



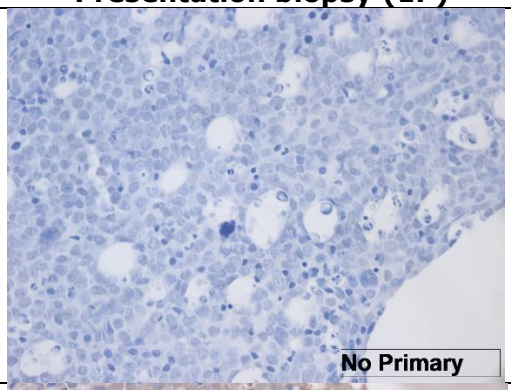
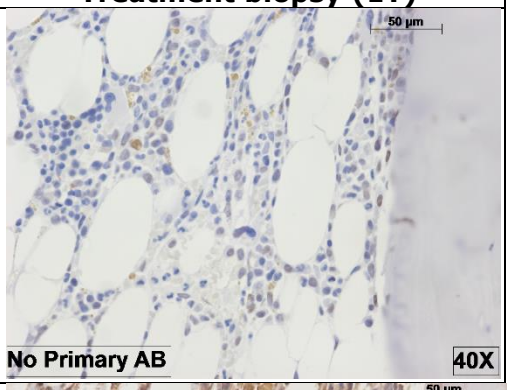
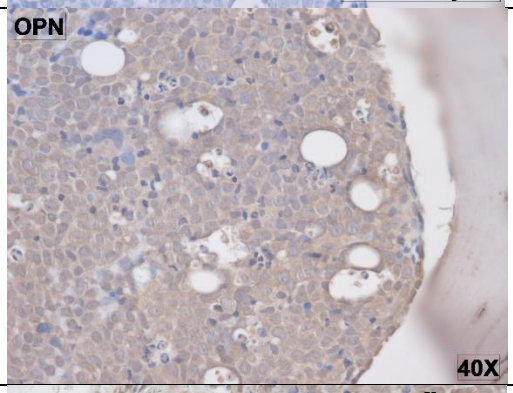
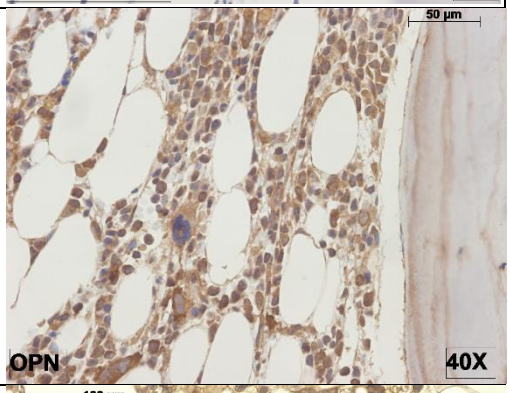
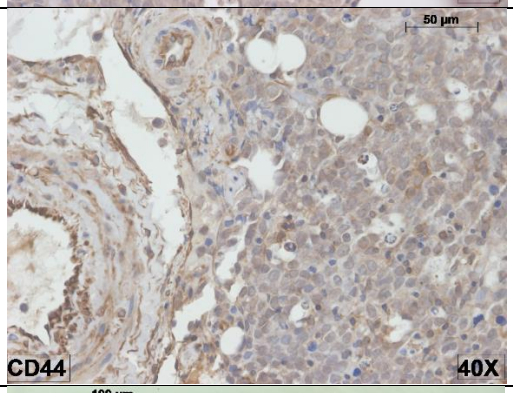
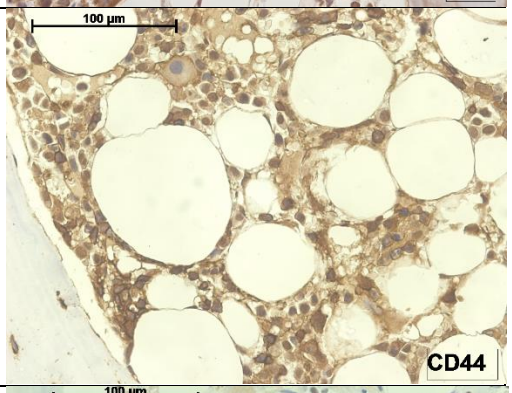
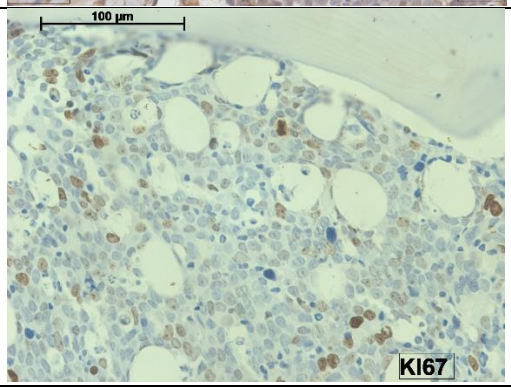
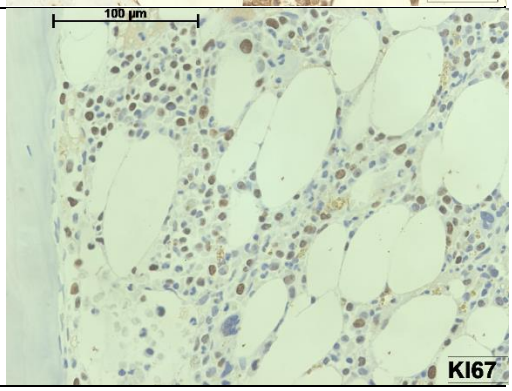

Melt Curve
ITGB3
Melt Curve
ITGB4
Melt Curve
ITGA3

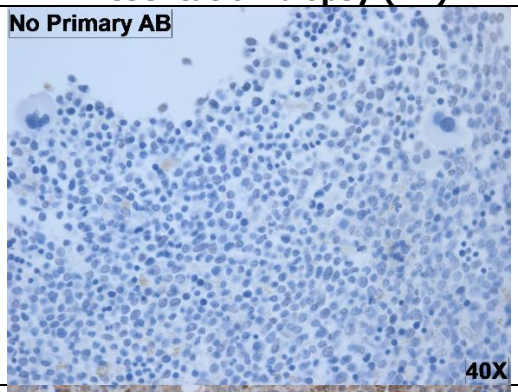
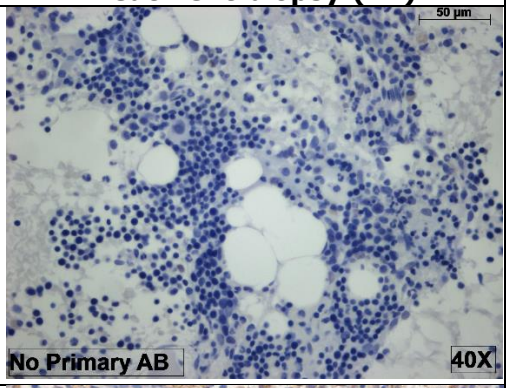
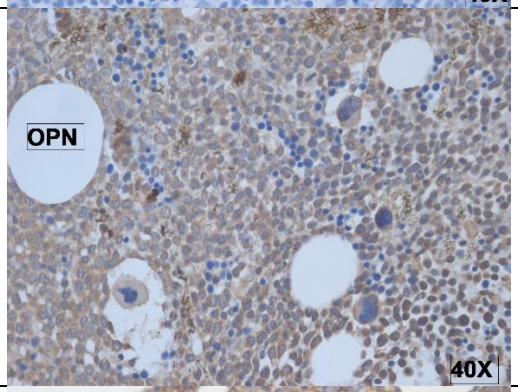
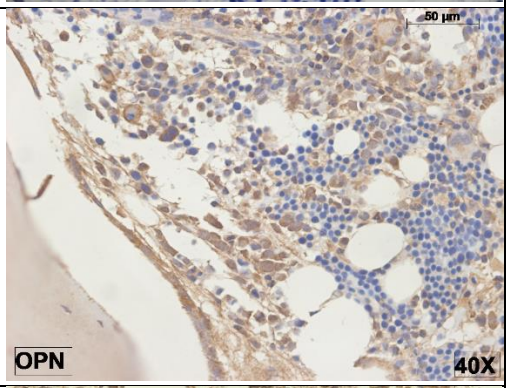
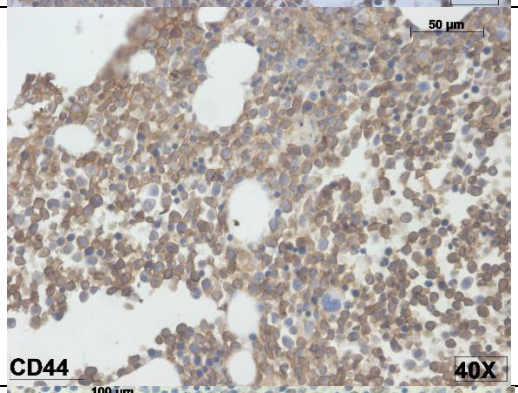
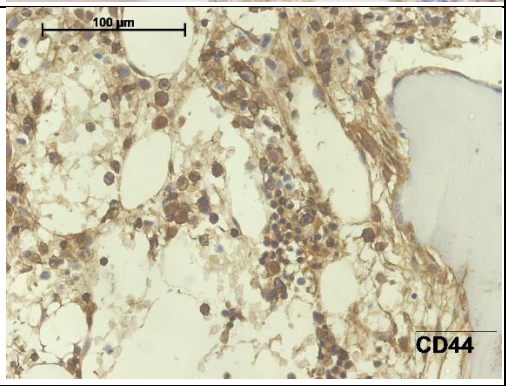
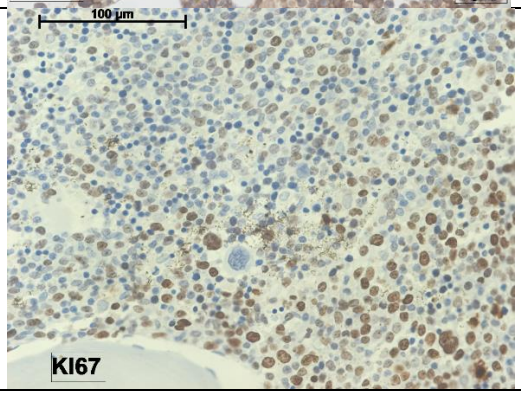
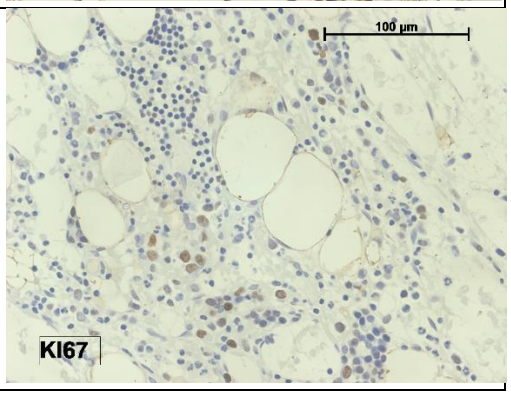
**Appendix A4:** RNA preps Integrity (measured by Agilent 2100 bioanalyzer) for the GEP analysis

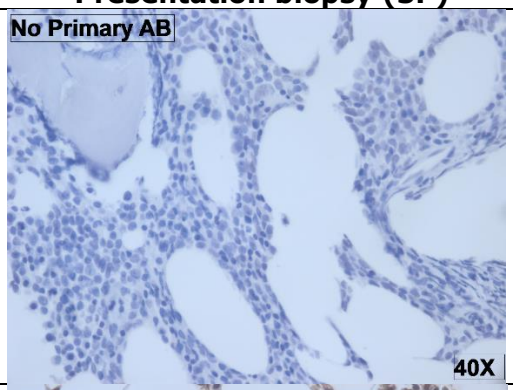
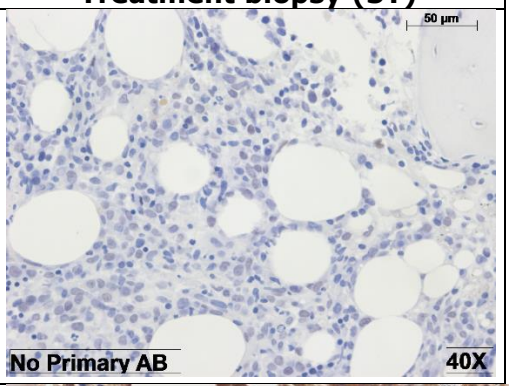
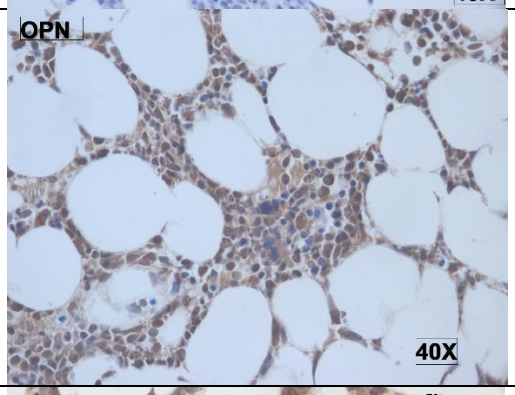
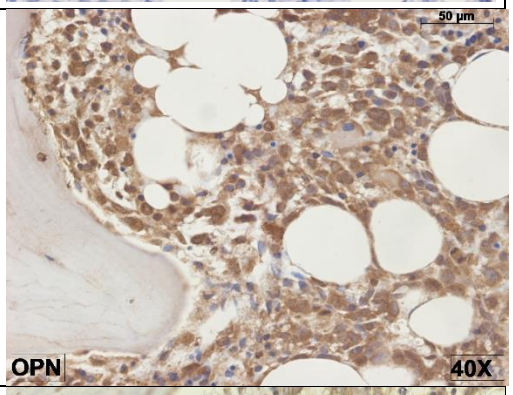
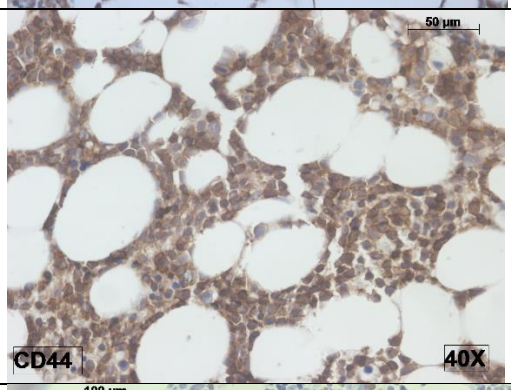
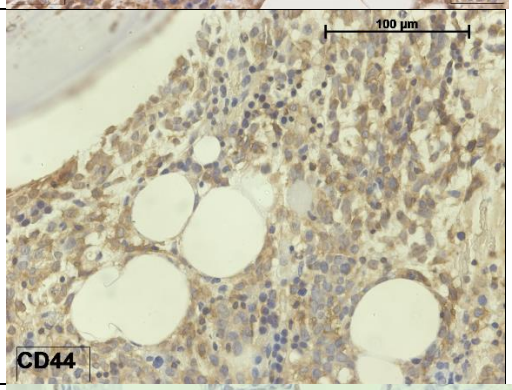
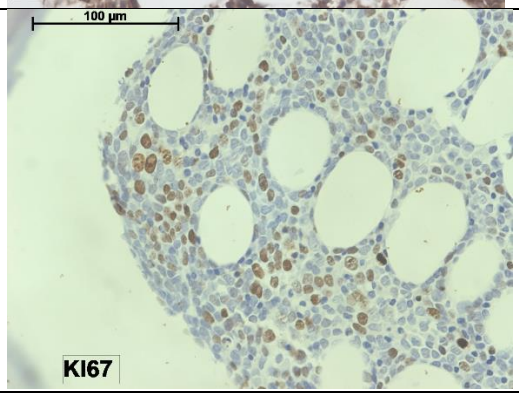
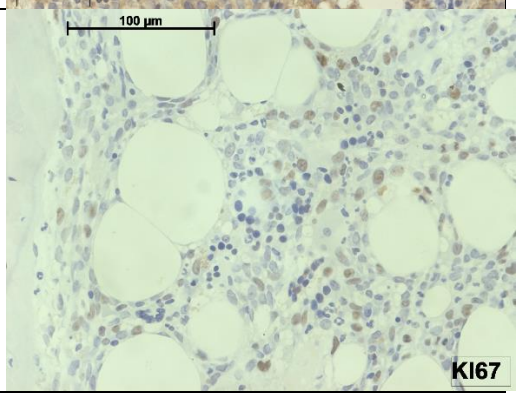


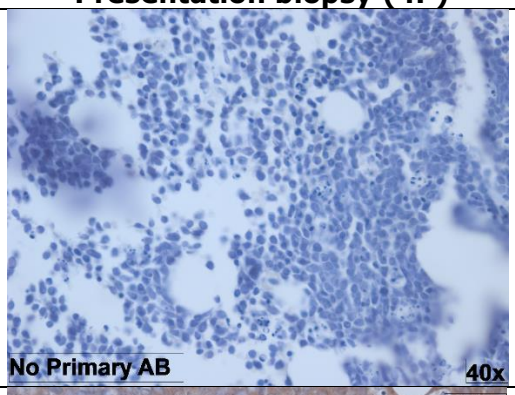
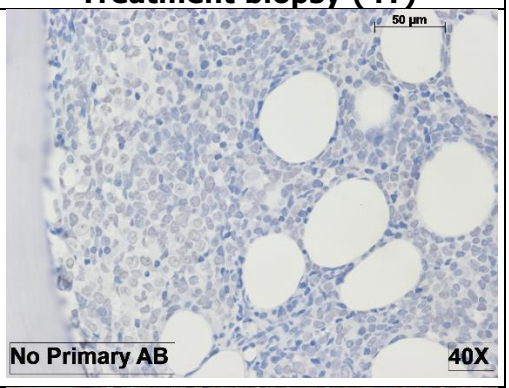
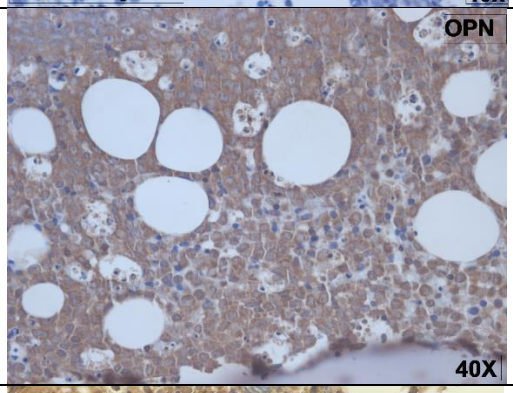
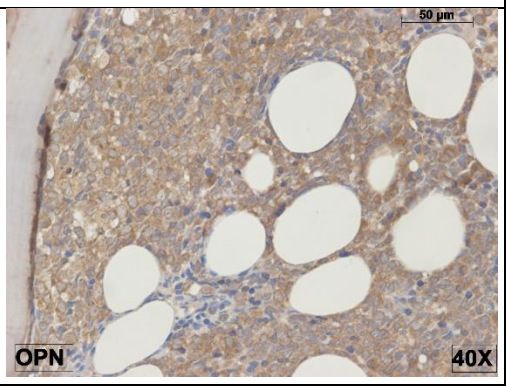
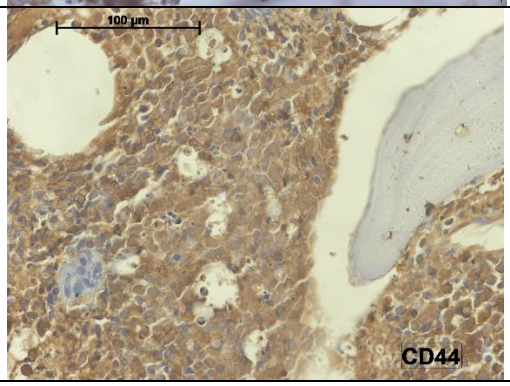
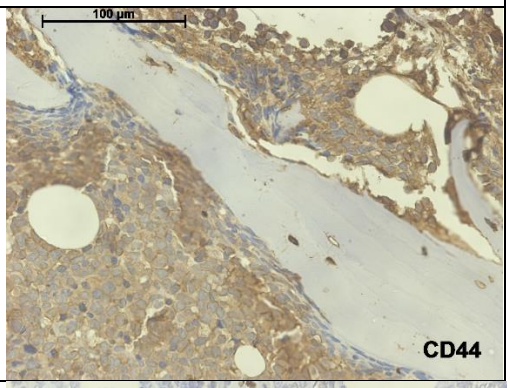
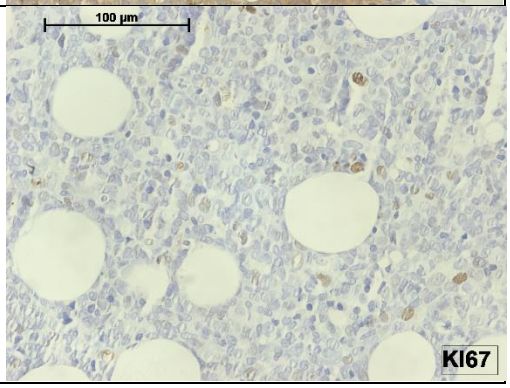



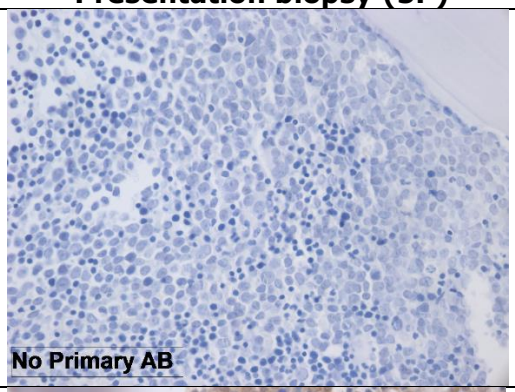
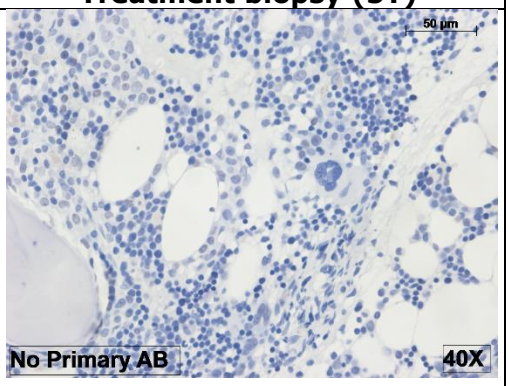
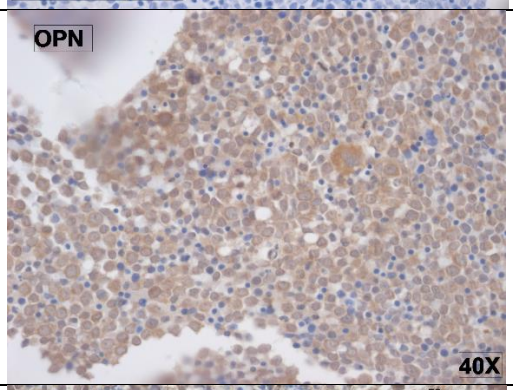
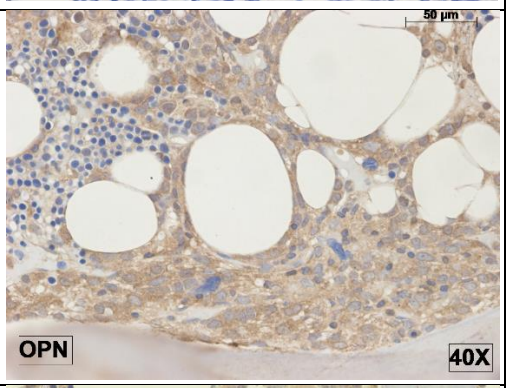
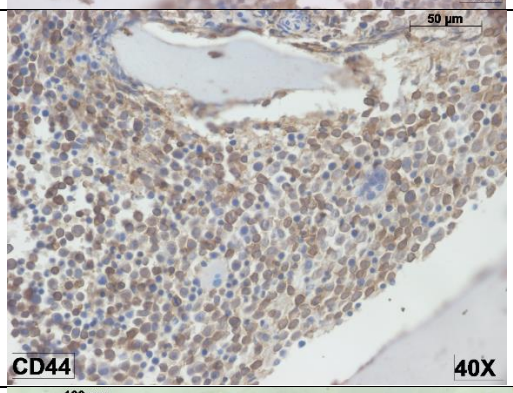
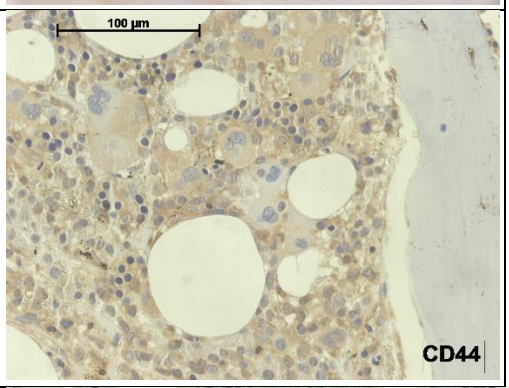
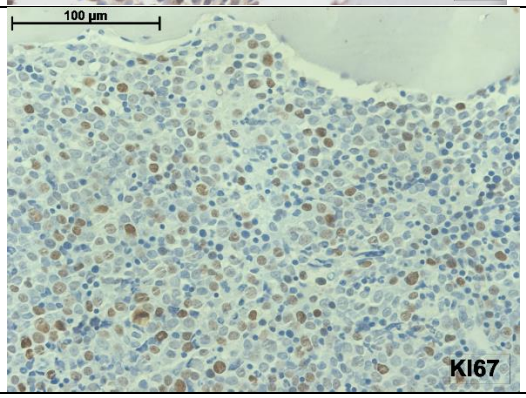
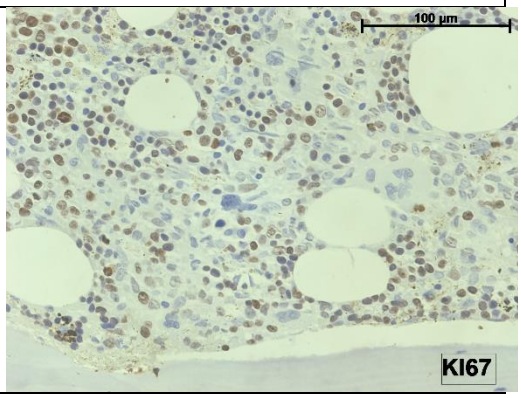
**Appendix A5:** The IHC pictures of the 7 presentation and 7 treatment BM biopsies covered in this study.

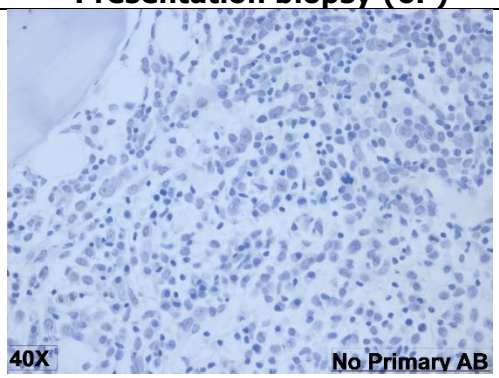
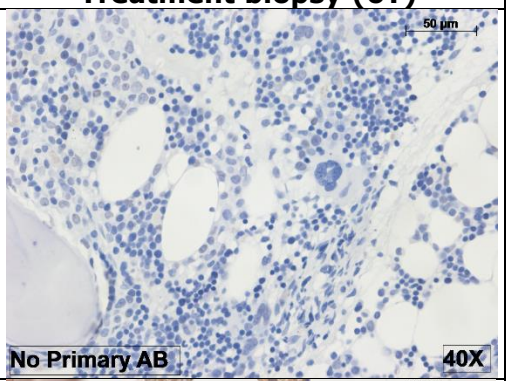
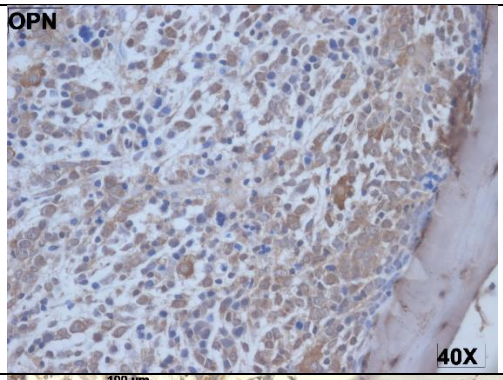
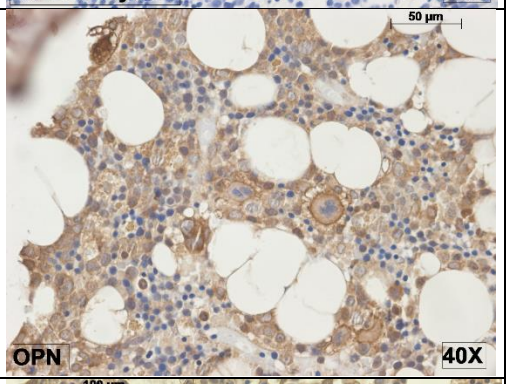
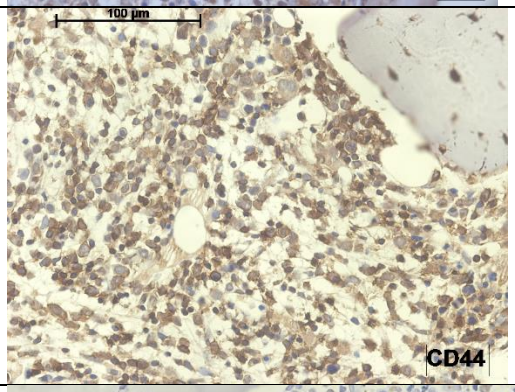
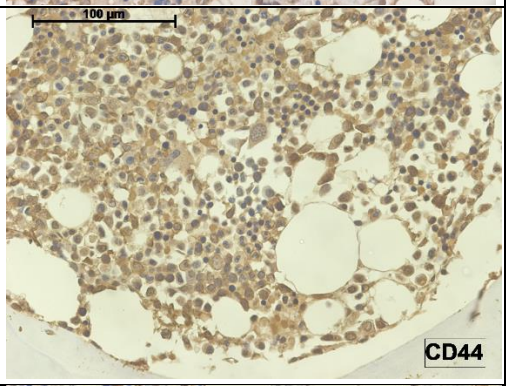
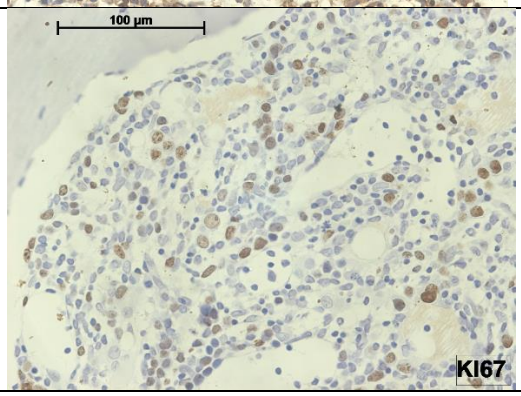
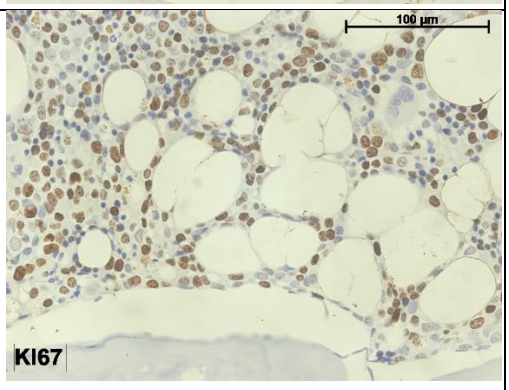
| Patient number one | | |
|---|---|---|
| | **Presentation biopsy (1P)** | **Treatment biopsy (1T)** |
| No primary AB control |  |  |
| OPN |  |  |
| CD44 |  |  |
| Ki67 |  |  |

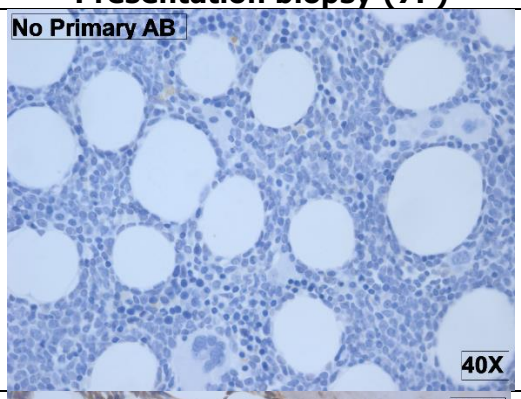
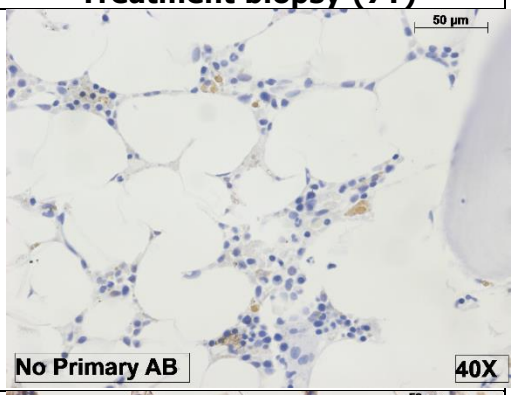
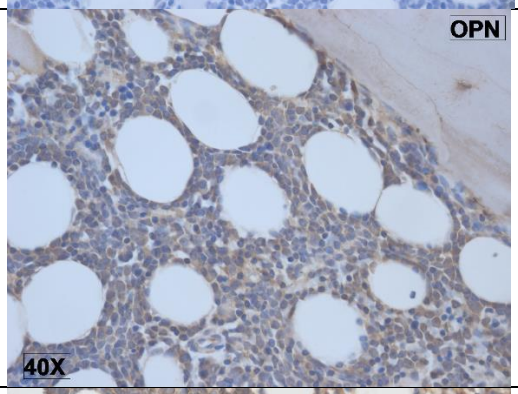
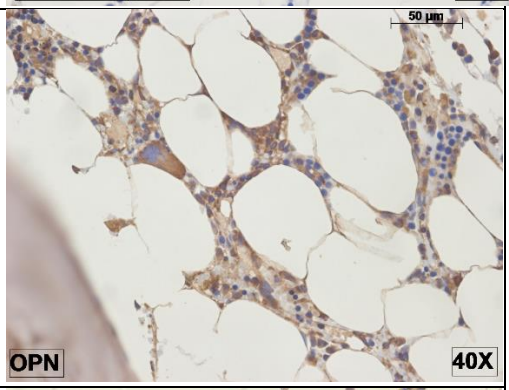
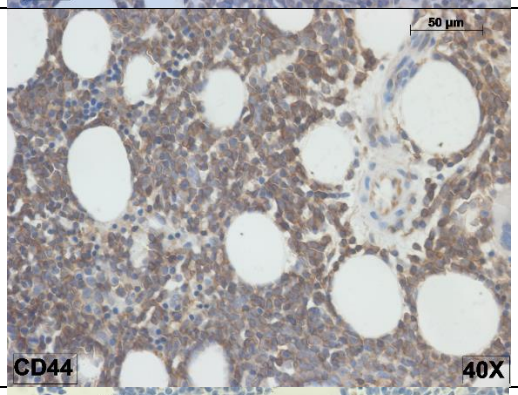
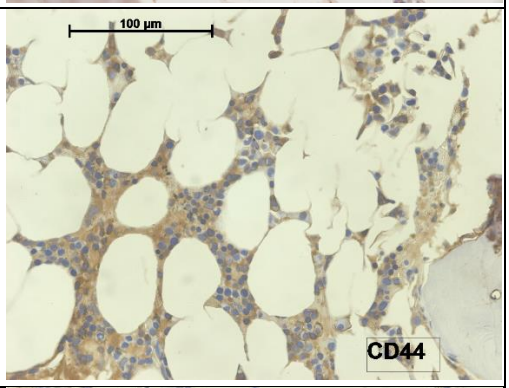
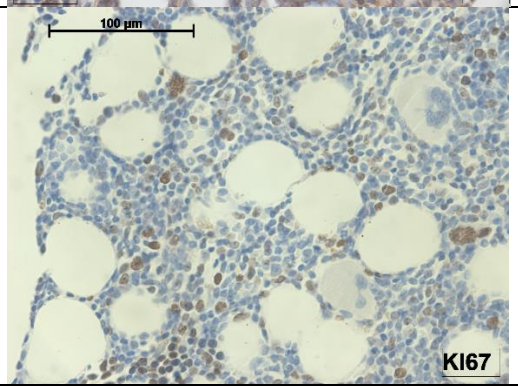
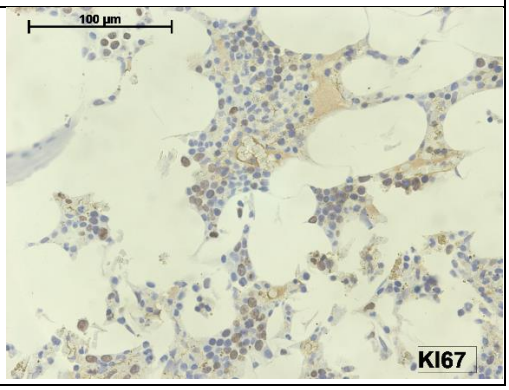
| Patient number two | | |
|---|---|---|
| | **Presentation biopsy (2P)** | **Treatment biopsy (2T)** |
| No primary AB control |  |  |
| OPN |  |  |
| CD44 |  |  |
| KI67 |  |  |

| Patient number three | | |
|---|---|---|
| | **Presentation biopsy (3P)** | **Treatment biopsy (3T)** |
| No primary AB control |  |  |
| OPN |  |  |
| CD44 |  |  |
| KI67 |  |  |

| Patient number four | | |
|---|---|---|
| | **Presentation biopsy (4P)** | **Treatment biopsy (4T)** |
| No primary AB control |  |  |
| OPN |  |  |
| CD44 |  |  |
| KI67 | Did not performed due to the inadequacy of BM biopsy sections |  |

| Patient number five | | |
|---|---|---|
| | **Presentation biopsy (5P)** | **Treatment biopsy (5T)** |
| No primary AB control |  |  |
| OPN |  |  |
| CD44 |  |  |
| KI67 |  |  |

| Patient number six | | |
|---|---|---|
| | **Presentation biopsy (6P)** | **Treatment biopsy (6T)** |
| No primary AB control |  |  |
| OPN |  |  |
| CD44 |  |  |
| KI67 |  |  |

| Patient number seven | | |
|---|---|---|
| | **Presentation biopsy (7P)** | **Treatment biopsy (7T)** |
| No primary AB control |  |  |
| OPN |  |  |
| CD44 |  |  |
| KI67 |  |  |

**Appendix A6:** Significantly enriched biological processes/signalling pathways in the sub-lethal genotoxicity signature of TF1-a cells surviving 6 days of etoposide treatment.*

| Signalling Pathway/Biological process | Enrichment Score | Enrichment p value | Genes in list in group | Genes not in list in group | GO ID |
|---|---|---|---|---|---|
| Cytokine-mediated signalling pathway | 21.64 | 0.00 | 10 | 149 | 19221 |
| Type 1 interferon-mediated signalling pathway | 15.65 | 0.00 | 6 | 59 | 60337 |
| Positive regulation of phosphorylation | 13.37 | 0.00 | 4 | 19 | 42327 |
| Integrin-mediated signalling pathway | 12.45 | 0.00 | 5 | 58 | 7229 |
| Platelet degranulation | 11.33 | 0.00 | 5 | 74 | 2576 |
| Immune response | 10.07 | 0.00 | 8 | 334 | 6955 |
| Positive regulation of angiogenesis | 9.96 | 0.00 | 4 | 49 | 45766 |
| Blood coagulation | 9.89 | 0.00 | 9 | 446 | 7596 |
| Chemotaxis | 9.39 | 0.00 | 5 | 113 | 6935 |
| Cellular response to interferon-alpha | 9.38 | 0.00 | 2 | 2 | 35457 |
| Positive regulation of cerebellar granule cell precursor proliferation | 9.36 | 0.00 | 2 | 2 | 21940 |
| Response to virus | 8.62 | 0.00 | 5 | 134 | 9615 |
| Negative regulation of type I interferon production | 8.54 | 0.00 | 3 | 27 | 32480 |
| Positive regulation of macrophage chemotaxis | 8.47 | 0.00 | 2 | 4 | 10759 |
| Regulation of defence response to virus | 8.47 | 0.00 | 2 | 4 | 50688 |
| ISG15-protein conjugation | 8.47 | 0.00 | 2 | 4 | 32020 |
| Platelet activation | 8.29 | 0.00 | 6 | 228 | 30168 |
| Chronic inflammatory response | 8.14 | 0.00 | 2 | 5 | 2544 |
| Negative regulation of interleukin-12 production | 7.85 | 0.00 | 2 | 6 | 32696 |
| Positive regulation of catenin import into nucleus | 7.85 | 0.00 | 2 | 6 | 35413 |
| Cellular homeostasis | 7.60 | 0.00 | 2 | 7 | 19725 |
| Macrophage chemotaxis | 7.38 | 0.00 | 2 | 8 | 48246 |
| Positive regulation of viral genome replication | 7.38 | 0.00 | 2 | 8 | 45070 |
| Negative regulation of blood vessel endothelial cell migration | 7.36 | 0.00 | 2 | 8 | 43537 |
| Positive regulation of blood vessel endothelial cell migration | 6.69 | 0.00 | 2 | 12 | 43536 |
| Regulation of cellular process | 6.46 | 0.00 | 4 | 126 | 0050794 |
| Negative regulation of viral genome replication | 6.42 | 0.00 | 2 | 14 | 45071 |
| Cell-matrix adhesion | 6.01 | 0.00 | 3 | 68 | 7160 |
| Cellular response to tumour necrosis factor | 5.97 | 0.00 | 2 | 18 | 71356 |
| Positive regulation of endothelial cell migration | 5.97 | 0.00 | 2 | 18 | 10595 |
| Negative regulation of protein binding | 5.97 | 0.00 | 2 | 18 | 32091 |
| Positive chemotaxis | 5.87 | 0.00 | 2 | 19 | 50918 |
| Negative regulation of cell death | 5.78 | 0.00 | 2 | 20 | 60548 |
| Response to bacterium | 5.78 | 0.00 | 2 | 20 | 9617 |
| Activation of MAPK activity | 5.67 | 0.00 | 3 | 77 | 187 |
| Flopodium assembly | 5.45 | 0.00 | 2 | 24 | 46847 |
| Innate immune response | 5.42 | 0.00 | 5 | 280 | 45087 |
| Intracellular protein kinase cascade | 5.31 | 0.00 | 3 | 88 | 17039 |
| Organ morphogenesis | 4.99 | 0.01 | 3 | 99 | 9887 |
| Peptidyl tyrosine phosphorylation | 4.92 | 0.01 | 2 | 32 | 18108 |
| Leukocyte migration | 4.89 | 0.01 | 3 | 103 | 50900 |
| Cellular response to lipopolysaccharide | 4.76 | 0.01 | 2 | 35 | 71222 |
| Regulation of biological process | 4.68 | 0.01 | 4 | 214 | 0050789 |
| Positive regulation of anti-apoptosis | 4.65 | 0.01 | 2 | 37 | 45768 |
| Activation of MAPKK activity | 4.65 | 0.01 | 2 | 37 | 186 |
| Regulation of cellular metabolic process | 4.60 | 0.00 | 2 | 36 | 0031325 |
| Cell differentiation | 4.41 | 0.01 | 6 | 501 | 30154 |
| Protein modification process | 4.01 | 0.02 | 3 | 144 | 6464 |
| Cell adhesion | 3.99 | 0.02 | 6 | 551 | 7155 |
| Wound healing | 3.83 | 0.02 | 2 | 58 | 42060 |
| Interferon-gamma-mediated signalling pathway | 3.66 | 0.03 | 2 | 64 | 60333 |
| Interspecies interaction between organisms | 3.51 | 0.03 | 4 | 307 | 44419 |
| Positive regulation of protein phosphorylation | 3.44 | 0.03 | 2 | 72 | 1934 |
| Cell migration | 3.37 | 0.03 | 2 | 75 | 16477 |
| | | | | | |

* The groups presented in this table were restricted to the groups that contain minimum of 2 genes.